LA-UR-21-25029
Approved for public release; distribution is unlimited.

Title: EXPLORING THE INTERACTION OF AMPHIPHILIC MYCOBACTERIAL LIPOARABINOMANNAN WITH LIPOPROTEINS: IMLICATIONS FOR BLOOD BASED DIAGNOSIS

Author(s): Jakhar, Shailja

Intended for: PhD Dissertation

Issued: 2021-05-25

Shailja Jakhar

Candidate

Biomedical Sciences

Department

This dissertation is approved, and it is acceptable in quality and form for publication:

Approved by the Dissertation Committee:

Dr. Harshini Mukundan, Ph.D., Chairperson

Dr. Steven W. Graves, Ph.D., Co-Chairperson

Dr. Douglas J. Perkins, Ph.D.

Dr. Pavan Muttil, Ph.D.

EXPLORING THE INTERACTION OF AMPHIPHILIC MYCOBACTERIAL LIPOARABINOMANNAN WITH LIPOPROTEINS: IMLICATIONS FOR BLOOD BASED DIAGNOSIS

by

SHAILJA JAKHAR

M.B.B.S, NATIONAL INSTITUTE OF MEDICAL SCIENCES, INDIA, 2010
MPH, EPIDEMIOLOGY/MATERNAL&CHILD HEALTH, SAINT LOUIS UNIVERSITY, 2015

DISSERTATION

Submitted in Partial Fulfillment of the
Requirements for the Degree of

Doctor of Philosophy
Biomedical Sciences

The University of New Mexico
Albuquerque, New Mexico

April 2021

DEDICATION

This work is dedicated to my parents D.R. Jakhar and Seema Jakhar. I couldn't have asked for more support and unconditional love that was always given to me. You have been my inspiration and strength throughout my life. All my success is owed to you. It would not have been possible without your support, sacrifices and encouragement throughout different phases of my life. I love you unconditionally.

ACKNOWLEDGEMENTS

I would like to thank my advisor Dr. Harshini Mukundan who guided and supported me to reach this milestone. She gave me opportunity to work independently and motivated and challenged me in ways that helped me become a better scientist.

Next, I would like to thank my committee members, Drs. Douglas J. Perkins, Pavan Muttil and Steven W. Graves, for their time, insight and guidance throughout the project.

I need to thank Dr. Susan Dorman who has been a great mentor always.

I would like to thank my labmates at Los Alamos National Lab for the immense role they have played. Firstly, I would like to thank Dr. Loreen Stromberg who trained me in the lab, asked critical questions, and helped me solve problems when I was stuck. Secondly, I would like to thank Dr. Jessica K. Sutherland who helped me pull this dissertation work through the end. I appreciate her mentorship as she was kind enough to train and guide me. I also need to thank Aaron Anderson, Dr. Dung Vu and Dr. Alexis A. Bitzer who provided technical support but were always there for emotional support through hard times. I would also like to thank other team members in the lab. A huge debt of gratitude is owed to my friends, Dr. Katie Davis-Anderson for her guidance and smiling company and Kiersten Lenz for always being there, especially when times were difficult. Thank you to the wonderful staff at Biomedical Sciences Graduate Program and Graduate Studies office and all the faculty.

Importantly, I would like to thank my family and friends for their immense support.

EXPLORING THE INTERACTION OF AMPHIPHILIC MYCOBACTERIAL LIPOARABINOMANNAN WITH LIPOPROTEINS: IMPLICATIONS FOR BLOOD-BASED DIAGNOSIS

by

Shailja Jakhar

M.B.B.S, National Institute of Medical Sciences, India, 2010

MPH, Epidemiology/Maternal and Child Health, Saint Louis University, 2015

Ph.D. Biomedical Sciences, University of New Mexico, 2021

ABSTRACT

Currently, over one-third of the global population is infected with tuberculosis (TB), one of the world's most deadly infectious diseases. The current gold standard for TB diagnosis is microbiological culture, which can take up to 6-8 weeks, which is not conducive to timely treatment. There are no reliable diagnostics for TB. Disease manifestation and outcome of diagnostic tests for TB is influenced by co-morbidities such as HIV co-infection, further complicating diagnostics development. Thus, there is a need for reliable diagnostics for TB. This is especially true in pediatric populations where the differential disease presentation further complicates outcomes.

This dissertation describes the development and evaluation of new tailored methods- lipoprotein capture and membrane insertion- for the discriminative detection of an amphiphilic mycobacterial biomarker, lipoarabinomannan (LAM), for diagnosis of TB in adult and pediatric populations. LAM is released by *Mycobacterium tuberculosis* during active infection and associates with serum lipoproteins such as high and low density lipoproteins (HDL/LDL) in the human host. The guiding hypothesis of this work is that the

sequestration of LAM in immune complexes and by lipoprotein carriers in the host contributes to difficulty in detection of the amphiphilic antigen in blood. To this end, we have evaluated the use of tailored amphiphile detection assays to process and measure sequestered LAM in host blood, and examined the application of this methodology in adults and children with TB disease. In addition, we have developed and studied an *in vitro* cell model to further extrapolate the impact of association of LAM with host carriers on its ability to induce innate immune processes, in order to better refine and design strategies for its direct detection. Overall, our conclusions indicate that the amphiphilic biochemistry of LAM and its interaction with lipoproteins is a feature which should be taken into account for the effective development of diagnostics.

TABLE OF CONTENTS

LIST OF FIGURES.....x
LIST OF TABLES..... xii

Chapter 1. Introduction

1.1 Tuberculosis disease burden and epidemiology 1
1.2 Disease presentation 5
1.3 Mycobacterium *tuberculosis*.....8
1.3.1 Pathogenesis.....9
1.4 Mycobacterial cell wall 10
1.4.1 Mycolic acid.....11
1.4.2. Lipoarabinomannan.....13
1.5 Diagnostics 17

Chapter 2. Goals and Overview of this Work.....26

Chapter 3. Current Status of Pediatric Tuberculosis Diagnostics, Needs, and Challenges

3.1 Overview and statement of problem 36
3.2 Challenges.....38
3.3 WHO goals for pediatric TB 39
3.4 Current TB diagnostic tools.....40
3.4.1 The lack of gold standard diagnostic and implications.....50
3.5 Pediatric TB in context of HIV 50
3.6 Research needed on pediatric TB.....52

Chapter 4. Pediatric Tuberculosis: The Impact of "Omics" on Diagnostics Development

4.1 Abstract.....54
4.2 Introduction 55
4.3 Current diagnostics for pediatric TB.....57
4.4 The role of "Omics" in TB diagnostic development 61
4.5 Conclusions.....78

Chapter 5. Detection of Lipid and Amphiphilic Biomarkers for Disease Diagnostics

5.1 Abstract....81
5.2 Introduction....82
5.3 Methods for detecting lipid and amphiphilic biomarkers....84
5. 4 Lipid biomarkers for infectious diseases....94
5.5 Lipid biomarkers for non-infectious diseases....98
5.6 Discussion....107

Chapter 6. Interaction of amphiphilic lipoarabinomannan with host carrier lipoproteins in tuberculosis patients: Implications for blood-based diagnostics

6.1 Abstract....112
6.2 Introduction....114
6.3 Methods....117
6.4 Results....126
6.5 Discussion....131

Chapter 7. The feasibility of serum lipoarabinomannan antigen detection in childhood tuberculosis

7.1 Abstract....138
7.2 Introduction....139
7.3 Results....142
7.4 Discussion....147
7.5 Methods....149

Chapter 8. A centrifugal microfluidic cross-flow filtration platform to separate serum from whole blood for the detection of amphiphilic biomarkers

8.1 Abstract....158
8.2 Introduction....158
8.3 Working principle....162
8.4 Methods....163
8.5 Results....167

8.6 Discussion.....170
Chapter 9. Impact of association of lipoarabinomannan with serum lipoproteins on innate immune signaling
9.1 Introduction 175
9.2 Materials and methods 177
9.3 Results and discussion 182
9.4 Conclusion 188
Chapter 10. Conclusions and future directions.....190

Appendix A: References 194
Appendix B: Supplemental information for chapter 6 233
Appendix C: Supplemental information for chapter 9.....239

LIST OF FIGURES

Figure 1.1. The global spread and impact of tuberculosis
Figure 1.2. Estimated tuberculosis incidence in 2019
Figure 1.3. Latent and active tuberculosis
Figure 1.4. The disease spectrum of tuberculosis
Figure 1.5. The structure of the mycobacterium tuberculosis cell wall
Figure 1.6. Steps of phagocytosis for mycobacterium tuberculosis
Figure 1.7. Pathway for disruption of mycobacterium tuberculosis- toll-like receptor signaling pathway
Figure 2.1. Specific aims schematic
Figure 4.1. Pediatric tuberculosis diagnostics—today and tomorrow
Figure 4.2. Representative cases for an “omics-based” approach to build a comprehensive understanding of the pathology of both adult and pediatric tuberculosis
Figure 5.1. Examples of biosensor techniques incorporating lipids for the detection of analytes
Figure 5.2. Immunoassay strategies to detect lipid and amphiphilic biomarkers
Figure 5.3. A comparison of the sensitivity of membrane insertion and lipoprotein capture technologies
Figure 6.1. Overview of lipoarabinomannan detection strategies
Figure 6.2. Assay optimization for the detection of lipoarabinomannan in human serum by lipoprotein capture assay
Figure 6.3. Measurement of lipoarabinomannan by membrane insertion assay, as a function of concentration
Figure 6.4. Direct detection of lipoarabinomannan in patient serum samples
Figure 6.5. Comparison of lipoprotein capture and membrane Insertion assay
Figure 7.1. Overview of tuberculosis diagnostic pathways and lipoarabinomannan detection strategies
Figure 7.2. Membrane insertion assay optimization for the detection of lipoarabinomannan in human serum

Figure 7.3. Direct detection of lipoarabinomannan in pediatric serum samples
Figure 8.1. A schematic depicting the difference between the separation of serum from blood
Figure 8.2. Schematic of microfluidic device
Figure 8.3. Schematics of phase separations on the microfluidic device
Figure 8.4. Average cell counts for the microfluidic device separation concept
Figure 8.5. Signal intensity of lipoarabinomannan after blood processing on microfluidic chip
Figure 9.1. Schematic of the conditions of LAM presentation in media
Figure 9.2. Cytokine profile of LAM exposed THP-1 cells in buffer and serum
Figure 9.3. Heat map distributions of cytokines induced by LAM under different physiological conditions
Figure S1. Antibody screening and selection by colorimetric sandwich immunoassays
Figure S1. Cell viability assay for THP-1 cells exposed to lipoarabinomannan

LIST OF TABLES

Table1.1. WHO endorsed tuberculosis diagnostic tests

Table1.2. Review of studies using different biomarkers and methods for detection of tuberculosis

Table5. 1. Advantages and limitations of sensors as clinical diagnostic tools for detecting lipid and amphiphilic biomarkers.

Table 5.2. Select lipid and amphiphilic biomarkers used for the diagnosis of infectious diseases

Table 5.3. Select lipid and amphiphilic biomarkers used for diagnosing non-infectious diseases

Table 6.1. Signal to noise ratios, by clinical group, for the lipoprotein capture assay

Table 7.1. Summary of patient demographics and laboratory test results for pediatric tuberculosis patients and controls.

Table S1. Selection of monoclonal antibodies for optimization of lipoprotein capture assay

Table S2. Patient demographics for Uganda tuberculosis patients

Table S3- CT values for gene expression analysis in THP-1 cells under different physiological conditions

Chapter 1.

Introduction

1.1 Tuberculosis Disease Burden and Epidemiology

Tuberculosis (TB) is one of the world's oldest and most formidable diseases[1]. Often referenced as a scourge on humanity[1], the disease has affected humans for thousands of years, and has caused more deaths in last 200 years than any other infectious disease worldwide. TB is so prevalent, that nearly one quarter of the world's population (~2 billion) is infected, and ~1.4 million people succumb to the disease every year[2,3]. So devastating is the effect of the disease, that the World Health Organization (WHO) declared TB a global health emergency in 1993[4–6]. Regardless of extensive research in therapeutics, vaccines, and diagnostics, TB is still a major cause of concern around the globe[7].

According to a 2020 report from the WHO, 10 million new people were infected, ~1.2 million HIV-negative individuals and ~208,000 HIV positive people (**Figure 1.1 A and B**) died from the disease. Eight countries accounted for two thirds of the global total: India (26%), China (8.4%), Indonesia (8.5%), the Philippines (6%), Pakistan (5.7%), Nigeria (4.4%), Bangladesh (3.6%) and South Africa (3.6%) (**Figure 1.2**). The estimate is

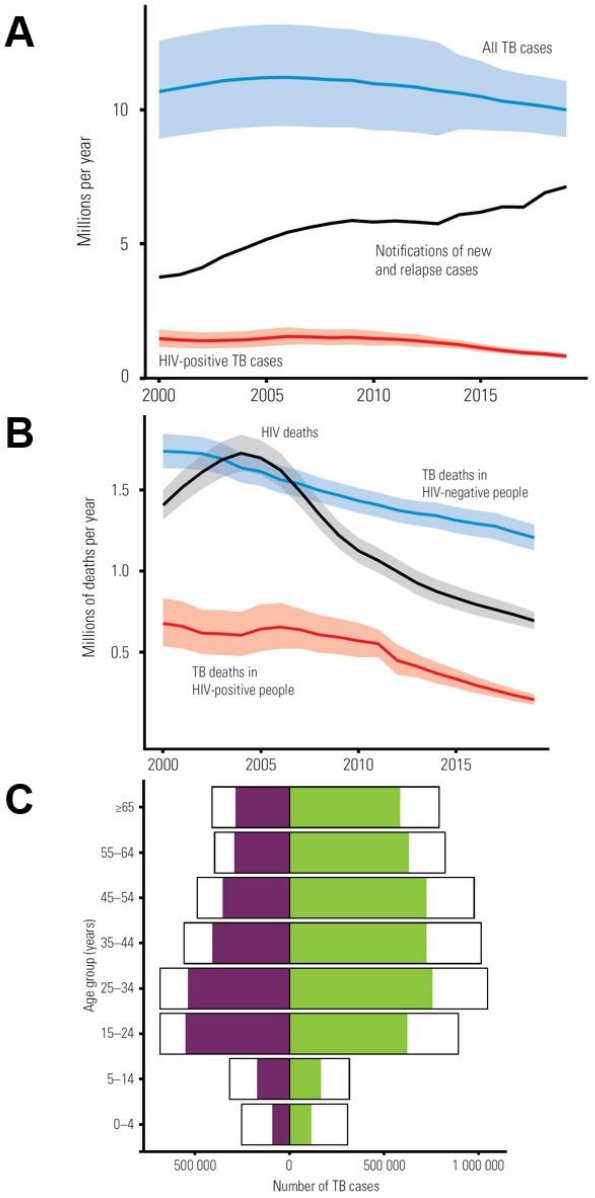

Figure 1.1. The global spread and impact of TB. A. Global trends in the estimated number of incident TB cases, 2000-2019. Shaded area represents uncertainty levels. B. Global trends in the estimated number of deaths caused by TB and HIV, 2000-2019. Shaded area represents uncertainty levels. C. Global estimates of TB incidence (black outline) and case notifications disaggregated by age and sex (female in purple; male in green), 2019. Reprinted with permission from WHO as per WHO guidelines. Global tuberculosis report, 2020, World Health Organization, https://www.who.int/tb/publications/global_report/en/, accessed on November 1, 2020.

slowly increasing in the Americas after several years of decline. Men and women of all ages are affected, but men represent a greater fraction (56% in 2019) compared to women (32%)[3]. Meanwhile, children (<15 years) account for 12% of all TB cases (**Figure 1.1 C**).

Historical evidence has demonstrated that TB-related mortality trends suffer from geographic inconsistencies[8]. Between the years 1900-1980, TB related deaths in Western Europe and the United States decreased by more than 100-fold. Since most of this decline was prior to the advent of anti-TB drugs, improvements in hygiene and

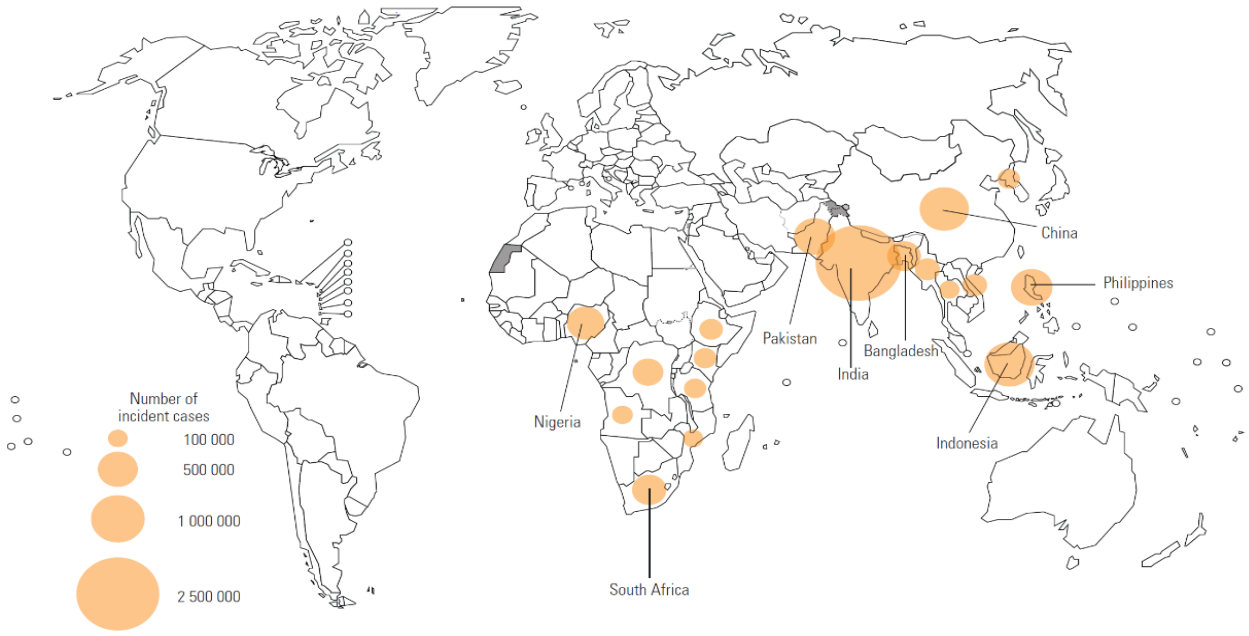

Figure 1.2. Estimated TB incidence in 2019, for countries with at least 100 000 cases. Reprinted with permission from WHO. Global tuberculosis report, 2020, World Health Organization, https://www.who.int/tb/publications/global_report/en/, accessed on November 1, 2020.

socioeconomic conditions were credited. As access to these interventions has improved over time, the mortality rate has become relatively stable overall. However, geographically, the disease mortality varies greatly with WHO African and South-East Asia regions accountable for 85% of total deaths in 2019 with India alone responsible for 31% of total TB deaths. Even though the overall number of incident cases and deaths fell between 2000 and 2019, additional work is still needed to end the TB epidemic. Faster reduction in TB deaths can be achieved with improving accessibility to TB diagnosis and treatment.

One of the complicating features of TB disease is the fact that many individuals infected with the pathogen are asymptomatic for extended periods of time – a condition referred to as latency (**Figure 1.3**). This latent period can last until the infected individual encounters one or more risk factors that challenge the immune system, and enables

activation of the disease. The transition from latency to active disease is defined as a spectrum – as described in disease presentation of this manuscript. Several factors influence activation of the disease from latency such as HIV co-infection (15-22x), malnutrition and air pollution[9], tobacco usage (2x risk)[10,11], excessive alcohol consumption (3x risk)[12] or affliction with diabetes mellitus[13]. Among all these, HIV is the most common co-infection for progression of disease to the active state[14]. Statistics indicate that up to 8.2% of all TB patients may be co-infected with HIV. Age is another major determinant in activation of TB disease. Infants are at much higher risk of developing active TB. Between 2-11 years of age, risk of developing active infection is much lower, but begins increasing again during adolescence until 25 years of age, where risk plateaus and remains high for the remainder of adult life[15].

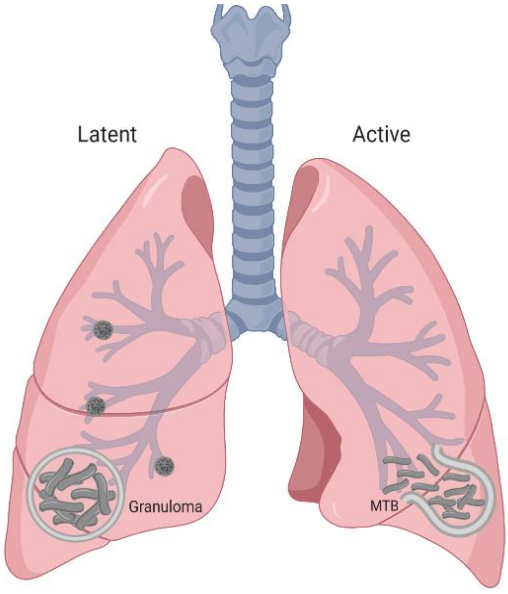

Figure 1.3. Latent and active TB. *Mycobacterium tuberculosis* (MTB) is contained in the granuloma (left) until the immune system is weakened and MTB escapes (right). BioRender.com

Aerosol transmission facilitates the rapid spread of TB, and influences its global burden. On average, a person with active TB infects 3-10 people per year, some of whom will progress to active TB[16]. In patients with active TB, the average period of communicability is >1 year (in high burden areas), which highlights the magnitude of the problem for controlling disease transmission[17], especially if the disease is left untreated. In fact, the true extent of TB disease remains unknown, with a large gap existing between

reported (7 million, 2019) and estimated (10 million, 2019) cases. Underreporting of detected cases and inadequate diagnosis are the most probable reasons for this gap[18]. These potential missing cases pose a major challenge to ongoing efforts geared towards controlling further transmission and spread of disease. This disparity is especially profound in younger populations, with estimates suggesting that 55% of pediatric cases have not been reported to surveillance programs[19]. This discrepancy amongst children further varies with the age group of children being considered, with 69% of cases unreported in children younger than 5 years of age compared to 40% in children 5-14 years[19]. These facts become especially poignant when one realizes that these children are living with TB, not receiving treatment, and possibly spreading the disease even further.

1.2 Disease presentation

One of the factors about TB disease that is responsible for the global prevalence and mortality is the complex nature of disease presentation.

Disease spectrum: Tuberculosis is a complex disease caused by the bacterium, *Mycobacterium tuberculosis* (MTB), and spreads *via* inhalation into the respiratory tract. Traditionally, TB has been characterized into latent and active infection stages depending on the absence or presence of clinical symptoms. However, recent work in animal models

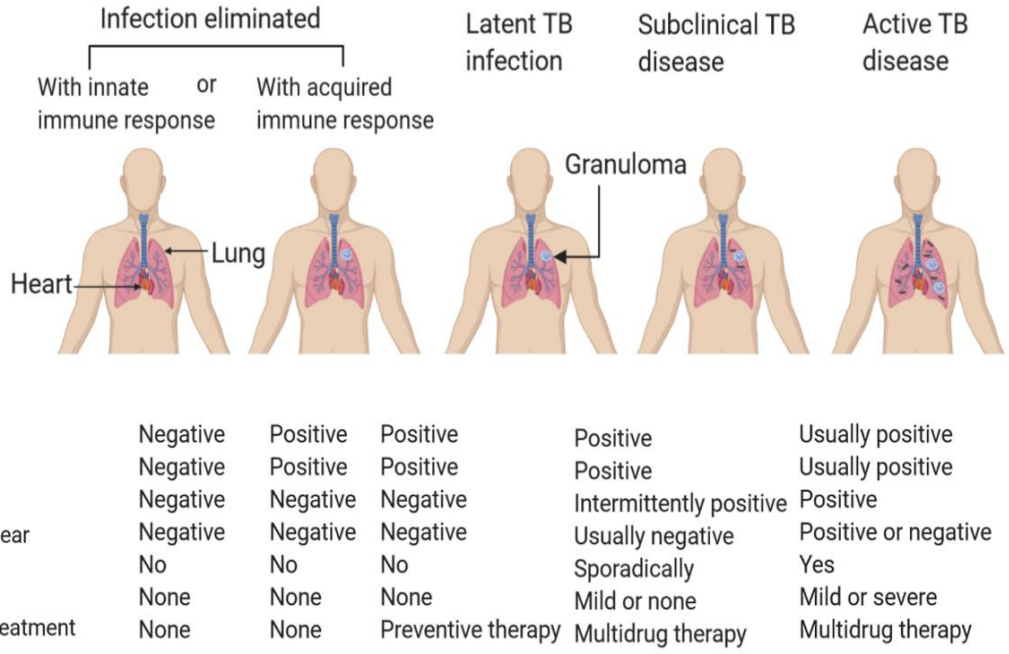

Figure 1.4. The disease spectrum of TB. *Mycobacterium tuberculosis* infection to active (pulmonary) TB disease, figure created with BioRender.com, adapted from Pai, M. *et al.* (2016) Tuberculosis *Nat. Rev. Dis. Primers* doi:10.1038/nrdp.2016.76

and humans show a more complex pathogenesis profile where infection can lead to either active disease or complete immune clearance[18]. As a result of these observations, TB disease is now described as a spectrum (**Figure 1.4**), spanning from asymptomatic infections to fatal disease[18,20,21]. To improve the characterization of clinical TB pathogenesis, Drain *et al*. proposed a new framework for dividing the TB disease spectrum into five infection stages: eliminated, latent, incipient, subclinical, and active. Eliminated individuals are those that have been exposed to MTB before but have successfully cleared it either owing to immune system or due to anti-TB drugs. In individuals with latent disease, MTB can stay dormant in the lungs for years with no clinical, radiological or microbiological evidence of active TB disease[22,23]. This is the most prevalent form of TB disease and affects almost one quarter of world's population. Incipient infection shares many similar traits with latent TB, and in this case, the patient expresses no clinical, radiological or microbiological evidence to confirm active disease

even though they are infected with viable bacteria. Subclinical disease involves a unique manifestation of the disease, where the patient shows microbiologic and radiologic symptoms indicative of active TB, but is still asymptomatic. The final aspect of spectrum of disease is individuals presenting with active TB, where patients are symptomatic with clinical and microbiological evidence and can transmit the disease[24]. Thus, whereas individuals that present with the disease in various ranges of the spectrum above can be contagious, some of them may not even be aware of their disease status, fueling further transmission of MTB.

Disease Presentation in Individuals with Active Disease: Another complicating aspect of active TB is that it can manifest as pulmonary or extra pulmonary forms. Pulmonary TB (PTB) commonly presents as a cough that lasts greater than 4 weeks, and is often accompanied by dyspnea, asthenia, chest pain, hemoptysis, persistent evening fever, night sweats, and weight loss. The hematogenous spread of MTB either due to reactivation of latent TB or progression of primary infection, results in extrapulmonary TB (EPTB). EPTB can be disseminated throughout the body and can manifest in the genitourinary, gastrointestinal, cerebral, lymphatic, or skeletal systems[25]. EPTB presents an even greater diagnostic challenge due to nonspecific clinical presentation. Because of the uncharacteristic presentation, the requisite treatment regimen is often unclear, making the disease much more difficult to treat and control in both children and adults.

Disease Presentation in Children: The disease presentation in children is different as compared to adults, more likely due to immature immune system. Children present with disseminated or EPTB more often than adults[26]. Pediatric TB and co-infection with both TB and HIV often results in paucibacillary disease, where clinical samples and isolates

from infected patients contain few bacteria, making culture and isolation of the causative agent challenging[27,28]. For this reason, pediatric TB is considered a minor contributor to the spread of infection. However, young children and people with HIV have a high risk of disease progression following infection, and are more likely to develop severe or disseminated disease. In children, these symptoms can be easily mistaken for other childhood respiratory diseases, making it more difficult to diagnose the disease. The childhood TB, disease presentation and diagnostics are discussed in more detail in chapter 3 of this manuscript.

1.3 Mycobacterium tuberculosis

MTB is the causative agent of TB and was discovered, isolated and cultured by Robert Koch in 1882[29]. These are rod shaped bacilli measuring about 1-4 µm in length and 30-60 nm in width[30]. MTB belongs to genus Mycobacterium, and are classified as acid- fast, since the cell wall is impermeable to the classic Gram stain, and therefore requires the use of heat and acid to visualize the bacteria. They are considered aerobic, intracellular, obligate pathogen and have no natural reservoir outside humans. MTB are slow growing mycobacteria, which are more virulent, have a doubling time of 15- 20 hours and usually produce visible colonies on a solid medium in 10-28 days[31]. The thick waxy cell wall of mycobacterium provides protection against the microbicidal mechanism of macrophages and plays an important role in host pathogen interaction.

1.3.1 Pathogenesis

Pathogenesis of MTB is a highly studied field, largely owing to the interesting strategies that the pathogen uses to evade immune recognition, thereby preventing its elimination from the host. In most instances, MTB enters the lungs *via* inhalation, reaches the alveolar space and comes in contact with mononuclear phagocytic cells such as alveolar macrophages and dendritic cells. The bacteria are then phagocytosed, which is the process by which bacteria is recognized, engulfed and destroyed (**Figure 1.6**)[32,33]. Phagocytosis is one of the responses of the host, which deploys a combination of innate and adaptive immune systems[34] to eliminate MTB.

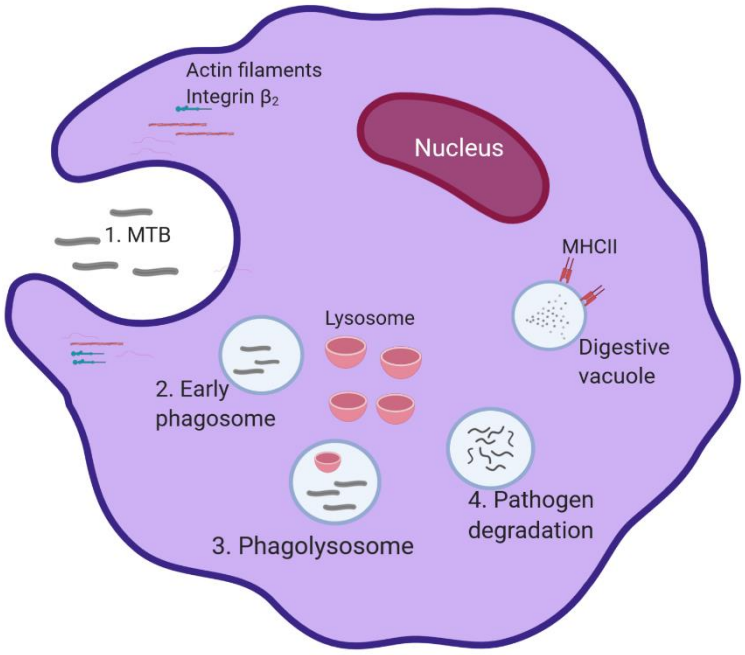

Figure 1.6. Phagocytosis involves 4 main steps: 1. Pathogen recognition 2. Development of early phagosome 3. Phagolysosome maturation 4. Pathogen degradation. Created with BioRender.com. Adapted from Carranza et al. (2019), Several Routes to the Same Destination: Inhibition of Phagosome-Lysosome Fusion by *Mycobacterium Tuberculosis;* N Am J Med Sci;

The process begins by recognition of pathogen associated molecular patterns (PAMP) such as LAM through specialized receptors such as (TLR)- 2, C-type lectin receptors, complement receptor type 3 (CR3) and mannose receptor (CD206) expressed on cell surface in the host. Once recognized, signaling pathways induce actin filament polymerization, which allows the cell membrane to elongate and form pseudopods that surround the MTB cell. Then the membrane seals around the engulfed

MTB, and forms an early phagosome. The final step in the destruction process takes place in phagolysosome, which is formed by fusion of phagosome and lysosome. Once MTB is internalized, a localized pro-inflammatory response occurs that leads to recruitment of other cells from nearby blood vessels leading to formation of granuloma. The granuloma is characteristic of TB disease and consists of a kernel of infected macrophages surrounded by foamy giant cells[35], forming a escape capsule for the long term survival and persistence of MTB. This encapsulation defines the latent stage of TB. Caseation of the granuloma under conditions where the host immune system is compromised, results in the dissemination of the contained MTB – causing active disease. Consequently, if bacteria are destroyed in the phagolysosome, the degraded antigens are then presented to T cells, resulting in the activation of adaptive immune response.

MTB exhibits remarkable abilities to evade host immunity, and block host-mediated phagocytosis in order to ensure pathogen survival, using several different strategies where ManLAM plays a crucial role in helping MTB evade host immune mechanisms as discussed later in LAM section.

1.4 Mycobacterial cell wall

The cell wall of mycobacteria plays a crucial role in MTB physiology, and comprises of the hallmark feature of mycobacteria- their abundance of unique in lipids [36]. The cell wall consists of the periplasm, a peptidoglycan layer, and the outer membrane[37]. The outer membrane contains mycolic acids, various glycolipids and phthiocerol dimycocerosates. All these mycobacterial cell wall lipid components are vital for interaction with the host

and its immune system. The lipids and lipoglycans also play an important role in MTB growth, survival and virulence[38–41].

1.4.1 Mycolic acid

Mycolic acids (MAs) are a main component of the cell wall of mycobacteria and important for regulating the permeability, viability and virulence of MTB. They are also responsible for the acid fast characteristic of MTB. These unique lipids are composed of meromycolate chains of up to 62 carbons with numerous modifications. MTB has 3 different structural classes of MAs namely, alpha-, methoxy- and keto-Mas[42], with the

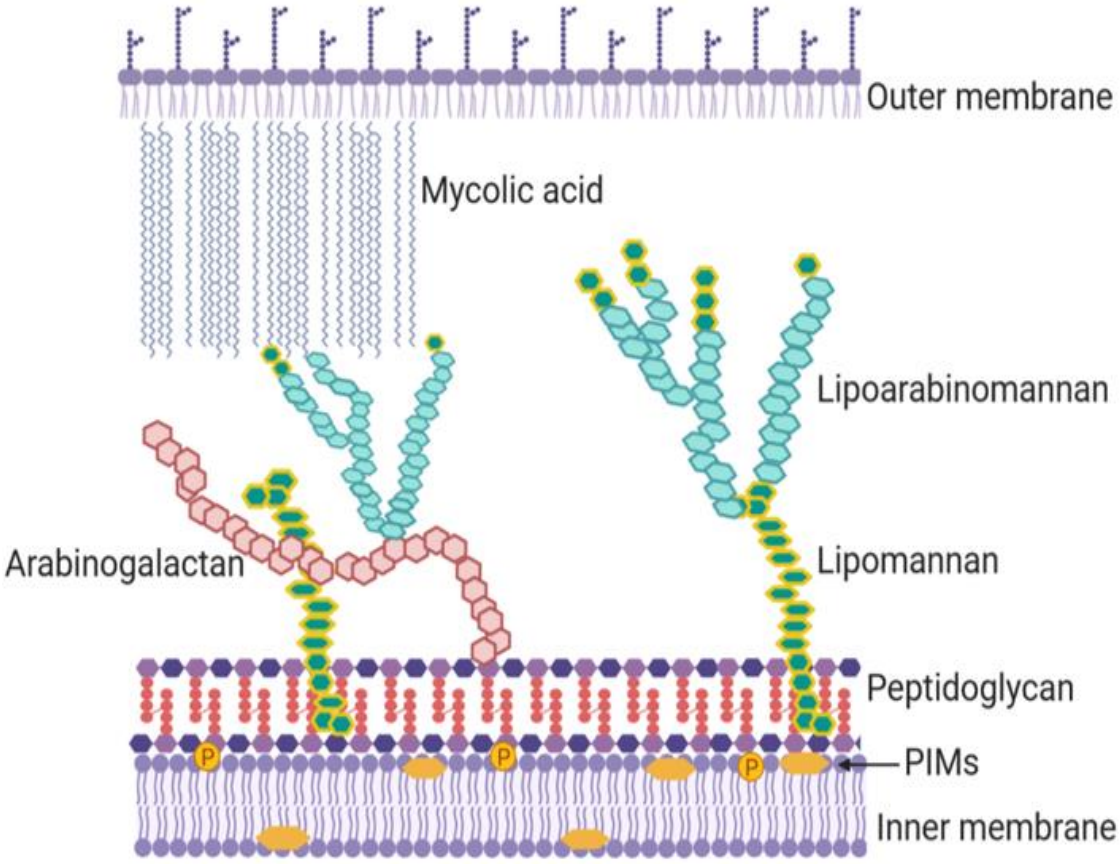

Figure 1.5. The structure of the Mycobacterium tuberculosis cell wall. This figure shows a schematic representation of the major components of the cell wall and their distributions. Figure created with BioRender.com. Adapted from: Vilchèze, C. Mycobacterial Cell Wall: A Source of Successful Targets for Old and New Drugs. Appl. Sci. **2020**, 10, 2278. doi.org/10.3390/app10072278

most abundant form being α -MA (>70%), and methoxy- and keto-MAs being minor components (10 to 15%)[43]. MA are synthesized in cytoplasm and transferred to the cell envelope *via* formation of trehalose monomycolate. The acids occur interlaced with trehalose- containing glycolipids and phthiocerol dimycoserates in the outer membrane of MTB. The internal layers of the cell wall of MTB consist mostly of arabinogalactan and peptidoglycans, as well as phosphalidyl-*myo*-inositol mannosides (PIMs), such as lipoarabinomannan (LAM) and lipomannan (LM) (**Figure1.5**)[29]. Many of these components provide vital functions for the cell, such as the polysaccharide, peptidoglycan, which provides rigidity, integrity, and shape to the cell[44]. The tensile strength and stability is achieved by interlaced pattern of peptidoglycan, which consists of alternating N-acetylglucosamine and muramic acid residues which are linked by β (1→4) bonds[45]. The molecule may also be anchored to an arabinogalactan complex via N-glycosylated- muramic acid residues[46]. Linear galactan and highly branched arabinans form the arabinogalactan, where arabinan anchors the mycolic acid forming the mycolyl-arabinogalactan-peptidoglycan (mAGP) complex. As mentioned earlier, the mycobacterial phospholipids are derivatives of phosphatidic acid and include phosphatidylglycerol, diphosphatidylglycerol, phosphatidylethanolamine and PIMs. These PIMs constitute major components of plasma membrane, and form the lipid base of LAM and LM[30]. Mannosylated- LAM (Man- LAM), LM, and PIMs all share a conserved mannosyl- phosphatidyl-*myo*-inositol (MPI) domain that likely secures the structures into the plasma membrane[47]. LAM is a critical virulence factor and plays an important role in host pathogenesis which makes it an ideal candidate for early diagnostics and

therapeutics, and is a major focus of this dissertation – hence discussed below in some detail.

1.4.2 Lipoarabinomannan

LAM is a critical cell wall lipoglycan originally isolated from a human infected with MTB in 1939[48–50]. Present day understanding of LAM structure comes from the pioneering work by Hunter, Chatterjee, Brennan and coworkers[51,52] that, together with others identified the antigen as an amphipathic molecule released from metabolically active or degrading bacterial cells[53]. This lipoglycan is comprised of three primary domains, including a glycophosphatidyl anchor and D-mannan with a D-arabinan core. The size and branching pattern of arabinan and mannan vary by strain, and differently modulate human immune response. Depending on the capping motif, LAM can be classified into 3 types: a) Man-LAM is comprised of mannosyl caps, and is associated with slow growing mycobacteria such as MTB, *M. leprae*, *M. bovis*. b) Phosphoinositol- capped LAM (PILAM) is characterized by the absence of a manno-oligosaccharide cap, and is found in non-pathogenic species such as *M. smegmatis.* c) AraLAM has an arabinan cap devoid of both mannose or phosphoinositol, and is found in *M. chelonae*[52,54]. The degree of mannose capping in ManLAM varies among different MTB strains, with 70% capping observed among the most virulent ones[52]. MTB H37Rv and *M. bovis* BCG both are known to have seven caps per molecule[55].

Despite much research, little is known about the orientation of LAM in the cell wall. Chatterjee and Khoo[48] described three possible hypotheses in 1997 (1) LAM is attached through lipids to the cell wall plasma membrane and the arabinose or mannose capped

arabinose units are exposed outside, (2) LAM is integrated by its PI-anchor into the external leaflet of a suggested outer-membrane analogue in mycobacteria, (3) LAM is a secreted molecule which has no permanent position in the cell wall. In 2012, Mukundan et al.[56] described three possible spatial models for LAM on a lipid bilayer: (1) LAM in a vertical orientation with its lipidic potion inserted into the membrane, (2) a flat position laying on top of the membrane, (3) and lying on its edge. Even in present day, it is clear that more studies are required in order to fully elucidate the structure and orientation of LAM in association with MTB and lipid architectures as LAM plays an important role in MTB pathogenesis. According to the first three-dimensional model of ManLAM, described by Mukundan et al., LAM is 14 nm long, and consists of 2139 atoms with a molecular weight around 16,100 Da[56]. Detailed understanding of LAM structure, presentation and orientation in cell wall, interaction with key molecules and how it plays a role in disease pathogenesis are key factors to develop much needed diagnostics and therapeutics for MTB.

Role of ManLAM in host pathogenesis: LAM is an important virulence factor released by MTB during active infection, and is recognized by innate immune system *via* pattern recognition receptors such as Toll like Receptor 2 (TLR-2). Beyond LAM, TLR-2 is activated by a large variety of conserved microbial components such as lipoproteins, lipoteichoic acid from gram positive bacteria and peptidoglycan[57]. The receptor can exist as heterodimer with either TLR1 or TLR6 which have been shown to discriminate between acylation states of lipoproteins[58–60]. TLR2/1 complex preferentially recognizes triacylated lipoproteins whereas TLR2/6 preferentially recognizes diacylated lipoproteins[57,58]. In any case, the interaction of LAM with TLR2 stimulates cytokine and chemokine signaling in

host macrophages. More details of the association of LAM with lipoproteins and the impact of presentation on the resultant stimulation of cytokines/chemokines is discussed in chapter 9.

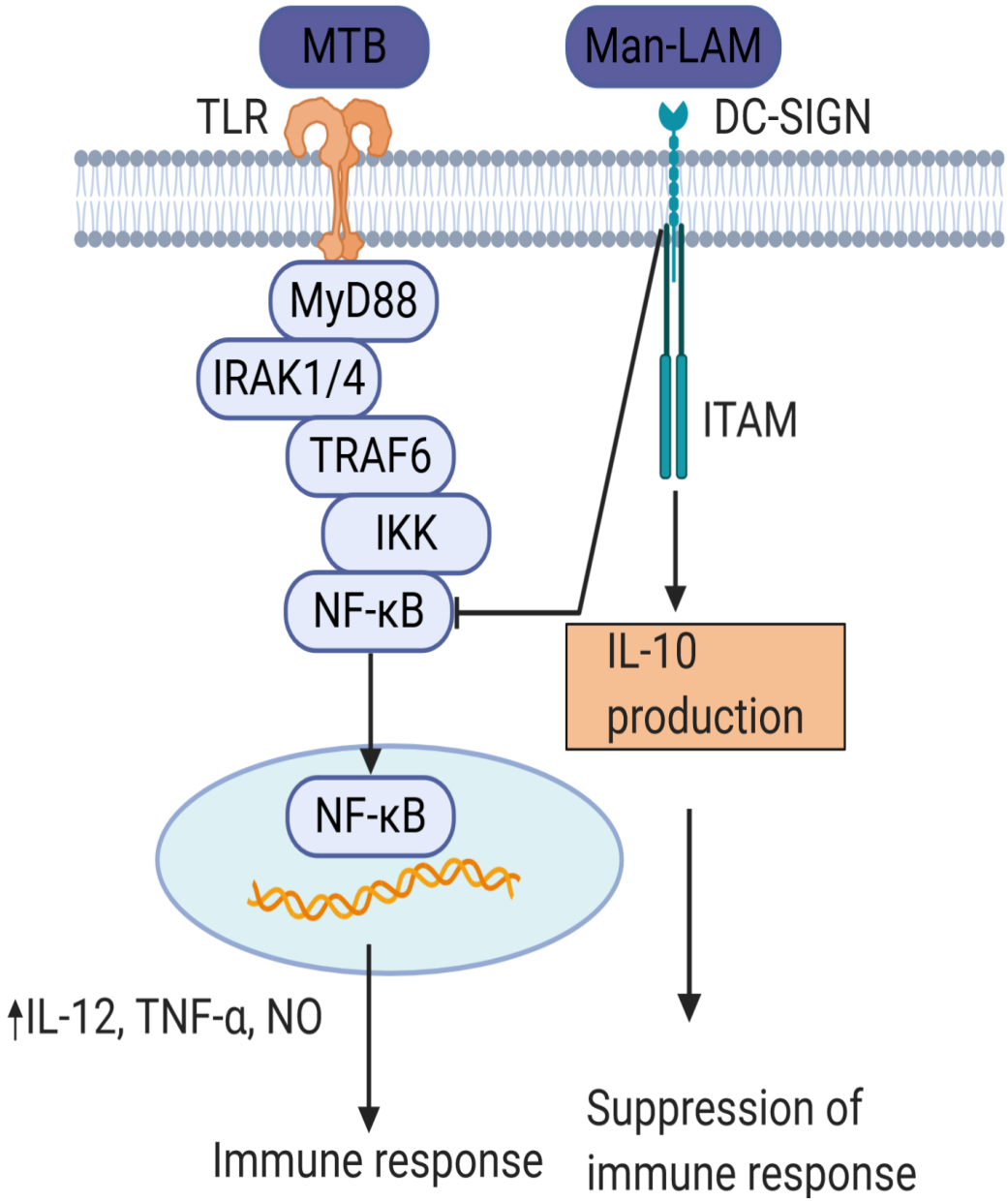

Figure 1.7. Disruption of MTB- TLR signaling pathway. Created with BioRender.com. Adapted from Koul et al. (2004), Interplay between mycobacteria and host signaling pathways. Nat. Rev. Microbiol.; doi:10.1038/nrmicro840. Abbreviations: MTB- Mycobacterium tuberculosis, TLR- Toll- like receptor, DC-SIGN- Dendritic cell- specific intracellular adhesion molecule-grabbing non-integrin, ITAM- tyrosine- containing activation motif, IRAK- interlukin-1 receptor-associated kinase, TRAF-6- TNF- receptor-associated factor 6, IKK- inhibitor of κB kinase.

ManLAM also alters the host apoptotic pathways by inhibiting increase in cytosolic Ca^{2+} concentration[61]. Ca^{2+} ions can promote apoptosis by increasing the permeability of mitochondrial membranes, stimulating the release of pro-apoptotic elements[62–64] . This is one of the ways by which ManLAM helps MTB in immune evasion.

Another MTB-Man LAM immune evasion strategy is by modulation of DC-SIGN (Dendritic cell- specific intracellular adhesion molecule- grabbing non- integrin) signaling pathway. DC-SIGN is a C-type lectin receptor found on surface of macrophages and dendritic cells. When MTB enters the host, it binds to TLRs and results in activation of NF-κB (**Figure 1.8**) through MyD88 signaling pathway leading to production of immunostimulatory cytokines that activate T cells and mediate killing of MTB [65]. However, in case of suppressed immune system in the host, Man-LAM binds to DC-SIGN and inhibits TLR signaling. This blocks the maturation of macrophages and dendritic cells that are attracted to the site of infection which causes suppressed T-cell activation and prevents appropriate immune response[66].

In conclusion, MTB is well adapted to the hostile environment of macrophages and other immune cells and uses various strategies for survival within host immune cells. Though our understanding of host-pathogen interaction is still incomplete, it is known that MTB disrupts host signaling machinery for intracellular survival. Further studies in the field of omics including proteomics, transcriptomics, lipidomics and metabolomics are needed to elucidate the exact mechanism by which MTB downregulates various signaling pathways. In addition, further understanding of the association of amphiphilic LAM with lipoproteins and its impact on immune signaling will provide insight into new improved diagnostic as well as therapeutic targets.

1.4.3 Diagnostics

The challenges associated with diagnosis of TB have been discussed in detail in **chapter 3 and 4** of this manuscript. Table 1.1 provides a brief summary descriptive of the various methods for the diagnosis of TB, which are currently endorsed by the WHO. There is a critical need for non-sputum based diagnostic tests for TB, especially those that can be used at the point of need, quickly and easily[67]. In this context, the detection of biomarkers such as LAM has garnered great attraction as a target for diagnostics development.[48,68–70]. Detection of LAM in several clinical matrices such as urine, sputum and serum has been evaluated, and several platforms have been developed to detect the biomarker (**Table 1.2**). However, the sensitivity and specificity of LAM tests developed so far does not meet WHO criteria for point of care diagnostic.

So far, urine remains the most evaluated matrix for LAM assay development and use. Yet, with disseminated and paucibacillary disease, and in individuals with HIV co-infection, blood may be a more reliable sample for LAM detection. The detection of LAM in blood, however, has been a challenge – and this difficulty is likely associated with the amphiphilic biochemistry of the molecule. ManLAM in aqueous solution has been shown to self-aggregate to form homogenous, regular spherical structures of around 30 nm and 200 nm of which 30 nm constitutes >99.5% of mass. This supramolecular organization has been attributed to hydrophobic interactions between acyl components of the molecule. More detailed understanding of LAM supramolecular structure comes from various biophysical approaches used by Riviere and colleagues, who estimated that there are about 452 ManLAM molecules per micelle[71]. These properties impact the orientation

Table1.1. TB diagnostic tests in use and endorsed by WHO

Method	Products	Intended and/or typical use	Main strengths	Main weaknesses
Smear microscopy for acid- fast bacilli	Light and light-emitting diode microscopy	Rapid point of care test for diagnosis and treatment monitoring	Requires moderate training, minimal infrastructure, minimal equipment	Low sensitivity, requires adequate sputum sample
Culture on solid and liquid media	Commercial liquid culture systems and rapid speciation Culture- based phenotypic DST using 1% critical proportion in LJ, 7H10, 7H11 and MGIT media	TB case detection and as prerequisite to drug susceptibility testing	Good sensitivity, liquid culture has better sensitivity than solid media	Slow time to growth (results take 6-8 weeks), higher contamination rate in some settings
Chest radiograph	N/A	Pulmonary TB case detection	Indications and use not restricted to TB	Low sensitivity and specificity, requires trained interpreter
Tuberculin skin test	Many commercialized reagents	Detection of MTB	Extensive practical and published experience	Sensitivity decreases with increasing immunocompromised; cross reaction with BCG vaccine
Interferon-γ release assays	T.SPOT.TB, Oxford Immunotec, UK QuantiFERON-TB gold plus, Qiagen, USA	Detection of MTB	Highly specific for MTB	Requires moderate training and equipment, imperfect sensitivity especially for immunocompromised persons
Molecular detection of TB and drug resistance (nucleic acid amplification test)	1.Xpert MTB/RIF and Xpert Ultra, Cepheid, USA 2.Line probe assays, Hain Lifescience, Germany and Nipro, Japan 3.Line probe assays, Hain Lifescience, Germany 4.TB LAMP, Eiken, Japan 5.Truenat MTB, MTB Plus and MTB-RIF Dx assays, Molbio Diagnostics, India	TB case detection and drug susceptibility testing	Good sensitivity, highly specific for MTB, less time to results	Xpert ultra cartridges have short shelf life, sensitivity decreases in immunocompromised, requires expensive equipment, line probe assays have high contamination risk due to open tube format, requires sputum as sample
Biomarker based assays	Alere Determine TB-LAM	TB detection in HIV infected individuals	Easy to use sample, easy to read results, less time consuming	Low sensitivity in HIV negative individuals

and stability of LAM in aqueous blood as well. Indeed, our team has demonstrated that amphiphilic LAM associates with host carriers, including high- and low- density lipoproteins (HDL and LDL)). HDL and LDL are composed of a core nanodisc lipidated structure that associates with the lipid moieties of LAM from MTB[72]. However, the interaction of LAM with host lipoproteins interferes with traditional methods for detecting these bacterial biomarkers directly in patient blood[73].

Immunoassays designed to target proteins display limited sensitivity when applied to amphiphiles in aqueous blood[73] due to the aforementioned host-pathogen interactions that sequester the biomarker[56,72,74]. Our team developed two novel assay methodologies that account for the amphiphilicity of LAM to achieve their ultra-sensitive detection in serum (discussed in detail in **chapter 6)**. The first assay, termed **membrane insertion** utilizes the passive interaction between an amphiphilic LAM and a lipid bilayer to capture the biomarker directly on the biosensor surface for interrogation with a labeled antibody. The second assay, termed **lipoprotein capture** exploits the interaction between LAM and host carrier lipoproteins in blood and thus requires prior knowledge of PAMP-lipoprotein association. In this second approach, an antibody targeting the lipoprotein carrier is used to capture a host-biomarker complex to the biosensor surface followed by interrogation with a labeled antibody targeting the biomarker of interest. Lipoprotein capture has been validated for the detection of LAM from MTB in patient serum and discussed in chapter 6 of this manuscript[72].

Rest of this manuscript describes in detail the challenges associated with diagnostics, evaluation and validation of lipoprotein capture and membrane insertion in

adults and pediatric population, in vitro THP-1 cell studies to understand the impact of LAM- lipoprotein association on immune signaling and future directions.

Table1.2. Review of studies using different biomarkers and methods for detection of TB

Sample Type	Biomarker(s)	Index test type	Sensitivity % (95% CI)	Specificity% (95% CI)	Reference
Urine	LAM	ELISA & Lateral Flow Assay (LFA)	ELISA- HIV positive- 0 (0-14.3) HIV negative- 3 (0.4-10.5) LFA: HIV positive- 65.2 (42.7-83.6) HIV negative- 42.4 (30.3-55.2)	ELISA- HIV positive- 95.2 (88.1-98.7) HIV negative- 95.9 (93.3-97.7) LFA: HIV positive- 56.6 (45.3-67.5) HIV negative- 61.7 (56.5-66.7)	[75]
Urine	LAM	ELISA & LFA	ELISA- HIV positive- 70 (35-93) HIV negative- 13 (0-53) LFA: HIV positive- 50 (19-81) HIV negative- 0 (0-37)	ELISA, LFA- 97 (85-100)	[76]
Urine	LAM	ELISA	Compared to microbiology/clinical- 83 Compared to microbiology- 33	Compared to microbiology/clinical- 85 Compared to microbiology- 60	[77]
Urine	LAM	LFA	43 (10-82)	91 (84-95)	[78]
Urine	LAM	FujiLAM, Alere Determine LAM, electochemiluminescence (EcILAM)	AlereLAM- 11 (6-18) FujiLAM- 53 (44-62) EclLAM- 67 (57-75)	AlereLAM- 92 (88-95) FujiLAM- 99 (97-100) EclLAM- 98 (96-99)	[79]
Urine	LAM	One- sided immunoassay	90	73.50	[80]
Urine	LAM	Immunomacroarray assay (Nanocage with a copper complex dye)	95	80	[81]
Urine	LAM	Determine TB LAM	23 (17-29)	93 (90-96)	[82]
Urine, Serum	LAM, ESAT6	Electochemiluminescence (EcILAM) assay	Urine- LAM- 93, ESAT-6- 65 Serum- LAM- 55, ESAT-6- 46	97	[83]
Urine	LAM	EcILAM assay	93 (80-97)	97 (85-100)	[84]

Sample Type	Biomarker(s)	Index test type	Sensitivity % (95% CI)	Specificity% (95% CI)	Reference
Urine	LAM	Magentic immunoassay	82	100	[85]
Urine	LAM	Determine TB LAM	12-45	80-100	[86]
Serum	LAM	Surface enhanced Raman scattering based immunoassay	87.50	100	[87]
Urine, Serum	LAM	ELISA	Serum- 33 (68-100) Urine- 40 (16-68)	92 (64-100)	[88]
Urine	LAM	Clearview TB ELISA	59 (52-66)	96 (91-99)	[89]
Urine	LAM	ELISA	51	88	[90]
Urine	LAM	Determine TB LAM	66 (57-74)	66 (57-74)	[91]
Urine, Sputum	LAM	Clearview TB ELISA	Urine- 6-21 Sputum- 86	Urine- 95-100 Sputum- 15	[92]
Sputum	LAM	ELISA	91	100	[93]
Urine	LAM	ELISA	93 (68-100)	95 (83-99)	[94]
Urine	LAM	Chemogen LAM ELISA	80	99	[95]
Urine	LAM	Single molecule fluoroscence assay	95	100	[96]
Urine	LAM	Chemogen LAM ELISA	44 (36-52)	89 (81-94)	[97]
Urine	LAM	Chemogen LAM ELISA	38	100	[98]
Urine	LAM	Clearview TB ELISA	46 (40-51)	89 (86-91)	[99]
Urine	LAM	Determine TB LAM	Overall-37 HIV positive-60	98	[100]
Urine	LAM	Clearview TB ELISA	15-70	NR	[101]
Urine	LAM	ELISA	74	89	[102]
Urine	LAM	LAM Strip test	56-64	95-98	[103]
Urine	LAM	Determine TB LAM	82	NR	[104]
Urine	LAM	Chemogen LAM ELISA	6-20	83-89	[105]
Sputum	MPT64	ELISA	86.9 (79-92)	92 (90-94)	[106]
PBMCs	IL-2	ELISPOT	100	81	[25]
Whole blood	ESAT-6, CFP-10	ELISA	85 (75-96)	60 (40-80)	[107]
PBMCs	Antibody in lymphocyte secreting assay	ELISA	91	87	[108]

Sample Type	Biomarker(s)	Index test type	Sensitivity % (95% CI)	Specificity% (95% CI)	Reference
Whole blood	51-gene mRNA signature	Microarray	**Validation cohort-** 82.9 (68.6–94.3) **IGRA**- 60.0 (33.3-86.67) **Xpert MTB/RIF assay**- 54.3 (37.1- 68.6)	**Validation cohort-** 83.6(74.6–92.7) **IGRA**- 83.3 (72.2-92.6) **Xpert MTB/RIF assay**- 100 (100- 100)	[109]
PBMCs	*MTB*-specific CD4+ CD27+ T-cells	ICS/Flow cytometry	83 (59– 96)	97(89–99)	[110]
Plasma	Cytokines	Milliplex human cytokine/chemokine kits with analyses conducted on a Luminex 200 analyzer	**ESAT-6** (IFN-γ- 90.9, IP-10- 95.5, TNF-α- 95.5, IL-1ra- 81.8, IL-2- 95.5, IL-13- 77.3, MIP-1β- 90.9) **CFP-10** (IFN-γ- 81.8, IP-10- 86.4, TNF-α- 86.4, IL-1ra- 77.3, IL-2- 90.9, IL-13- 63.6, MIP-1β- 77.3) **PPD** (IFN-γ- 95.5, IP-10- 95.5, TNF-α- 95.5, IL-1ra- 50, IL-2- 100, IL-13- 77.3, MIP-1β- 81.8)	**ESAT-6** (IFN-γ- 97.3, IP-10- 96.0, TNF-α- 88.0, IL-1ra- 69.3, IL-2- 97.3, IL-13- 89.3, MIP-1β- 70.7) **CFP-10** (IFN-γ- 89.3, IP-10- 93.3, TNF-α- 85.3, IL-1ra- 78.7, IL-2- 94.7, IL-13- 86.7, MIP-1β- 68) **PPD** (IFN-γ- 97.3, IP-10- 81.3, TNF-α- 84.0, IL-1ra- 46.7, IL-2- 96.0, IL-13- 69.3, MIP-1β- 60.0)	[111]
Whole blood	71 genes	ribonucleic acid sequencing	Diagnostic gene list comparison to published gene list for pediatric dataset -38-100, Treatment response- 70-80	Diagnostic gene list comparison to published gene list for pediatric dataset - 48- 93, Treatment response- 40-80	[112]
Whole blood	3 genes (GBP5, DUSP3, and KLF2)	Studies with microarray-based whole genome expression profiles	TB vs healthy- 93 Latent TB- 88 Other diseases- 82	TB vs healthy- 97 Latent TB- 85 Other diseases- 79	[113]

Sample Type	Biomarker(s)	Index test type	Sensitivity % (95% CI)	Specificity% (95% CI)	Reference
Whole blood	116 gene signature set	Microarray	TB vs Latent TB- ACOT7- 67, AMPH- 56, CHRM2- 56, GLDC- 67, HBD- 67, PIGC- 55, S100P- 89, SNX17- 56, STYXL1- 56, TAS2R46- 67	TB vs Latent TB- ACOT7- 86, AMPH- 52, CHRM2- 62, GLDC- 79, HBD- 93, PIGC- 76, S100P- 76, SNX17- 65, STYXL1- 65, TAS2R46- 72 TB vs healthy- ACOT7- 76, AMPH- 76, CHRM2- 46, GLDC- 73, HBD- 78, PIGC- 89, S100P- 35, SNX17- 86, STYXL1- 30, TAS2R46- 84	[114]
PBMCs isolated from whole blood	CRP, Ferritin, Mycobacterial antibody secreting cell assay (MASC)	ELISA	MASC-78, Ferritin- 89, CRP- 67	MASC-86, Ferritin- 75, CRP-83	[115]
Whole blood	12 host markers	Luminex platform	IFN-a2- 89.5 (66.9-98.7), IL-1Ra-26.3 (9.1-51.2), sCD40L- 42.1 (20.3-66.5), VEGF- 83.3 (58.6-96.4), MCP-3- 26.3 (9.1-51.2)	IFN-a2- 52.6 (39.0-66.0), IL-1Ra-98.2 (90.6-99.9), sCD40L- 93.0 (83.0-98.0), VEGF- 61.4 (47.6-74.0), MCP-3- 98.3 (90.6-99.9)	[116]
Whole blood	Interferon gamma inducible protein 10 (IP-10)	ELISA	NR	NR	[117]
Whole blood	IP-10	ELISA	QFN-G-IT and T-SPOT.TB- 91.7, IP-10- 66.7	NR	[118]
Whole blood	IP-10	Microsphere based assay on luminex platform	NR	NR	[119]

Sample Type	Biomarker(s)	Index test type	Sensitivity % (95% CI)	Specificity% (95% CI)	Reference
Whole blood	18 cytokines	Cytometric bead array- T helper 13-plex assay and a custom 5-plex assay (LEGENDplexTM, BioLegend) and analysed using a 2-laser flow cytometer (FAC- SCaliburTM, Becton Dickinson).	NR	NR	[120]
Peripheral blood	21 cytokines	Milliplexe Human 10 Cytokine Kit (Millipore, Billerica, MA, USA). phycoerythrin fluorescence measured using Bio-Plex 200 System	NR	NR	[121]
Whole blood	Cytokines	Bioplex Pro Human Cytokine Group 1 assay (Bio-Rad Laboratories, Hercules, CA, U.S.)	IFN-γ- 79 (66.1-88.6), IL-1ra- 80.7 (68.1-90), IL-2- 75.4 (62.2-85.9), IL-13- 80.7 (68.1-90), IP-10- 80.7 (68.1-90), MIP-1β- 70.2 (56.7-81.6), TNF-α- 30.9 (19.1-44.8), IL-2, IL-13, IP-10- 84.2 (72.1-92.5)	IFN-γ- 83.8 (76.5-89.6), IL-1ra- 68.4 (59.9-76.1), IL-2- 99.3 (96-100), IL-13- 93.4 (87.8-97), IP-10- 86 (79.1-91.4), MIP-1β- 67.7 (59.1- 75.4), TNF-α- 88.2 (81.6-93.1), IL-2, IL-13, IP-10- 82.4 (74.9-88.4)	[122]
Whole blood and urine	IP-10	ELISA	**HIV negative-** IP-10 blood- 79, IP-10 urine- 53, QFT-IT- 53, TST- 61 **HIV positive-** IP-10 blood- 100, IP-10 urine- 54, QFT-IT- 17, TST- 23	**HIV negative**- IP-10 blood- 53, IP-10 urine- 66, QFT-IT- 83, TST- 82 **HIV positive**- IP-10 blood- 17, IP-10 urine- 61, QFT-IT- 82, TST- 94	[123]
Whole blood	IFN-γ	ELISA	TST- 88.2 (79.4-94.2), QFT-IT - 89.6(79.7-95.7), T SPOT- 88.5 (80.4-94.1)	TST- 86.3 (83.9-88.6), QFT-IT - 95.4(93.8-96.6), T SPOT- 96.8 (94.2-98.5)	[124]

Sample Type	Biomarker(s)	Index test type	Sensitivity % (95% CI)	Specificity% (95% CI)	Reference
Whole blood	13 cytokines	Luminex or ELISA, Chemiluminiscence immunoassay for ferritin and 25 (OH)D	IP-10, IFN-γ, ferritin, and 25(OH)D- 93.2	IP-10, IFN-γ, ferritin, and 25(OH)D- 90	125
Whole blood	198 genes	dual-color-Reverse-Transcriptase-Multiplex-Ligation-dependent-Probe-Amplification (dcRT-MLPA)	7 and 10 transcript signature- 91.7 (71.5-98.5)	7 transcript signature- 80.8 (60.0-92.7), 10 transcript signature- 88.5 (68.7-96.9)	126
Peripheral venous blood	Cytokines	Bio-Plex multiplex ELISA cytokine assay system, Luminex	NR	NR	127
Serum	Metabolic signatures	1H nuclear magnetic resonance (NMR) spectroscopy and mass spectrometry (MS)	1H NMR - 69 (56-73), MS-67 (60-71)	1H NMR - 83 (73-93), MS-86 (75-93)	128
Serum	119 antigens	Multiplex baed based luminex assay to meaasure IgG antibody	60	60	129
Plasma	17 plasma metabolites	1H NMR spectroscopy	L-valine, pyruvic acid and betaine Training set- 85.7 (66.4-95.3) Independent validation cohort- 82.4 (55.8-95.3)	L-valine, pyruvic acid and betaine Training set- 94.6 (80.5-99.1) Independent validation cohort- 83.9 (65.5-93.9)	130
Peripheral blood	Transcriptional and translational biomarkers	Dual colour Reverse Transcriptase-Multiplex Ligationdependent Probe Amplification	NR	NR	131
Whole blood	45 genes and 10 cytokines	Dual-color Reverse-Transcriptase Multiple Ligation-dependent Probe-Amplification and bioplex assay for cytokines	NR	NR	132
Whole blood	29 miRNA	Microarray, RT-PCR	TB vs Healthy - 95.8	TB vs Healthy - 100	133
Plasma	20 circulating immune markers	Multiplex ELISA using Luminex	NR	NR	134

Chapter 2.

Goals and Overview of this Work

TB affected 10 million people in 2019, with nearly 1.4 million deaths[3], a statistic that can be greatly controlled if reliable diagnostics and therapeutics were available. The current gold standard for TB diagnosis is microbiological culture, which can take up to 6-8 weeks to result, and therefore, not conducive to timely treatment[135]. Several additional diagnostics have been approved for use in adults, as discussed in Section diagnostics, chapter 1 of this manuscript. Co-morbidities such as HIV not only influence the likelihood of presenting with active disease, but also the outcome of the diagnostic results. [136].

Current diagnostic assays for TB largely use sputum as the sample of choice, making them ineffective in individuals with extra-pulmonary and disseminated forms of the disease. Biomarker assessments use urine samples, but the poor sensitivity of these assays limits their use only to certain subsets of infected individuals. Thus, there is a clear need for better diagnostic tests for TB. Many a time, a combination of these diagnostics is required for confirmation of disease, which is a challenge with respect to implementing countermeasures in a timely manner.

This challenge is especially grave in in pediatric populations where the manifestation of the disease can be very different than in adults as discussed in chapter 3 of this manuscript in detail[137]. Children can manifest extra-pulmonary and disseminated forms of the disease. In addition, the disease is often paucibacillary in children, which makes extrapolation of culture and microscopic outcomes unreliable.

Based on complex presentation of the disease and current diagnostic tests, the WHO has identified the need for a non-sputum, biomarker- based diagnostic test for TB[67]. Direct detection of these pathogen biomarkers in infected patients can allow for a rapid, sensitive and reliable method of diagnosis for TB, and is a concept that has been studied by our group and other investigators[94,138–140]. LAM is one such biomarker that has garnered lot of attention recently and use of this antigen as a biomarker and its biochemistry and molecular biology has been discussed in chapter 1. LAM detection in urine has been studied by many researchers , but has shown consistently poor sensitivity in HIV negative individuals[139,141,142]. The detection of LAM in blood, however, has been a challenge – and this difficulty is likely associated with the amphiphilic biochemistry of the molecule. Yet, with disseminated and paucibacillary disease, and in individuals with HIV co-infection, blood may be a more reliable sample for LAM detection. ***The guiding hypothesis of this work is that the sequestration of LAM in immune complexes/lipoprotein carriers is responsible for the difficulty in detection of the amphiphilic antigen in blood, and also impacts immune induction in patients.*** To test this hypothesis, the following three specific aims were investigated (**Figure 2.1**).

Aim 1. Detection of LAM in serum using the Lipoprotein Capture and Membrane Insertion Assay, with subsequent validation in adult TB patient samples.

Aim 2. Validate feasibility of LAM in serum as a diagnostic biomarker for pediatric TB disease

Aim 3. Understand the impact of LAM interaction with lipoproteins such as HDL/LDL on TLR2-mediated cytokine production

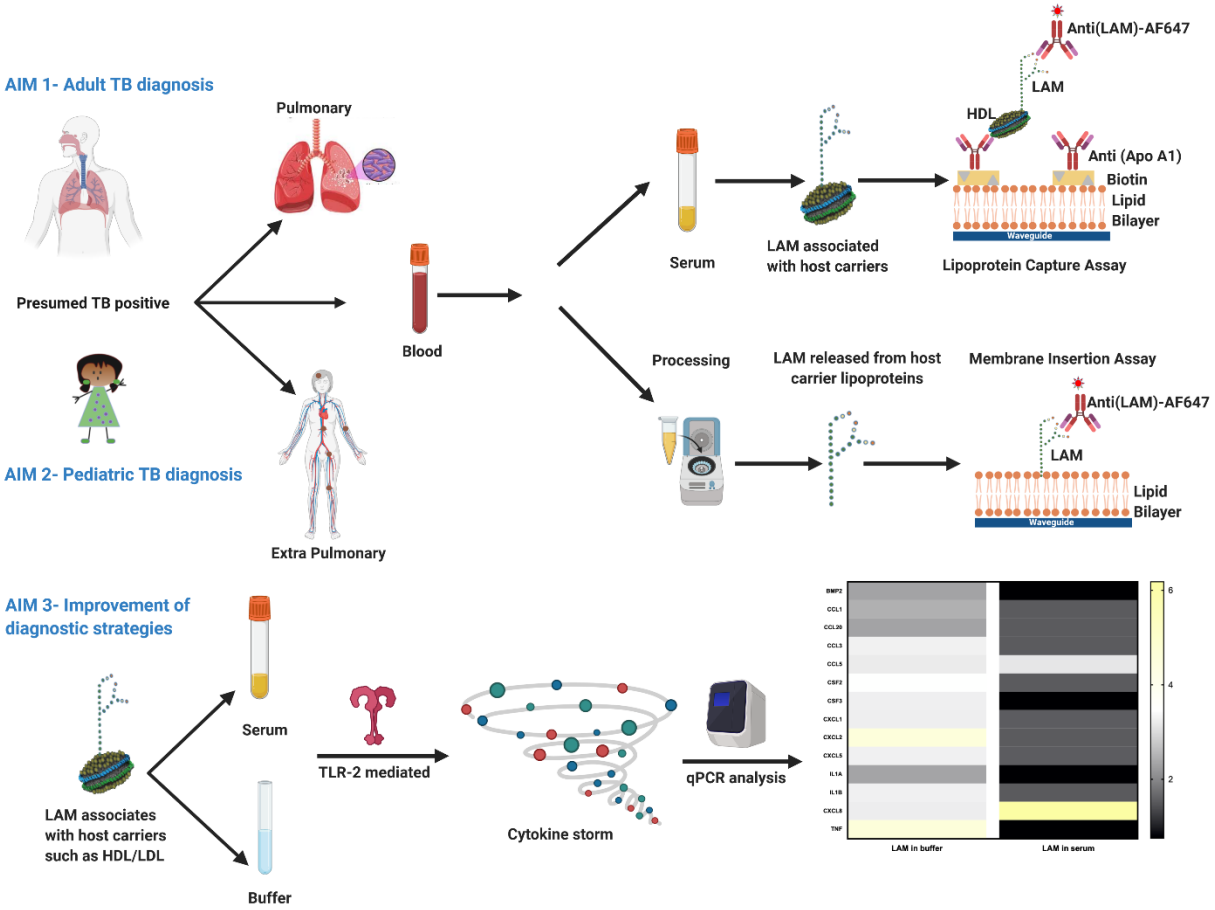

The primary goal of this work was to develop and integrate a blood-based assay for detection of LAM in adult and pediatric TB patients. While a seemingly simple goal, the underlying complexities of the disease made this task quite challenging. The research conducted to test the hypothesis and investigate each aim is outlined as individual chapters throughout the manuscript and are summarized below.

The work presented in **Chapter 3**, was published as a book chapter in the book *Diagnosis and management of tuberculosis.* This work was researched by me as primary author, Kiersten Lenz and Harshini Mukundan. In this chapter, we reviewed the challenges associated with diagnosis of pediatric TB due to differential disease presentation in children, WHO goals for controlling pediatric TB, as well as current diagnostic tools

available to diagnose TB in children. We also described the addition of complexity to disease detection due to presence of HIV.

Chapter 4 reviews current technology used for diagnosis of TB, and presents the value of incorporating lipidomics, transcriptomics and proteomics approaches for disease diagnosis. The work was published in *International Journal of Molecular Sciences.* The chapter was researched by me as primary author, Alexis A Bitzer, Loreen R. Stromberg and Harshini Mukundan. The chapter describes in detail genomics, transcriptomics, proteomics, lipidomics and metabolomics techniques including studies used to study biomarkers for diagnosis of TB – and expands on the value of a multi-omic approach towards developing comprehensive diagnostics that can address the spectrum of TB disease.

Chapter 5 describes the difficulties associated with detection and measurement of amphiphilic biomarkers, including LAM, and the various techniques and methods that are used to detect them. We address the significance of amphiphiles associated with the disease as well as their suitability for use as diagnostic target. This review was published in *Biosensors* with Jessica Z.Kubicek-Sutherland as first author. Dung M. Vu, Heather M. Mendez and I assisted with the review, under guidance of Harshini Mukundan. The use of varied detection approaches including mass spectrometry, NMR- based sensor, optical, mechanical and electrochemical biosensors for amphiphiles, are discussed in great detail. The waveguide based biosensor used for detection of LAM in this research work is also discussed.

Details, optimization and clinical validation of lipoprotein capture and membrane insertion assays are described in **chapter 6**, which is currently under review for publication in PLOS One. As the primary author of this manuscript, my role was to optimize the lipoprotein capture and membrane insertion assays for the detection of LAM in serum. I also performed the clinical validation of both assays in serum from adult TB patients from Uganda. The antibody characterization for lipoprotein capture was done by Ramamurthi Sakamuri using Enzyme linked immunosorbent assay (ELISA). The antibodies were generously provided by Emmanuel Moreau at the Foundation of Innovative New Diagnostics (FIND). Loreen R. Stromberg played a critical role in training me on biosensor platform used for this work. Priya Dighe and Dung M. Vu assisted with conducting initial assays. Lipoprotein capture and membrane insertion assays were developed by Harshini Mukundan and her team at LANL, including Basil Swanson who helped conceive the initial approach with her. The clinical study was in collaboration with Susan E. Dorman, then at Johns Hopkins University (recently transitioned to Medical University of South Carolina) who provided clinical specimens and her expertise in analyzing the work. Harshini Mukundan served as primary investigator, and helped with experimental design, insight, troubleshooting, data analysis and manuscript editing. Laura Lilley and Nicolas Hengartner assisted with the statistical analysis for amphiphile assays.

The purpose of this work was to explore feasibility of detection of LAM in patient serum using two tailored assays-lipoprotein capture and membrane insertion. All assays were performed on a waveguide based biosensor developed at Los Alamos National Laboratory. The assays targeted amphiphilic LAM associated with carrier moieties, or liberated using a sample processing method. Using lipoprotein capture assay, we were

able to detect LAM in most of the clinical samples, and no LAM was detected in healthy controls. To further explore the reason for missed LAM detection in some clinical samples, we hypothesized that positive HIV status of patients might alter lipoprotein levels and thus LAM detection. Therefore, we measured lipoprotein levels in HIV positive and negative serum samples and found out that HIV positive patients have significantly less HDL concentrations compared to HIV negative. These findings showed that an assay strategy independent of lipoprotein levels might result in increased LAM detection Therefore, to evaluate serum LAM levels without dependence on host lipoprotein concentrations, we adapted sample processing method to liberate LAM from associated host lipoprotein assemblies followed by direct detection of the pathogen biomarker using the membrane insertion approach. The latter approach improved the sensitivity of LAM detection in serum, and improved the sensitivity of LAM detection by 10-fold. This study validated membrane insertion with sample processing method as a reliable method for detection of LAM in serum from TB patients. It also led to critical questions about further implications of LAM/host lipoprotein associations for diagnostic assay performance and TB pathogenesis.

The validation of membrane insertion assay for detection of LAM in serum from pediatric patients is presented in **Chapter 7**. After successfully detecting LAM in adults, as described in chapter 6, we asked the question if similar approach was feasible for diagnosis of TB in pediatric patients. The work is under preparation for publication. I performed all the clinical assays using membrane insertion method. The study was in collaboration with Dr. D.J. Perkins at the University of New Mexico, who provided serum samples from a clinical site in Siaya, Kenya. Harshini Mukundan is the principal

investigator, provided project design, supervision, experimental oversight and data interpretation.

In this study, we demonstrated the direct detection of LAM in pediatric serum for the first time ever using membrane insertion assay. The study validated membrane insertion as a reliable method for detection of LAM in serum from pediatric TB patients.

The work in **Chapter 7** describes functional assessment of microfluidic device allowing improved biomarker retention compared to benchtop method of sample processing. The manuscript is accepted for publication in *scientific reports*. The idea originated from work in chapter 5 where membrane insertion using sample processing proved to be more sensitive for the detection of LAM. Thus, we attempted to develop a strategy to easily and effectively perform the required sample processing at the point of need. Kiersten Lenz lead the development and design of microfluidic chip and is the primary author on this manuscript. As the second author on manuscript, I validated the device using membrane insertion to detect LAM. Jing Chen, Dylan Purcell, Omar Ishak assisted with device design. Harshini Mukundan was the principal investigator, and provided project vision, supervision, experimental oversight and data interpretation. Pulak Nath was the fabrication laboratory lead, and responsible for the the microfluidics work. Other authors were Aaron Anderson, Jessica Kubicek-Sutherland, Jennifer Harris, Leyla Akhadov helped with concept development, experimentation and manuscript review. The outcome of the study was that we were able to achieve excellent retention of LAM using the microfluidic chip compared to traditional benchtop methods. The device can be broadly used for separation of serum from blood at the point of need, and is compatible with both

hydrophilic and hydrophobic biomarkers secreted by other pathogens. Kiersten Lenz is working further on validation of the device for the extraction of lipids from blood.

The research described in chapters 6 and 7 led us to our final aim - to understand the impact of LAM interaction with lipoproteins on TLR-2 induced cytokine expression in order to refine and improve LAM detection strategies. The outcome of this work is discussed in **Chapter 9**, and a manuscript is under preparation. I developed the TLR-2 and knock-out cell system, and performed the majority of experiments. Dr. Jessica Kubicek Sutherland provided guidance on design of experiments, and trained me on the new techniques and instruments used for this work. Kiersten Lenz and Katja Klosterman are other authors on the manuscript who helped with experiments. Harshini Mukundan is the principal investigator who provided project direction, supervision, experimental oversight and data interpretation.

All the assays performed for detection of LAM in chapter 6 and 7 were done on a lipid bilayer system on the LANL waveguide biosensor platform. Although complex bilayers provide a more stable system and molecular insight into detection of amphiphiles, they do not signify the entire intricacy of cell membranes. Therefore, we studied LAM interaction with lipoproteins using human cell line under different physiological conditions. Our hypothesis was that cytokine expression due to LAM-lipoprotein interactions would be different based on the presentation of the amphiphile - in serum versus buffer. These outcomes cast further insight into the impact of amphiphile carrier associations on innate immunity, and define optimal conditions for performing physiologically relevant cell studies. Further studies will continue to explore the use of nanodisc (synthetic

lipoproteins) in cell-based system to sequester amphiphilic biomarkers and improve diagnostic and therapeutic strategies.

Though each chapter focuses on very specific aspect of this dissertation work, taken as a whole, it represents a comprehensive approach to developing and optimizing blood-based strategies for detection of LAM, faciliatating improved TB diagnosis. We present a vigilant optimization and validation of lipoprotein capture and membrane insertion assays in serum from adult and pediatric TB patients. The assays are platform and antigen ambivalent, and can be easily transitioned to other detection platforms and for diagnosis of other infectious and non-infectious pathogens that secrete amphiphilic biomarkers. The work is concluded with future directions at the end **(Chapter 10)**.

Chapter 3.

Current Status of Pediatric Tuberculosis Diagnostics, Needs, and Challenges

Shailja Jakhar[1], Kiersten Lenz[1], Harshini Mukundan[1,2]

1: MSJ567, Physical Chemistry and Applied Spectroscopy, Chemistry Division, Los Alamos National Laboratory, Los Alamos, New Mexico 87545

2: To whom correspondence is addressed, harshini@lanl.gov

3.1 Overview and statement of problem

Tuberculosis (TB) is a chronic bacterial disease caused by *Mycobacterium tuberculosis* (Mtb). About one third of the world's population is infected with Mtb, of which only 5-10% develop clinical symptoms and progress to an active disease state. The rest of the population are carriers of the disease, a condition referred to as latent TB infection (LTBI). The transition from latent carriers to active disease can be influenced by many factors such as HIV co-infection, age, co-morbidities such as malaria and other factors, and poses a problem for reliable diagnosis of TB[20].

TB is a major public health concern in all age groups, but presents a bigger challenge in pediatric populations, primarily owing to the lack of reliable diagnostics. Young children (<3-4 years of age) are most commonly exposed to Mtb infection from adults in the family. Some of the factors that increase risk of exposure are age, physical structure of the child's house, and sleeping practices. The chance of infection differs with age: there is a 20-30% risk in children aged 1-2 years, 5% risk in children aged 3-5 years, 2% risk among children 5-10 years, and 5% risk among children older than 10 years.[143] The burden of TB is much higher in developing countries due to various factors including poverty, malnutrition, HIV, HIV-TB co-infection, and increased drug resistance. TB reporting gaps are the most profound among younger children, as 55% of children estimated to have the disease are not reported to national monitoring and surveillance programs, as compared to a rate of 35% in adults. This reporting disparity amongst children varies with age: 69% of cases are unreported in children younger than 5 years of age, and 40% of cases are unreported in children 5-14 years[19]. Because of

the disease progression and risks to children, more focus needs to be placed on understanding, diagnosing, and treating pediatric TB.

There are three major challenges associated with presentation of TB disease in pediatrics, which complicate diagnostics and therapeutic intervention:

1. Pediatric TB is paucibacillary – i.e. clinical samples and isolates from infected children contain few bacteria, making culture and isolation of the causative agent challenging[27]. For this reason, pediatric TB is considered a minor contributor to the spread of infection in a population. However, young children have a high risk of disease progression following infection, and are more likely to develop severe or disseminated disease. Indeed, in some of the higher burden regions, children account for more than 20% of TB cases[144].

2. Pediatric TB is also often disseminated. As with adults, disseminated TB is much more difficult to treat and control, because of the uncharacteristic presentation and unclear treatment regimens. This same challenge also extends to children presenting with drug-resistant forms of the disease, because the dosage and regimens for treatment in children have not been well established. Dodd *et al*. reported that of the estimated 850,000 children diagnosed with TB in 2014, about 7% were isoniazid resistant, 3% were multidrug resistant (MDR), and 4.7% of MDR cases were extreme drug resistant (XDR). It has been demonstrated that more children are infected with drug resistant TB than are actually diagnosed[145]. Thus, drug resistant TB presents an significant challenge in children, especially those living in the vicinity of adults with similar variants of the pathogen, because it is difficult to diagnose, track, and treat in this population.

3. TB can manifest itself in pulmonary and extra pulmonary forms, of which extra pulmonary TB (EPTB) is more difficult to diagnose, especially in pediatric populations. Pulmonary TB (PTB) commonly presents as a cough that lasts greater than 4 weeks, dyspnea, asthenia, chest pain, hemoptysis, persistent evening fever, night sweats, and weight loss. In children, these symptoms can be easily mistaken for infections associated with other respiratory, and present with similar clinical and radiological findings, making it more difficult to diagnose the disease in this population. EPTB presents an even greater challenge. The disease can be disseminated, or it can present in the genitourinary, gastrointestinal, cerebral, lymphatic, or skeletal systems[25].

Together, these factors complicate our ability to identify and control pediatric TB. The goal of this chapter is to summarize the problems, challenges, promising future avenues, and future needs for combating the problem of pediatric tuberculosis, with specific emphasis on diagnosis of the condition.

3.2 Challenges

The inability to diagnose TB poses the biggest challenge to management of the disease in children. Early symptoms of TB are very similar to other childhood diseases, including viral and bacterial infections, pneumonia, and other respiratory diseases. As mentioned earlier, TB presents in paucibacillary form in children[146]. Sputum culture, which is the gold standard diagnostic for adults, remains negative in ~70% of pediatric cases because of the low bacterial load in this population[144]. This problem is further confounded by the fact that many children present with disseminated disease, thereby producing no sputum. And even in those with pulmonary disease, young children are

unable to expectorate sputum, making it a difficult approach for reliable diagnosis in this population. These factors and the differential pathology of the disease impact diagnosis by traditional culture-based methods, sputum microscopy, and newer approaches such as Gene Xpert based detection. Indeed, the percentage of children with active TB that were missed by confirmatory tests are 40% missed by culture, 50% by gene Xpert, and 77% by microscopy[147]. Therefore, the diagnosis of childhood TB is currently based on history, clinical symptoms, the Tuberculin skin test (TST), and chest radiography[26], each of which is associated with high rate of failure and unreliability. The consequent alarming percentage of missed diagnoses points to an urgent need for a rapid and sensitive point-of-care diagnostic for tuberculosis in children.

3.3 WHO goals for pediatric TB (2018)

Throughout the world, TB remains the leading cause of pediatric mortality from a single infectious agent. In 2017, 1 million children younger than 15 years of age (10% of total TB cases) developed TB, of which 52% were less than 5 years of age. 80% of TB-related pediatric deaths were among children 5 years old or younger, and 17% of those were co-infected with HIV. 15% (233,000) of the pediatric TB-related deaths were among children that had poor access to diagnosis and treatment. There were about 150-400 cases per 100,000 people in high-burden, low income countries, as compared to only about 10 cases per 100,000 in high income countries. This disparity highlights the need to increase access to proper diagnosis and treatment in low income regions, which would help prevent many of the TB-related deaths in children. Because of these reasons, the World Health Organization (WHO) is on a mission to reduce the absolute

number of TB deaths by 90% and incidence rate by 80% by the year 2030 (as compared to 2015)[148].

The WHO report clearly identifies the need for an effective diagnostic in pediatric populations in order to achieve this goal. According to the WHO, successful diagnosis and treatment of TB can prevent millions of deaths each year. In order to develop a successful diagnostic, understanding the reasons for under-diagnosis are critical. Today, under-diagnosis of TB in pediatric and adult populations can be due to various factors such as poor access to healthcare, lack of symptoms, healthcare providers failing to test for TB, in addition to the poor sensitivity and specificity of the diagnostic itself. These factors are all compounded in pediatric populations owing to the differential presentation of the disease. Further, most of the gaps in detection and treatment were observed in African regions, where HIV-TB coinfection rate is significantly high, and in resource-poor regions of the world (e.g., parts of India and China)[149]. To close the gap between detection and treatment, a new WHO initiative called "Find. Treat. All." was established in 2018. The goal of this initiative is to detect and treat 40 million people, including 3.5 million children, from 2018-2022. Such initiatives and the WHO report establish the clear need for new and effective diagnostics for pediatric TB.

3.4 Current TB diagnostic tools

Approaches to diagnose Mtb infection can be broadly divided into two categories:

1. Detection of the human immune response to Mtb infection (e.g.; detection of antibodies and activated T cells); and

2. Direct detection of Mtb and Mtb Signatures (e.g.; microscopy, culture, antigen and nucleic acid detection assays)

   Several diagnostics have been developed under each of these categories for the diagnosis of TB infection, and many have been adapted or evaluated in pediatric populations. A complete review of all of them is beyond the scope of this chapter. Thus, we will primarily focus on non-nucleic acid-based diagnostics for pediatric TB in this manuscript.

Assays for the detection of the human immune response to Mtb infection:

Tuberculin skin test (TST) - One of the earliest diagnostic assays that was developed for the diagnosis of TB infection is the Tuberculin skin test (TST). The technique involves the application of tuberculin/purified protein derivative to the skin, and is also known as the Mantoux test, Mendel- Mantoux test, Heaf test, or Pirquet test. The antigen is injected intradermally and the human immune response to the pathogen-specific antigens is assessed by measuring the diameter of the inflammatory response on the skin. If the diameter of induration is greater than 10 mm within two days after injection, the result is considered positive for TB exposure. Thus, the results are subjective, qualitative, and require two visits to the physician for final diagnosis[150]. TST cannot discriminate exposure from infection, and is currently only prescribed for the diagnosis of LTBI. Another disadvantage of the TST is poor specificity in individuals with prior exposure to non-tuberculous *Mycobacteria* (NTM), or those who have been vaccinated with Bacillus Calmette-Guerin (BCG), both of which can result in false positive outcomes. TST may also have low sensitivity in younger children and those with advanced TB, immunity, or malnutrition.[151] The sensitivity of this test is

reported to be 63-75% in immunocompetent TB-suspected individuals, 44-56% in malnourished individuals, and 36-69% in HIV-infected individuals[147,152].

Depending on the antigen preparation and methods used, there is significant disparity in the efficacy and use of the TST. This also depends on the population in question, and health care infrastructure therein. A Gambian study showed that TST is slightly more sensitive than enzyme linked immune absorbent spot (ELISpot, which measures release of IFN γ, a host immune biomarker, see below for further information) in children exposed to Mtb, and it is not confounded by prior BCG vaccination[153]. On the other hand, a study performed in the UK showed that ELISpot had a higher sensitivity when compared to TST in children exposed to a confirmed TB case in school[154]. . Similarly, a study in children with a history of exposure to TB showed that a variant of the ELISpot assay, focused on measuring IFN γ release, named T.SPOT, resulted in a test sensitivity of 50%, and was no better than TST (80%) in culture-confirmed cases. Thus, TST cannot be used to exclude active disease[155]. However, another study performed in Australia showed higher specificity of QGIT compared to TST and a high discordance between both tests[156]. It is noted that both IGRAs (see below) and TST measure the host immune response to the pathogen, and hence, can be influenced by infection with similar organisms, or previous infection with the pathogen in question.

Interferon gamma release assays (IGRAs)– Originally developed by Oxford Immunotec, UK, Qiagen, USA, the IGRA is based on the release of interferon γ (IFN γ) when T cells of individuals are exposed to Mtb. This release of IFN γ can be measured quantitatively *in vitro*, which makes the assay less subjective as compared

to TST. This technique has currently been approved by the WHO for diagnosis of LTBI. Mtb antigens such as the Culture Filtrate Protein 10 (CFP10) and Early Secretory Antigenic Target 6 (ESAT6), proteins encoded by genes within the Region of Difference 1 (RD1) of Mtb genome, elicit interferon γ response in the human host, *via* activation of innate immune receptors. The BCG vaccine strain of Mtb, and some non-mycobacterial species, do not contain these two antigens. Hence, even though they are based on host recognition mechanisms, IGRAs have been shown to have better sensitivity and specificity than the TST, and can differentiate between BCG vaccination and infection, unlike TST in a variety of studies[150]. Some of the commercially available IGRAs include QuantiFERON-TB Gold (QFT-G), QuantiFERON-TB Gold in-tube (QFT-G-IT) and T-SPOT TB (T-SPOT)[150], which vary in the mode of detection (lateral flow assays, ELISA-based, and other). However, there exist some studies which question the superior performance of IGRAs over TST. For instance, Kampmann *et al*. showed that TST had better sensitivity than IGRA (QFG-IT and T-SPOT.TB) in predicting definite TB cases, but showed similar performance of both IGRA tests in LTBI cases. Further, TST and T-SPOT.TB had reduced sensitivity in EPTB compared to PTB, whereas QFG-IT demonstrated similar performance in both[157].

IGRAs have been evaluated for diagnostic efficacy in pediatrics. Connell *et al.* showed similar concordance (93%) between both IGRAs in LTBI children[158]. Bianchi *et al.* showed a good agreement between positive QFG-IT and active disease, and an intermediate agreement between IGRA and TST[151]. A meta-analysis done by Laurenti *et al.* showed no difference in sensitivity between TST, QFT-IT, and T-SPOT.TB

among immunocompetent children, but found that the specificity of QFT-IT and T-SPOT.TB was much greater in this population when compared to TST[124]. Other reviews support the observation that IGRAs demonstrate higher specificity over TST, but suggest that their sensitivity is in fact lower (66% pooled sensitivity from 20 different studies) than TST[159]. ELISpot assays have been shown to demonstrate a sensitivity of 83% in all TB cases, and ~75% in individuals with HIV co-infection and/or malnutrition[152]. Most recently, Lehman *et al.* performed an analysis of the use of IGRA in children, as compared to TST. They found that IGRA testing has greater specificity compared to TST in children > 5 years of age, and recommended it to be the test of choice for diagnosing TB in this age group. However, in younger children (< 5 years of age) , both TST and IGRAs were shown to have similar sensitivity. In all of these studies, a negative IGRA does not rule out TB, particularly in children < 1 year of age and those with central-nervous system affliction, suggesting that better and more reliable methods are required for pediatric disease, especially EPTB.

On the whole, these findings suggest that IGRAs are a valuable platform for the diagnosis of TB. In theory, because IGRAs measure host immune recognition of Mtb antigens, they should be effective in PTB as well as EPTB. However, the efficacy of this method in EPTB and pediatric populations has not been well established[160]. IGRAs are more expensive compared to TST, but have the advantages of being free from human errors, and they only require one visit to a clinic[67,152,161].

Assays for direct detection of Mtb and Mtb Signatures

Sputum smear microscopy – The acid-fast nature of Mtb provides for a simple staining based microscopic identification in people presenting with PTB[162–165]. This is the

primary method to diagnose TB in low- and middle-income countries. Both light and light emitting diode microscopes have been endorsed by the WHO for diagnosis and treatment monitoring of TB using this method. The technique is simple, rapid, and inexpensive, with high specificity in high burden TB areas and the sensitivity is moderate in PTB patients[162–166].

There are several challenges in the use of this technique for the reliable diagnosis of TB. For one, the WHO requires at least two (but preferably three) sputum specimens to be collected from each patient suspected of having PTB. The results depend on the skill of a microscopist, and are impacted by the overall health of the patient and ability to expectorate sputum, complicating results and therapeutic intervention. Since sputum microscopy requires the actual presence of bacteria in the chest expectorate, the method cannot be applied to patients with EPTB[167–169]. Even in cases of PTB, collecting adequate sputum samples from children and immunocompromised individuals presents another challenge[170]. Only 15% of children diagnosed with TB have a positive smear from either sputum or from gastric aspirate[171]. The sensitivity of the method is reported to be between 12-22% in immunocompetent TB-suspected individuals, while the specificity is 100%[147,172]. One challenge in the application of the method for diagnostics in pediatric populations is the paucibacillary nature of the disease, which complicates the ability to acquire three repeated positive smears from a single patient. Further, the sensitivity of microscopy for induced sputum as compared to culture range from 20-57% in children[173], making it unreliable for diagnosis. A sputum sample is extremely infectious; handling and processing of the sample for microscopic characterization increases the risks associated with this

method.

Culture-based methods - Culture is the current gold standard TB diagnostic in adults, but even this method fails quite often in children because of the differential manifestation of the disease. Mtb can be cultured, albeit requiring a longer time compared to most common bacterial pathogens, and the requirement of laboratory infrastructure and trained personnel complicates the process as well. The two culture-based diagnostic systems approved by the WHO are 1) the liquid culture system with rapid speciation, and culture-based phenotypic drug sensitivity testing (DST) using 1% critical proportion in LJ,7H10,7H11 (culture media) and 2) the mycobacterial growth indicator tube (MGIT) media. Of the two, MGIT provides a significantly faster diagnosis when compared to conventional solid culture, but has the disadvantage of a high cost[148]. A lower cost alternative to these methods is microscopic observation drug susceptibility (MODS), which has also been shown to be more sensitive in pediatric populations[148] when compared to conventional modalities, and allows for the simultaneous assessment of drug resistance. The main disadvantage of culture-based methods is they may take up to 12 weeks for the test results to come back due to the slow reproduction rate of *Mtb*. The ability to culture the pathogen in clinical samples varies with various factors such as age, HIV status, disease progression, and clinical presentation[148].

Whereas culture is well established in adults, there is a scarcity of data in children. The paucibacillary nature of pediatric TB results in reduced sensitivity of culture in children[174]. Only 40% of children diagnosed with TB receive a positive culture test result[175]. The sensitivity ranges from 44-60% in immunocompetent TB-suspected

individuals, while specificity is 100%[147,172]. A study in Vietnam showed a sensitivity of 81.3% for MODS and 88.6% for liquid culture.[176] As with smear microscopy, negative culture results cannot be used to rule out TB in children[177], due to the complications associated with presentation of the disease. However, when positive, culture can be useful to distinguish between non-mycobacterial and mycobacterial disease in HIV-TB coinfection[177]. With the PTB and EPTB presentation of the disease, and the paucibacillary nature of pediatric TB, culture cannot be used to exclude the disease when negative, but is definitely confirmatory when positive. The choice of the sample, and the concentration of the bacteria for growth are critical considerations in the use of culture.

Rapid molecular tests - Xpert Mtb/RIF assay (Cepheid, USA) is the only rapid molecular test currently recommended by the WHO for pediatric TB today, and can provide results within 2 hours of sample collection. Current policy recommends it be used as an initial diagnostic test in children suspected of having MDR-TB or HIV-associated TB. The WHO acknowledges the inability to get microbiological confirmation in children, and allows for the use of data from adults to guide this recommendation in children. The test can simultaneously detect TB and resistance to Rifampicin, by detecting a DNA sequence specific to Mtb through polymerase chain reaction. Steingart *et al.* showed a sensitivity of 65.1-75.9% for children[178]. In order to increase accessibility to rapid molecular testing for TB, Cepheid developed the Edge platform, which is a single-module instrument that connects to a tablet, facilitating storage and transfer of data. This allows for the instrument to function in more

decentralized settings, at the same level as microscopy, as it includes an auxiliary battery.

The WHO meeting report shows that the next-generation Xpert Mtb/RIF Ultra cartridge will offer enhanced sensitivity as compared to current Xpert Mtb/RIF cartridge in detecting *Mtb* in paucibacillary specimens, including smear-negative culture-positive specimens (e.g. those from people living with HIV), extrapulmonary specimens (notably cerebrospinal fluid), and specimens from children[148]. The sensitivity is 49% in immunocompetent TB-suspected individuals, while specificity is 100%[147]. However, the Ultra cartridge has the disadvantage of a short shelf life, which makes it difficult to use in low-resource countries. Yet, Xpert offers the most promise for the application of molecular diagnostic technologies for the diagnosis of pediatric TB, and variant manifestations of the disease.

Detection of Lipoarabinomannan, an Mtb Biomarker– Lipoarabinomannan (LAM) is one of the most studied Mtb biomarkers[179,180]. LAM is secreted by Mtb, and is a conserved lipoglycan involved in virulence. The biomarker is known to activate Toll-like receptor 2 mediated innate immune pathways during Mtb infection[181]. Investigators have demonstrated the secretion of LAM in urine and its presence in blood[94,182]. Detection of LAM in multiple patient samples, as described below, offers a promising strategy for the diagnosis of TB.

LAM in urine - Detection of LAM in urine has allowed for the development of point-of-care tests for TB. However, most of these tests present with low sensitivity and hence, are not suitable for use as general screening tests for TB. However, the sensitivity for the diagnosis of TB among individuals coinfected with HIV, especially among patients

with low CD4 counts, is significantly elevated and these assays are therefore being widely used in this population. The urine LAM strip-test (Determine®-TB Alere, USA) is currently recommended by the WHO in HIV-positive adults with CD4 counts less than or equal to 100 cells/μL with signs and symptoms of TB. Since 2015, new evidence has emerged that might justify the use of the test in a broader group of people living with HIV[19]. LAM detection in urine has the advantage that it allows for simple, non invasive, sample collection, is associated with low cost, less bench time, and does not require highly trained personnel. A WHO update on LAM assays reported a pooled sensitivity of 47% and pooled specificity of 82% among various studies performed in children with HIV[183].

LAM in blood - LAM produced by Mtb at the site of infection quickly enters the blood stream. However, LAM is amphiphilic, as are other bacterial pathogen associated molecular patterns (PAMPs) that activate immune recognition, and is unstable in aqueous blood[52,184]. Because of this biochemistry, LAM seeks to associate with host membranes or carrier complexes for biochemical stability. In blood, host lipoproteins such as high- and low-density lipoprotein (HDL, LDL) sequester LAM, resulting in modulation of the inflammatory response[72,73,185,186]. Understanding this host-pathogen biology, Mukundan *et al.* have developed a novel lipoprotein capture assay using a biosensor platform developed at Los Alamos National Laboratory to directly and quantitatively detect LAM in blood[72]. The fact that LAM is expressed, albeit hidden in lipoproteins, in the blood of patients with active TB, and that this expression occurs irrespective of whether the patient has pulmonary or disseminated disease makes it a promising target for diagnosis of pediatric TB[186,187].

3.4.1 The lack of gold standard diagnostic and implications

One of the major challenges in diagnosing childhood pulmonary TB is the lack of a reliable gold-standard diagnostic, which leads to significant under or over treatment of children with suspected disease[135,170,188–190]. Culture is considered the gold standard in adults, but has been shown to be imperfect in detecting childhood TB[170,188]. Less than 15% of pediatric cases are sputum smear positive, and culture detects around 30-40%, due to reasons outlined earlier in this chapter. Therefore, childhood TB is diagnosed based on a triad of close contact with a TB patient, positive TST, and abnormal chest radiograph[170], which results in significant misdiagnosis and under diagnosis, both of which have societal and individual implications.

Evaluation of new diagnostic tools for the detection of childhood TB is difficult due to the absence of accurate comparative matrices and reference assays[147]. One of the key factors that can be considered when evaluating new diagnostics is the duration and proximity of suspected case of pediatric TB to confirmed cases – i.e. transmission cohort studies. Some studies have emphasized the significance of exposure to confirmed TB cases, as positive results increased with increased exposure[153,154].

3.5 Pediatric TB in context of HIV

TB is the most common opportunistic infection and leading cause of death in people with HIV, including children. The immunocompromised status of HIV positive individuals may allow for the activation of TB in latent carriers, increase risk and

susceptibility in non-carriers, and enhance unconventional disease presentation and possibility of disseminated disease, all of which challenge conventional diagnostic approaches. Children with a low CD4 count have a five-fold risk of contracting TB as compared to those with mild immunosuppression[191]. The risk of infection by drug-resistant TB also increases with HIV coinfection[192]. HIV-TB coinfected patients are 37% more likely to develop resistance to at least one drug, versus 19% of patients with TB only[193]. HIV-TB coinfection has been reported to be over 50% in some high burden African settings[194]. Globally, 11% of HIV-positive TB patients died during treatment, and the possible reason for poor outcome is late detection of HIV-associated TB, as well as delayed start of treatment. Whereas most of this data is accrued on adult populations, the ramifications apply to children – if only more significantly than to adults. Therefore, the WHO has recommended treatment for latent TB infection in HIV individuals and children under 5 years, who are living in households with individuals/family members with bacteriologically confirmed TB. The 2018 WHO report recommended the use of GeneXpert assays and lateral flow urine LAM assays in HIV clinics to help ensure early diagnosis and reduced mortality[195]. The relationship between TB and HIV coinfection, and the implications of this association on disease manifestation, need to be considered in making treatment decisions.

3.6 Research needed on pediatric TB

The WHO has developed a roadmap to end TB in children and adolescents, with the goal of developing new diagnostic approaches for systematic TB detection in

vulnerable children and to develop child-friendly point of care tests with requisite accuracy by the year 2023. According to the WHO 2018 report, a major technological breakthrough is required by 2025 so that TB incidence rate can fall to much lower levels, and the spread of the disease can be curtailed. There is a significant dearth in the investment and development in new diagnostics, which has delayed such breakthroughs and effective control of disease spread. Consequently, there is an urgent need for a new diagnostic that can minimize barriers to healthcare access, ensure quality testing in difficult to diagnose groups, is affordable to use, and has low maintenance costs, especially in pediatric populations. Early diagnostic tests, which are usable at the point of care, and can accurately diagnose PTB and EPTB in children with/without HIV co-infection can provide that much required breakthrough and allow for the realization of the WHO goals for global TB control.

Chapter 4.

Pediatric Tuberculosis: The Impact of "Omics" on Diagnostics Development

Shailja Jakhar, Alexis A. Bitzer, Loreen R. Stromberg and Harshini Mukundan *

Physical Chemistry and Applied Spectroscopy, Chemistry Division, Los Alamos National Laboratory, Los Alamos, NM 87545, USA; sjakhar@lanl.gov (S.J.); abitzer@lanl.gov (A.A.B.); loreen@lanl.gov (L.R.S.)

* Correspondence: harshini@lanl.gov; Tel.: +1-(505)-606-2122

Received: 31 July 2020; Accepted: 17 September 2020; Published

4.1 Abstract

Tuberculosis (TB) is a major public health concern for all ages. However, the disease presents a larger challenge in pediatric populations, partially owing to the lack of reliable diagnostic standards for the early identification of infection. Currently, there are no biomarkers that have been clinically validated for use in pediatric TB diagnosis. Identification and validation of biomarkers could provide critical information on prognosis of disease, and response to treatment. In this review, we discuss how the "omics" approach has influenced biomarker discovery and the advancement of a next generation rapid point-of-care diagnostic for TB, with special emphasis on pediatric disease. Limitations of current published studies and the barriers to their implementation into the field will be thoroughly reviewed within this article in hopes of highlighting future avenues and needs for combating the problem of pediatric tuberculosis.

Keywords: pediatric tuberculosis; diagnostics; omics; biomarkers; lipoarabinomannan

---

4.2 Introduction

Tuberculosis (TB) is one of the most common infectious diseases worldwide and continues to pose a substantial threat to pediatric health[196]. According to the World Health Organization (WHO), roughly 10 million individuals were infected with TB in 2019, which resulted in ~1.2 million deaths. Children (<15 years) account for approximately 14% of all TB deaths, and 11% of all TB cases. Of these cases, only 35% of all pediatric TB cases are accurately diagnosed, leading to a delay or lack of treatment[197]. Within this pediatric population, 69% of cases in children under the age of 5, and 40% of cases in children 5–

14 years of age remain unreported and undiagnosed, partially accounting for the high infection and mortality rates in this population[19]. Thus, the availability of reliable empirical diagnostics will greatly facilitate improved treatment and survival in children with pediatric TB. However, such diagnostics are currently nonexistent for pediatric TB infection.

A key contributing factor in our inability to effectively diagnose and treat pediatric TB, is the continued lack of understanding of host-pathogen interactions and disease manifestation in this population. The exact immune mechanisms of underlying TB disease in children are unclear, but some pathways have been elucidated. TB is caused by the bacterium *Mycobacterium tuberculosis* (MTB). In pulmonary manifestation of the disease, the bacteria enter the body via inhalation and colonize terminal alveoli of the lungs after crossing many physical barriers[198]. MTB then activates the host immune response, causing macrophages and lymphocytes to migrate to the infection site. Here, the immune cells begin granuloma formation where MTB can persist in a latent stage for an extended time. Changes in host immune status can cause latent infection to become active at any time[199]. Thus, it is the dynamic balance between bacterial pathogenicity and the host immune system that determines the clinical presentation of TB disease. This balance is influenced by several factors including the infectious dose, virulence and persistence of the pathogen, host health and co-morbidities (HIV/AIDS, diabetes, and others), and the interplay between the innate and acquired immune system[200–204].

According to the WHO, successful diagnosis and prompt treatment of TB could prevent millions of deaths each year [2]. However, pediatric TB is not effectively diagnosed by strategies developed for adult infection. Less than 15% of pediatric cases are sputum smear positive, and only 30%–40% of all cases are confirmed by culture[205].

The high failure rate of existing diagnostic tests in pediatrics is largely due to the differential presentation of disease in this population.

For one, the incomplete maturation of the immune system in pediatrics has been shown to be a contributing factor in disease manifestation and progression[206]. Children aged 1–2 years present with a 20%–30% risk of disease activation, whereas the risk decreases to 5% between ages 3–5, and can potentially further decrease to 2% between 5–10 years of age[143]. Additionally, the developing immune system of children can result in a varied response depending on the stage of disease manifestation, which consequently leads to increased risk of active TB with different disease outcomes[206]. Secondly, childhood TB is often disseminated making it harder to detect via traditional sputum-based diagnostics[144]. Additionally, young children are often unable to expectorate sputum, making the reliance on sputum-based diagnostics difficult for this population[78]. Moreover, pediatric clinical isolates contain fewer bacteria (paucibacillary), making culture and isolation even more challenging. These factors contribute to the challenge of diagnosis of pediatric TB, and render adult diagnostic tests ineffective when applied to children. For instance, while bacterial culture from blood or sputum sample from a presumptive positive patient is the current gold standard TB diagnostic in adults, the method has reportedly low sensitivity when used in children[207]. As a result of the above mentioned factors, a reliable diagnostic for pediatric TB has proved challenging and remains an elusive goal[135,170,188–190]. The following section provides a comprehensive assessment of current diagnostic methods with **Figure 4.1** providing a comparison of current approaches for diagnosis of pediatric TB with an “omics” future.

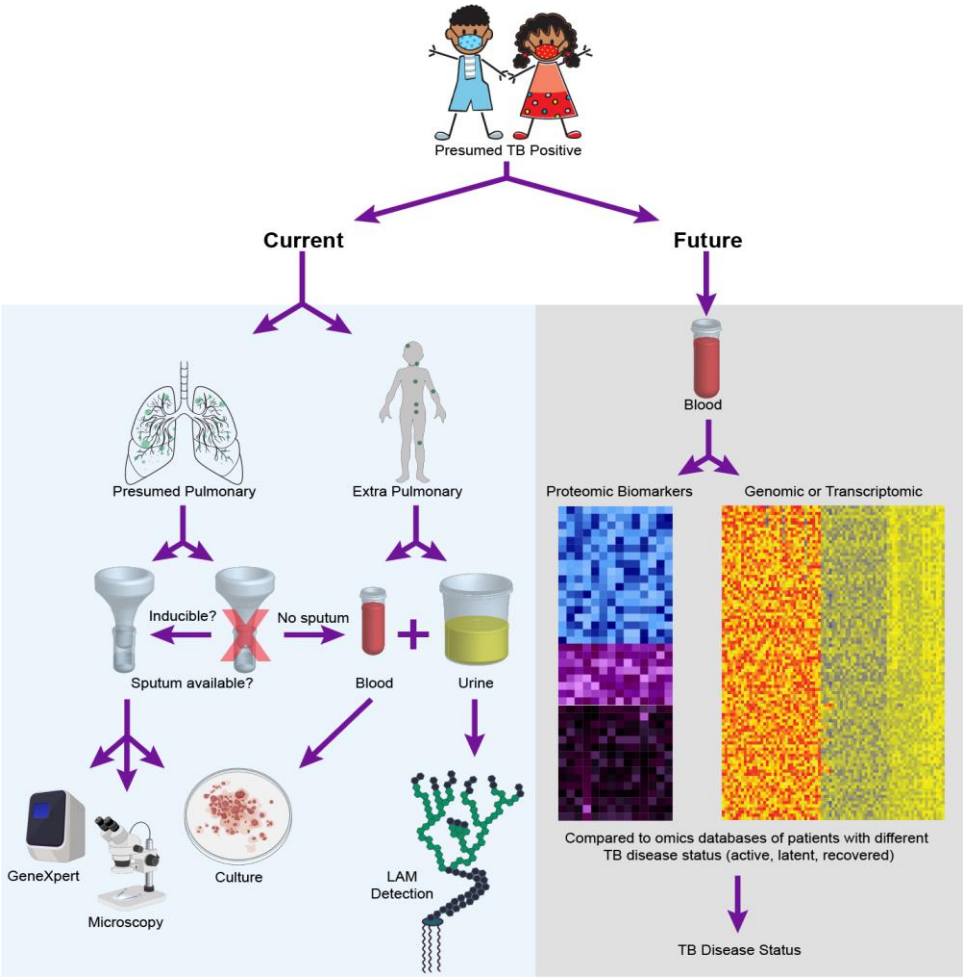

Figure 4.1. Pediatric tuberculosis (TB) diagnostics—today and tomorrow. The figure outlines the diagnostic choices and decisions that are made when a child is presumed positive for TB disease today, while highlighting that these choices and challenges may be entirely alleviated with the realization of empirical diagnostics as facilitated by one of the many potential omics strategies discussed in this review. To create the cumulative figure, images 379758506 by katy_k20 and 394943974 by janista were obtained from DepositPhotos and used under the standard license agreement. Additional images were downloaded from BioRender.com and used under licensed agreement.

4.3 Current Diagnostics for Pediatric TB

TB can manifest in the latent form in many individuals, and only activates in some patients based on various influencing conditions. Depending on the design, approach, and sensitivity of an assay, a method can be approved for either diagnosis of latent or active forms of the disease in pediatric or adult populations. For instance, the tuberculin skin test (TST) has historically been used worldwide and is currently recommended by WHO

for diagnosis of latent TB infection in adult and pediatric populations[197]. In this test format, the tuberculin/purified protein derivative is injected intradermally and the diameter of the inflammatory response on skin is measured. A diameter of greater than 10 mm within two days is considered positive for TB exposure[25]. TST cannot discriminate between latent and active infection, requires two visits to clinic, and is based on subjective interpretation of the spot size[150]. Despite approval for use in children, TST suffers from lower sensitivity in this population, along with poor specificity in individuals exposed to non-tuberculous Mycobacteria or prior bacille Calmette-Guerin BCG vaccination[151].

Another test that has been endorsed by WHO for diagnosis of latent TB infection is the interferon gamma release assay (IGRA). This method is based on the quantitative measurement of interferon gamma (IFN γ) released upon activation of innate immune receptors when exposed to MTB antigens, in whole blood. The MTB antigens used includes culture filtrate protein 10, early secretory antigenic target 6, and proteins encoded by genes within the region of difference 1 of the MTB genome[156]. The sensitivity and specificity of IGRA is better than TST, and can differentiate between BCG vaccination and MTB exposure[161]. The assay concept has been commercialized by multiple companies, and available IGRAs include QuantiFERON-TB Gold (QFT-G), QuantiFERON-TB Gold in-tube (QFT-G-IT), and T-SPOT TB (T-SPOT), which vary in the mode of detection (such as lateral flow assays, enzyme-linked immunosorbent assays (ELISA), and ELISpot). The need to draw blood and immediately perform the test is a limiting factor, especially in resource limited areas.

An inexpensive and simple method commonly used to diagnose active pulmonary TB in low and middle income countries is the sputum smear, which uses microscopic

identification of stained MTB in infected samples[162–165]. WHO has endorsed both light microscopy-based and light emitting diode microscope-based formats of this assay modality for use in both adult and pediatric TB patients. This technique is simple, rapid, and inexpensive, with moderate sensitivity in adults with pulmonary TB[162–166]. However, a drawback of the method is that two sputum specimens are necessary, which are difficult to obtain in all patients, but especially from children[208]. Thus, the value of sputum microscopy for effective diagnosis of pediatric infections is very limited.

Culture is the gold standard for the diagnosis of active TB infection. However, the technique is time-consuming, due to the slow growth rate of MTB. There are two culture-based diagnostic systems approved by the WHO: (1) the liquid culture system with rapid speciation, and culture-based phenotypic drug sensitivity testing (DST) using highly specialized culture media and (2) the mycobacterial growth indicator tube (MGIT). Of the two, MGIT provides higher yield of MTB and significantly faster diagnosis when compared to conventional solid culture, but has the disadvantage of a high cost[148]. However, the paucibacillary and disseminated nature of pediatric TB results in reduced reliability of culture as a gold standard in children[75]. Because of these pediatric TB disease states, culture cannot be used to exclude the disease when negative, but is definitely confirmatory when positive. The choice of sample, and the concentration of bacteria for growth are critical considerations in the use of culture as a confirmatory diagnostic. Thus, while culture is considered the gold standard for TB diagnosis in adults, the technique often produces unreliable results in detecting childhood TB[170,188].

The Gene-Xpert MTB/resistance to rifampicin (RIF) assay (Cepheid® USA) was developed to detect DNA sequences specific to MTB, using polymerase chain reaction

(PCR). This test has been recommended by the WHO to improve adult and pediatric case detection and identification, and can provide results within 2 h of sample collection[148,209]. Current policy recommends it be used as an initial diagnostic test in children suspected of having multi-drug resistant TB or HIV-associated TB[197]. However, the sensitivity of this assay suffers when bacterial burden is low in samples, as is common in pediatric and HIV positive populations[178]. Furthermore, the assay relies on sputum as a sample, which is a limitation in children, given their inability to expectorate.

Detection of the biomarker lipoarabinomannan (LAM) is a highly promising strategy for pediatric TB because of the non-reliance on sputum as the diagnostic sample[67]. As a result, the MTB cell wall antigen-LAM has gained attention over time. WHO has recommended the use of the lateral flow urine LAM (LF-LAM) assay (Determine™ TB LAM Ag, Abbott) for detection of active TB in severe HIV positive cases. LF-LAM assay involves application of a 60 µL unprocessed urine sample on the test device and results are read visually within 30 min[142]. Another commonly used method to detect LAM in urine are immunoassays, such as ELISA. Here, the capture antibody is used in a multi-well plate, followed by addition of sample and a detection antibody[75,77,210]. However, LAM detection is not yet approved for use in diagnosis of HIV negative pediatric TB, likely because of the lower sensitivity of current diagnostic strategies. Researchers are working on the evaluation of the use of ultra-sensitive sensors in order to circumvent this problem[56,72,83,137,211,212]. The use of samples such as urine and blood favors application of this approach to children, and individuals with disseminated infection.

While there are promising developments, there are currently no reliable diagnostics for pediatric TB. The percentage of children with active TB that were incorrectly diagnosed

by current diagnostic tests, as outlined above, are 40% by culture, 77% by microscopy, and 50% by gene Xpert[147]. The poor reliability of current pediatric diagnostics have caused the diagnosis of childhood TB to be based almost entirely on medical history, clinical symptoms, TST results, and chest radiography[213], and the WHO has a prescribed process for syndromic diagnostics. Therefore, there is an urgent need for development of diagnostics using non-sputum based, reliable biomarkers for detection of tuberculosis in children[137].

Approaches targeting diagnostics development for pediatric TB can broadly be classified into three major categories: (1) detection of antigens or other biomarkers produced by the pathogen, (2) measurement of host immune response to MTB antigens (both humoral and cellular), and (3) unbiased “omics” approaches utilizing genomics, transcriptomics, proteomics, lipidomics, and metabolomics characterization. The use of pathogen signatures and host biomarkers for TB diagnostics have been broadly discussed elsewhere, and is briefly summarized above. This manuscript explores the third approach, using “omics”, for diagnosis of pediatric TB and how this can be applied to pediatric TB diagnosis.

4.4 The Role of “Omics” in TB Diagnostic Development

Empirical diagnostics can potentially traverse the challenges associated with various presentations and manifestations of TB disease in children, as well as address the varied manifestations of TB disease in adults (disseminated, extra-pulmonary, drug-resistant, and latent)[214]. Molecular signatures to facilitate such diagnostics can belong to any of the “omic” categories of relevance and the use of omics as a tool for biomarker discovery has advanced greatly over the past decade, facilitating such development. As depicted in

Figure 4.2, a well-rounded omics approach for investigating TB pathology includes genomics, transcriptomics, proteomics, metabolomics, and lipidomics. Such a high throughput approach can provide researchers with an unbiased multi-dimensional understanding of disease progression and outcomes, to better develop an all-encompassing diagnostic test.

In comparison to current diagnostics, the average response times for the various omics technologies discussed in this manuscript vary greatly at this point in development. For instance, a technically naive health care worker can accomplish running an Alere LAM assay at the point of need, within 30 min for a low cost. However, running a genomics panel on patient sputum samples is far more expensive (hundreds of dollars, depending on the method), and may require pathogen concentration via culture. This is technically intensive and time consuming and requires extensive bioinformatics capabilities, which in turn require skilled capabilities and complex laboratory infrastructure. Whereas, the Alere immunoassay interrogates for one single biomarker of interest, genomic arrays can provide a pan-diagnostic approach for discriminative diagnosis of infection. Further, genomic technologies are advancing with respect to ease of use and operation at unprecedented rates, and, in fact, have defied Moore's law[215]. Field forward sequencing capabilities that can be used quickly and in an automated version at the point of need are rapidly emerging[216]. Many culture-free sequencing capabilities are also emerging, decreasing the time to result, especially when combined with deployable and easy to use informatics pipelines[217]. Similar to genomics, proteomic and metabolomic arrays are also time consuming, labor intensive, and expensive in their current form. However, this is also changing rapidly, albeit not as quickly as evidenced with genomics. Service centers

providing proteomic microarray development and validation are emerging, and despite the research required and custom development involved, are now available for ~$100 per sample[218]. Thus, all of these omics-based methods hold more promise for the future, because of their holistic nature, flexibility, and agility to being applied to a variety of human health challenges. These properties are especially relevant to pediatric TB, where the reliability of current diagnostics is very poor. A novel omics future promises a superior, more reliable strategy for pediatric TB diagnosis. Currently, there are various researchers working on the development of deployable and easy to use informatics pipelines for proteomics, genomics, and other omics strategies[219–222].

An omics approach would expand our knowledge of diagnostic biomarkers and could also facilitate better understanding of MTB pathogenesis and drug resistance mechanisms to aid in the development of suitable therapeutics and vaccine candidates. An example of this would be using proteomics to measure cellular activity to provide deeper insight into pathogen or host cellular processes during different stages of infection[223]. Additionally, whole genome sequencing (WGS) can be used to identify signatures of drug resistance in the pathogen before or during drug therapy to provide a customized pharmaceutical regimen to improve treatment efficacy[224]. With the evolution of machine learning and artificial intelligence based computational capabilities, an “omics” approach can be utilized in many ways to identify host or pathogen signature patterns for diagnostics and targets for therapeutics.

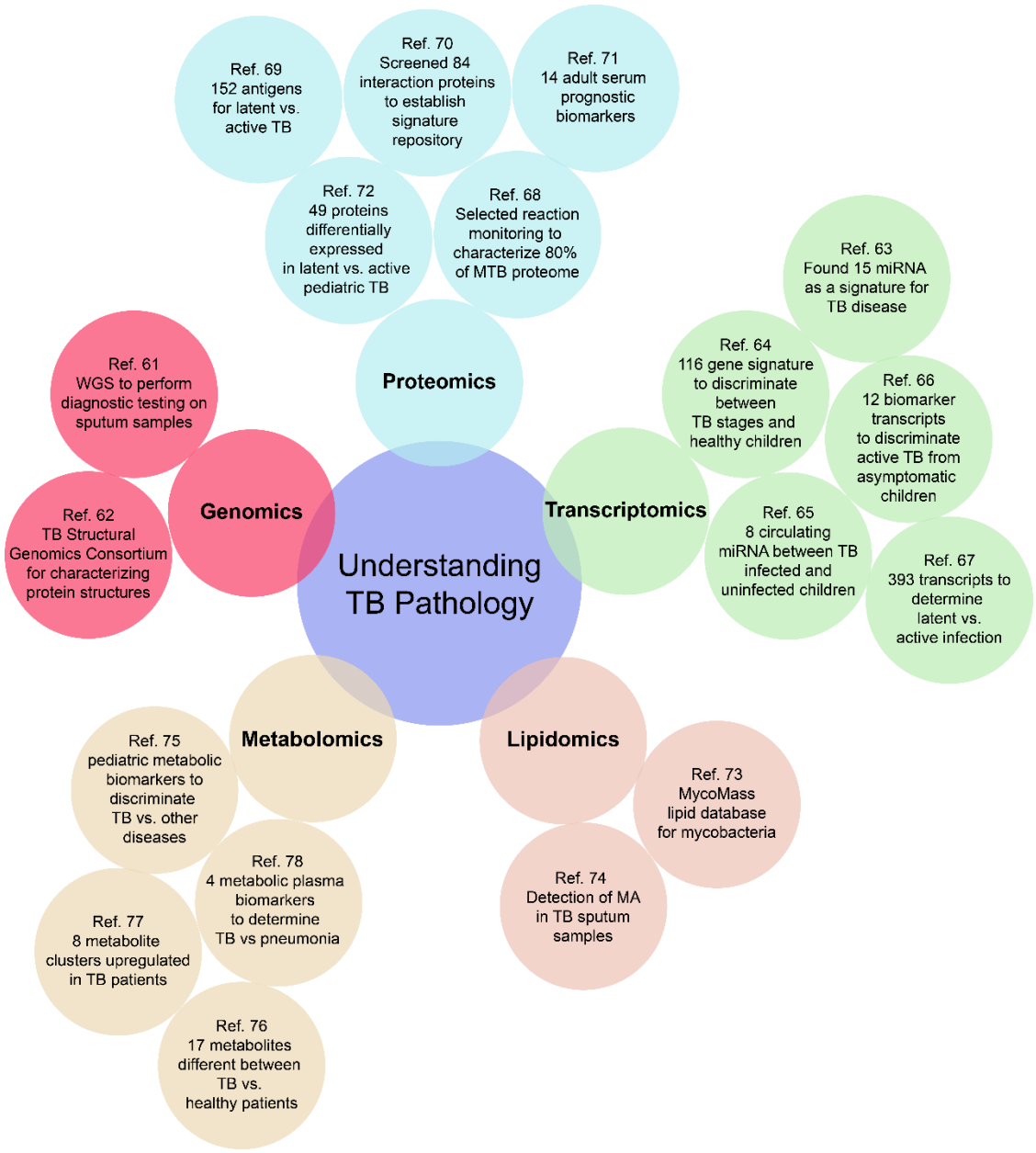

Figure 4.2. Representative cases for an "omics-based" approach to build a comprehensive understanding of the pathology of both adult and pediatric TB. There are still many omics-based approaches to be further investigated, especially for pediatric TB[114,128,131,133,225–238].

Genomics

WGS of MTB presents an exciting opportunity with respect to improved strategies for diagnosis of TB, irrespective of disease state. Recent advances in genomics have allowed for the use of WGS in order to discriminate between reinfection versus relapse

of TB infection. Unlike serological techniques, WGS as a diagnostic tool can confirm the presence of current MTB infection [79]. While most WGS-based work has required prior culture of the pathogen, there have been two recent studies using WGS as a confirmatory diagnostic test by sequencing MTB genomes directly from uncultured sputum samples[239]. This is of great relevance in the progress towards using this technique as a diagnostic strategy. However, it is important to note that MTB DNA was also detected in samples that were culture and smear negative. Therefore, DNA-based genomic detection cannot distinguish between active and cleared infections where residual DNA may be present from dead bacteria[233].

One critical advantage of WGS-based diagnosis of TB infection is the ability to identify, and appropriately treat mixed MTB infections (up to 50% in certain TB endemic regions), which are defined as disease caused by more than one distinct MTB strain[240,241]. Existing platforms have consistently demonstrated lower sensitivity in mixed infections, suggesting that WGS may fill a major gap in this arena. For instance, the Xpert assay for rifampicin resistance on mixed infections has a lower sensitivity of (80%), compared to 93% on homogenous infections[241]. A second advantage of WGS is the data on its application towards the determination of drug resistance. Sequencing data consistently agrees with conventional DST, and is associated with shorter turnaround times, especially when done from early cultures[224]. The same reasons that make WGS suitable for tackling these challenging problems, also make it an excellent candidate for tracking multiple TB presentations in pediatric populations. However, most often, WGS requires culture prior to sequencing, which can delay diagnosis, and complicate application in paucibacillary pediatric cases. More studies such as the ones noted above need to be performed on

non-sputum samples to explore culture-free WGS strategies. In addition to diagnostics, DNA microarray chips have been explored for the rapid detection of MTB resistance to different therapeutics. One such study collected sputum samples from 42 patients with TB and determined a 92.8% susceptibility and 93.8% specificity for the identification of resistance to the antimycobacterial drug, rifampicin[242]. A similar study assessed 176 clinical isolates on an array with 12 pairs of primers, and 60 nucleotide polymorphisms of 9 different MTB genes, and compared the results to culture-based DSTs, GenoType MTBDR*plus*, and MTBDR*sl* tests. It was found that the array was able to detect for resistance to isoniazid with a sensitivity of 100% and a specificity of 96.7%, whereas for rifampicin it was observed to be 99.4% and 96.7%, respectively. These outcomes present excellent suitability for reliable use in a clinical setting for the identification and monitoring of resistant strains. Development of such methods could have a large impact not only on diagnosis of MTB, but also on disease prognosis[243].

Aside from diagnostics, genomics has proved to be a powerful tool for understanding the molecular epidemiology of TB, mechanism of drug resistance, and for unraveling protein and structural information. Analysis of WGS information is also useful for epidemiological characterization and tracing transmission[239,244,245], and the genetic sequence data provides a code for protein structure. The TB Structural Genomics Consortium is an organization dedicated to determining protein structures for MTB proteins on a genome wide scale. Large scale structural determination could help researchers design smarter drugs to combat disease[234].

Transcriptomics

Compared to genomics, transcriptomics is more readily adaptable for rapid diagnostic development. Analysis of host coding RNA can be used to investigate gene expression patterns throughout the course of the disease, and potentially with varied manifestations, making them ideal targets for investigation of pediatric TB diagnostics. Non-coding RNA, which does not encode for any protein, is frequently linked to regulatory functions, which may be altered during different disease states. A recent study identified 15 non-coding micro RNA (miRNA) as a signature for TB disease[235]. In this study, researchers compared the miRNA profiles from different genetic backgrounds, adult patients with active pulmonary and extra-pulmonary infections, TB/HIV co-infections, and latent TB. Using miRNA as a marker was found to have an overall sensitivity of 86% and a 79% specificity for diagnosis of active TB infection in these varied populations. Using RNA sequencing of whole blood samples, researchers examined the use of small non-coding RNA population such as miRNA, PIWI-interacting RNA (piRNA), small nucleolar RNA (snoRNA), and small nuclear RNA (snRNA) as host biomarkers for active and latent MTB in a systematic manner[246,247]. From this approach, one miRNA and two piRNAs were identified as potential biomarkers for latent MTB[248], but further studies are required for their validation in such an application.

There have also been several transcriptomic studies in pediatric populations with TB in the last 10 years[109,112–114,126,131,133]. However, the broader implications of these results towards the development of a pediatric diagnostic are limited by the lack of diversity in population sampling. Host circulating miRNA profiles from whole blood in a pediatric TB population, were analyzed by Zhou et al. who demonstrated that a combination of eight miRNA signatures provided a 95.8% sensitivity and 100% specificity for the discrimination of children infected with TB versus uninfected healthy controls[133]. Using the GeneChip

Human Exon 1.0 ST Arrays (Affymetrix), a 116 gene signature set from whole blood was identified in 27 Warao Amerindian children (9 active TB, 9 latent TB, and 9 healthy controls)[114], again suggesting that a transcriptomic profile assessment can provide a reliable strategy for diagnosis of pediatric TB. The researchers further validated the ten genes in an independent cohort of 54 children by using quantitative real time polymerase chain reaction (qRT-PCR), and found that five out of ten genes were sufficient to achieve 78% sensitivity and 100% specificity in this population[249]. Additionally, a recent study with Indian children explored transcriptomic profiles from peripheral blood in various stages of disease presentation, and identified 12 transcriptional immune biomarkers that could differentiate between infected and asymptomatic children[131]. Whereas a comprehensive and well-characterized pathogen transcriptomic study is required in order to benchmark relevant signatures, the early developments in this field show promise for the application of these signatures for pediatric TB diagnosis.

A modified approach to transcriptomic diagnosis is to track changes in host cells, rather than the pathogen. For example, by focusing on transcripts from whole blood samples of patients infected with TB, researchers identified a profile of 86 host transcripts which can potentially distinguish TB infections from others, and an additional 393 which further characterize the infection as active or latent[236]. Similar studies in pediatric cohorts would help further understanding of TB-host interaction, and also facilitate differentiation of latent and active disease, thereby advancing diagnostic applications. Transcriptional signatures are independent of bacterial load, which strengthens the argument for using this technique for diagnosing low burden cases such as in paucibacillary disease, as evidenced in children.

Proteomics

Proteomics profiling has been used to measure cellular activity, and can provide a deep insight into cellular processes in complex clinical backgrounds. Understanding the wide array of proteins expressed by both MTB and the host in response to MTB infection could shed light on pathways responsible for pathogenesis and persistence[250,251]. Such proteomic studies could target the pathogen-specific proteome, or host signatures in response to MTB infection, both of which have been attempted extensively, and examples from which are discussed below[252,253].

The function of about one-quarter of the MTB coding genome and the precise activity and protein networks of most of the associated proteins remain poorly understood. Protein mass spectrometry and functional proteomics have provided new insights into making this information more accessible to diagnostics development. Early proteomic studies used two-dimensional gel electrophoresis (2D-GE) to analyze proteins from bacterial fractions and culture supernatants of MTB [59]. However, the low resolution of this method limited the analysis to only a few hundred proteins[254–256], which is insufficient to provide a clear assessment of the signature array. The use of liquid chromatography-tandem mass spectrometry (LC-MS/MS) shotgun proteomic methods in both targeted and non-targeted studies has allowed for the expansion of this capability to several thousand proteins at a given time[237,257]. More advanced MS techniques, such as selected reaction monitoring, have allowed for the quantification of ~80% of the MTB proteome, and do not require cell fractionation or separation[237]. In addition to MS, proteome microarrays have also been used to profile thousands of protein interactions in a single experiment[258,259]. Proteomic arrays have enabled researchers to define an immunoproteome for MTB. Until recently

much of biomarker discovery has relied on traditional methods for separation and identification, however, as alternative methods are being constantly described the field has grown. To date there are three proteome-wide screening approaches that have been employed for the identification of candidate antigens for CD4+ T cell responses to MTB. All three studies found that a relatively small percentage of the proteome was responsible for the majority of the immune response[253,260,261].

In addition to an immunoproteome, a proteomic microarray approach has been used to screen 4262 MTB antigens from 40 adult TB patients which allowed for the identification of 152 MTB antigens that were differentially elevated among patients with active versus latent disease[238]. Yet another study used a two-way proteome microarray approach to screen 84 potential host MTB interactors in infected adults, developing a signature repository that can be further used to understand MTB pathogenesis[225]. Deng et al. identified 14 adult serum biomarkers to differentiate between patients with active disease and those that have recovered from TB infection, facilitating monitoring of treatment outcomes[226]. In addition to presenting the proteome library, the investigators were also able to begin to explore the use of such microarrays in determining protein–protein interactions, biomarker discovery, and differentiating between individuals with active disease and those that had recovered from TB infection, demonstrating the potential usefulness of such platforms for real-world applications.

From a longitudinal cohort of 6,363 MTB positive, HIV-negative adolescents of ages between 12–18 years in South Africa, host protein signatures associated with MTB were systematically assessed. In this study, the cohort was followed for 2 years and investigators reported that 46 individuals developed microbiologically confirmed MTB

disease, while 106 non-progressors were identified. As such, 3000 human host proteins from plasma were quantified, of which 361 were found to demonstrate significant difference in abundance between individuals with microbiologically confirmed TB and non-progressors. From these 361 proteins, a 5-protein signature, TB risk model 5 (TRM5), was further sub-selected for use in discriminatory diagnostics. A second 3-protein pair (3PR) was further added to this sub-selection in order to improve the efficacy of the diagnostic platform. However, neither the TRM5 or 3PR achieved the minimum criteria for an incipient TB test as defined by the Foundation for Innovative New Diagnostics (FIND) or WHO, and, therefore, additional work is still needed to improve these signature-based protein assays[262]. Additionally, a subset of proteins that are exported, termed the exportome, could be potential source of additional disease biomarkers. Efforts to identify exported proteins have been typically limited to in vitro work. However, recently an in vivo method has been described and termed EXIT (exported in vivo technology) for the discovery of MTB exported proteins, as demonstrated in murine infection models. Over 500 proteins were revealed to be exported, several of which were induced in vivo. Proteins discovered by this technique should be further explored as potential biomarkers for adult and pediatric MTB disease markers[263].

In a third study, researchers identified an eight-protein host signature which had ramifications for the diagnosis of TB disease. In this study, three separate cohorts were enrolled for a total of 640 individuals. The initial cohort of individuals was used for the screening of protein biomarkers of TB, the second to establish and test the predicted model, and the third for biomarker validation. The initial round of screening involved a

microarray comprised of 16 non-overlapping arrays to measure 640 human proteins. Sixteen proteins of interest were then further analyzed in a second array. Using a series of mathematical models, a diagnostic model was built using an eight-protein signature. In the second test cohort the signature had an 83% specificity and a 76% sensitivity. The third cohort, in which the signature was validated, the specificity and sensitivity was 84% and 75%, respectively. While this study was done with adults, a similar study could be designed for pediatric MTB to develop a pediatric specific model[264].

Proteomic profiles can allow for the diagnosis of pediatric TB, and despite the disease's varied manifestations, several researchers have begun to specifically explore that possibility. For instance, a quantitative proteomics approach using LC-MS/MS was employed to characterize plasma from 72 children in different test groups (active TB, inflammatory disease control, and healthy control) at a Beijing Children's Hospital. The study identified 49 proteins in pediatric cases that were differentially expressed between active and latent TB[227]. One study characterized the plasma proteins in children at different MTB infection stages (active TB and LTBI), and identified four proteins—XRCC4, PCF11, SEMA4A, and ATP11A—to be signatures of active TB disease using proteomics[227]. Given the differential presentation of pediatric TB disease, it is likely that a combinatorial approach exploring varied biomarker signature profiles may provide a greater reliability of identification rather than a single factor approach[265].

Lipidomics

Lipids are an essential player in biological processes, both within the host and the pathogen. MTB is known to have one of the most complex lipid envelopes in nature, which forms the barrier between the pathogen and the host, and a substantial lipid biosynthesis capacity within their genome[31]. The multilayered cell wall contains both an inner phospholipid bilayer as well as an outer lipid layer consisting of mycolic acid. Lipids from both layers have strong potential to be used as a biomarker for diagnosis.

With considerable advances in mass spectrometry over the past decade, the field of lipidomics has advanced MTB research. The large-scale characterization and quantification of lipids has led to the development of MycoMass, a database for mycobacterial lipids[228]. The database currently contains 58 lipid types. More than 40 of these mycobacterial lipids lack any similarity to other eukaryotic or Gram-negative organisms, making them unique signatures for diagnostics development and therapeutic targeting. The unique Mycobacterial lipidome is, thus, a signature repository that requires further characterization[266]. When comparing the lipid profile from normally grown MTB with dormant and reactivated bacteria, analysis revealed a total of 4187 significant features with 2480 features found to have significant variation during the transition from normoxial growth to dormancy. Across the three different stages a total of 74 fatty acyls showed significant variations. Findings such as these could play roles in the discovery of biomarkers for various different stages of MTB[267].

Mycolic acids (MAs) are a main component of the cell wall of mycobacteria. The cell wall of mycobacterium provides protection against a host immune response by mediating macrophage trafficking events, and by helping the bacterium to grow within host

macrophages[268–270]. MTB has three different structural classes of MAs namely, alpha-, methoxy-, and keto-MAs[42], with the most abundant form being α-MA (>70%), and methoxy- and keto-MAs being minor components (10% to 15%)[43]. MA-classes play a crucial role in virulence and are present in high concentrations in the bacterial cell wall. While they are unique to Mycobacteria, these lipids differ considerably between different Mycobacterial species/strains, a factor which could be helpful for differential diagnosis. For example, the detection of all three forms of MAs in bacterial extracts and gamma irradiated whole bacteria, using surface enhanced Raman spectroscopy[271]. While some studies have used a surface plasmon resonance (SPR) technique to detect serum antibodies to MAs, the method has not been validated clinically[272]. Using a biosensor platform to detect antibodies against MAs from patient serum improved MA detection (sensitivity 91.3% in TB and HIV positive patients) compared to ELISA[273]. Other techniques used to detect MAs are LC-MS and high-performance liquid chromatography, which are both expensive and require advanced user training to operate and interpret data, making them difficult to use in resource-poor settings[271,274]. MAs were detected in adult TB sputum by Shui et al. The study demonstrated a sensitivity of 94% and specificity of 93% in discriminating between TB cases and controls[229]. The authors speculated that the method “might offer advantages in specialized situations such as pediatric cases (where sputum volume is very limited)”, although clinical validation of this has yet to be performed. Lipidomic and metabolomic analysis of MAs in samples such as urine and serum in pediatric and adult patients is needed to establish the effectiveness of this lipidic signature as a potential diagnostic biomarker[275].

Other prominent mycobacterial cell wall components include lipoglycans such as trehalose dimycolate (TDM), phosphatidyl-myo-inositol mannosides (PIM), LAM, and lipomannan (LM)[48–50]. Animal studies have shown that lipids on mycobacterial surface interfere in their interaction with phagocytes, thereby influencing pathogenesis[276]. However, not much is known about the molecular mechanism with exception of key lipoglycans, LAM and LM[276,277].

LAM is an amphipathic molecule released from metabolically active or degrading bacterial cells resulting in the activation of host immune response[51–53]. In 2001, Hamasur et al. discovered that LAM was detectable in the urine several hours after intra-peritoneal injection of crude MTB cell wall extract into mice[94]. The observation provided researchers with an opportunity to evaluate LAM as a biomarker for the development of non-invasive[94,182] point-of-care tests for TB. As a result, a lateral flow urine LAM assay is currently available (Determine™ TB LAM Ag, Abbott Biotechnologies), with a sensitivity of 45% and specificity of 92% in HIV positive patients[278] and is recommended by the WHO only for use in HIV-positive adults with CD4 counts less than or equal to 100 cells·μL^{-1} presenting with symptoms of TB[142]. The guidelines for use of urine LF-LAM assay are similar in children, based on data from adults[142]. Previous work from our team demonstrated the detection of urinary LAM at a maximal concentration of 350 pM in individuals without HIV co-infection using a sandwich immunoassay on an ultra-sensitive waveguide based optical biosensor[56]. The conclusions of this work are supported by a recent study using an improved chemiluminescence readout, with sensitivity and specificity of 93% and 97%, respectively[83]. These findings show that a more sensitive assay format is required in immunocompetent individuals.

Despite advances in LAM diagnostics testing for adults, data on pediatric testing is still scarce. A WHO update on urine LAM assays reported a pooled sensitivity of 47%, and a pooled specificity of 82% among various studies performed in children with HIV[158], which is also reflected in independent assessments of both lateral flow and ELISA formats of detection[75,76,78]. These studies show that LAM measurement is more reliable in immunocompromised children, and that measured concentrations of the antigen decrease with anti-TB treatment[76], which suggests potential for this biomarker to be used as a prognostic indicator. Longitudinal studies demonstrating antigen concentrations as a function of disease progression and treatment must be performed in order to validate this hypothesis, as previously demonstrated for the measurement of lipomannan in *M. bovis* infection[279–282].

Previous work from our group has demonstrated that LAM is associated with high-density lipoproteins (HDL) in host blood[72]. This association should be considered when developing diagnostics, as with membrane insertion and lipoprotein capture methodologies[74,211,279,283–285], because traditional strategies for measuring the monomeric antigen are likely to be unsuccessful in this conformation. To date there are only a few studies showing detection of LAM in blood from adults[83,182,212] and none in a pediatric population.

Lipidic profiles of mycobacteria are unique—and targeting these differential biomarkers can definitely provide a unique strategy for the diagnosis of active disease. It is important to develop capabilities for the characterization and measurement of pathogen and host lipids, and further improve our understanding of pathogen lipid profiles in order to advance this field of science. Furthermore, the genes and enzymes that regulate these

specific lipids can be identified and pave a way to integrate other omics approaches, such as metabolomics.

Metabolomics

Metabolomics can be used to study changes in host metabolism and associated processes in response to TB infection. A recent study in children from the United Kingdom and Gambia demonstrated alterations in host metabolism using ^{1}H NMR spectroscopy and MS, to provide a signature repertoire for diagnostic applications. ^{1}H NMR data was analyzed to discriminate between children with TB, and those infected with other diseases, and demonstrated a sensitivity and specificity of 69% and 83%, respectively, for the diagnosis of TB. MS characterization of metabolic profiles had similar results with a sensitivity and specificity of 67% and 86%, respectively[128]. The study also showed raised levels of ceramide, a type of sphingolipid found in high concentration in cell membranes. Ceramides have been shown to contribute to maturation of the phagosome in macrophages infected with MTB, causing increased killing of pathogenic MTB[286], and can serve as unique metabolic signatures of pathogenesis. Similar alterations in metabolic markers have been seen in adult studies[230–232]. Thus, metabolomics studies can provide some useful insights into understanding pediatric immune response mechanisms to MTB. However, large scale and controlled studies are required for the identification of metabolomic processes and signatures that can be used for diagnostic applications. Yet, the change in host metabolome in response to TB infection can likely provide useful information for pediatric TB diagnosis and understanding of pathogenesis.

4.5 Conclusions

Pediatric TB is a devastating problem worldwide with no reliable diagnostic tests to differentiate between latent and active TB cases or help guide treatment to success. Current pediatric diagnostics are typically based on difficult-to-collect sputum samples, are time consuming, and associated with lower sensitivity. Further, current diagnostic tests do not address the varied challenges of differential presentation of TB disease in children when compared to adults. Some of the current approaches can potentially be refined and re-aligned for pediatric applications. For instance, assay modalities with enhanced sensitivity or blood-based detection methods can greatly improve the use of LAM as a diagnostic marker for pediatric TB disease. However, there is a distinctive need for a broader search for empirical signatures, validated strategies, comprehensive and reproducible assessments, and clinical studies that target pediatric presentation of TB. Due to incredible complexity of TB pathology in various populations, using an "omics-based" approach can facilitate the identification of suites of biological signatures necessary for developing a universal TB diagnostic test. While many "omics" studies have been done in adult populations, these results only provide a road map for building further understanding of pediatric TB pathology. Additional investigation of how TB stages differ and progress to active disease in a pediatric population would aid development of an all-encompassing specific and sensitive diagnostic test.

Funding: This work was supported by an NIAID NIH R21 Research Grant (5R21A1130663) to Harshini Mukundan, Principal Investigator. SJ was supported by this grant as a graduate student. LS was supported by a Laboratory Directed Research and Development Reines Postdoctoral fellowship, and AB by a Laboratory Directed Research

and Development Director’s Postdoctoral fellowship, both from the Los Alamos National Laboratory.

Acknowledgments: The authors thank the chemistry for biomedical applications team, the multiple collaborations on tuberculosis research efforts in the United States and elsewhere, for their support of this work. Many thanks to our team mentor, Basil I Swanson (retired Laboratory Fellow).

Conflicts of Interest: The authors declare no conflict of interest.

Chapter 5.

Detection of Lipid and Amphiphilic Biomarkers for Disease Diagnostics

Jessica Z. Kubicek-Sutherland [1], Dung M. Vu [1], Heather M. Mendez [2], Shailja Jakhar [1], and Harshini Mukundan [1,*]

[1] Physical Chemistry and Applied Spectroscopy, Chemistry Division, Los Alamos National Laboratory, Los Alamos, New Mexico, USA

[2] Department of Chemical and Biological Engineering, University of New Mexico, Albuquerque, NM, USA; The New Mexico Consortium, Los Alamos, NM, USA

***** Correspondence: harshini@lanl.gov; Tel.: +01-505-606-2122

Received: date; Accepted: date; Published

5.1 Abstract

Rapid diagnosis is crucial to effectively treating any disease. Biological markers, or biomarkers, have been widely used to diagnose a variety of infectious and non-infectious diseases. The detection of biomarkers in patient samples can also provide valuable information regarding progression and prognosis. Interestingly, many such biomarkers are composed of lipids, and are amphiphilic in biochemistry, which leads them to be often sequestered by host carriers. Such sequestration enhances the difficulty of developing sensitive and accurate sensors for these targets. Many of the physiologically relevant molecules involved in pathogenesis and disease are indeed amphiphilic. This chemical property is likely essential for their biological function, but also makes them challenging to detect and quantify *in vitro*. In order to understand pathogenesis and disease progression while developing effective diagnostics, it is important to account for the biochemistry of lipid and amphiphilic biomarkers when creating novel techniques for the quantitative measurement of these targets. Here, we review techniques and methods used to detect lipid and amphiphilic biomarkers associated with disease, as well as their feasibility for use as diagnostic targets, highlighting the significance of their biochemical properties in the design and execution of laboratory and diagnostic strategies. The biochemistry of biological molecules is clearly relevant to their physiological function, and calling out the need for consideration of this feature in their study, and use as vaccine, diagnostic and therapeutic targets is the overarching motivation for this review.

5.2 Introduction

The utility of a diagnostic is measured by its ability to provide rapid and reliable information to guide treatment. The past century has seen a rise in molecular diagnostic strategies for measuring disease-specific signatures in patient samples (e.g. blood, urine, tissue and others) using a variety of biosensor technology. A biosensor utilizes a biological component or biocatalyst to detect the presence of an analyte and a transducer to create a quantifiable signal from this interaction. For a biosensor to be used feasibly in a clinical setting, it must be highly specific for the target analyte, accurate in patient samples, rapid and reliable, and resistant to non-specific interactions in clinical samples. In addition, for some applications, especially in resource-poor conditions, it is also desirable for the sensor to be cost-effective and easy-to-use[287]. In order to avoid false positive (signal in the absence of analyte) and false negative (analyte present without signal) signals, the biocatalyst and transducer must be carefully considered for each target analyte.

Identifying target analytes and their presentation in a host during disease is of crucial importance for the success of such molecular diagnostic technologies. Biomarkers are indicators of biological processes and disease-specific biomarkers are of great clinical value for diagnostics. Understanding the interactions between the biomarker and its host is key to developing assays for the detection of such analytes in clinical samples. Because of the ease of purification and detection, proteins and nucleic acids have been extensively used as diagnostic targets. Traditionally, nucleic acids and proteins have been targeted as biomarkers for the diagnosis and detection of disease, primarily because of the availability of a variety of sensitive and tailored methods for the detection of these biochemical signatures. However, another category of biomolecules that play important

roles in a variety of cellular processes, and can therefore serve as indicators of disease and analytes for biosensors are lipids and amphiphiles[288]. Besides membrane formation, lipids also play a crucial role in cell signaling (steroids) and energy storage. The brain is composed of 40-81% lipid, with the myelin sheath being 78-81% lipidic in biochemistry[289]. Many of the bacterial virulence factors recognized by the human innate immune response, such as lipopolysaccharide (LPS) and lipoteichoic acid (LTA), are amphiphilic lipoglycans[290–296]. The structure of lipids is far more diverse than that of proteins, nucleic acids or carbohydrates, allowing for highly specific biomarkers for a variety of diseases. However, all lipids contain at least one hydrocarbon chain that is insoluble in water making them difficult to detect in aqueous solutions such as blood, which has largely limited their application as diagnostic targets. Indeed, currently, rapid detection of lipidated targets is largely achieved via methods that were originally designed for proteins. Here, we review advancements in methods for detection of lipid and amphiphilic biomarkers associated with both infectious and non-infectious diseases describing the advantages and limitations of each approach in clinical diagnostics (**Table 5.1**).

Table5. 1. Advantages and limitations of sensors as clinical diagnostic tools for detecting lipid and amphiphilic biomarkers.

Method	Advantages	Limitations
Mass spectrometry	Sensitive Specific Works in patient samples	Expensive Sample preparation can be extensive Requires highly trained personnel Requires laboratory infrastructure
NMR-based sensors	Rapid Reproducible Works in patient samples	Low sensitivity Low specificity Sample preparation can be extensive Requires highly trained personnel Requires laboratory infrastructure
Optical biosensors		

SPR-based sensors	Rapid Specific	Low sensitivity in patient samples
Interferometry-based sensors	Low-cost Sensitive	Low specificity in patient samples
Waveguide-based sensors	Rapid Reproducible Sensitive Specific Works in patient samples	Short shelf-life of labeled reagents
Electrochemical biosensors	Rapid Reproducible	Low sensitivity in patient samples Low specificity in patient samples
Mechanical biosensors	Rapid	Low sensitivity in patient samples Low specificity in patient samples Reproducibility

5.3 Methods for Detecting Lipid and Amphiphilic Biomarkers

Storage and processing of patient samples

Sample collection and preparation is a critical consideration for the detection any biomarker[297], but lipidic targets warrant further attention[298]. Common lab methods such as freeze/thaw and chemical extractions can have a profound effect on the viability of amphiphilic biomarkers[299,300]. Further, depending on the sample, lipid and amphiphilic biomarkers are often sequestered by host factors, further reducing their availability for direct detection[72]. Therefore, any biosensor designed to detect amphiphilic biomarkers must account for their unique biochemical properties.

Mass spectrometry

Lipidomics requires a thorough characterization of the structure and the function of lipids within a living system. The study of amphiphilic biomarkers, as described here, is a composite of lipidomics, but involves the consideration of the hydrophilic components of

the biomarker in addition to the hydrophobic lipids. Since its inception in the early 20th century, mass spectrometry (MS) has played a significant role in characterization of lipids[301–303], and this has been extensively reviewed. Here, we will focus on the adaptive application of MS to amphiphilic biomarkers.

MS ionizes lipids and sorts ions based on their mass-to-charge ratio. It has been widely used to characterize lipids[304–308], especially with the development of soft ionization techniques such as electrospray ionization (ESI) and matrix-assisted laser desorption ionization (MALDI). Lipid extraction is usually the first step for lipid analysis, and separates the lipidic components (organic phase) from other components such as proteins and nucleic acids (aqueous phase). Most widely used extraction methods have been adapted from Folch[309] or Bligh and Dyer[310], in which a mixture of methanol, chloroform and water are applied for phase separation. However, shotgun lipidomic methods have also been developed which omit the chromatographic separation and sample processing described above, and analyzes all lipid classes together, instead using ionization additives to provide discriminative identification[301]. This method might be more suitable especially for biomarker-discovery, wherein there is no prior art regarding the biomarkers being identified/measured.

Chromatographic methods such as gas chromatography, thin-layer chromatography, high-performance liquid chromatography (HPLC), or ultra-performance liquid chromatography (UPLC)[306,311] are used for separation of lipid mixtures. HPLC and UPLC are have broader applications in lipid analysis[305,311] and can be performed in normal phase (lipid class separation based on their different polarities and dipole moments) or reverse phase (separates lipid according to their hydrophobicity and is based on fatty-

acyl compositions). Coupling of separation with LC methods allows lipids to be resolved sequentially with greater ionization yields, decreased ion suppression from major lipid classes, and increased sensitivity[305,312]. However, this LC step can be bypassed, with direct infusion (shotgun lipidomics) of lipid samples, which simultaneously analyzes the lipid species in the crude lipid extract[313,314]. This method does not require *a priori* decisions on which lipid species to measure, is relatively simple, high-throughput, and fast with short data acquisition times. However, a major limitation of this method is that highly abundant lipids can compete for ionization with the minor species, and mask detection of the latter.

MALDI-MS is based on the utilization of an ultraviolet–absorbing matrix that initially absorbs the energy of the laser and mediates the generation of ions[315,316]. ESI-MS uses a high voltage electrospray to aerosolize the lipid sample and generate ions to charge the lipid molecule[304,317]. MALDI or ESI ionization can be combined with several types of mass analyzers such as triple quadrupole, time-of-flight (TOF), ion trap, and orbitrap to further characterize different lipid classes and species[317,318]. Both quadrupole and TOF mass analyzers are commonly used and their configuration together (e.g. triple quadrupule (QqQ), quadrupole time-of-flight (QTOF)) as tandem mass spectrometric instruments to break down the precursor ions into fragmented product ions, can provide further chemical and structural resolution on the lipid species[319,320]. As an example, ESI-MS has been successfully applied to characterize cardiolipin[320]. Cardiolipin, a biomarker implicated in heart disease and cancer, is a phospholipid present in mitochrondria and is a component of bacterial membrane[321,322]. The diversity of cardiolipin molecular species is found in both the identity and position of its four fatty acyl moieties. Minkler and Hoppel showed

that reverse-phase ion pair HPLC coupled with a triple quadrupole MS/MS linear ion trap mass spectrometer to generate MS/MS was highly effective in characterizing cardiolipin from different species (e.g. rat liver, mouse heart, bovine heart, dog heart)[320], with the spectra facilitating deduction of the structure of cardiolipin: the diacylglycerol phosphate region, the monoacylglycerol region, and the fatty acid region[320].

Mass spectrometry has been used by clinical laboratories to rapidly diagnose both infectious and non-infectious diseases, detect drug toxicity, monitor treatment as well as to discover new biomarkers[323]. However, clinical mass spectrometry systems such as VITEK® MS by BioMerieux are expensive to set up and maintain and require trained personnel to perform and analyze the tests limiting its utility as a point-of-care diagnostic tool.

Nuclear magnetic resonance (NMR)

NMR spectroscopy is one of the most powerful analytical techniques for lipid analysis of biological matrices (e.g., cells, tissue, and biological fluids), owing to the natural abundance of hydrogen in such samples[324–328]. This method is nondestructive, nonselective, and provides detailed molecular information, which can be of extensive value in analyzing amphiphilic biomarkers. Specifically, high-field proton nuclear magnetic resonance (^{1}H-NMR) spectroscopy is used for molecular profiling[329,330], allowing for identification of biomarkers associated with diseases such as tuberculosis[331], cancer[332,333], heart disease[334]; and others, identifying underlying causes of disease[335], and identifying diagnostic biomarkers and new therapeutic strategies[336]. High-resolution, one-dimensional (1D) ^{1}H NMR is reproducible and simple[324,334]. It has been applied for

metabolomics since the 1980s[324,327], specifically, for plasma[333], serum[337], urine[338], and feces[339]. Tissues are normally examined intact[328] and spectra can be obtained rapidly (< 5 min)[324] with detection limits around 1 to 10 µM at > 500 MHz[327,335] MS and NMR are often used in conjunction with one another[335,340]. Although NMR has decreased sensitivity in comparison to MS[335,341], it has other advantages such as being a non-destructive technique with minimal sample preparation, and providing quantitation of molecular structures[303,341]. Coupling the two method yields significantly greater sensitivity (attomole to femtomole)[342].

Lipidomic NMR is associated with many challenges. A substantial number of biomolecules in complex matrices have similar resonances, due to similar proton chemical shift ranges[327,343] resulting in considerable peak overlap[327,344] and a low signal-to-noise ratio[345]. Minimizing peak overlap and increasing sensitivity can be resolved by using high resolution spectrometers (800 to 950 MHz)[346]. Resonance line broadening[347] attributed to the formation of micelles in an aqueous environment or constrained molecular movement as a result of lipid aggregation into bilayers[327] is another challenge that is overcome by chemical or physical treatment of the sample[327].

The use of two-dimensional (2D) NMR[348,349] can also overcome the above challenges of 1D ^{1}H NMR. 2D techniques such as the heteronuclear single quantum coherence (HSQC) method are better suited for lipid profiling because of its ability to detect resonances for both ^{1}H nuclei and ^{13}C nuclei[345], thus allowing for correlation between ^{1}H and ^{13}C chemical shifts and providing elucidation of C-H bonds within a structure[335]. Although detection of ^{13}C is possible with HSQC, the natural abundance of ^{13}C[350] is relatively low requiring prior enrichment of cells with ^{13}C[331], 2D NMR is more time

consuming (> 1 hr/spectrum) in comparison to 1D ^{1}H NMR (< 10 min)[335,338,351]. Absolute quantitation of lipids using NMR remains a challenge[352].

High resolution NMR has been shown to detect a variety of diseases directly in human tissue and fluid samples[353]. Portable NMR-based biosensors have also been developed for use as medical diagnostics[354]. However, portable NMR sensors suffer from low sensitivity and specificity while high-resolution NMR tools require expensive equipment and trained personnel to analyze results.

Biosensors

Broadly defined, biosensors recognize target molecules and produce a measurable signal. Optical, electrochemical and mechanical biosensors (**Figure 5.1**) have been adapted for the detection of lipidic and amphiphilic biomarkers, using a variety of assay methodologies which can be categorized as a) labeled and b) label-free. Labeled assays indirectly measure binding of an analyte to the target molecule, using a reporter molecule (an indicator). Labeled assays have the advantage of readily multiplexing, highly desirable in clinical applications. Label-free assays measure signal changes directly associated with either target binding or cellular processes, without the need for an external reporter. The advantages of label-free biosensors include reduced assay complexity, cost and decreasing interference of the label on binding between ligand and target.

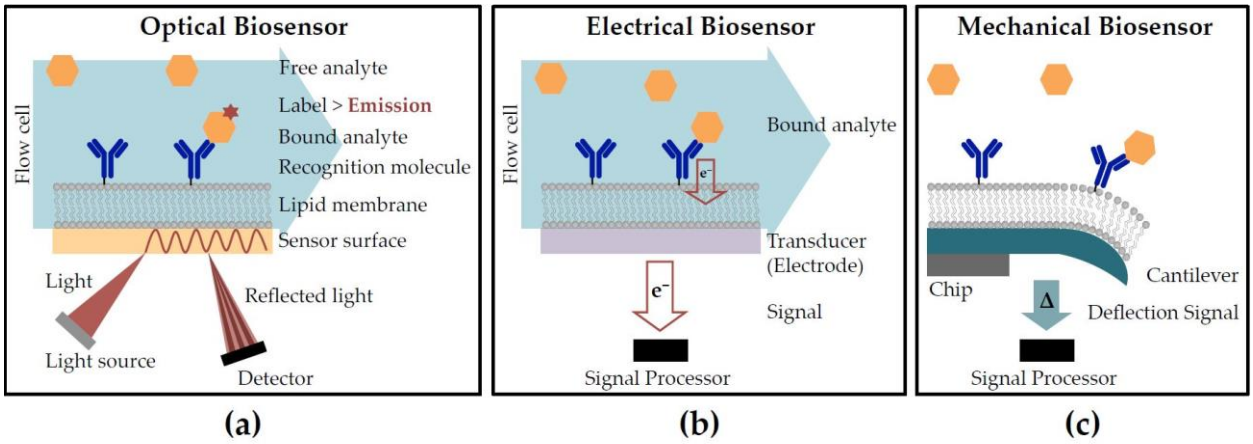

Figure 5.1. Examples of biosensor techniques incorporating lipids for the detection of analytes include (a) optical (b) electrical and (c) mechanical.

Optical biosensors detecting lipids

Optical biosensors measure binding-induced changes in light from the sensor surface. Surface plasmon resonance (SPR) is a label-free technology that has been used to detect the interaction of amphiphilic molecules with lipid bilayers, for ligand screening and biomarker discovery[355]. In SPR sensing, a ligand is immobilized on a gold-coated surface while an interacting molecule is injected in aqueous solution, and the change in resonance associated with binding is measured optically using a spectrometer. SPR has been optimized for measuring protein-protein affinities using the BIAcore™ (GE Healthcare) system. In original iteration, SPR systems lack resolution, cannot multiplex, and are difficult to miniaturize. However, several researchers are working on overcoming these limitations, which may provide for more robust sensors in the future[356]. SPR is not conducive for detection of amphiphiles in biologically relevant conditions, as required for diagnostic applications.

Interferometry, particularly Backscattering interferometry (BSI), allows for label-free detection of both surface-bound and free-solution molecules[357]. In BSI, excitation of a microfluidic channel containing the sample, as well as the channel surface, usually made

of polydimethylsulfoxide or glass, yields interference fringes. Changes in fringes associated with binding of two molecules are measured in the backscatter region. BSI detects interactions of amphiphiles with lipid bilayers[358] directly in human serum[359]. However, in complex samples, non-specific interactions and associated changes in refractive index can prove challenging, but can be limited using suitable surface functionalization chemistry[360]. BSI is inexpensive, sensitive and very versatile, making it a promising candidate for detection of amphiphilic biomarkers in patient samples.

Ellipsometry measures the refractive index of a thin film, and has been utilized in label-free assays where changes in refracted light are measured upon interaction of giant lipid vesicles with a poly-$_L$-lysine coated surface, using a biosensor based on total internal reflection imaging ellipsometry (TIRIE)[361]. This sensor can detect μm size particles such as cells, capsules and liposomes. However, the ability to detect such particles in tissues, as well as the overall clinical utility of this system is yet to be demonstrated.

An optical assay based on UV absorption of lipid-functionalized gold nanorods has been used to detect the lipopeptide myristoyl-Lys-Arg-Thr-Leu-Arg, and a variety of other lipid biomarkers, in serum[362]. However, the low specificity of this label-free technique requires mass spectrometry analysis in order for multiplexing.

In labeled assays, the target molecule is immobilized on the surface of a biosensor and then probed with an analyte, typically an antibody, coupled to a label (fluorophore, quantum dot, radioisotope, enzyme)[363]. Mukundan *et al*. have employed an optical waveguide-based biosensor measuring only surface-bound fluorescent signals from labeled antibodies for the sensitive and specific detection of lipid and amphiphilic targets directly in clinical samples[184,364,365]. This system utilizes the interactions of these

biomarkers with lipid bilayers and lipoproteins to capture them directly to the waveguide surface, followed by probing with labeled-antibodies excited by waveguide-coupled laser light (**Figure 5.2**). This system has been demonstrated to effectively detect amphiphilic biomarkers associated with *Mycobacterium tuberculosis*[56,72], *M. bovis*[280], *Escherichia coli*[366], *Salmonella* Typhimurium[74], influenza[367], tumor markers[368,369] oftentimes directly in human serum, proving potential utility as a diagnostic tool[184,365]. These assays have

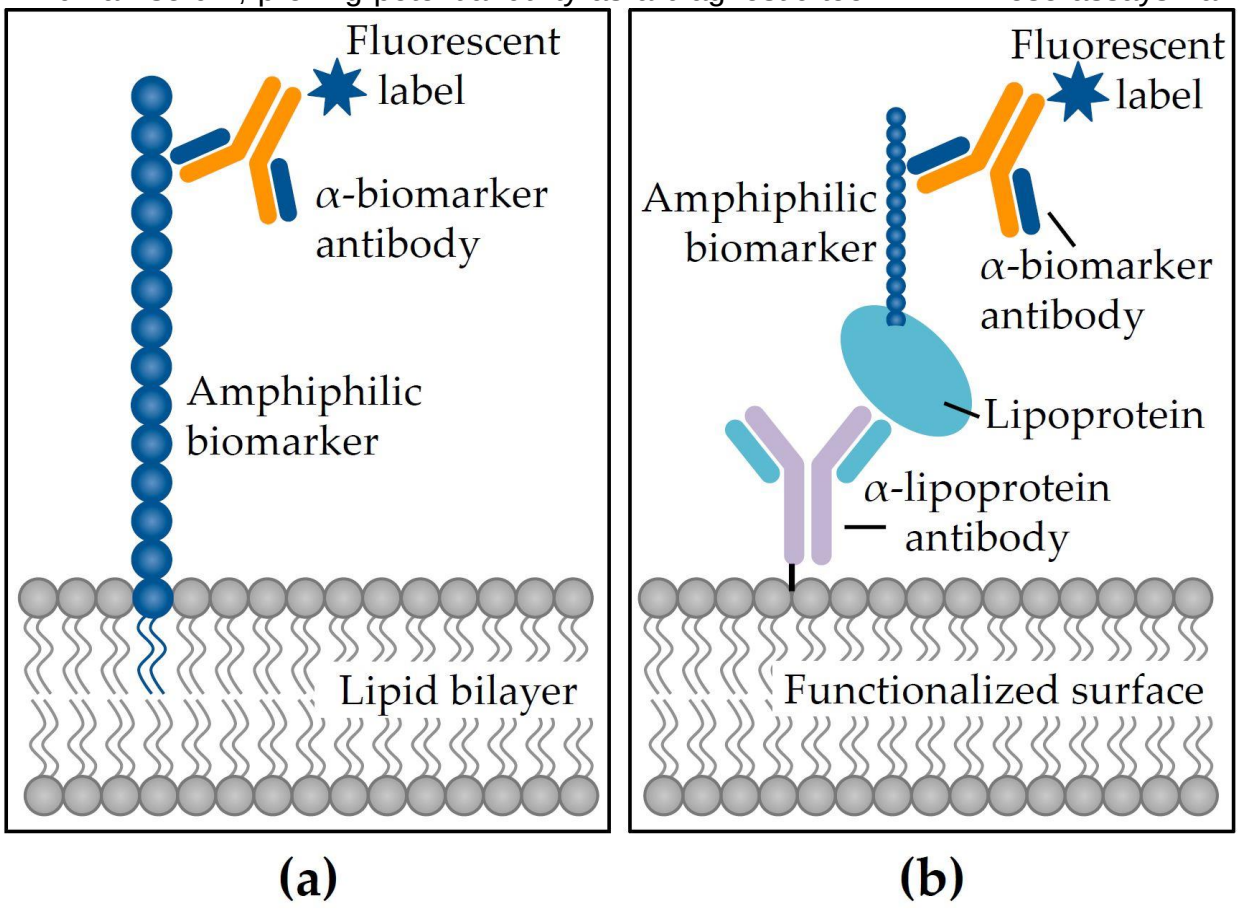

Figure 5.2. Immunoassay strategies to detect lipid and amphiphilic biomarkers using (a) membrane insertion or (b) lipoprotein capture.

been multiplexed for the simultaneous detection of several biomarkers[364]. However, the main disadvantage of using labeled reagents is the time and cost of the labeling process, and shelf life of the labeled ingredients[370].

Electrochemical biosensors detecting lipids

Electrochemical sensing is a label-free method where an electrode is used to directly detect associated reactions[371]. Electrochemical biosensors have had the greatest commercial success (glucose monitors) due to their low-cost, ease of use and miniaturization properties[372]. Amperometric sensors measure current typically as a result of electron transfer during the binding between a molecule, and chemically functionalized surface, as exemplified in the detection of LPS using redox diacetylenic vesicles on a sol-gel thin-film electrode[373]. Another example is the binding of cholera toxin to a glycosphingolipid ganglioside GM1 coated gold surface, which has been developed into a sensitive, low-cost sensor[374]. Potentiometric sensors measure potential or charge accumulation and have been used to detect lipid antigens[375] such as amphiphilic cholesterol using lipid films[376,377], without interference from ascorbic acid, glucose, urea or other proteins and lipids. In addition, label-free electrochemical biosensors have been developed for the detection of lipids such as low-density lipoprotein (LDL) with high sensitivity and specificity[378,379]. These sensors have also displayed long-term stability and high reproducibility with small sample volumes, which make for a promising clinical tool. However, a problem with electrochemical detection of biomarkers is specificity of detection in complex biological samples, as these platforms are more sensitive to even small perturbations in the background, which is always a possibility in clinical measurements.

Mechanical biosensors detecting lipids

Mechanical biosensors provide rapid and sensitive measurements without extensive sample processing, ideal for clinical application. The two main mechanical sensing techniques are based on cantilever and quartz crystal microbalances (QCM), both of which are label-free. QCM detects changes in resonance frequency on the sensor surface from increased mass due to analyte minding[372]. QCM has been used to observe the formation of supported lipid bilayers in real-time[380] and lipid exchange between a bilayer and vesicle[381]. The latter measures mechanical bending of a receptor-functionalized microcantilever upon binding of the target molecule, as demonstrated for LPS[382]. Another example is the measurement of the interaction between amyloid-β and the cell membrane as an early indicator of Alzheimer's disease[383]. A major drawback to cantilever sensors is that they often operate in air, rather than liquid samples, limiting their clinical utility

5.4 Lipid Biomarkers for Infectious Diseases

Rapid diagnosis is important to halt the spread of both endemic and emerging pathogens, as well as multi-drug resistant organisms[384]. Infectious diseases are caused by bacterial, viral, fungal and parasitic organisms and are routinely diagnosed using culture, microscopy, serology and genetic tests[385], all of which are time-consuming and performed by trained laboratory personnel. Several biosensors have been developed for diagnosis of infectious diseases[297], however all come with challenges that limit their application in the clinic. Many biomarkers associated with infectious diseases are amphiphiles, which are difficult to detect, especially in aqueous blood (**Table 5.2**).

Biomarker	Disease	Location	Interacting molecules	Reference
Lipopolysaccharide (LPS)	Sepsis	Blood	LBP, HDL, LDL, holotransferrin	386,387 388
	Urinary tract infection	Urine	n.d.	389
	Antimicrobial resistance	Any sample	n.d.	390
Lipoteichoic acid (LTA)	Sepsis	Blood	HDL, LDL, VLDL LBP, holotransferrin	387,391 388
Lipoarabinomannan (LAM)	Tuberculosis	Urine	n.d.	211
		Blood	HDL	72
Lipomannan (LM)	Bovine tuberculosis	Blood	HDL	280
OmpK36 porin	Antimicrobial resistance	Any sample	n.d.	390
Hemozoin (HZ)	Malaria	Blood	LBP, HDL, LDL, VLDL, apolipoprotein E, α-1-antitrypin	392

LBP: LPS-binding protein; HDL: high-density lipoprotein; LDL: low-density lipoprotein; VLDL: very low density lipoprotein; n.d.: not determined

Table 5.2. Select lipid and amphiphilic biomarkers used for the diagnosis of infectious diseases.

Sepsis

Sepsis is an infection of the bloodstream resulting in uncontrolled activation of the immune system[393]. Morbidity and mortality results from organ failure, which can be avoided with early and effective treatment, which in turn, requires rapid diagnostics[394]. There are several lipid and amphiphilic biomarkers associated with sepsis. LPS (also known as endotoxin) is a classic pathogen associated molecular pattern (PAMP) shed by Gram-negative bacteria. LPS activates the innate immune receptor, Toll-like Receptor 2, resulting in a cytokine cascade, which is the mechanism of endotoxic shock[395]. The presence of LPS in patient blood is a clear indicator of sepsis. However, detection of LPS in aqueous blood is complicated by the molecule's amphiphilic biochemistry, which drives it to associate with host carrier lipoproteins[396] and other molecules such as LPS-binding protein (LBP), high-density lipoprotein (HDL), low-density lipoprotein (LDL), very low-density lipoprotein (VLDL) and bactericidal/permeability-increasing protein[388]. Similarly,

LTA is an amphiphilic cell wall component of Gram-positive bacteria whose presence in blood also indicates sepsis. *Staphylococcus aureus* LTA in human blood preferentially binds to HDL (68%), then to LDL (28%), and minimally to very low density lipoprotein (4%)[391]. LBP also binds to LTA[388]. These associations complicate the detection of amphiphilic LPS and LTA in blood.

Mycobacterial infections

Lipoarabinomannan (LAM) is a biomarker for diagnosis of tuberculosis (TB)[179,180,185,397]. LAM is an amphiphilic heat stable lipoglycan, which forms an integral component of the mycobacterial cell wall[179,185], and is secreted during TB infection. LAM has proved to be an excellent diagnostic target especially in smear negative patients (HIV-positive, pediatric population and others). Some limitations of LAM include assay cross reactivity with common oral flora like Candida and Actinomyces that can result in lower predictive value of detection[92]. LAM assays can be improved using standardized sample processing methods and more sensitive sensor technology, as well as more specific antibodies[150]. LAM is readily detected in urine (88,89), but not in blood, likely because it associates with HDL in blood[72]. To this end, lipoprotein capture assays that utilize antibodies to target HDL have been used to pull down bound LAM in serum samples[56,72,280]. This method targets host pathogen interactions, can be applied to other amphiphilic biomarkers in blood[56]. Pathogen biomarker based measurements can be used in both human and animal hosts[211,280]. However, high cost of such technology, and biochemical nature of LAM are current challenges to the development of such assays[150].

Antimicrobial resistance

The global spread of antimicrobial resistance underlines the need for rapid and accurate assays for the determination of resistant organisms prior to antibiotic treatment. A common mechanism of antibiotics is inhibition of bacterial cell wall components, which are lipid or amphiphilic molecules[398]. Modifications of membrane lipids are common mechanisms of antimicrobial resistance in bacteria[399,400] and the direct detection of such changes would support effective treatment. In fact, targeting PAMPs that are highly conserved, such as membrane lipids, for molecular diagnostics has a tremendous benefit over approaches targeting more rapidly evolving aspects of bacterial physiology (i.e. PCR). MALDI-TOF MS has been used to detect antibiotic resistance caused by lipid alterations[390]. E.g.; detection of LPS alterations that reduce the molecules net negative charge resulting in resistance to antimicrobial peptides such as colistin, and OmpK36 porin loss in *Klebsiella pneumoniae* resulting in resistance to carbapenems. However, the initial cost of setting up a clinical MALDI-TOF system is prohibitive toward application in routine diagnostic settings.

Malaria

Hemozoin is an insoluble amphiphilic crystalline byproduct formed from the degradation of blood by parasites such as *Plasmodium falciparum*, the causative agent of malaria[392]. Hemozoin is released into circulation upon erythrocyte lysis, and its presence in patient blood is a direct indication of malarial infection[401]. Detection of hemozoin has mostly been achieved using microscopy and flow cytometry in blood[402]. The amphiphilic nature of hemozoin hampers its direct detection in blood due to sequestration by host immune

components[401] such as apolipoprotein E and LBP[392]. Methods like Lipoprotein capture can potentially be adapted for the detection of amphiphilic hemozoin in blood.

5.5 Lipid Biomarkers for Non-infectious Diseases

Non-infectious diseases including cancer and cardiovascular disorders are a result of a malfunction in normal physiological processes. Therefore, identifying specific biomarkers for diagnosing non-infectious diseases presents a major challenge. Rather than targeting a foreign molecule that is absent in a healthy patient, the diagnosis of non-infectious diseases often measures irregularities in expression of host-derived molecules[403,404]. Many lipid and amphiphilic molecules associated with human metabolism can be used as biomarkers when differentially detected in diseased versus healthy individuals (**Table 5.3**). Detection of such biomarkers can potentially be used to determine prognosis, monitor recurrence, evaluate disease progression, and predict a patient's risk of developing a particular disease[405].

Table 5.3. Select lipid and amphiphilic biomarkers used for diagnosing non-infectious diseases.

Biomarker	Disease	Location	Interacting lipoproteins	Reference
Cholesterol	Cardiovascular disease	Blood	HDL, LDL	406,407
	Cancer	Blood	HDL, LDL	408,409
	Preeclampsia	Blood	HDL, LDL	410,411
	Lipotoxicity	Blood	HDL, LDL	412
Triglycerides (TG)	Cardiovascular disease	Blood	LDL, VLDL	404,413,414
	Cancer	Blood	LDL, VLDL	408,409,415–420
	Preeclampsia	Blood	LDL, VLDL	410,411,421,422
	Lipotoxicity	Blood	LDL, VLDL	412,423,424
Cardiolipin (CL)	Cardiovascular disease	Blood	LDL, HDL, VLDL	425
	Cancer	Brain tissue,	n.d.	322,426

Prostate tissue	

HDL: high-density lipoprotein; LDL: low-density lipoprotein; VLDL: very low density lipoprotein; n.d.: not determined

Cardiovascular Diseases and Disorders

Cardiovascular diseases (CVD)[427] account for 17.5 million deaths, accounting for 31% of all deaths worldwide[427]. Heart attacks and strokes, mainly caused by a blockage that prevents blood from flowing to the heart or brain account for about 80% of all CVD deaths. In many cases, dyslipidemia, or abnormal levels of lipids in the blood, is a major mediator of CVD[428]. It is typically characterized by increased levels of total cholesterol, increased levels of low density lipoprotein cholesterol (LDL-C), increased levels of TG, decreased levels of high density lipoprotein cholesterol (HDL-C), modified function of lipid molecules, or a combination of some or all of these factors[428–430]. Cholesterol is a major component of cell membranes, and contributes to their structural integrity and fluidity[403]. Cholesterol is also a precursor of vitamin D and important steroid hormones such as progesterones, glucocorticoids (cortisol), androgens (testosterone) and estrogens[403,431]. Cholesterol homeostasis is critical to cardiovascular health. High cholesterol can raise CVD risk[407,432] by creation of sticky plaque deposits along arterial walls, eventually blocking blood flow, causing heart attacks and strokes. LDL and HDL are important carriers of cholesterol. Increased levels of LDL-C can cause cholesterol buildup in arteries, resulting in their narrowing, raising cardiovascular risk[433]. HDL is a scavenger, carrying cholesterol away from the arteries and back to the liver for breakdown[406]. A high TG level combined with high LDL-C and low HDL-C is linked with fatty buildups in artery walls[404,413,414].

Assessing CVD risk largely involves serum lipid profiling, focused on measuring total cholesterol, HDL-C, LDL-C, and TG levels[434], largely by use of labeled optical immunoassay platforms. For instance, the Alere Cholestech LDX® System combines enzymatic optical detection with solid-phase technology to rapidly and sensitively measure total cholesterol, HDL cholesterol, triglycerides and glucose in a finger prick of blood. Cholesterol is measured enzymatically in serum in a series of coupled reactions that hydrolyze cholesteryl esters and oxidize the 3-OH group of cholesterol, byproducts of which are measured colorimetrically[435–437]. TGs are measured enzymatically in serum *via* a series of coupled reactions that produce glycerol, which is oxidized using glycerol oxidase. H_2O_2, one of the reaction products, is measured colorimetrically[435]. In clinical practice, the standard measure of HDL is quantification of its cholesterol content after precipitation of apolipoprotein B (coat protein for LDL)[435]. Other techniques to determine HDL-C in serum include ultracentrifugation, electrophoresis, HPLC, precipitation-based method, direct measuring methods, and NMR[435,438].

LDL-C is often determined using the “Friedewald formula” which incorporates measured values for total cholesterol, HDL-C, and TG as: LDL-C = (total cholesterol) – (HDL-C) – (TG/5)[439]. This equation assumes that the ratio of TG to cholesterol is constant, which is not always the case. The Friedewald formula can thus underestimate LDL-C at lower levels of LDL-C, and higher levels of TG (>400 mg/dL)[440]. Modifications to the Friedewald formula have tried to address these shortcomings[440]. Direct LDL-C measurements (e.g. ultracentrifugation, electrophoresis, chemical precipitation, immunoseparation, and homogenous assays) are available, but standardization and extensive validations are needed for use in clinical measurements[440]. For clinical

sampling, serum lipid serum profiles are determined using diagnostic test kits, and analyzed with chemical automated continuous flow analyzers that use photometric and colorimetric testing (Hitachi 7180/7020 Hitachi Clinical Analyzers, Randox RX Series Clinical Chemistry Analyzers), and point-of-care devices (Alere Cholestech LDX microfluidic device system, Professional CardioChek PA test strip system, Accutrend Plus test strip system).

Many CVDs cannot be explained by these current standards[441], as many patients have lipid levels within the recommended range. Thus, there is a need for additional biomarkers for early diagnosis and prevention of CVD. Several biomarkers have been identified and are being explored for diagnostic potential. Cardiolipin is one such biomarker, reduced concentrations and altered composition of which have been implicated in cardiomyopathy associated with Barth Syndrome[442,443]. Diabetic cardiomyopathy is characterized by altered lipid composition and mitochondrial dysfunction[443,444] and reduced cardiolipin metabolism has been implicated here as well. Mitochondrial dysfunction due to reactive oxygen species effect has been shown to be associated with cardiac ischemia/reperfusion[306,308]. Mitochondrial cardiolipin have been proposed to undergo lipid peroxidation because of either their high content of unsaturated fatty acids or because of their location in the mitochondria[443,445]. Oxidized cardiolipin, a natural antigen that has pro-inflammatory effects, is also associated with atherosclerosis[443,446]. Current methods to detect the pro-inflammatory effects and thrombosis induced by cardiolipin rely on determination of antibodies against oxidized cardiolipin with commercially available standard enzyme-linked immunosorbent kits (e.g. Orgentec Anti-Cardiolipin Screen, Germany)[443,446].

Cancer

Cancer is the leading cause of death worldwide, with 8.8 million deaths in 2015[427]. Most cancers are initially diagnosed either because of the appearance of signs or symptoms of the disease, or via screening, which is not always available[447]. Definitive diagnosis is by biopsy of the affected tissue. The main treatments for many cancers are surgery, chemotherapy, and radiation therapy. The effectiveness of these treatments depends on early diagnosis, which results in a higher chance of survivability[447]. Therefore, there is a need for more research on molecular diagnostics based screening and early detection of cancer.

Dyslipidemia has been proposed to have an association with an increased risk of cancer, particularly breast and prostate cancers. Some studies exploring causal associations between serum lipids and breast cancer have observed increased levels of total cholesterol, TG, and LDL-C and decreased levels of HDL-C[408,415,417,420]. However these trends are not always consistent[448,449]. Similar observations were made for prostate cancer, with some studies showing an abnormal lipid trend, similar to breast cancer[149,408,409,418,419]. Other studies found no correlation or opposite trends[450–452]. Thus, we clearly do not have a good understanding of the pathophysiological effects of how lipids levels contribute to cancer. Methods to detect serum lipid levels are similar to those that are currently being applied to assessing cardiovascular disease, described in the CVD section.

Nobel laureate Otto Warburg claimed that cancer originated from irreversible injury to mitochondrial respiration, the structural basis for which is still unclear[453,454]. A possible hypothesis is that mitochondrial dysfunction induced by oxidative stress can cause lipid

peroxidation that contributes to the development of cancer[322]. One of the culprits implicated as a candidate for lipid peroxidation is cardiolipin[322]. Kiebish *et al*. found abnormalities in cardiolipin content or composition in several types of mouse brain tumors, compared to normal brain[322]. These abnormalities were closely associated with significant reductions in energy-generating activities[322]. ESI-MS showed that the cardiolipin composition was significantly different in prostate tissue isolated from normal individuals versus cancer patients[426].

More discovery efforts need to be undertaken to understand the roles lipids play in cancer[455–458]. Most of the findings suggest that there are abnormal levels of lipids- phosphatidylcholines, phosphatidylethanolamines, lysophosphatidylcholine, lysophosphatidic acid, LysoPI, ceramides, cholesteryl oleate- in biological samples from cancer patients than in normal ones[455–458].

Detection of lipidated biomarkers has been explored for many cancers. For instance, the carcinoembryonic antigen (CEA) has been implicated in a variety of cancers such as breast, colorectal, pancreatic and others[459–461]. Detection of CEA is mainly performed using targeted antibodies, and optical detection platform – labeled immunoassays. Studies have found that serial CEA measurements can detect recurrent colorectal cancer with ~80% sensitivity and 70% specificity, 5 months in advance of other diagnostics! CEA has been suggested to be the most frequent indicator of recurrence in asymptomatic patients and detection of this biomarker is the most cost-effective test for the preclinical detection of resectable disease. CEA is most useful for the early detection of liver metastasis in patients with diagnosed colorectal cancer. The biomarker is also valuable as a prognostic indicator for breast cancer[462]. In addition to optical colorimetric

measurements, radioimmunoassays have also been used for CEA measurement[463–467]. Our team has developed and validated the measurement of CEA in serum and nipple aspirated fluid from patients with abnormal mammograms using a fluorescence sandwich immunoassay on a waveguide-based optical biosensor platform, demonstrating picomolar sensitivity of detection of the antigen[368,369]. The challenges with CEA detection include the fact that the biomarker has been implicated with other non-cancerous conditions such as smoking, and that the presence of the biomarker in blood is not specific indicator of a type of cancer.

Another significant cancer biomarker family, the Carbohydrate antigens, are also amphiphilic and belong to the mucin-class of molecules, which promote cancer cell proliferation and inhibits anti-cancer immune responses[468]. Of these, CA125 is best known as a biomarker to monitor epithelial ovarian cancer and for the differential diagnosis of pelvic masses[469,470]. Serum levels of CA125 are routinely monitored in patients with ovarian cancer as prognostic indicators of cancer recurrence. Genway Biosystems has developed a colorimetric immunoassay for this biomarker, which is just one of several such assays available for this target. CA15-3 (MUC1) is yet another biomarker, which has been extensively implicated in a variety of cancers, and is routinely used as a prognostic indicator, and a measure of cancer severity[471]. Again, immunoassay methods, including radioimmunoassay methods are used for the measurement of these antigens in serum. These assays lack sensitivity and specificity, and are associated with a high false-positive rate, which needs to be addressed to increase their clinical utility. For example, Roche Laboratories has developed an electro-chemiluminescence assay for the detection of CA15-3 in blood. These immunoassays utilize a ruthenium-complex

and tripropylamine. The chemiluminescence reaction for the detection of the reaction complex is initiated by applying a voltage to the sample solution resulting in a precisely controlled reaction.

Detection of exosomes has been explored for many cancers. Exosomes are small heterogeneous extracellular vesicles (40 – 150 nm) released by most cell types in bodily fluids such as urine, plasma, saliva and breast milk[472,473]. While their exact function is still relatively unknown, the current theories are that they are involved in intracellular communication and cellular waste disposal[472,473]. The lipid composition of exosomes includes many different lipid classes as well as DNAs, RNAs and proteins. The exosomes are believed to contain the molecular constituents of the cell that they were derived from. In particular, exosomes have been identified as a potential biomarker for early detection and prognosis of cancer as they promote tumorigenesis, growth, progression and metastasis[472–475]. Exosome secretion by cancer cells is considerably up regulated compared to non-cancerous cells. RNAs (messenger RNA, microRNA, long non-coding RNA), DNAs (mitochondrial DNA, single stranded DNA, double stranded DNA), and proteins (small Rab family GTPases, annexins, survivin, CD9, CD 24 and CD34) are endosomal payloads that have been found to be elevated or altered in cancer cells compared to non-cancerous cells[474–476]. Quantitative real-time polymerase chain reaction, nucleic acid sequencing, antibody-based methods for detection and quantitation (e.g. Western blot, ELISA), nanoparticle tracking, dynamic light scattering, flow cytometry, transmission electron microscopy have all been applied to the detection and quantification of endosomes as well as the characterization of the contents of the endosomes[474–476].

Preeclampsia

Preeclampsia (PE) is a complex pregnancy disorder that is characterized by hypertension and proteinuria[477]. PE affects 2-8% of pregnancies worldwide. It is the most common pregnancy complication and is associated with high maternal and perinatal mortality. PE may be life-threatening for both mother and child, increasing both fetal and maternal morbidity and mortality[478,479]. In the mother, PE may cause premature cardiovascular disease, such as chronic hypertension, ischemic heart disease, and stroke[478,479]. Children birthed from preeclamptic pregnancies have an increased risk of stroke, coronary heart disease, and metabolic syndrome[478,479]. While the pathophysiology of PE remains unclear, this disorder is mediated abnormal placentation that trigger endothelial dysfunction, resulting in vasoconstriction, thrombosis, and end-organ ischemia[477]. Dyslipidemia has been shown to be associated with an increased risk of preeclampsia[411,480]. Several meta-analysis studies, which involved PE case-control studies as well as prospective cohort studies show that while this abnormal lipid pattern may involve increased TC, TG, LDL-C and decreased HDL-C, the results are not always consistent[410,411,421,422]. However, in many of these studies there seems to be a clear consensus of raised TC levels, resulting in hypertriglyceridemia[410,411,421,422]. It is still unclear whether hypertriglyceridemia is a risk factor for preeclampsia or whether there is any causal association between them[411,421,422]. More studies need to be done to understand the role maternal TG plays the pathophysiology of PE. Because PE display an abnormal serum lipid profile, many of the bioassays and methods developed for CVD are readily applied to test for PE. These bioassays and methods have been discussed in the CVD section. Recent mass spectrometry based lipidomic studies have revealed several potential lipid biomarkers associated with PE[319,481]. These include oxidized

cholesterol, cholesteryl ester, oxidized sphingomyelin, ceramide, glycerophosphocholine, and lysophosphatidylcholines.

Lipotoxicity

Lipotoxicity is a metabolic disorder characterized by excessive accumulation of fatty acids within the cell and has been implicated in the development of heart failure, obesity and diabetes[482,483]. Adipose tissues play a critical role in energy storage[484]. Adipocytes, the primary cells forming adipose tissue, contain cytosolic lipid droplets composed of a core of neutral lipids, including sterol esters and TGs, surrounded by a phospholipid monolayer[484–490]. Lipotoxicity is the abnormal accumulation of lipid droplets in non-adipose tissues, which leads to mitochondrial dysfunction, inhibition of ATP generation, and ultimately cell death by apoptosis[483,491,492]. Manifestation of lipotoxicity typically occurs in kidney, liver, heart and skeletal muscle[483]. For example, a disease estimated to affect 10 to 24% of the global population[493] is the accumulation of fat within the liver termed nonalcoholic fatty liver disease (NAFLD)[494]. NAFLD is characterized by increased hepatocyte accumulation of TGs within the cytosol[495] and can progress from fatty liver accumulation to liver fibrosis and cirrhosis[493,496]. Serum TG and cholesterol have been implicated as potential biomarkers for lipotoxicity and are currently detected using serum lipid profiling as described in the CVD section[412,423,424].

5.6 Discussion

Amphiphilic and lipidic molecules are significant mediators in a variety of biological processes associated with infectious diseases and non-infectious conditions such as

cancer and CVD. Many of the PAMPs secreted by bacteria are amphiphilic, as are a significant proportion of biomarkers associated with neurological processes. Many cancer signatures are also lipidated. Thus, ignoring this unique category of molecules will only limit our understanding of host-pathogen biology and disease processes. Because of the challenges in raising antibodies to such targets, and developing sensitive labeled assays, many of these biomarkers are not efficiently used in the diagnosis of disease. The biochemistry of these molecules should be considered in the design and execution of these assays. For instance, the conformation of the amphiphilic biomarkers changes dramatically depending on the milieu in which they are present (**Figure 5.3**), and the critical micelle concentrations of these molecules. Lipidated biomarkers adhere to plastic surfaces, decreasing sensitivity of their detection. These characteristics also manifest themselves in physiological samples such as blood. Amphiphilic molecules, depending on their critical micelle concentration, will either self-aggregate into micelles, or associate with carrier moieties such as HDL and LDL, making their direct and rapid detection more challenging (**Figure 5.3**). Understanding the biochemical characteristics of the amphiphilic targets and anticipating the impact of these features in physiological systems can allow for the development of tailored, sensitive assays for their detection.

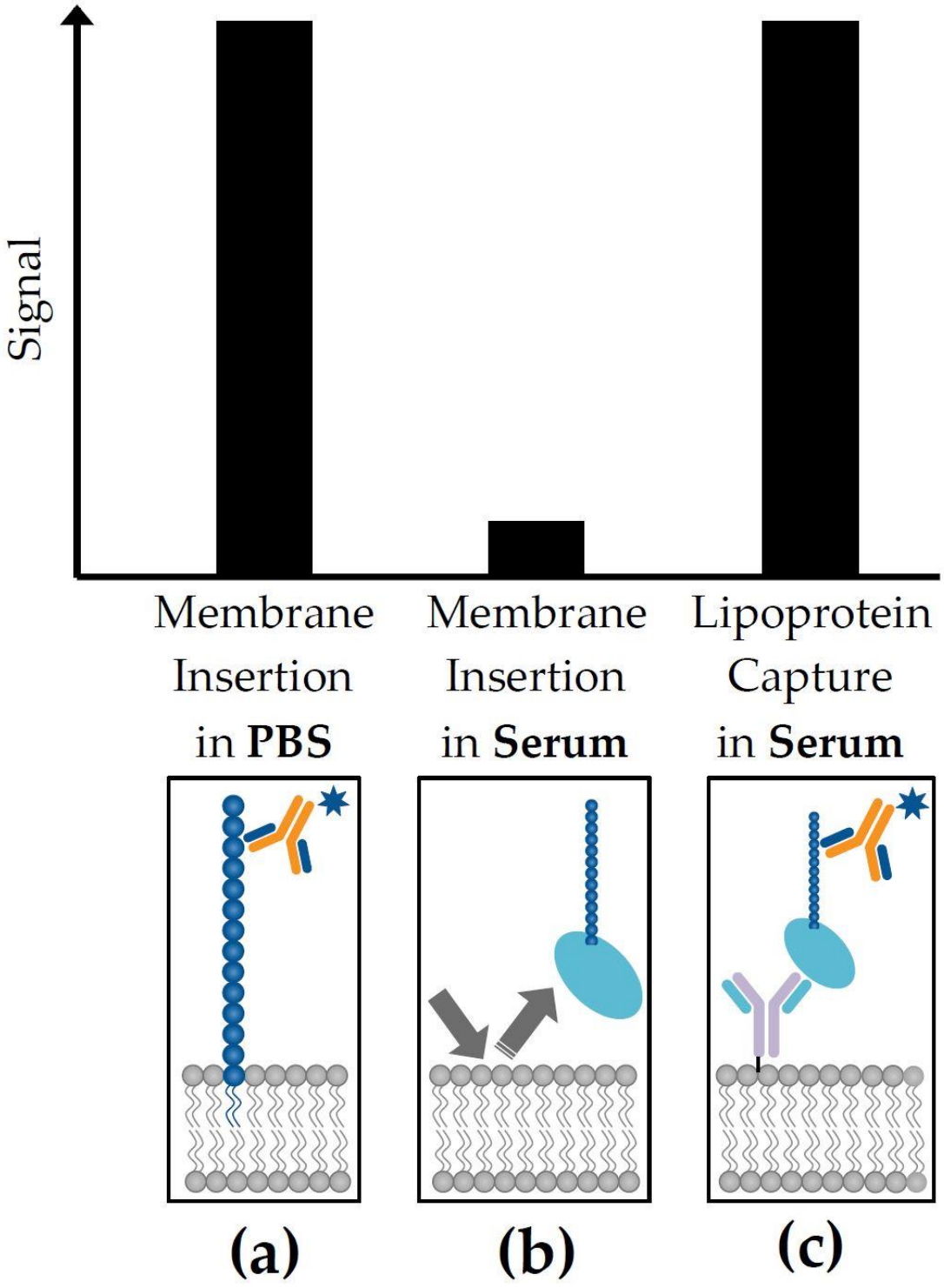

Figure 5.3. A comparison of the sensitivity of membrane insertion and lipoprotein capture technologies for the measurement of amphiphilic biomarkers based on the medium of presentation (serum *vs.* buffer). Biomarkers that are readily detected in (a) phosphate buffered saline (PBS) can be poorly observed in (b) serum when utilizing a membrane insertion assay strategy, because of the uptake of these signatures by host serum carrier molecules. This signal can be recovered if (c) lipoproteins are incorporated in the assay format, exploiting the host pathogen interaction for maximal sensitivity of detection.

Acknowledgments: The writing and compilation of this manuscript was supported by Los Alamos National Laboratory Directed Research Award (Mukundan and McMahon). Mendez was supported by Agriculture and Food Research Initiative Competitive Grant No. 2012-68003-30155 from the United States Department of Agriculture's National Institute of Food and Agriculture. The authors thank Aaron Anderson (LANL), Basil Swanson (retired Laboratory Fellow, co-inventor of the Lipoprotein capture methodology), Benjamin McMahon (LDRD PI) and Steven Graves (UNM) for their support.

Author Contributions: J.Z.K.-S., D.M.V., H.M.M., S.J. and H.M. contributed to the writing and editing of this manuscript.

Conflicts of Interest: The authors declare no conflict of interest.

Chapter 6.

Interaction of amphiphilic lipoarabinomannan with host carrier lipoproteins in tuberculosis patients: Implications for blood-based diagnostics.

Shailja Jakhar[1], Ramamurthy Sakamuri[1, 2], Dung Vu[1, 4], Priya Dighe[3], Loreen R. Stromberg[1], Laura Lilley[1], Nicolas Hengartner[g], Basil I. Swanson[3], Emmanuel Moreau[5], Susan E. Dorman[6] and Harshini Mukundan[1, *]

[1] Physical Chemistry and Applied Spectroscopy, Chemistry Division, Los Alamos National Laboratory, Los Alamos, New Mexico, United States

[2] Bako Diagnostics, Georgia, United States (current)

[3] Biosecurity and Public Health, Bioscience Division, Los Alamos National Laboratory, Los Alamos, New Mexico, United States

[4] Actinide Analytical chemistry, Chemistry Division, Los Alamos National Laboratory, Los Alamos, New Mexico, United States

[5] Foundation for Innovative New Diagnostics, Geneva, Switzerland

[6] Department of Medicine, Medical University of South Carolina, Charleston, South Carolina, United States

* Corresponding Author: Tel. +1 (505) 606-2122; Email: harshini@lanl.gov (H.M.)

6.1 Abstract

Lipoarabinomannan (LAM), an amphiphilic lipoglycan of the *Mycobacterium tuberculosis* cell wall, is a diagnostic target for tuberculosis. Previous work from our laboratory and others suggests that LAM is associated with host serum lipoproteins, which may in turn have implications for diagnostic assays. Our team has developed two serum assays for amphiphile detection: lipoprotein capture and membrane insertion. The lipoprotein capture assay relies on capture of the host lipoproteins, exploiting the biological association of host lipoprotein with microbial amphiphilic biomarkers to "concentrate" LAM. In contrast, the membrane insertion assay is independent of the association between pathogen amphiphiles and host lipoprotein association, and directly captures LAM based on its thermodynamic propensity for association with a supported lipid membrane, which forms the functional surface of an optical biosensor. In this manuscript, we explored the use of these assays for the detection of LAM in sera from adults whose tuberculosis status had been well-characterized using conventional microbiological tests, and endemic controls. Using the lipoprotein capture assay, LAM signal/noise ratios were >1.0 in 29/35 (83%) individuals with culture-confirmed active tuberculosis, 8/13 (62%) individuals with tuberculosis symptoms but no positive culture for *M. tuberculosis*, and 0/6 (0%) symptom-free endemic controls. To evaluate serum LAM levels without bias associated with potential differences in circulating host lipoprotein concentrations between individuals, we subsequently processed available samples to liberate LAM from associated host lipoprotein assemblies followed by direct detection of the pathogen biomarker using the membrane insertion approach. Using the membrane insertion assay,

signal/noise for detection of serum LAM was greater than that observed using the lipoprotein capture method for culture-confirmed TB patients (6/6), yet remained negative for controls (2/2). Taken together, these results suggest that detection of serum LAM is a promising TB diagnostic approach, but that further work is required to optimize assay performance and to decipher the implications of LAM/host lipoprotein associations for diagnostic assay performance and TB pathogenesis.

6.2 Introduction

Tuberculosis (TB) is the leading cause of global mortality associated with a single infectious disease, and is estimated to afflict 10 million people worldwide (2018), with ~ 1.3 million deaths[197]. The World Health Organization has identified the need for a non-sputum diagnostic test for TB, particularly extrapulmonary TB and pulmonary TB associated with low bacillary burden in airways, as can occur in young children and in individuals with HIV co-infection[67].

Accordingly, several biomarkers have been explored for the empirical diagnosis of TB, with lipoarabinomannan (LAM) arguably being the most studied[70,497,498]. LAM is an amphiphilic lipoglycan component of the *Mycobacterium tuberculosis* (MTB) cell wall that has in vitro immunomodulatory activity including activation of the Toll-like receptor 2 pathway[284,499,500]. Following the findings of Hamasur *et al.* that LAM was detectable in mouse urine within one day after intra-peritoneal injection of crude MTB cell wall extract, most clinical diagnostic work focused on detection of LAM in urine[85,94,501,502]. One lateral flow urinary LAM assay is now commercially available (Alere Determine™ TB LAM Ag, Abbott Biotechnologies). However, the sensitivity of the Alere assay is suboptimal – ranging from 42% in HIV-negative TB patients to 53% in TB patients with advanced HIV disease, a condition in which total mycobacterial burden can be very high and occult renal TB can be present[47,499,503]. The next generation Fujifilm SILVAMP TB-LAM (FujiLAM; Fujifilm, Tokyo, Japan), a lateral flow test incorporating high-affinity monoclonal anti-LAM antibodies and, has 30% better sensitivity compared to Alere LAM but needs further validation in clinical settings[141]. Several other LAM assay formats including FujiLAM with enhanced sensitivity are in development[85,141].

The amphiphilic biochemistry of LAM confers instability in aqueous milieu such as blood. Previous work from our team has shown that, in human blood, LAM associates with host lipoproteins such as high density lipoproteins (HDL). In aqueous blood, HDL is a stable lipidic assembly comprised of a core lipid nanodisc stabilized by coat apolipoproteins[73,141,503]. While LAM has been extracted from blood of TB patients[504], direct measurement of LAM in blood or serum has proved to be more elusive, and achieved mainly in individuals with advanced HIV disease[211,504,505]. We hypothesized that sequestration of LAM in host lipoprotein assemblies may contribute to the difficulty in detecting the antigen in blood. In parallel assessment of LAM in serum and urine from TB patients using an electrochemiluminescence immunoassay, Broger *et al.* showed substantially lower assay sensitivity in serum than in urine, but that matrix inhibition of serum could largely be reversed by heat treatment, resulting in substantial increases in LAM signal in tested sera[83].

To evaluate the impact of serum sequestration of LAM in host lipoprotein complexes, we measured serum LAM using two methods tailored for the detection of amphiphilic biomarkers in aqueous matrices (**Fig 6.1**) – lipoprotein capture and membrane insertion. The lipoprotein capture assay (**Fig 6.1**) relies on capture of host lipoproteins, exploiting their biological association with the pathogen amphiphile to "concentrate" LAM[72,506]. In contrast, the membrane insertion assay (**Fig 6.1**) is independent of that host lipoprotein/LAM association, and directly captures LAM based on its thermodynamic propensity for association with a supported lipid membrane which forms the functional surface of a biosensor[184,211,506]. Although both of these assays are platform ambivalent, we used enzyme linked immunosorbent assays (ELISA) and fluorescence

measurements from a waveguide-based biosensor platform developed at the Los Alamos National Laboratory for this study[72,365]. There are two limitations that impact the use of conventional plate-based methods for the detection of LAM. 1) LAM is an amphiphile and therefore, sticks to plastics and other surfaces, reducing assay reliability, sensitivity and reproducibility. 2) In clinical samples, LAM is already sequestered by host lipoproteins and not available in free-form[72]. It has to be detected in this conformation or liberated from it to facilitate detection. In this manuscript, we have attempted to develop methods that address both these limitations. Both the assays are performed on a surface functionalized with lipid bilayer, and therefore override the challenges of using plastic ELISA plates in concert with amphiphiles. Further, we have consistently shown that the use of the waveguide platform offers at least 10X greater sensitivity than conventional plate-based ELISA, which is an advantage when it comes to sensitive detection of pathogen antigens in complex clinical samples[285,369].

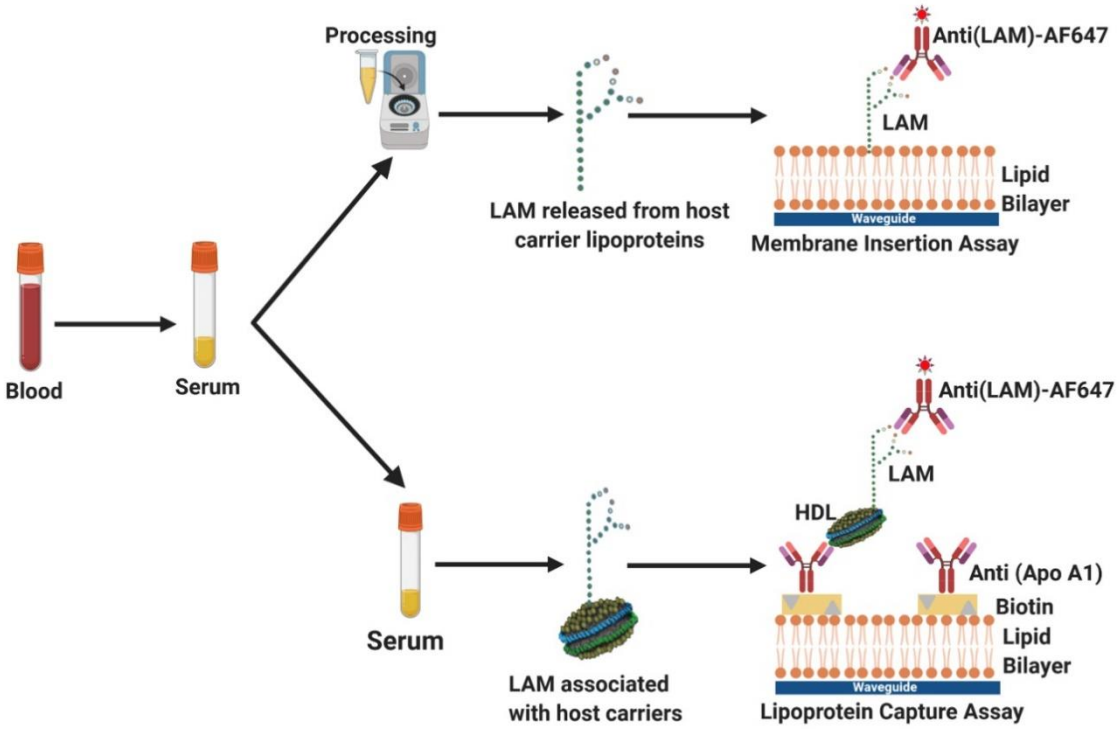

Figure 6.1.

Overview of Lipoarabinomannan (LAM) detection strategies. When LAM is associated with a host lipoprotein carrier such as HDL, detection can be performed using lipoprotein capture, which requires two antibodies, as well as prior knowledge of LAM-lipoprotein carrier associations. An antibody targeting apolipoprotein A1, the coat protein of HDL, is used to capture the nanodiscs on the assay surface, followed by detection with a fluorescently labeled antibody targeting LAM. In the absence of sequestration by a host lipoprotein carrier, LAM can be directly detected by membrane insertion, which requires only one antibody. The amphiphilic antigen, LAM, is allowed to partition into a supported lipid bilayer interface, followed by detection with a specific fluorescently labeled antibody. Graphic representations are not drawn to scale. Figure created with BioRender.com.

In this manuscript, we evaluated the use of the above two assays- lipoprotein capture and membrane insertion- for the direct detection of LAM in serum from carefully characterized samples from tuberculosis patients, and endemic controls.

6.3 Methods

Clinical specimens

This study used existing stored specimens that previously had been obtained from participants in Uganda for a study that evaluated the diagnostic accuracy of the Alere Determine™ TB LAM Ag assay[100]. That diagnostic accuracy study enrolled HIV-positive

adults suspected of having active tuberculosis based on the presence of at least one of cough, fever, night sweats, or weight loss. Individuals were excluded if they had received more than two days of anti-tuberculosis treatment. At enrollment, each participant provided two sputum specimens, each of which was cultured in liquid and solid media. One mycobacterial blood culture, performed using the Myco/F LYTIC system (Becton and Dickinson, Franklin Lakes, NJ), was performed for each participant at enrollment. A participant was considered to have active TB if *M. tuberculosis* was isolated in culture from any specimen. Neither Xpert MTB/RIF nor other nucleic acid amplification test was performed on sputum, since those tests were not available on-site at the time of study enrollment. At enrollment, blood was drawn into a BD Vacutainer serum separator tube (Becton and Dickinson), and serum was subsequently withdrawn and immediately frozen at -80°C until used for this study. For this exploratory study, one of the investigators (SED) selected specimens based on knowledge of participant microbiological classification, with intent to include a representative spectrum of participants with and without culture-confirmed TB. Samples were selected on the basis of culture results and sent to LANL in a double blinded fashion. Additionally, we used existing de-identified serum specimens from six Ugandan adults who did not have TB symptoms and were not known to be HIV-positive; no additional meta-data were available for these specimens. Samples were thawed immediately prior to use for the studies described here. If multiple assays were performed on a single serum sample, lipoprotein capture was performed first with the fewest possible freeze/thaw cycles to avoid degradation of lipoprotein carriers.

Ethics

This study was approved by ethics committees of Johns Hopkins University School of

Medicine, the Joint Clinical Research Centre (Kampala, Uganda), and Los Alamos National Laboratories. All participants provided written informed consent.

Reagents and materials

Anti-LAM monoclonal antibody (CS40), rabbit anti-LAM polyclonal antibody, and purified LAM (H37Rv) used in validation and optimization assays were obtained from Biodefense and Emerging Infections Resources (BEI resources, Manassas, VA). Anti-LAM monoclonal antibodies used in the reporter cocktail (see below) were a generous gift from the Foundation of Innovative New Diagnostics (FIND, Geneva, Switzerland). Biotinylated anti-ApoA1 antibody (ab27630) was purchased from Abcam (Cambridge, MA). Alexa Fluor 647 conjugated streptavidin (S21374), 1-Step Ultra TMB-ELISA Substrate Solution (34028), EZ-Link Plus Activated Peroxidase kits, Alexa Fluor 647 labelling kits, and polystyrene flat-bottom 96 well plates (Corning 9017) were purchased from Thermo Fisher Scientific (Waltham, MA). Bovine serum albumin (BSA, A7906) and Dulbecco's phosphate buffered saline (PBS, D1408) were obtained from Sigma Aldrich (St. Louis, MO). Human serum was obtained from Fischer Scientific Inc (Catalogue. No. BP2657100). 1, 2-Dioleoyl- sn-glycero-3-phosphocholine (DOPC) and 1, 2-dioleoyl-sn-glycero-3-phosphoethanolamine-N- (cap biotinyl) (sodium salt) (cap Biotin) were obtained from Avanti Polar Lipids (Alabaster, AL).

Waveguide-based optical biosensor

The waveguide-based optical biosensor was developed at Los Alamos National Laboratory and is described in detail elsewhere[365]. Waveguides were custom engineered

by nGimat Inc (Norcross, GA) and the surface chemistry was performed at Spectrum Thin Films (Hauppauge, NY). Silicone gaskets for waveguide assembly were from Grace Bio-Labs (Bend, OR) and Secure seal spacers (9 mm diameter x 0.12 mm deep) were from Electron Microscopy Sciences (Hat- field, PA). Glass microscope slides used as coverslips were purchased from Thermo Fisher Scientific (Rockford, IL).

Waveguide preparation and flow cell assembly

Single mode planar optical waveguides were used for functionalization as previously described[363]. Briefly, waveguides and glass coverslips were cleaned by sequential sonication in chloroform, ethanol and water (5 min each), followed by drying under argon stream and exposure to UV-ozone (UVOCS Inc., Montgomeryville, PA) for 40 min. Flow cells for immunoassays were assembled using clean waveguides and cover slips, which were bonded together with a silicone gasket containing a laser cut channel creating a flow cell. Following assembly, the flow cell was injected with 70 µl of lipid micelles (preparation described below) and then incubated overnight at 4 °C to facilitate vesicle fusion and lipid bilayer stabilization.

Lipid micelle preparation

1, 2-Dioleoyl-sn-glycero-3-phosphocholine (DOPC) and 1, 2-dioleoyl-sn-glycero-3-phosphoethanolamine-N- (cap biotinyl) (sodium salt) (cap biotin) were obtained from Avanti Polar Lipids (Alabaster, AL), resuspended in chloroform and stored at −20 °C. Lipid micelles for use in waveguide experiments were prepared as described previously[211]. Briefly, 2 mM DOPC and 1% cap biotinyl (mol/mol) were combined in a glass tube then

the chloroform was evaporated off under argon gas. Lipids were rehydrated in PBS, incubated in the dark for 30 min at room temperature with shaking (100 rpm) on an orbital shaker. Lipid solutions then underwent 10 rapid freeze/thaw cycles alternating between liquid nitrogen and room temperature water. Finally, lipids were probe sonicated for 6 min total (1.0 sec pulse on/off, 10% amplitude) using a Branson ultrasonic generator. Once the lipids were stabilized, the addition of biotin allowed for the bilayer integrity to be evaluated during immunoassay experiments by probing with 50–100 pM of a streptavidin Alexa Fluor 647 conjugate[184,363].

Waveguide-based assays

All incubations occurred at room temperature. Dilutions of all reagents were made in PBS. Flow cells were prepared as described above and the lipid bilayer was blocked for 1 hr with 2% BSA in PBS (w/v). All incubations were immediately followed by a wash with 2 mL of 0.5% BSA in PBS (w/v) to remove any unbound constituents. Incident light from a 635 nm laser (Diode Laser, Coherent, Auburn, CA) with power adjusted to 440−443 μW was coupled into the waveguide using a diffraction grading. The response signal was adjusted for maximum peak intensity using a spectrometer (USB2000, Ocean Optics, Winter Park, FL) interfaced with the instrument and an optical power meter (Thor Labs, Newton, NJ)[74].

The background signal associated with the lipid bilayer and 2% BSA block was recorded, and then the integrity of the lipid bilayer was assessed by incubation of 50−100 pM streptavidin, AF647 conjugate (Molecular Probes, S32357) for 5 min. The two control steps are performed in every experiment as intrinsic controls. The remaining assay steps

depended on the particular assay as described below. The antibodies used in this assay (FIND Clones 171 and 24) were labeled with AF-647, and the optimal combination of antibodies and their concentrations were determined using Enzyme Linked Immunosorbent Assays (S1 Fig., Section S1, Supplemental Information). The incubation times for the assays were optimized in all cases by standard measurements using LAM spiked into commercially procured human serum. The antigen titrations were performed on the waveguide-based biosensor.

Lipoprotein capture assay. Host HDL lipoproteins are nanodiscs of lipids that are held together by a coat protein, Apolipoprotein A1. The lipoprotein capture assay utilized an anti-apoA1 capture antibody for the capture of HDL lipoproteins onto the sensing surface. Following the test for lipid bilayer integrity (instrument controls), 10 nM unlabeled streptavidin was added and incubated for 10 min to saturate the biotin embedded in the lipid bilayer. Next, 100 nM of biotin conjugated α-apoA1 (α-HDL) antibody was added and incubated for 45 min, allowing for the capture antibody to adhere to the surface via biotin-streptavidin interaction. The surface is now functionalized with the capture antibodies for the lipoprotein capture assay. Prior to experimental measurement, however, the non-specific signal was determined by incubation of the fluorescence reporter antibody, FIND antibody cocktail labeled with AF647 (15nM each antibody, for 45 min), with control human serum on to the waveguide surface. This allows for the determination of the fluorescence signal associated with the interaction of the reporter antibody with the surface and control serum, in the absence of the antigen (no-antigen control).

Upon completion of the control measurements above, the antigen was added, and specific interaction between LAM and the reporter antibody cocktail was measured. To

generate standard LAM concentration curves, varying concentrations of MTB H37RV LAM (100, 250, 500, 1000, 1500, 2500, 5000 nM) were spiked into commercially procured human serum, and incubated for 24 hours to allow for complete association with lipoproteins. For clinical specimens, 200 µL of serum was used for each assay, and directly added to the flow cell. Upon incubation, the FIND reporter cocktail was again added, and the specific signal associated with the binding of LAM with the antibodies was measured via the spectrometer interface.

Three sets of controls were performed (n=25 each). The instrument background signal is an assessment of the biosensor function and bilayer integrity. No antigen control experiments were performed using control serum, in the absence of LAM. Specificity controls were performed using anti-LAM antibodies (FIND 171 and 24), and measuring the signal associated with their interactions with LAM functionalized on the biosensor surface. In all experiments, raw data were recorded as relative fluorescence units (RFU) as a function of wavelength (nm). The specific/non-specific ratio (S/N) was determined by taking the maximum RFU value for the specific signal, subtracting out the RFU value for the instrument controls, specificity and no-antigen controls (henceforth referred to as the background) and dividing this by the maximum RFU value for the non-specific signal minus the maximum RFU value for the background [**Equation (1)**].

$$S/N = \frac{(Specific - Background)}{(NS - Background)}$$

Equation (1)

Membrane insertion assay. For this assay, LAM is released from host lipoprotein complexes prior to detection via a pre-established sample processing method[310]. Briefly processing was performed using a modified single-phase Bligh and Dyer

chloroform:methanol extraction. Chloroform, methanol and LAM sample (either standard or clinical) were combined in a siliconized microfuge tube (Fisher Scientific, 02-681-320) at a 1:2:0.8 (v/v) ratio. The chloroform, methanol, and serum mixture was combined by gentle pipetting using low-retention pipet tips to avoid lipid adherence to the plastic, and then the mixture was centrifuged for 1 min at 2,000 x g to separate the proteins (supernatant) from the lipid/amphiphilic molecules (pellet). The supernatant was discarded and the LAM-containing pellet was resuspended in PBS by gentle pipetting. Following a 5 sec pulse spin to settle debris that could clog the septum of the biosensor flow cell, the LAM-containing solution was used as the biomarker sample for immunoassays.

There is no need for a capture antibody (reduces assay time by 40 min.) in the membrane insertion assay format, as it relies on the direct interaction of the LAM antigen (liberated from carrier assemblies as described above) into the supported bilayer interface. To generate standard concentration curves, LAM antigen was diluted to the desired concentration in control human serum in high-recovery glass vials (Thermo Scientific, Waltham, MA) C5000-995 and incubated overnight (18−24 hrs) at 4 °C to allow for association with lipoproteins in serum, as described above the lipoprotein capture assay. The samples were serially diluted, as described above for the lipoprotein capture assay. Each dilution was then subject to the sample processing method, and evaluated in the assay format in order to generate the standard curve. For the clinical samples, 50ul of each serum sample from patients and controls was subjected to the sample processing method, and used in the assay.

For this set of assays, the three control measurements described above (instrument controls, no-antigen control and specificity controls) were performed (n=10 each) as well, and the concentration of the reporter antibodies was the same as used for the lipoprotein capture assay above (15nM for 45 min.). For the experimental measurements, 200 uL of the processed sample was incubated in the flow cell, allowing for association of amphiphilic biomarkers with the lipid bilayer. Then the FIND antibody cocktail was added again, and incubated (15nM for 45 min) for assessment of the specific signal. Raw data were recorded as relative fluorescence units (RFU) as a function of wavelength (nm).

For both the lipoprotein capture assay and the membrane insertion assay, a S/N ratio > 1.0 was considered a positive result, and each sample measurement was repeated two times in order to assess reproducibility. The laboratory team performing LAM assays using participant specimens was blinded to participant group assignment and other clinical information, and it was held by one of the team members (SED) as described earlier.

For use of waveguide based sensor at the point of need, our team has simplified the waveguide-based optical biosensor for field deployment, and validated assay performance on this new portable (<10Lbs) instrument with optical components integrated and the software for functionality on a phone-based application. For easier use of sample processing method, we have developed and validated the first microfluidics device which is capable of performing lipid extractions within minutes at the point of need.

Statistical analysis

S/N ratios are presented as means ± standard deviation. Welch's t test and Mann Whitney U test was used to determine statistical significance. A significance level (P) of less than 0.05 was considered statistically significant (***P < 0.001, **P < 0.01, or *P < 0.05). Outlier analysis was performed using Chauvenet's criterion, which identifies the probability that a given data point reasonably contains all samples in a data set. LAM concentration curve and all significance tests were performed using GraphPad Prism8.

Limit of detection

The limit of detection (LOD) was obtained as described in **Equation (2)**. For a given sample concentration, the average non-specific signal for all replicates was obtained and added to three times the standard deviation (σ), multiplied by the sample concentration, and divided by the average specific signal for that concentration. Sample concentration and LOD will be in the same units, so if sample concentration is in nM then LOD will be in nM.

$$\mathrm{LOD} = \frac{(NS + 3\sigma)[\mathrm{Sample}]}{Specific}$$

Equation (2)

6.4 Results

Antibody selection and optimization:

For both the lipoprotein capture assay and the membrane insertion assay, antibodies were selected and concentrations determined by Enzyme Linked Immunosorbent Assays (ELISAs) (S1 Fig., Section S1). Briefly, antibodies were chosen based on sensitivity and specificity for LAM detection, and a combination of two different monoclonal antibody clones (24 and 171) yielded best outcomes for LAM detection in serum samples. These

two antibodies were used as a cocktail at 15 nM each for both the membrane insertion and lipoprotein assay formats.

Optimization of the lipoprotein capture assay: Fig 6.2a shows a representative spectral measurement on the waveguide-based biosensor[211,365] for the measurement of LAM (1.5 μM) spiked and incubated overnight in control human serum. RFU is plotted as

a

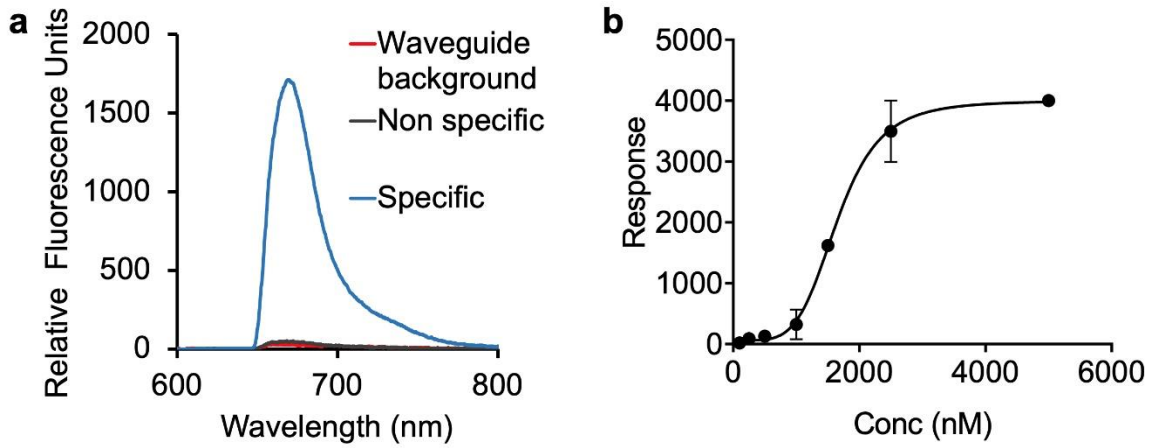

Figure 6.2. Assay optimization for the detection of LAM in human serum by lipoprotein capture assay. Measurement of LAM by lipoprotein capture assay, as a function of concentration. (a) Representative spectral measurement of LAM (1.5 □M) incubated overnight at 4 °C in control human serum, with the specific signal (Relative Fluorescence Units, RFU) from the detection α-LAM antibody (15 nM) as a function of emission wavelength (nm). The background and non-specific signals are measured before the addition of LAM. **(b)** Lipoprotein capture assay was performed for the detection of LAM spiked into control serum at various concentrations and incubated overnight to allow incorporation of the amphiphile into carrier assemblies. Results are plotted as RFU as measured on the waveguide-based optical biosensor, at increasing concentrations of LAM. All values given in **(b)** are the mean ± standard deviation derived from at least two independent determinations (n = 2). Statistical significance was determined by Welch's t test using Graph pad Prism 8.

function of emission wavelength (nm), as measured on the spectrometer interface associated with the instrument. LAM concentration curve (**Fig 6.2b**) shows a sigmoidal fit with a R^2 value of 0.999 and limit of detection- 69nM, which corresponds to a concentration of 1900 ng/mL LAM.

Optimization of the membrane insertion assay: Fig 6.3a shows a representative spectral measurement for LAM (0.5 uM, RFU), using the membrane insertion assay following extraction from spiked serum. The LAM concentration curve (**Fig 6.3b**) using this method shows a sigmoidal fit with a R^2 value of 0.998 and limit of detection- 3.3nM, which corresponds to a concentration of 114 ng/mL.

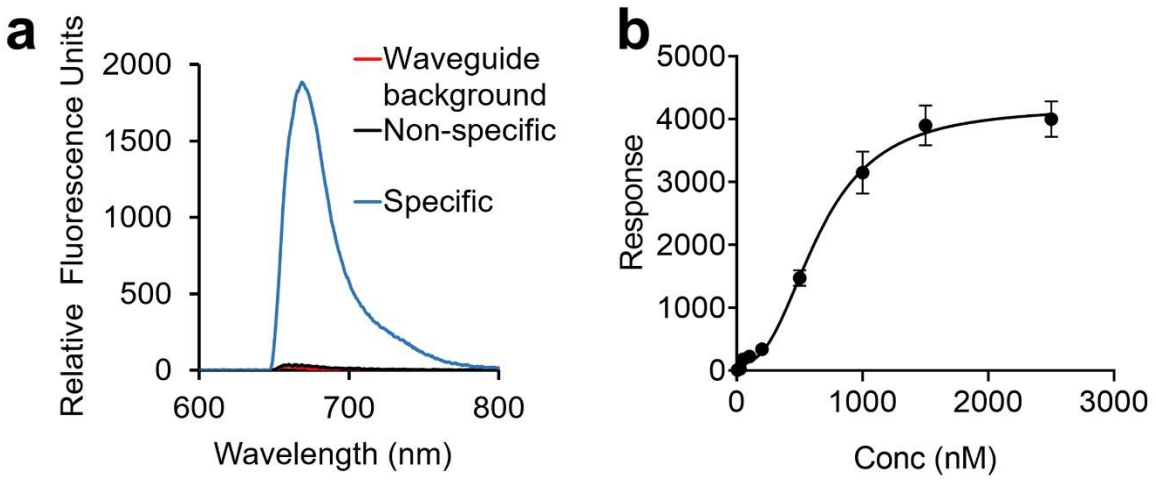

Figure 6.3. Measurement of LAM by membrane insertion assay, as a function of concentration. (a) Representative spectral measurement of LAM (.5 □M) incubated overnight at 4 °C in control human serum, with the specific signal (Relative Fluorescence Units, RFU) from the detection α-LAM antibody (15 nM) as a function of emission wavelength (nm). The background and non-specific signals are measured before the addition of LAM. (b) Membrane insertion assay was performed for the detection of LAM spiked into control serum at various concentrations and incubated overnight to allow incorporation of the amphiphile into carrier assemblies. Sample processing was done to remove lipoproteins. Results are plotted as RFU as measured on the waveguide-based optical biosensor, at increasing concentrations of LAM. All values given in (b) are the mean ± standard deviation derived from at least two independent determinations (n = 2). Statistical significance was determined by Welch's t test using Graph pad Prism 8.

Detection of LAM in clinical samples:

Using the lipoprotein capture assay, LAM signal/noise ratio (S/N) was > 1.0 in 29/35 (83%) culture-confirmed TB patients, 8/13 (62%) individuals with TB symptoms but no positive cultures, and 0/6 (0%) healthy controls (**Fig 6.4**). Mean S/N ± SD values were 3.8 ± 4.7, 1.9 ± 1.4, and 0.6 ± .20, respectively (**Table 6.1**).

To further understand the LAM lipoprotein capture assay performance, we stratified culture-confirmed TB patients by specimen source (sputum and/or blood) of positive MTB culture(s). Surprisingly, there was no association between MTB detected in blood culture, and LAM detected in serum. Serum LAM S/N was >1.0 in 10/12 (83%) culture-confirmed TB patients with MTB in blood cultures vs. 19/23 (83%) culture-confirmed TB patients whose blood culture was negative for MTB (relative risk 1.01, 95% CI 0.68, 1.28). Median (IQR) LAM S/N was 2.2 vs 1.3 among culture-confirmed TB patients with vs. without MTB in blood cultures (Table 1).

Table 6.1. Signal to noise ratios, by clinical group, for the lipoprotein capture assay

Clinical Group	**% with SNR >1.0 (n/n)**	**S/N Median (IQR)**	**S/N Mean (SD)**
Culture-confirmed TB (HIV-positive)	**83 (29/35)**	**2.2 (2.6)**	**3.8 (4.7)**
Sputum culture-MTB, blood culture MTB	100 (9/9)	2.2 (6.2)	5.0 (6.4)
Sputum culture negative, blood culture MTB	33 (1/3)	0.9 (5.7)	2.8 (2.7)
Sputum culture MTB, blood culture negative	83 (19/23)	2.5 (2.5)	3.5 (4.0)
TB symptoms but all cultures negative	**62 (8/13)**	**1.3 (0.4)**	**1.9 (1.4)**
Controls	**0 (0/6)**	**0.6 (2.3)**	**0.6 (.20)**

Abbreviations: TB, tuberculosis; MTB, *Mycobacterium tuberculosis*; S/N, signal to noise ratio; SNR, signal to noise ratio; IQR, inter quartile range; SD, standard deviation

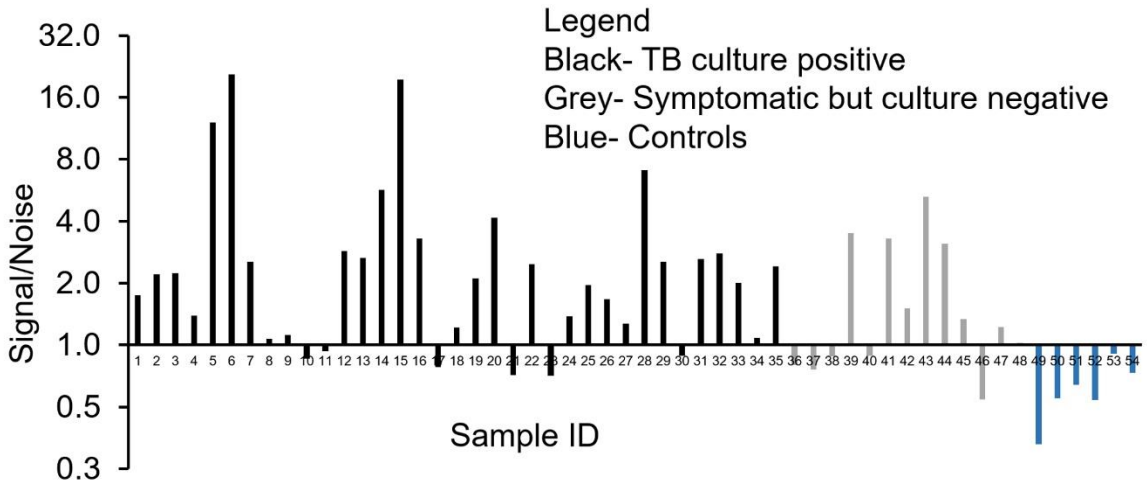

Figure 6.4. Direct detection of LAM in patient serum samples. Detection of LAM in clinical serum samples using the lipoprotein capture assay. Data are presented as the Signal/Noise (S/N) ratio with a value above 1.0 indicating a positive result. The measured S/N in sera from 54 patients from 3 different categories (see legend) is plotted. Results of urine testing using the Determine™ TB LAM Ag assay at the time of enrollment into the clinical study: patients 1-20 were positive, patients 21-48 were negative, and healthy controls 49-54 were not tested.

We hypothesized that, if host HDL concentration impacted the outcome of the lipoprotein capture assay, then use of a LAM assay approach that was independent of host lipoproteins – membrane insertion- might increase assay analytical sensitivity. **Fig 6.5a** shows the comparison of the two methods for detection of LAM in a serum sample spiked with 500 nM of LAM, with all other parameters held constant. Specific signal was significantly greater (x10) using the membrane insertion assay as compared to the lipoprotein capture assay (p value= 0.04, R^2= 0.99).

Subsequently we performed the membrane insertion and lipoprotein capture assay in parallel for the same eight clinical samples with sufficient volume for comparative testing

(**Fig 6.5b**). For serum from culture-confirmed TB patients, the S/N was uniformly higher for the membrane insertion assay than for the lipoprotein capture assay; no specific signal was detected in healthy control sera by either assay.

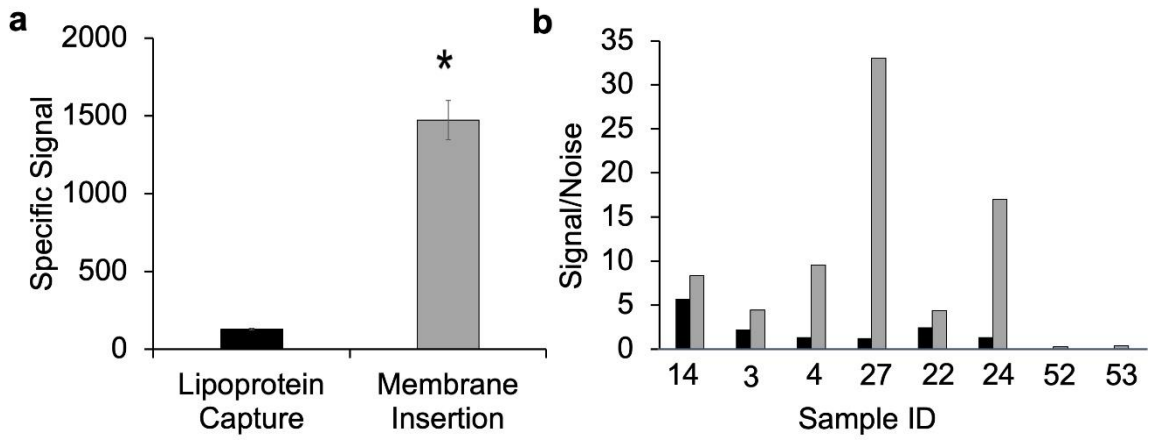

Figure 6.5. Comparison of Lipoprotein capture and Membrane Insertion. **(a)** Representative measurement of LAM (0.5 μM), by lipoprotein capture (black bars) and membrane insertion assay (grey bars), incubated overnight at 4 °C in control human serum, with the specific signal (RFU) from the detection of α-LAM antibody (15 nM). Values are the mean ± standard deviation derived from at least two independent determinations (n = 2). Statistical significance was determined by Welch's t test (*P<0.05). **(b)** Comparison of LAM detection signal by lipoprotein capture (black bars) and membrane insertion assay (grey bars) in patient serum samples. Data are presented as the S/N ratio with a value over 1 indicating a positive result. Samples 14, 3, 4, 27, 22 and 24 are positive for LAM by either blood or sputum culture methods, whereas samples 52, 53 are healthy controls.

6.5 Discussion

In this exploratory study, we compared and contrasted the use of two tailored methods for the detection of amphiphilic biomarkers in aqueous samples – lipoprotein capture and membrane insertion – for the measurement of serum LAM.

Both these methods were able to directly measure LAM in serum, with a demonstrated enhancement of sensitivity using the membrane insertion method.

In our initial evaluation in serum from adults whose TB status had been rigorously characterized by conventional mycobacteriology testing, we observed a clear difference between culture-confirmed TB cases and adult controls with regard to both proportion

with detectable LAM signal and LAM S/Ns. This finding demonstrates the applicability of these two tailored methods for serum amphiphilic LAM detection.

Clinically, there were two unexpected findings. Our working hypothesis – that serum LAM was associated with presence of MTB in blood cultures – was not supported by the lipoprotein capture assay data, as serum LAM was detected in the majority of culture-confirmed TB patients whose blood cultures were negative for MTB, and further, was not detected in the few patients whose blood cultures were positive for MTB. This outcome can be either because of an absence of serum LAM, or simply be associated with a failure to pull-down host lipoprotein/ failure to detect LAM due to LAM epitopes being hidden by the lipoprotein matrix.

In order to evaluate these two possibilities, we used a membrane insertion assay that is independent of host serum lipoproteins. Compared to lipoprotein capture, the membrane insertion assay resulted in higher S/N in all tested TB patients, but the magnitude of the difference varied from patient to patient. In all, our results indicate clearly that an assay modality that is independent of variable host factors (membrane insertion) is more sensitive than one that is dependent on them (lipoprotein capture). The enhanced sensitivity of membrane insertion compared to lipoprotein capture is based on the optimization assays and the 8 clinical samples. The increased sensitivity of the membrane insertion assay over lipoprotein capture assay, even in spiked samples, indicates some of the LAM associated with lipoproteins is not readily detected. Indeed, a variety of factors can impact host lipoprotein concentrations, including HIV/AIDS[507,508]. Because of insufficient volume of clinical samples, we were not able to quantitate lipoprotein concentrations to formally establish an association between serum concentrations of

these host lipoproteins and LAM S/N in TB patients, and this is a weakness of our study. HIV is associated with quantitative and qualitative lipid abnormalities including low levels of HDL, disordered HDL metabolism, and reduced Apo A levels[509–511]. It is intriguing to speculate that HIV effects on host lipoproteins might influence host handling of MTB LAM, thereby impacting TB disease pathophysiology in addition to impacting performance of our lipoprotein capture assay. A better understanding of the mechanisms and kinetics of LAM sequestration and clearance could have important implications for understanding tuberculosis and inflammation more broadly.

The second unexpected finding was that serum LAM was detectable (using the lipoprotein capture assay and threshold S/N > 1.0) in over half of TB symptomatic individuals whose sputum and blood cultures all were negative for MTB. There are two possible explanations for this: 1) These are false positive results, and detected signal in the absence of LAM; or 2) MTB LAM was present in serum, but sputum and blood cultures were falsely negative. Our existing data cannot tease apart these possibilities. However, we note that all of these individuals were enrolled with suspected TB disease, and that our assay did not have any false positive measurements in the control group (0/6). Further, the recognized sensitivity limitations of mycobacterial culture as a gold standard as well as the recognition that “TB” is nonbinary and represents a spectrum of conditions including incipient and subclinical TB, support further investigation of serum LAM as a biomarker[21,512].

There are important limitations of our exploratory study. The sample size was small, and adult controls all were HIV-negative whereas individuals with TB symptoms all were HIV-positive. Second, as noted above, serum specimen volumes precluded performance of

both LAM detection methods and HDL quantitation on all specimens, and therefore we were not able to comprehensively characterize the associations between serum LAM, host lipoproteins, and HIV serostatus. We hope to address these limitations in future clinical evaluations that are curated to address out needs.

In conclusion, we present two tailored assay strategies for the direct detection of amphiphilic serum LAM. Our findings highlight the role that host pathogen interactions play in pathogen amphiphile presentation and the need to account for these interactions in the design of diagnostic assays. Our findings also raise the intriguing possibility that serum LAM might be an informative TB biomarker of incipient or subclinical TB.

Acknowledgements

We thank Mr. Aaron S. Anderson and Dr. Jessica Kubicek-Sutherland for technical guidance, assistance and helpful discussions during the course of this work. We are grateful to the patients from Uganda for their participation in the study. The authors thank Dr. Mark Perkins, who was then at the Foundation for Innovative New Diagnostics and now, at the World Health Organization, for his help in establishing the initial collaborations essential for this work.

Funding statement

This work was supported by Los Alamos LDRD Directed Research Grant (Co-PI Mukundan) and grant R21 AI03599 to Dr. Susan Dorman from the National Institutes of Health. Los Alamos National Laboratory, an affirmative action equal opportunity employer, is managed by Triad National Security, LLC for the U.S. Department of Energy's NNSA, under contract 89233218CNA000001. The funder provided support in

the form of salaries for authors [HM, SJ and RMS from LDRD; SD and HM from NIAID], but did not have any additional role in the study design, data collection and analysis, decision to publish, or preparation of the manuscript. The specific roles of authors are articulated in the ‘author contributions’ section.

Author contributions

H.M., S.J. and S.D. designed the experiments. S.J., D.M.V., R.S., and P.D. performed experiments. S.J., D.M.V., R.S., E.M., S.D., and H.M. analyzed the data. S.J. and H.M. wrote the manuscript, with extensive input from S.D and E.M. E.M. assisted with procurement of key reagents and requirements for the study. S.D. led the clinical enrollment and recruitment for the study. All authors assisted in editing the manuscript.

Competing financial interests

Scientists from the Los Alamos National Laboratories, operated by the Triad LLC, that are authors on this manuscript, do not have competing interests, and are not consultants for any competing interests.

Ramamurthy Sakamuri was a post-doctoral researcher at Los Alamos National Laboratory when he conducted this research. Bako Diagnostics did not participate or were not involved in the research presented in this manuscript in any way. This does not alter our adherence to PLOS ONE policies on sharing data and materials.

Supporting information

S1 Fig. Antibody screening and selection by colorimetric sandwich immunoassays. Performance of antibody clones 24 (square), 27 (circle) and 31(triangle), using antibody 171 as the reporter, as assessed by sandwich colorimetric immunoassays is plotted as a function of concentration (n=3, per antibody, per concentration). Plot shows highest absorbance of clone 31, followed by 24, and finally, 27.

S1 Table. Selection of monoclonal antibodies

S2 Table. Patient demographics

S1 File. Supporting information

Chapter 7.

Serum lipoarabinomannan antigen as a biomarker for childhood tuberculosis- A feasibility study

Shailja Jakhar[1], Emmanuel Moreau[2], Susan E Dorman[3], Benjamin H. McMahon[4], Douglas J. Perkins[5], Harshini Mukundan[*1]

[1] Physical Chemistry and Applied Spectroscopy, Chemistry Division, Los Alamos National Laboratory, Los Alamos, New Mexico, United States

[2] Foundation for Innovative New Diagnostics, Geneva, Switzerland

[3]Department of Medicine, Medical University of South Carolina, Charleston, South Carolina, United States

[4]Theoretical Biology and Biophysics, Theoretical Division, Los Alamos National Laboratory, Los Alamos, New Mexico, 87545, United State

[5]Center of Global Health, Department of Internal Medicine, University of New Mexico Health Sciences Center, Albuquerque, New Mexico, United States

* Corresponding Author: Tel. +1 (505) 606-2122; Email: harshini@lanl.gov (H.M.)

7.1 Abstract

Tuberculosis (TB) in children remains underdiagnosed and underreported. Pediatric TB is paucibacillary and often disseminated, making traditional culture and sputum-based diagnosis ineffective. There are no gold standards for the diagnosis of TB in children, and there is an urgent need for effective detection methods to address this problem. Our team has utilized the mechanism of host-pathogen interactions between amphiphilic lipoarabinomannan (LAM), a biomarker released by *Mycobacterium tuberculosis*, with host lipoproteins in blood to develop a method for the direct detection of infection. Herein, we apply this assay format, membrane insertion, for the rapid diagnosis of pediatric TB using the ultra-sensitive waveguide-based optical biosensor developed at the Los Alamos National Laboratory. Our two-step approach involves a rapid sample processing step to liberate LAM from serum lipoproteins, followed by its detection on the biosensor by membrane insertion. Herein, we evaluate the measurement of serum LAM in 24 TB positive patients and age-matched controls using this approach. LAM signal-to-noise ratios were > 1.0 in 12/12 (100%) of children classified as TB positive by WHO clinical criteria, and 0/12 (0%) in symptom-free age-matched controls. To our knowledge, this is the first study demonstrating the direct measurement of LAM in serum from infected children. Additionally, this work provides preliminary evidence that the detection of LAM can be used to track disease progression. Further testing and qualification of these findings is required; however, these early findings offer promise for the ability of this approach to provide diagnostic solutions for pediatric TB.

7.2 Introduction

According to the World Health Organization (WHO), there were 1.2 million new cases of childhood tuberculosis (TB) and 233,000 TB-related deaths in 2019[3]. However, globally, only about 35% of all pediatric TB cases are accurately diagnosed, leading to underestimation of incidence and mortality, as evidenced by several studies[78,197,513,514]. Further, the mortality and morbidity associated with pediatric TB is particularly high among children co-infected with HIV[515].

Lack of reliable diagnostics for pediatric TB clearly contributes to the exacerbation of the severity of this problem. Microbiological confirmation of pulmonary TB is challenging, as it is difficult for young children to expectorate sputum, the sample needed for diagnosis[135]. In a study by Zar et al., only 25% of children (62/250) suspected of having pulmonary TB were positive by either smear microscopy (29/62) or culture (58/62)[171], which is consistent with the confirmation rates reported by other studies in the literature[516]. Even when sputum can be induced, smear microscopy is rarely positive in children due to the paucibacillary nature of the disease[171,517,518]. *M. tuberculosis,* which causes TB disease, is a Gram-indeterminate pathogen with a very high lipid content, making it difficult to culture and characterize in the laboratory. Mycobacterial culture, which has positivity rates of up to 30% and takes 6-8 weeks before results are available, is often required for confirmation of disease, thereby delaying the treatment decisions[75,171,518–521]. Therefore, the only accepted criteria for the diagnosis of pediatric TB are clinical symptoms reported by the WHO. Joel et al. demonstrated the efficacy of

this method, and their correlation with actual TB disease in a large pediatric study of 1394 patients[522].

Based on challenges associated with current TB diagnostics, the WHO has called out the need for biomarker-based tests to diagnose TB. GeneXpert MTB/RIF, which measures pathogen load in sputum samples *via* polymerase chain reaction (PCR), has been endorsed by the WHO for pulmonary TB diagnosis in children[523]. However, young children develop disseminated TB more often than adults do, making the reliance on a sputum-based approach challenging. Biomarker detection in urine or blood samples, which can be of value in individuals with extrapulmonary TB, would therefore be more useful than diagnostics based on sputum samples[75].

Lipoarabinomannan (LAM), an immunogenic glycoprotein component of the mycobacterial cell wall, is a biomarker that has been extensively researched for the diagnosis of TB[49,94,102,182] and a lateral flow urine LAM assay (Determine™ TB LAM Ag, Abbott Biotechnologies) is currently recommended by for use in HIV-positive adults with CD4 counts less than or equal to 100 cells·μL^{-1} that have symptoms of TB[142]. The test has a reported sensitivity of 45% and specificity of 92% in adult HIV-positive patients[278]. The increased use of LAM as a biomarker for diagnosis of TB in adults has led to the exploration of its potential use in pediatrics[83,182,212]. Studies in pediatric populations using lateral flow and immunoassay methodologies show a pooled sensitivity of 47%, and a pooled specificity of 82%[75–78,517,524]. Based on the above findings, the WHO has published guidelines for the use of LAM as a diagnostic biomarker in children[75,78,142,525]. However, there is a clear need to improve the sensitivity of this assay in this population. Recently, Nicol et al evaluated the FujiLAM SILVAMP TB LAM assay (Fuji LAM assay)

in urine samples from pediatric patients, and it showed a similar sensitivity to Alere LAM immunoassays (42% vs 50%) . However, the sensitivity of the Fuji LAM assay was significantly higher in both HIV-positive (60%) and malnourished children (62%). The specificity of Fuji LAM was also much higher compared to Alere LAM (92% vs 66%)[526]. Studies have also demonstrated that LAM concentrations decrease with anti-TB treatment[76], which suggests potential for this biomarker to be used as a prognostic indicator.

LAM is an amphiphilic lipoglycan, and previous work from our team has shown that it associates with human high- and low- density lipoproteins (HDL and LDL) in infected individuals. Thus, serum lipoproteins serve as carriers for lipidic and amphiphilic pathogen signatures such as LAM, and this interaction interferes with traditional methods for detecting the biomarker directly in aqueous matrices such as blood. Based on this understanding, we developed a rapid and gentle sample processing method to liberate the antigen from host lipoproteins. The antigen can then be directly detected using a tailored method for amphiphile detection called membrane insertion (**Figure 7.1**)[73,211,368,527–530]. This approach has been previously validated successfully for the detection of LAM in HIV-positive adults[531]. In this manuscript, we evaluated the ability of this tailored membrane insertion assay to detect LAM in serum from pediatric TB patients, with and without HIV, and age-matched controls. To our knowledge, this is the first preliminary study evaluating the detection of LAM in serum for pediatric TB diagnosis.

Whereas the detection assay is compatible with any immunoassay sensor, we have used an ultra-sensitive waveguide-based optical biosensor that was engineered at the

Los Alamos National Laboratory for the work presented in this manuscript[73,284,364,365,527,529].

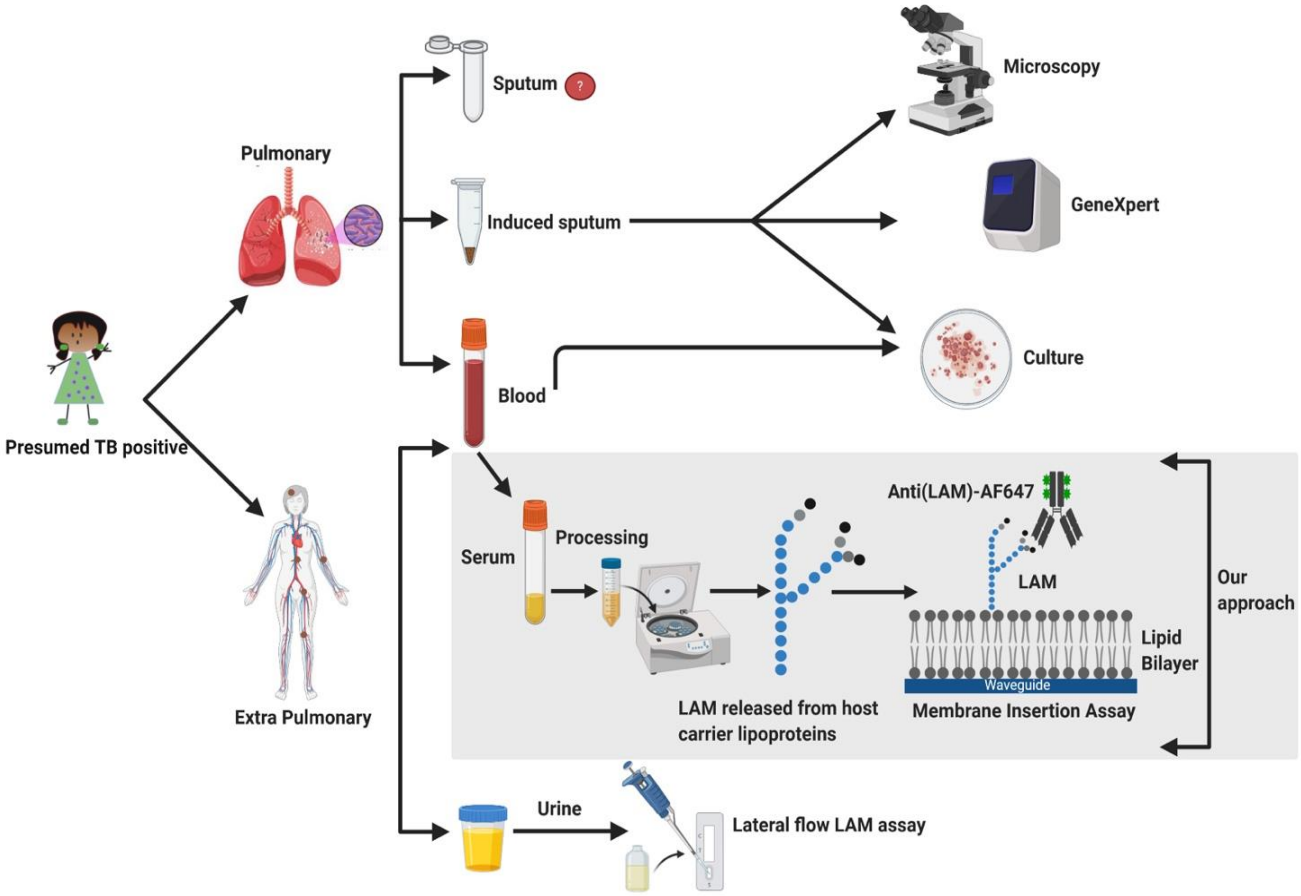

Figure 7.1. Overview of TB diagnostic pathways and LAM detection strategies. In current practice, a child suspected to be infected with TB is assessed on the basis of clinical symptoms and chest X-ray, and classified as either positive or negative. Further assessment of pulmonary vs. extrapulmonary TB is also made. For presumed pulmonary TB patients, sputum is analyzed by one of three methods: GeneXpert, microscopy, or culture. But, if sputum is unavailable, blood and urine sample is obtained, for culture and LAM detection, respectively. Membrane insertion assay (described in text, schematic representation in grey), presented in this manuscript, can be used as a reliable alternative for LAM detection from blood in individuals with both pulmonary and extrapulmonary TB. Graphic representations not drawn to scale. Created using Biorender.com.

7.3 Results

Optimization of the membrane insertion assay

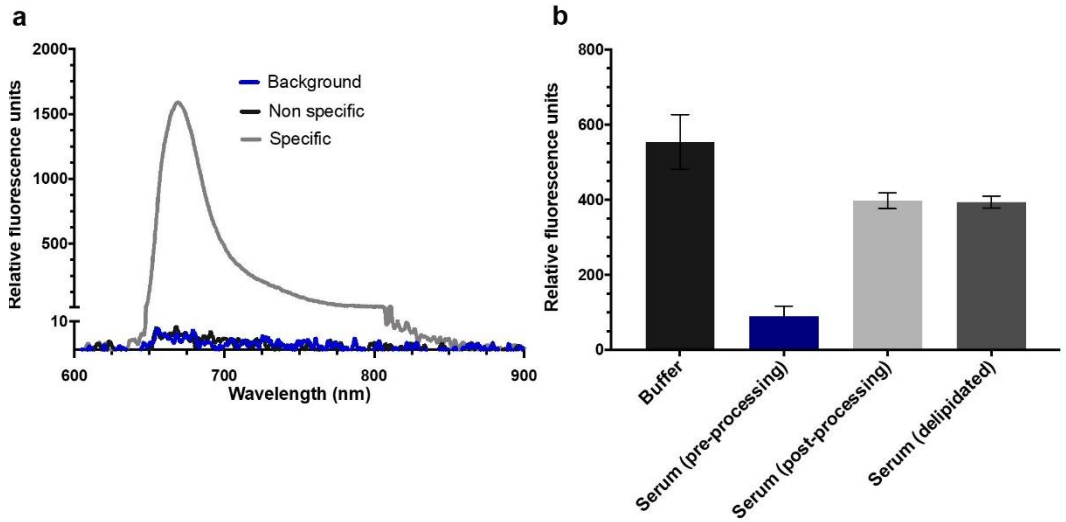

Figure 7.2. Optimization of detection of LAM in human serum by membrane insertion on the waveguide based optical biosensor. (a) Representative spectral measurement of LAM (500nM) in control human serum (grey curve), with the specific signal (Relative Fluorescence Units, RFU) from the detection of α-LAM antibody (15 nM) as a function of emission wavelength (nm). Background (blue) and non-specific signal (black) are shown. **(b)** Detection of LAM (100nM) in various conditions - spiked into buffer (black), c serum (pre-processing) (blue), serum (post processing) (light grey) and serum (delipidated) (dark grey). Results are plotted as RFU measured on the waveguide-based optical biosensor, as a function of experimental condition. All values given in **(b)** are the mean ± standard deviation derived from at least two independent determinations (n = 2). P value<.05. Statistical significance was determined by one way ANOVA using Graph pad Prism 9.

Figure 2a shows a representative spectral measurement for LAM (500nM), using the membrane insertion assay following extraction from spiked serum using our sample processing method. Relative fluorescence units (RFU) was plotted as a function of emission wavelength (nm), as measured on the spectrometer interface associated with the instrument. Background (measurement of intrinsic impurities in the waveguide itself, 3RFU, blue), non-specific background (interaction of anti-LAM antibody with serum, in the absence of LAM antigen, 5 RFU, black), and specific signal (signal associated with the interaction of the fluorescently labeled antibody cocktail with serum LAM, 1565 RFU, blue) are measured in every experiment. The signal/noise ratio (S/N) for the representative spectrum in Figure 7.2 a is 781 and was determined by taking the maximum RFU value for the specific signal, subtracting out the corresponding value for the instrument controls,

specificity, and no-antigen controls (henceforth referred to as the background) and dividing this by the maximum value for the non-specific (NS) signal minus the maximum signal intensity measured for the background [**Equation (1)**].

$$S/N = \frac{(Specific - Background)}{(Non\text{-}specific\ (NS) - Background)}$$

Equation (1)

Figure 7.2b assesses the efficacy of our sample processing method in extracting LAM sequestered by serum lipoproteins. 100nM of LAM spiked into PBS (not sequestered by host carriers) was used as positive control, and a S/N of 554 was measured by membrane insertion under these conditions. 100nM LAM was spiked into serum to mimic its presentation in host blood, and under this condition, the S/N measured decreases significantly to 89, and a signal intensity of 127 RFU was measured compared to 606 RFU in the positive control. This lost signal intensity is partially recovered when serum containing LAM (100 nM) is subject to sample processing. Under this condition, a signal intensity of 411 RFU and a S/N of 397 is observed. This is comparable to the signal intensity observed in delipidated serum (serum lacking host lipoproteins such as HDL and LDL), with a signal intensity to 406 RFU, corresponding to a S/N of 394. This demonstrates that the sample processing method is capable of recovering all the LAM associated with serum lipoprotein carriers.

Detection of LAM in pediatric serum samples

Table 7.1 collates the patient clinical and demographic information for 12 pediatric patients and 12 age-matched controls evaluated in this preliminary feasibility study. The

average age of children in both groups was 9.5 years, with 9/12 males, 3/12 females in TB positive group and 5/12 males, 7/12 females in TB negative group. Children in the TB positive group had co-morbidities such as HIV (4/12), malnutrition (4/12), malaria (5/12), sepsis or anemia (7/12), whereas none of the children in the healthy group had HIV or malnutrition. However, 4/12 children in the healthy group had malaria, and 3/12 had sepsis/anemia.

Table 1. Patient clinical profile and demographic information.

Characteristics		Total	TB patients, n(%)	Healthy controls, n(%)
Participants		24	12 (50)	12 (50)
Age (year)		9.5	9.7	9.3
Sex (male, female)		14 (58%), 10 (42%)	9 (75), 3 (25)	5 (42), 7 (58)
BCG vaccine		24	12 (50)	12 (50)
Comorbidities				
HIV infection		4	4 (33)	0
Malnutrition		4	4 (33)	0
Malaria		9	5 (42)	4 (33)
Sepsis/Anemia		10	7 (58)	3 (25)
Diagnostic correlation				
Positive (WHO criteria)		12	12 (100)	0
Serum LAM S/N	Mean (SD)		15.6 (21)	0.5 (0.2)
	Median (IQR)		8 (16)	0.5 (0.2)

Figure 7.3a shows the S/N calculated in pediatric serum samples for the measurement of LAM by membrane insertion, with a value of 1 or greater indicating a positive outcome. Among children who had confirmed TB on the bassis of the WHO

clinical criteria the S/N for LAM measurement was > 1.0 in 12/12 (100%). None of the healthy controls (0/12 (0%)) we positive for LAM measurement using this method. Mean S/N ± SD values were 15.6 ± 21 and 0.5 ± 0.2, respectively. The median was 8.0 and 0.5, respectively (Table 1). Thus, comparison of our assay results with WHO-based clinical criteria for diagnosis of TB yielded 100% corroboration with disease status, irrespective of co-morbidities.

Longitudinal serum samples were available from two patients, and we evaluated the LAM signal at both these time points, as shown in **figure 7.3b and c**. Both patients were classified as TB-negative by WHO clinical criteria when they visited the clinic for the first time, for their annual health assessment, otherwise referred to as the "well-child" visit. Interestingly, these two children returned for clinical assessment months later, and were then classified as TB-positive by WHO clinical criteria. Patient 1 (14 years old) came to the clinic with fever, night sweats, and had an abnormal chest X-ray during the second visit, which was 3 months after the first, and was diagnosed as positive for pulmonary TB and sepsis. Membrane insertion showed a higher LAM signal on the second visit **(Figure 7.3b)** (S/N= 7.0, black bar), compared to the first visit (S/N= 4.7, grey bar). Patient 2 (7 years old) returned to the clinic 2 months after the first visit, and presented with an abnormal chest X-ray, and was diagnosed with pulmonary TB and malaria. Patient 2 also had a household member who was diagnosed with TB and was subsequently initiated on TB treatment. Membrane insertion showed a positive signal on the second visit **(Figure 7.3c)** (S/N= 1.7, black), compared to the first visit (S/N= 0.80, grey) (**Figure 7.3b**). These longitudinal measurements further support the feasibility of using serum LAM measurements for diagnosis of pediatric TB.

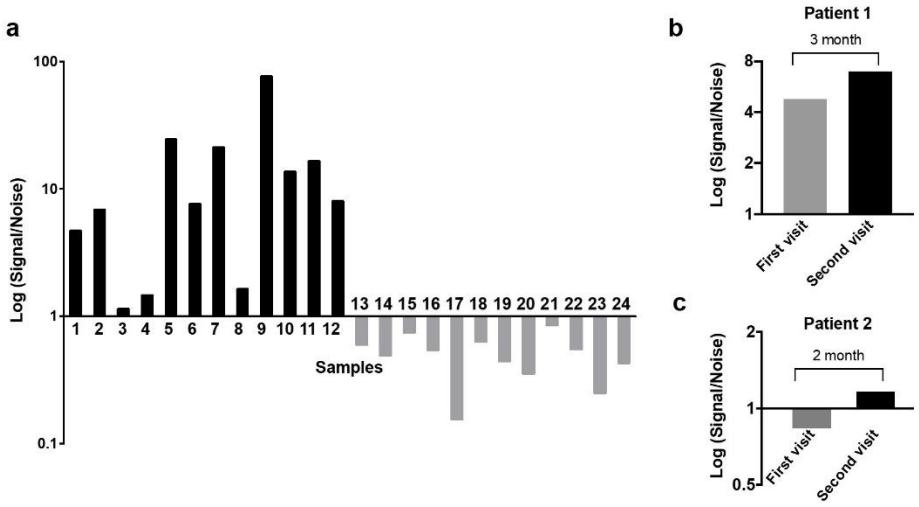

Figure 7.3. Direct detection of LAM in pediatric serum samples. Detection of LAM in clinical sera using membrane insertion. Data are presented as log(Signal/Noise (S/N)) ratio, with a value above 1.0 indicating a positive result. a) S/N measured in 24 pediatric patients. Black bars indicate TB positive, and grey bars indicate healthy children. b) and c) Longitudinal variability in LAM signal in patients between visits (n=2). Grey bars represent first visit, and black, second. The cross-bar indicates the period between the two sample collections.

7.4 Discussion

In this exploratory study, we assessed the feasibility of a tailored method for the detection of amphiphilic biomarkers in aqueous serum- membrane insertion – for the measurement of LAM in serum from children suspected of pediatric TB. Of the 24 individuals tested in this early assessment, we observed 100% corroboration with disease status. All twelve patients with TB disease (diagnosed by WHO clinical criteria) had co-morbidities such as HIV, malaria, anemia, malnutrition, and sepsis. This demonstrates that LAM can be detected in pediatric serum using this approach irrespective of presence of co-morbidities, garnering support for further investigation of this method as a diagnostic for pediatric TB.

We had longitudinal samples for two (2/24) individuals enrolled in this study. Both of them had provided samples during their annual well-visit, and then subsequently returned to the clinic following presentation of respiratory symptoms.

Interestingly, patient 1 tested positive for LAM during both the first and second visits, with a greater signal intensity evidenced during the second visit. This raises the possibility that the individual was already TB-positive but did not present with symptoms and was not diagnosed using the clinical criteria. It also suggests that LAM can be detected early in disease progression, allowing for timely diagnosis to guide treatment. This observation requires further evaluation and validation in a longer longitudinal cohort.

Patient 2 was negative during the well visit, and presented with a positive LAM signature during the second visit. This individual also had a TB positive household contact, which correlates with previous literature that the risk of secondary TB is greater among young children than in adults with a positive household contact[532–534].

With the lack of reliable gold standard diagnostics for pediatric TB, we compared our assay outcomes against the WHO's clinical method of diagnosis – which is the method used for clinical decision making in Siaya, Kenya. In future, we hope to study a larger pediatric cohort and compare the performance of membrane insertion against other diagnostic methods such as lateral flow assays for urinary LAM measurement, mycobacterial culture, and GeneXpert (Cepheid, USA). None of these methods has currently been accepted as the confirmatory diagnostic for pediatric TB, and has limitations when applied to this population, as discussed previously [75,78]. The relative

performance of these methods in children presenting with TB disease can offer further insights into pathophysiology and disease manifestation.

In conclusion, we present a tailored assay strategy – membrane insertion- which offers promise direct detection of amphiphilic serum LAM in pediatric populations, as evaluated in a small clinical cohort. Our findings highlight the importance of the amphiphilic biochemistry of LAM and the need to account for this property in the design of diagnostic assays, and warrant the need for follow on evaluations of novel biomarker based methods for pediatric TB.

7.5 Methods

Materials- Bovine serum albumin (BSA, A7906) and Dulbecco's phosphate buffered saline (PBS, D1408) were obtained from Sigma Aldrich (St. Louis, MO). Control human serum was obtained from Fischer Scientific Inc (Catalogue No. BP2657100), 1 mL aliquots were stored at −20 °C and thawed only once prior to use. Control delipidated human serum was obtained from Alfa Aesar (Catalogue No. BT-931), 1 mL aliquots were stored at −20 °C and thawed only once prior to use. 1, 2-Dioleoyl- sn-glycero-3-phosphocholine (DOPC) and 1, 2-dioleoyl-sn-glycero-3-phosphoethanolamine-N- (cap biotinyl) (sodium salt) (cap Biotin) were obtained from Avanti Polar Lipids (Alabaster, AL). Purified LAM (H37Rv) used in validation and optimization assays were obtained from Biodefense and Emerging Infections Resources (BEI resources, Manassas, VA) AND resuspended to 1mg/mL in sterile nanopure water. 60 µL aliquots were stored in low retention tubes at -80 °C and thawed immediately prior to use. Anti-LAM monoclonal antibodies used in the reporter cocktail (see below) were a generous gift from the Foundation of Innovative New Diagnostics (FIND, Geneva, Switzerland). Alexa

Fluor 647 conjugated streptavidin (S21374) was obtained from Thermo Fisher Scientific. LAM antibodies were fluorescently-conjugated using Alexa Fluor® 647 (AF647) antibody labeling kits purchased from Life Technologies (Thermo Fisher Scientific, Grand Island, NY) according to manufacturer instructions. Antibody concentration and degree of labeling was measured using a NanoDrop 1000 instrument (Thermo Fisher Scientific).

Clinical specimens

Clinical samples were obtained from pediatric patients (ages 1month- 17 years) recruited at the Siaya County Referral Hospital in western Kenya between 2016 to 2020 as part of a longitudinal study examining the pathogenesis of tuberculosis and related co-morbidities. Blood and sputum samples were collected. Serum samples were isolated from venous blood and stored at –80 °C until use. Samples were thawed immediately prior to injection in the waveguide assays. For membrane insertion assays, 50 µL of clinical serum sample was used.

Ethics

The scientific and ethical review committees of the Kenya Medical Research Institute and the institutional review boards of the University of New Mexico and LANL approved all protocols in this study involving human patients. All samples were collected following written informed consent by the parents or guardians of the patient, and patients participating in this study were treated according to the Kenyan Ministry of Health guidelines.

Waveguide-based optical biosensor

The waveguide-based optical biosensor was developed at Los Alamos National Laboratory and is described in detail elsewhere [365]. Waveguides were custom engineered by nGimat Inc (Norcross, GA) and the surface was coated with a 10 nm SiO_2 to enable functionalization at Spectrum Thin Films Inc. (Hauppauge, NY). Silicone gaskets for waveguide assembly were from Grace Bio-Labs (Bend, OR) and Secure seal spacers (9 mm diameter x 0.12 mm deep) were from Electron Microscopy Sciences (Hat- field, PA). Glass microscope slides used as coverslips were purchased from Thermo Fisher Scientific (Rockford, IL).

Waveguide preparation and flow cell assembly

Single mode planar optical waveguides were used for functionalization as previously described [211,363,364,368]. Briefly, waveguides and glass coverslips were cleaned by sonication in chloroform, ethanol and water (5 min each). Next, waveguides and cover slips were dried completely under argon gas and irradiated using UV-ozone (UVOCS Inc., Montgomeryville, PA) for 40 min and stored dry until use. Flow cells for immunoassays were assembled using clean waveguides and cover slips, which were bonded together with a silicone gasket containing a laser cut channel creating a flow cell. Following assembly, the flow cell was injected with 70 µl of lipid micelles (preparation described below) and then incubated overnight at 4 °C to enable vesicle fusion and lipid bilayer stabilization.

Lipid micelle preparation

1, 2-Dioleoyl-sn-glycero-3-phosphocholine (DOPC) and 1, 2-dioleoyl-sn-glycero-3-phosphoethanolamine-N- (cap biotinyl) (sodium salt) (cap biotin) were obtained from Avanti Polar Lipids (Alabaster, AL), resuspended in chloroform and stored at −20 °C. Lipid micelles for use in waveguide experiments were prepared as described previously [211]. Briefly, 2 mM DOPC and 1% cap biotinyl (mol/mol) were combined in a glass tube then the chloroform was evaporated off under argon gas. Lipids were rehydrated in PBS, incubated for 30 min at room temperature with shaking (100 rpm) on an orbital shaker. Lipid solutions then underwent 10 rapid freeze/thaw cycles alternating between liquid nitrogen and room temperature water. Finally, lipids were probe sonicated for 6 min total (1.0 sec pulse on/off, 10% amplitude) using a Branson ultrasonic generator. Once the lipids were stabilized, the addition of biotin allowed for the bilayer integrity to be evaluated during immunoassay experiments by probing with 50–100 pM of a streptavidin Alexa Fluor 647 conjugate [184,363].

Waveguide-based assays

All incubations occurred at room temperature. Dilutions of all reagents were made in PBS. Flow cells were prepared as described above and the lipid bilayer was blocked for 1 hr with 2% BSA in PBS (w/v). All incubations were immediately followed by a wash with 2 mL of 0.5% BSA in PBS (w/v) to remove any unbound constituents. Incident light from a 635 nm laser (Diode Laser, Coherent, Auburn, CA) with power adjusted to 440−443 μW was coupled into the waveguide using a diffraction grading. The response signal was adjusted for maximum peak intensity using a spectrometer (USB2000, Ocean Optics, Winter Park, FL) interfaced with the instrument and an optical power meter (Thor Labs, Newton, NJ) [74].

The background signal associated with the lipid bilayer and 2% BSA block was recorded, and then the integrity of the lipid bilayer was assessed by incubation of 50−100 pM streptavidin, AF647 conjugate (Molecular Probes, S32357) for 5 min. The two control steps are performed in every experiment as intrinsic controls. The remaining assay steps depended on the particular assay as described below. The antibodies used in this assay (FIND Clones 171 and 24) were labeled with AF-647, and the optimal combination of antibodies and their concentrations were determined using Enzyme Linked Immunosorbent Assays as described before[531]. The incubation times for the assays were optimized in all cases by standard measurements using LAM spiked into commercially procured human serum. The antigen titrations were performed on the waveguide-based biosensor.

Membrane insertion assay. Here, LAM is released from host lipoprotein complexes prior to detection via a pre-established sample processing method [310]. Briefly processing was performed using a modified single-phase Bligh and Dyer chloroform:methanol extraction. Chloroform, methanol and LAM sample (either standard or clinical) were combined in a siliconized microfuge tube (Fisher Scientific, 02-681-320) at a 1:2:0.8 (v/v) ratio. The chloroform, methanol, and serum mixture was combined by gentle pipetting using low-retention pipet tips to avoid lipid adherence to the plastic, and then the mixture was centrifuged for 1 min at 2,000 x g to separate the proteins (supernatant) from the lipid/amphiphilic molecules (pellet). The supernatant was discarded and the LAM-containing pellet was resuspended in PBS by gentle pipetting. Following a 5 sec pulse spin to settle debris that could clog the septum of the biosensor flow cell, the LAM-containing solution was used as the biomarker sample for immunoassays.

Antibody selection criteria, methods to generate standard curve and limit of detection have been discussed previously[531]. Briefly, to generate standard LAM concentration curves, varying concentrations of MTB H37RV LAM (6, 25, 50, 100, 200, 500, 1000, 1500, 2500 nM) were spiked into commercially procured human serum, and incubated for 24 hours to allow for complete association with lipoproteins. Each dilution was then subject to the sample processing method, and evaluated in the assay format in order to generate the standard curve. For the clinical samples, 50ul of each serum sample from patients and controls was subjected to the sample processing method, and used in the assay.

Three sets of controls were performed (n=10 each). The instrument background signal is an assessment of the biosensor function and bilayer integrity. No antigen control experiments were performed using control serum, in the absence of LAM. Specificity controls were performed using FIND antibody labeled with AF-647 and measuring the signal associated with their interactions with LAM functionalized on the biosensor surface. The concentration of the reporter antibodies was 15nM for 45 min. For the experimental measurements, 200 uL of the processed sample was incubated in the flow cell, allowing for association of amphiphilic biomarkers with the lipid bilayer. Then the FIND antibody cocktail was added again, and incubated (15nM for 45 min) for assessment of the specific signal. In all experiments, raw data were recorded as relative fluorescence units (RFU) as a function of wavelength (nm). The specific/non-specific ratio (S/N) was determined by taking the maximum RFU value for the specific signal, subtracting out the RFU value for the instrument controls, specificity and no-antigen controls (henceforth referred to as the background) and dividing this by the maximum RFU value for the non-specific signal minus the maximum RFU value for the background [**Equation (1)**].

$$S/N = \frac{(Specific - Background)}{(NS - Background)}$$

Equation (1)

A S/N ratio > 1.0 was considered a positive result. The laboratory team performing LAM assays using participant specimens was blinded to participant group assignment and other clinical information, and it was held by one of the team members (DJP).

Statistical analysis

S/N ratios are presented as means ± standard deviation. Welch's t test was used to determine statistical significance. A significance level (P) of less than 0.05 was considered statistically significant (***P < 0.001, **P < 0.01, or *P < 0.05). Statistical analysis was performed using GraphPad Prism9.

Chapter 8.

A centrifugal microfluidic cross-flow filtration platform to separate serum from whole blood for the detection of amphiphilic biomarkers

Kiersten D. Lenz[1], Shailja Jakhar[ǂ 1], Jing W. Chen[ǂ 2], Aaron S. Anderson[1], Dylan C. Purcell[2], Mohammad O. Ishak[3], Jennifer F. Harris[3], Leyla E. Akhadov[3], Jessica Z. Kubicek-Sutherland[1], Pulak Nath*[2^], Harshini Mukundan*[1]

[1] Los Alamos National Laboratory, Physical Chemistry and Applied Spectroscopy, Los Alamos NM, USA

[2] Los Alamos National Laboratory, Applied Modern Physics, Los Alamos NM, USA

[3] Los Alamos National Laboratory, Biosecurity and Public Health, Los Alamos NM, USA

[^] Currently employed at Sandia National Laboratory, Albuquerque NM, USA

*Corresponding authors: pulakn.lanl@gmail.com and harshini@lanl.gov

[ǂ] These authors contributed equally to this work

8.1 Abstract

The separation of biomarkers from blood is straightforward in most molecular biology laboratories. However, separation in resource-limited settings, allowing for the successful removal of biomarkers for diagnostic applications, is not always possible. The situation is further complicated by the need to separate hydrophobic signatures such as lipids from blood. Herein, we present a microfluidic device capable of centrifugal separation of serum from blood at the point of need with a system that is compatible with biomarkers that are both hydrophilic and hydrophobic. The cross-flow filtration device separates serum from blood as efficiently as traditional methods and retains amphiphilic biomarkers in serum for detection.

8.2 Introduction

The separation of serum from whole blood is a necessary first step in many clinical diagnostic blood tests, since serum contains important biomarkers, whether autogenic or pathogenic, for disease diagnosis and monitoring[535–537]. Our focus is on the detection of amphiphilic bacterial biomarkers that are released into the host's blood stream rapidly after infection[72,211,283,529,538]. Early detection and specific treatment of bacterial infections is necessary to help prevent the spread of antimicrobial resistance, save lives, and reduce the chances of outbreaks. Ideally, diagnosis will occur at the point of need and provide rapid intervention solutions. The development of rapid, simple, automated, safe, and inexpensive processing of blood samples can therefore benefit many diagnostic assays.

We are working towards a universal diagnostic strategy for all bacterial pathogens, including the development of novel assays to quickly detect biomarkers indicative of

bacterial infection[285]. Our universal bacterial sensing strategy mimics innate immune recognition in the laboratory, facilitating diagnosis of all bacterial infection from a single clinical sample: blood. The bacterial biomarkers targeted by our assays are the same as those targeted by our human innate immune response, and are most often lipidated sugars (lipoglycans or glycolipids, such as lipopolysaccharide, lipoteichoic acid, and lipoarabinomannan). Previous work from our laboratory and others has shown that the amphiphilic biochemistry of these biomarkers causes them to be sequestered by host lipoprotein carriers, including high- and low-density lipoproteins (HDL and LDL)[72,73,506,528]. Because of this sequestration, it is necessary to liberate the amphiphilic biomarkers from their lipoprotein carriers in order to enable sensitive measurement. Detection can then occur via enzyme-linked immunosorbent assays (ELISA's), waveguide-based biosensor[211,283,529] or other methods[73].

The focus of the work presented in this manuscript is the separation of serum from blood within a microfluidic device that preserves the integrity of relevant amphiphilic biomarkers present in serum. Our current sample processing method, while reliable, requires trained personnel and a multi-step laboratory procedure[284]. For use in a point-of-care setting, sample preparation should be automated in order to save time and ensure user safety, while preserving sample quality[539]. The platform must be able to process small volumes of whole blood, have a low cost of production, and offer minimal loss of sample integrity during processing. It is also beneficial to have the ability to integrate additional processing steps as dictated by the specific application.

While there have been many reported microfluidic devices that separate serum from blood, most to our knowledge have emphasized the preservation of protein and nucleic

acid signatures[539–550]. Lipidic and amphiphilic biomarkers present a unique challenge, as they tend to adhere to many different surfaces, including certain plastics and dialysis membranes.

Centrifugal microfluidics is a promising area of research for the automation of a variety of processes, including biological assays and sample preparation[551–553]. The field is especially appealing for point-of-care and deployable devices, due to the fact that minimal instrumentation is needed, and the centrifugal force present is inherently effective for density-based separations[553]. This applies to our system, as the extraction of serum from blood is essentially a phase separation. We have applied the concepts of centrifugal microfluidics in order to develop a cross-flow filtration scheme for the gentle separation of serum from blood[552–554].

During the process of cross-flow filtration, the sample passes tangentially across a filter, which is achieved *via* the centrifugal force acting on the platform. Components smaller than the membrane's pores are driven through the filter as pressure increases, while larger components pass over the membrane surface[555]. In contrast, dead-end filtration can result in clumping of particles that clog the filter (**Figure 8.1**). Cross-flow filtration decreases the chances of clogging, which in turn decreases the chances of red blood cell (RBC) lysis. Lysis of RBCs is of concern, since the release of hemoglobin (a fluorescent molecule) from the cells can interfere with fluorescence-based detection methods[556–558].

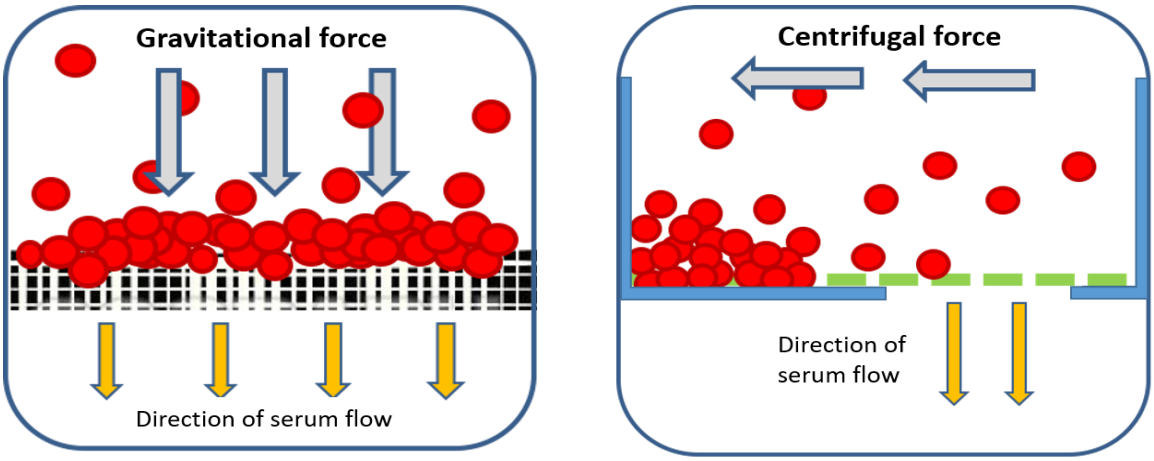

Figure 8.1. A schematic depicting the difference between the separation of serum from blood via dead-end filtration (left), which tends to cause clogging of membrane pores, and cross-flow filtration (right). Red circles represent RBCs

Based on these observations, we chose to develop a cross-flow centrifugal microfluidic platform for the separation of serum from whole blood that is compatible with the biochemistry of amphiphilic biomarkers. While this is not the first time a cross-flow filtration method has been integrated into a centrifugal microfluidic chip, it is the first to our knowledge to specifically preserve amphiphilic molecules within serum[559–561]. The design was optimized to purify serum to commercial standards, as validated by performing cell counts on all samples. Materials used for the fabrication of the centrifugal platform were compatible with our sample processing criteria, as confirmed by testing samples from the device on our waveguide-based optical biosensor for the retention of amphiphilic biomarkers of interest[211,365,366,529]. This development greatly simplifies the sample processing requirements for our biosensing assays and facilitates the transition of such technologies to the point-of-need. In addition, this method can be applied to other detection techniques that require the separation and preservation of

serum from whole blood, including in resource limited settings, inexpensively and rapidly.

8.3 Working Principle

The device consists of multiple chambers stacked on top of each other, separated by a membrane, according to the layout in **Figure 8.2a and 8.2b**. Four separation units are present on the centrifugal disc (**Figure 8.2c**), enabling multiple simultaneous experiments on one chip, which could be used for various assays or replicates of the same sample. The following steps take place within each separation unit (**Figure 8.2a**):

Step 1: Blood is introduced into the platform though the sample inlet. The ports are sealed, and the disc is placed on a motor to impart centrifugal force onto the sample at a given revolutions per minute (RPM). The centrifugal force causes the blood to flow away from the center of rotation. RBCs cluster toward the bottom of the sample reservoir in pellet trap #1 due to their density.

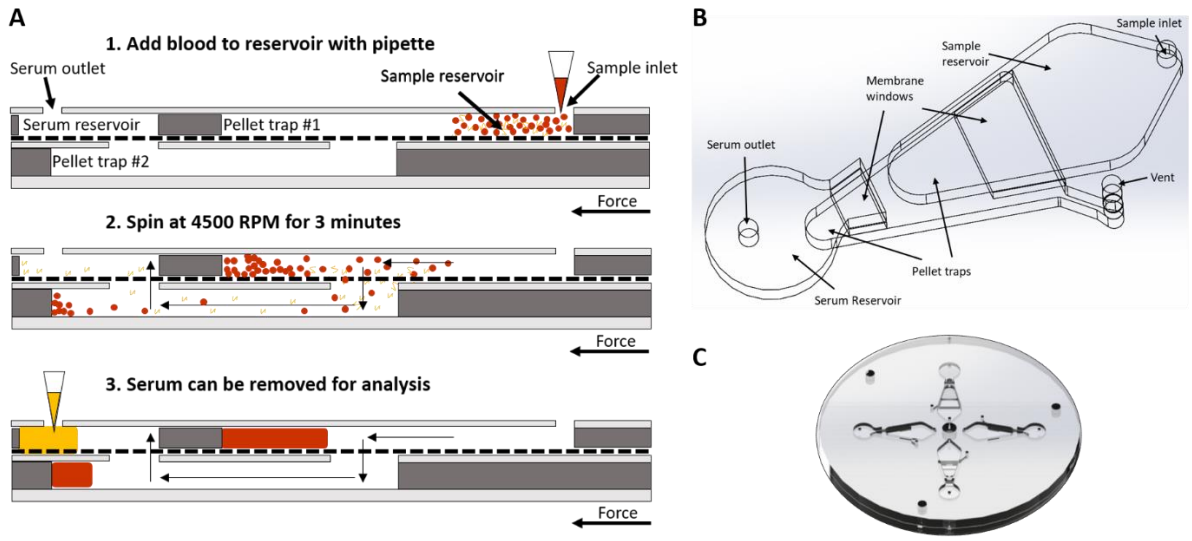

Figure 8.2. A) Edge view of one cross-flow filtration unit and separation concept; B) Top-view schematic of one separation unit; C) One completed disc with four separation units.

Step 2: As the pressure increases in the sample reservoir, serum is able to flow through the embedded membrane, while RBCs are largely prevented from flowing through due to their size. A small number of RBCs may squeeze through the pores of the membrane.

Step 3: Excess RBCs that went through the membrane are caught in pellet trap #2. As RBCs accumulate in pellet trap #2, the serum flows up into the serum reservoir, passing through another membrane section that serves as a secondary filtration step for RBCs. The serum is then collected through the serum outlet.

Our initial cross-flow filtration design included only one pellet trap, but we observed that some RBCs were able to get through the membrane. We realized we could easily integrate another filtration step, without changing our fabrication process, by adding another pellet trap to the design.

8.4 Methods

Device Fabrication

The cross-flow filtration platform consists of five structural layers of plastic and one thin plastic membrane layer. The device was fabricated using a rapid prototyping method involving laser-based micropatterning and lamination. A pressure-sensitive adhesive (91022, 3M^{TM}) was used to facilitate the lamination process. Layer schematics were drawn using SolidEdge10 2D drafting software. Alignment holes were included on all layers for assembly on a jig. The layers were cut using a CO_2 laser cutter (M360, Universal Laser Systems) from stock cast acrylic (McMaster Carr Supply Company), polycarbonate (McMaster Carr Supply Company), and membrane sheets (Sterlitech

Corporation). After cutting, the plastic layers were cleaned by bath sonication in water with dish soap for 15 minutes followed by a manual wash by wiping with isopropyl alcohol.

The membrane layers are Sterlitech Corporation's track-etched hydrophilic polycarbonate with 5 µm pores. The polycarbonate membrane was coated by the manufacturers with polyvinylpyrrolidone (PVP) to ensure hydrophilicity38. The membrane sheets are reported by the manufacturer to be between 3-24 µm thick, making them delicate to work with[562]. In order to obtain reproducible separation by the membranes, it was important to integrate suspended membranes that are flat. We have developed a method for membrane integration, described in the Electronic Supplementary Information (ESI), which consistently produces a surface that is free from visible indentations or imperfections.

Device Testing and Optimization

Device functionality was verified in a series of systematic experiments that determined ideal RPM (from 3500-5000, tested in 500 RPM increments), time (from 2-5 min, tested in 1 min increments), membrane type (polycarbonate and polyester; 2, 3, and 5 µm pore sizes), and geometric design parameters (pellet trap sizes, tested in 0.5 mm height increments) for phase separations. An example of these systematic testing schemes is described in the ESI. In order to test different conditions, the disc was placed on the jig, and 90 µL of whole sheep's blood was pipetted into each inlet hole. The inlets were designed to be the same diameter as the pipette tip in order to create a seal and prevent leakage. A one-sided custom polycarbonate tape was aligned on top of the disc to seal all ports and prevent the escape of fluids during processing. A microcentrifuge

(Scilogex) was used to test different RPM and time profiles. A central hole (**Figure 8.2c**) was cut into the microfluidic disc to fit over the rotor, and the cap from the microcentrifuge was securely fastened over the disc.

Blood/Serum Separation Efficiency

Serum purity, defined as the percentage of cells removed from whole blood, was determined by using a TC20 Automated Cell Counter (Bio-Rad Laboratories, Inc.). Cell counts from whole blood (Sheep; ThermoFisher Scientific, Inc.) were compared to counts on serum from the microfluidic device, and purity was calculated using the following formula[563]: **serum purity (SP) (%) =**

$$SP = \frac{(\#\ of\ cells\ in\ whole\ blood) - (\#\ of\ cells\ in\ serum)}{(\#\ of\ cells\ in\ whole\ blood)} \cdot 100$$

Cell counts were also performed on commercially-available sheep serum produced by ultracentrifugation (ThermoFisher), and serum separated from whole blood in our lab by traditional benchtop methods, for comparison. Results were analyzed by a Student's t-test for significance.

Biomarker Retention

We validated the ability of our microfluidic device to retain serum biomarkers of interest by comparing the efficacy of the process against the benchtop method developed by our team[211,283,364,366,368,529]. Because the bacterial biomarkers of interest are amphiphilic in nature, this step also ensured that the biomarkers were retained in the sample and not adsorbed to the plastic device materials.

Initial biomarker retention experiments were performed on the Los Alamos National Laboratory's waveguide-based optical biosensor, which is used for the detection of

biomarkers from Gram-negative, -positive, and -indeterminate bacteria[211,366,529]. The technology is described in detail elsewhere[211,365,366,368,529].

The ability to retain and subsequently detect lipoarabinomannan (LAM), the virulence factor associated with *Mycobacterium tuberculosis*, was chosen as an assessment of biomarker retention. LAM is an amphiphilic biomarker, and previous work has shown that the antigen associates with HDL[72,95]. We have evaluated the benchtop sample processing method for the extraction of carrier-associated LAM, followed by its detection on the waveguide biosensor using a tailored method called membrane insertion[366,529]. Herein, we compared benchtop and microfluidic methods by measuring the sensitivity of detection of LAM in serum.

In order to test biomarker retention, whole blood was spiked with LAM to a concentration of 0.05 µM and incubated overnight at 4°C. The next day, serum was separated from blood using either the microfluidic device or by traditional benchtop separation, depending on the assay. For extractions using the microfluidic device, 90 µL blood was pipetted into each inlet hole, and the disc was centrifuged at 4500 RPM for 3 minutes. This RPM and time combination was optimized as described earlier. For traditional methods, 500 µL whole blood was pipetted into a microcentrifuge tube and centrifuged at 4500 RPM for 3 minutes. The serum from each method of separation was analyzed by cell counting, and sample processing was finished by benchtop methods in both cases. 120 µL of serum was mixed by pipetting with 150 µL chloroform and 300 µL methanol in low-retention microcentrifuge tubes. The mixture was spun at 5500 RPM for 1 minute on a microcentrifuge, and the supernatant was discarded. The pellet containing biomarkers of interest was re-suspended in 120 µL of 1X PBS, which was

injected into the flow cell of the waveguide and incubated for 45 minutes at room temperature. After incubation, the flow cell was washed, and the specific signal was measured on the waveguide-based optical biosensor. Complete details for the waveguide-based assays can be found in the ESI.

8.5 Results

Device Functionality

We found that spinning the disc at 4500 RPM for 3 minutes yielded serum with the least amount of RBCs remaining in it. Sterlitech's polycarbonate membrane with 5 µm pores was the most effective at filtering out RBCs. Our design includes two pellet traps for RBC collection (**Figure 8.2**). Pellet trap heights of 5 mm and 2 mm for pellet trap #1 and #2, respectively, were found to be the most effective. A two-step filtration design was determined to be more successful at separating serum from blood when compared to a one-step method, as described in the Working Principle section. **Figure 8.3** shows cross-sections of the one-step vs. two-step filtration designs and the resulting phase separations.

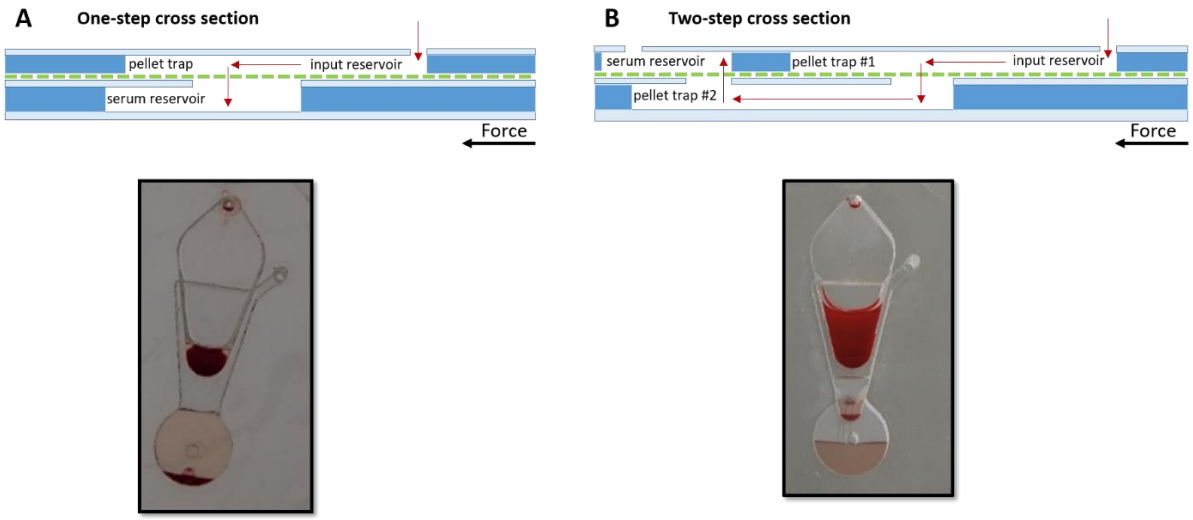

Figure 8.3. Schematics of one-step (**A**) vs. two-step (**B**) cross-flow filtration, with corresponding photos of phase separations on the microfluidic device; **A**) The one-step filtration method was ineffective at separating a large fraction of blood cells from serum; **B**) The two-step filtration method was successful at separating serum from blood.

Serum Purity

We compared the RBC count of serum separated on the microfluidic device to serum separated by traditional centrifugation and to commercially-available serum. The serum processed on our microfluidic platform had a statistically significantly lower cell count (P = 0.0179 for microfluidics vs. benchtop; P = 0.0128 for microfluidics vs. commercial serum). A bar graph of cell counts for whole blood compared to different methods of separating serum is shown in **Figure 8.4**. Serum purity was calculated for benchtop methods of separation and for the microfluidic separation. Both methods yielded a high percentage of cells removed from whole blood, greater than 99.99%.

We determined that our device is suitable for blood/serum separation, a common first step of many sample processing methods. The serum processed on the microfluidic device had a lower cell count than either the serum processed using the benchtop

separation method or commercially-available serum, which indicates higher serum purity.

Biomarker Retention

We validated biomarker retention for blood separated on the microfluidic chip and compared the results to our benchtop sample processing method. After serum from the microfluidic device was determined to have a significantly lower cell count (**Figure 8.4**)

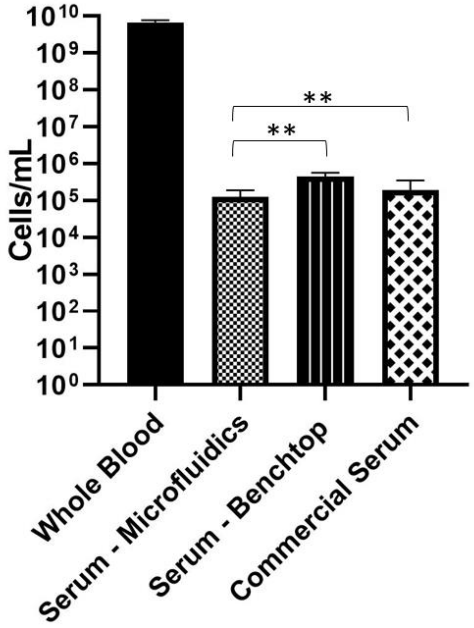

Figure 8.4. Average cell counts (n=3) on whole blood ($6.8x10^9$ cells/mL), serum processed on the microfluidic device ($1.27x10^5$ cells/mL), serum processed by benchtop methods ($4.45x10^5$ cells/mL), and commercially-available serum ($1.9x10^5$ cells/mL). ** indicates statistical significance.

than serum from the benchtop or commercially-available serum, we further validated the device by testing for biomarker retention in the sample. LAM was spiked in whole blood at 0.05 μM before separating serum from blood on the microfluidic device. Blood from the same aliquot was used for benchtop blood/serum separation in microcentrifuge tubes. After separation, the serum was analyzed on our waveguide-based optical biosensor, as described in the Experimental Section. There was no statistically

significant difference between LAM levels in serum processed on the microfluidic device vs. by benchtop methods (P = .9392), indicating that the microfluidic device preserves amphiphilic biomarkers present in serum as effectively as benchtop processing methods, and the device's materials are suitable for our application. A comparison is shown in **Figure 8.5**.

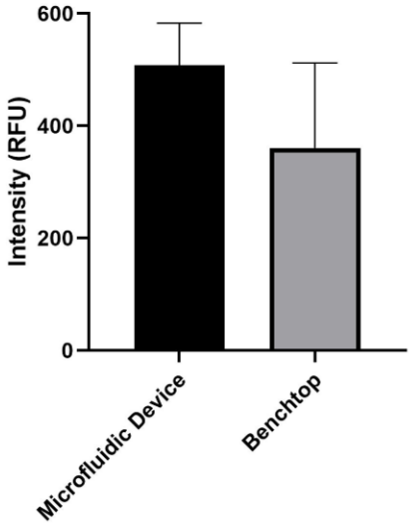

Figure 8.5. Signal intensity (n=3) of LAM from whole sheep's blood separated on the microfluidic device vs. benchtop methods. Higher intensity indicates higher concentration of biomarker retained in the serum sample. There was no significant difference between signals, indicating that our cross-flow filtration chip is suitable for the separation of serum from blood and subsequent detection of amphiphilic biomarkers. The fact that serum processed on the microfluidic disc yielded a similar signal intensity indicates that the microfluidic device preserves amphiphilic biomarkers present in serum as effectively as benchtop processing methods.

8.6 Discussion

We have integrated a multi-stage cross-flow filtration system into a centrifugal microfluidic platform to perform blood/serum separation. To our knowledge, this is the first cross-flow based microfluidic device capable of the separation of serum from blood with a documented ability to preserve lipidic biomarkers with the same efficiency as

benchtop processing. Serum processed on our device contained fewer RBCs when compared to serum separated using benchtop methods and to commercially-available serum. The serum separated on our microfluidic chip was over 99.99% pure. There was no significant loss of signal for detection of the model biomarker of interest, LAM, when compared to benchtop methods of separation, indicating the suitability of our device for amphiphilic and lipidic signature retention.

This method of blood/serum separation offers several advantages. The platform requires only 90 µL of whole blood, which reduces invasiveness and is of importance when working with potentially dehydrated patients at the point-of-care. It is simple to manufacture, disposable, and does not rely on pumps or valves for fluidic movement. It does not interfere with amphiphile detection as validated on our optical biosensor, nor does it require the dilution of blood. The chip itself is modular, as shown by the decision to use two pellet traps instead of one. This highlights the ease with which the design can be adapted for other phase-separation applications, without changing the manufacturing process we developed. Finally, the platform is a promising design for the complete automation of sample processing at the point-of-care, whether for bacterial biomarkers or other lipidic signature.

Data availability

The datasets generated during and/or analyzed used in this manuscript are available from the corresponding author on reasonable request.

Competing interests

The authors declare no competing interests.

Acknowledgements

This work was supported by the Los Alamos National Laboratory, Exploratory Research Project (Engineering category, PI Mukundan); and Defense Threat Reduction Agency (DTRA R-00634-19-0 - DOD: Fieldable Automated Biosensor for Universal Diagnostics and Discriminating Bacterial vs. Viral Pathogens, PI Mukundan), program manager, Dr. D. Dutt. Many thanks to Dr. Kirsten McCabe, LANL program manager and Dr. Caitlin Coob, DTRA program administrator, for their support with this work. Many thanks to Aneesh R. Pawar for spending part of his student internship fabricating devices. We appreciate the guidance, suggestions and participation of the Los Alamos National Laboratory Chemistry for Biomedical Applications team members.

Author contributions

H.M. devised the main conceptual design of the project, acquired funding, managed and coordinated research execution, and supervised biological assay experiments.

P.N. and K.D.L. conceived the centrifugal cross-flow filtration concept. P.N. trained K.D.L to investigate cross-flow filtration and supervised the microfluidic experimental workflow.

S.J. and K.D.L. performed biological assay experiments. S.J. developed the LAM waveguide-based assay used for validation.

K.D.L. and J.W.C. carried out the microfluidic testing experiments for optimization of RPM, time, and design parameters. K.D.L, J.W.C., D.C.P, and M.O.I. carried out fabrication of device designs and optimized the membrane integration technique used in the fabrication of devices.

L.E.A. optimized the use of a custom motor set-up.

J.K.S. developed the sample preparation protocol that was semi-automated in this work.

A.S.A., J.F.H., and J.K.S. provided guidance and resources to contribute to the validation of this device.

K.D.L. performed data analysis and figure creation.

K.D.L. wrote the initial draft of the manuscript with input from P.N. and H.M.

All authors discussed the results and reviewed and/or edited the final manuscript.

Chapter 9.

Impact of mycobacterial lipoarabinomannan association with serum lipoproteins on innate immune signaling

Shailja Jakhar[a], Kiersten Lenz[a], Katja Klosterman[a], Loreen R. Stromberg[a], Harshini Mukundan[a], Jessica Z. Kubicek-Sutherland[a*]

[a]Physical Chemistry and Applied Spectroscopy, Chemistry Division, Los Alamos National Laboratory, Los Alamos, New Mexico, United States

* Corresponding Author: Tel. +1 (505) 412-8264; Email: jzk@lanl.gov (J.Z.K.S.)

9.1 Introduction

Lipoarabinomannan (LAM) is a pathogen associated molecular pattern (PAMP) that is released by *Mycobacterium tuberculosis* (MTB) during active infection[564]. Mannose capped LAM (ManLAM), a type of LAM, is produced by pathogenic and slow growing mycobacterial species including MTB[55]. It is an amphiphilic lipoglycan component of the mycobacterial cell wall that plays an important role in modulating key aspects of the host's innate and adaptive immune responses to mycobacterial infections[31,565,566].

LAM has been shown to circulate as an immune complex or occurs associated with serum lipoproteins in aqueous blood[101,567]. Studies from our lab have shown that bacterial amphiphiles including lipopolysaccharide (LPS), lipoteichoic acid (LTA), and LAM[72,279,283] associate with lipoproteins such as high-, low-, and very low-density lipoproteins (HDL, LDL, and VLDL). These carrier proteins transport amphiphilic molecules in aqueous blood and play an important role in mediating the protective inflammatory response on host cells.

LAM is recognized by several pattern recognition receptors (PRRs), including Toll-like receptor 2 (TLR2) and other receptor heterodimers such as TLR2/TLR1 and TLR2/TLR6, which are mostly expressed on the surface of macrophages and dendritic cells during early MTB infection[568,569]. Binding with PRRs subsequently triggers the MyD88-dependent signaling pathway, leading to the production of pro- and anti-inflammatory cytokines[570,571]. There have been contradictory findings from a limited number of studies with respect to the mechanism of interaction of TLR2 with mycobacterial lipoproteins such as

ManLAM. Some studies have suggested there is a strong interaction between TRL2 and ManLAM,[564,570] while others indicate a weak association[572,573]. We argue that this contradiction could be due to the differential interaction of LAM with host lipoproteins, and that such associations should be considered in the design of physiologically relevant *in vitro* experimental models.

Extensive literature exists on the interaction of LPS with serum binding proteins.[279,387,574] But the global understanding of the association of LAM with lipoproteins, and its impact on immune signaling is still very limited, despite the fact that LAM is currently the most researched biomarker for MTB diagnosis. Whereas an enormous amount of effort is being put into improving the sensitivity of LAM assays for MTB detection, the design and evaluation of these assays is limited by our limited comprehension of the pathophysiology of the interaction of the biomarker with host. Previous research on LPS from our lab demonstrated a dramatic difference in cytokine profiles when the antigen was presented in media versus serum. A stark suppression of pro-inflammatory cytokines expression was observed in serum[279]. These findings indicated that the amphiphilic biochemistry of bacterial PAMPs, and their association with host lipoproteins, impacts host-pathogen interaction and is an important feature to be considered in the design of experiments.

The majority of cell studies with LAM have been performed in either media or serum, without considering the impact that interaction of LAM with lipoproteins could have on the observed response. In fact, THP-1 cells (a human monocytic cell line) are primarily cultured in media containing 10-20 % serum for optimal cell

growth, which can have significant effect on the interaction of LAM with the cells. Given that serum concentrations *in vivo* is around 90%, a physiologically relevant *in vitro* system that accurately represents the LAM-induced cytokine expression as it occurs in infected hosts does not currently exist. Here, we explore the impact of LAM presentation on immune stimulation in human differentiated macrophage [THP-1 monocytes differentiated to macrophages using phorbol 12 myristate 13 acetate] cell line, as the first step towards developing a physiologically relevant cell-based model of innate immunity. Specifically, we investigated whether the association with lipoproteins found in serum alter the LAM-associated pro-inflammatory cytokine profile as compared to LAM in a system devoid of lipoproteins.

9.2 Material and methods

Materials. Human monocyte cell line THP-1 (TIB-202), was purchased from the American Type Culture Collection (ATCC). Human THP-1 TLR2 (-/-) cell line was custom engineered by Horizon inspired cell solutions (HD204-038). RPMI-1640 (30-2001) and fetal bovine serum (FBS) (30-2020) were from ATCC. 2-mercaptoethanol (M6250) and phorbol 12 myristate 13 acetate (PMA) (P8139) was from Sigma-Aldrich. RNeasy Mini Kit (74106), RT^2 First Strand Kit (330404), RT^2 Profiler PCR Array Human Cytokines & Chemokine (PAHS150ZC6EA), RT^2 SYBR Green ROX qPCR Mastermix (330529) were from Qiagen. Individual RT^2 primer assays (330011 (PA-031), 330001 (PPH00701B, PPH00192F, PPH00564C, PPH00566F, PPH00703BPPH00576C, PPH007723B,

PPH00696C, PPH00552F, PPH00698B, PPH00694B, PPH00586A, PPH00580C, PPH00690A, PPH00171C, PPH00568A, PPH00341F, PPH00073G, PPH01018C, PPH21138F, PPX63340A, PPH00549C)) were purchased from Qiagen. Human very low density lipoproteins (LP1), Chylomicrons (SRP6304), low density lipoproteins (L7914) and high density lipoproteins (L8039) were from Sigma. Purified Man LAM (H37Rv) used in validation and optimization assays were obtained from Biodefense and Emerging Infections Resources (BEI resources, Manassas, VA) AND resuspended to 1mg/mL in sterile nanopure water. 60 µL aliquots were stored in low retention tubes at -80 °C and thawed immediately prior to use. Control human serum was obtained from Fischer Scientific Inc (Catalogue No. BP2657100), 1 mL aliquots were stored at −20 °C and thawed only once prior to use. Control delipidated human serum was obtained from Alfa Aesar (Catalogue No. BT-931), 1 mL aliquots were stored at −20 °C and thawed only once prior to use.

Cell culture. Cells were revived in T-25 flask with RPMI-1640 supplemented with 0.05 mM 2-mercaptoethanol and 20% FBS. Cells were maintained in T-75 tissue culture flasks with RPMI-1640 supplemented with 0.05 mM 2-mercaptoethanol and 10% FBS (growth media) and incubated in 5% CO_2 at 37 °C. THP-1 cells double every 24-48 hours and were sub cultured by addition of fresh growth media before concentration reached 10^6 cells per mL.

Cell viability assay. To evaluate cytotoxicity of LAM, viability assays were performed with THP-1 cells. 5 x 10^4 cells per well with LAM (10 µg/mL and 50

μg/mL) in RPMI 1640 growth media were added in 24-well tissue culture plate and allowed to incubate in 5% CO_2 at 37 °C for 24 h. After 24 h, cytotoxicity was assessed by incubating cell cultures with the resazurin-based PrestoBlue at 37 °C for 1 h. Measurements were taken using a SpectraMax Gemini EM plate reader (Molecular Devices, Sunnyvale, CA) with excitation at 560 nm and emission at 590nm. Percent cell viability was determined by dividing the relative fluorescence units (RFU) of LAM-containing wells by the RFU of the media-only wells. Assays were performed with at least four replicates.

THP-1 adaptation to 2.5% FBS. To assess gene expression between serum, no serum conditions, cells were adapted to RPMI-1640 supplemented with 0.05 mM 2-mercaptoethanol and 2.5% FBS. To do so, FBS concentration in RPMI 1640 was reduced to half on every subsequent sub culture (20%, 10%, 5%, and 2.5%).

Differentiation of THP-1 cells using PMA. THP-1 cells were differentiated to macrophages using PMA. Once cells were adapted to 2.5 % FBS in RPMI-1640, cells were added to 20nM PMA-media (RPMI 1640 with 0.05 mM 2-mercaptoethanol and 2.5 % FBS). 8 x 10^4 cells/mL/well were plated in a 24 well tissue culture plate and allowed to incubate in 5 % CO_2 at 37 °C for 24 h after which cells become adherent. PMA-media was aspirated off cells after 24 h and wells were rinsed gently 2 times with RPMI growth media (2.5%FBS). 1mL growth media was added again and cells were allowed to differentiate for another 48-72 h in 5 % CO_2 at 37 °C. Once differentiated, supernatant was discarded and different solutions as described below were added.

Conditions of LAM exposure to THP-1 cells. Condition 1 is when 10 μg/mL of LAM/no LAM is presented to TLR2 (+) cells in serum. 10 μg/mL of LAM was spiked into 20 % serum and incubated at 4 °C overnight to allow time for association before adding to RPMI 1640 media with no serum. Condition 2 is when LAM is presented to TLR2 (+) cells in delipidated serum. 10μg/mL of LAM was spiked into 20 % delipidated serum and incubated at 4 °C overnight to allow time for association before adding to RPMI 1640 media with no serum. Condition 3 is when 10 μg/mL LAM/no LAM is presented to TLR2 (+) cells in media (serum free) with and without lipoproteins. Condition 3a is media with LAM/no LAM. Condition 3b is LAM added to HDL (0.5 mg/mL)/no HDL in media. Condition 3c is LAM added to LDL (1 mg/mL)/no LDL in media. Condition 3d is LAM added to VLDL (0.15 mg/mL)/no VLDL in media. Condition 3e is LAM added to chylomicrons (0.1 mg/mL)/no chylomicrons in media. The different lipoprotein concentrations were based on normal physiological concentrations as mentioned in literature[575–577].

0.5 mL of solution per well was added to 24 well plate and incubated in 5 % CO_2 at 37 °C for 24 hours after which supernatant was collected in low retention tubes and stored at -80 °C. Wells were washed with PBS suitable for cell culture and RNA extraction was done as described below.

Gene expression analysis. To evaluate changes in gene expression between condition 1, 2 and 3, RNA was extracted from THP-1 cells after 24 h of exposure to 10 μg/mL of LAM with and without lipoproteins (HDL/LDL/VLDL/Chylmicrons)

in RPMI-1640 media without FBS using a RNeasy Mini Kit [Qiagen, 74106.]. Cells from at least four technical; and three biological replicates were pooled for RNA analysis. cDNA synthesis from RNA samples was performed using the RT^2 First Strand Kit [Qiagen, 330404.]. Initial gene expression analysis to screen for select genes was performed on cDNA samples using an RT^2 Profiler PCR Array Human Cytokines & Chemokines in a 96-well plate format [Qiagen, PAHS150ZC6EA]. Each array contained 84 different human cytokines and chemokines, five housekeeping genes, proprietary controls to monitor genomic DNA contamination, first-strand cDNA synthesis, and real-time PCR efficiency. Gene expression analysis for rest of the conditions was performed on cDNA samples using individual RT^2 qPCR primer assays in a 96 well plate format [Qiagen, details in materials section]. 18 cytokines and chemokines included on basis of initial screen were: BMP2, CCL1, CCL2, CCL20, CCL3, CCL5, CSF2, CSF3, CXCL1, CXCL2, CXCL5, IL15, IL16, IL18, IL1A, IL1B, CXCL8 AND TNF; 3 housekeeping genes; ACTB, HPRT1 and RPLP0 and 3 controls to monitor genomic DNA contamination (GDC), reverse transcription control (RTC) and no template control were ran on every 96 well plate. PCR arrays were run on Applied Biosystems StepOnePlus thermocycler using RT^2 SYBR Green ROX qPCR Mastermix [Qiagen, 330529]. data analysis suite and Graphpad Prism 9.0.

Statistical analysis

CT values were uploaded onto the data analysis web portal at http://www.qiagen.com/geneglobe. Samples contained controls and test groups.

CT values were normalized based on Manual selection using ACTB, HPRT1 and RPLP0 as reference genes.

Independent Student's *t*-tests were used for statistical analyses between two groups in RT^2 Profiler PCR Arrays and quantitative real-time-PCR. Experimental values are described as the mean±standard deviation, *P*-values<0.05 indicated a significant difference between two groups. Statistical analysis was performed using Graphpad Prism 9.0.

9.3 Results and discussion

We studied the differences in cytokine and chemokine signaling of human

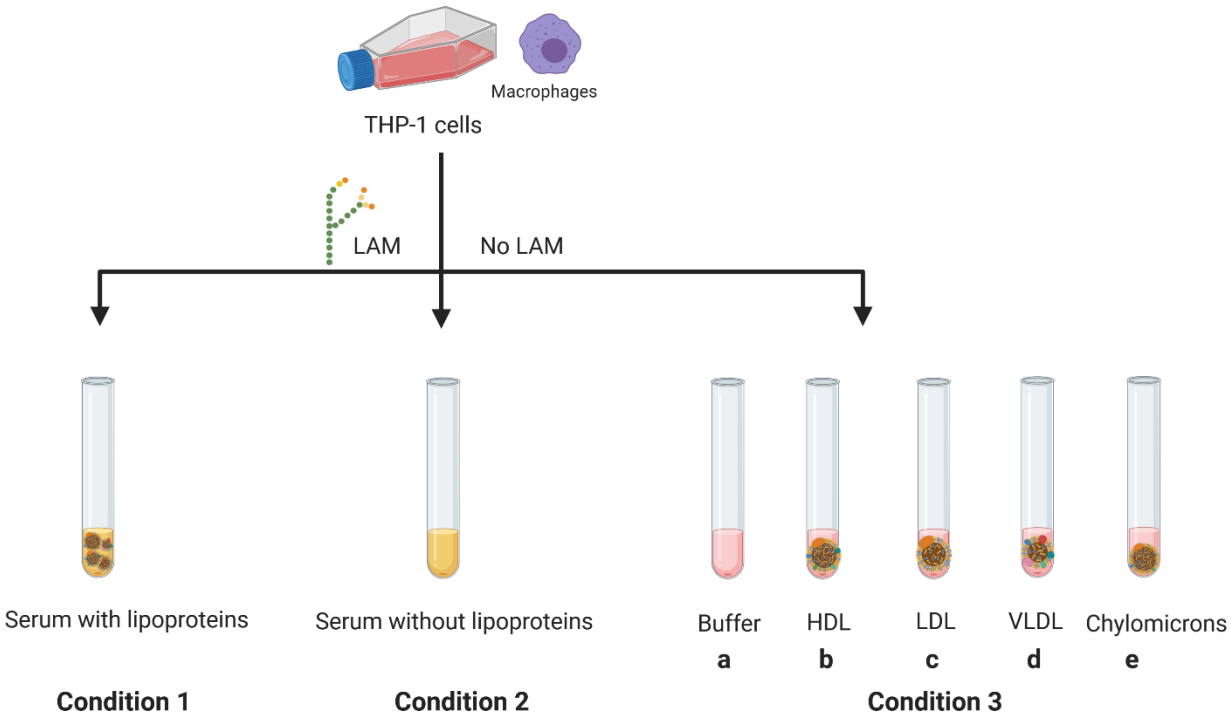

Figure 9.1. Schematic representation of research approach. LAM/No LAM was exposed to THP-1 cells under 3 different conditions. Condition 1 association of LAM with some of the common lipoproteins present in serum: HDL, LDL, VLDL and chylomicrons. Condition 2 shows presentation of LAM to cells with de-lipidated serum, when lipoproteins such as HDL, LDL, VLDL and chylomicrons are inactivated by de-lipidation. **Condition 3** is when LAM is presented to cells in a) just serum- free media or with either b) HDL c) LDL d) VLDL e) Chylomicrons. Schematic via Biorender.com.

macrophages when LAM was presented under three different conditions (**Figure 9.1**): condition 1- LAM presented in 20 % human serum supplemented culture media, condition 2- LAM presented in 20 % de-lipidated human serum and media, and condition 3a- LAM presented in just media (serum-free), or with either 3b- HDL, 3c- LDL, 3d- VLDL and 3e- chylomicrons. These three experimental conditions will be referred to as 1, 2, and 3a, b, c, d and e, respectively. The conditions of the study were chosen after extensive literature review, and a LAM concentration of 10 μg/mL and exposure time of LAM to THP-1 cells for 24 hours were used[38,61,64,181,572,578–590].

Before commencing on the experimental evaluation, an intrinsic assessment of toxicity of LAM to THP-1 cells was measured. Cells were exposed to 10 and 50 μg/mL of ManLAM for 24 hours. Figure S1 shows that LAM was not cytotoxic to THP-1 cells at either concentration, validating the use of the cell line with the given concentration of LAM for this study. Cells were adapted to minimum serum (2.5%) conditions to assess cytokine signaling when exposed to conditions 1, 2 and 3 as described in detail in the methods section. Cells were then differentiated using PMA to assess cytokine expression under different physiological conditions.

Initially, we examined LAM/no LAM- dependent expression using a high-throughput array of 94 cytokines and chemokines expressed by the THP-1 human macrophage cell line following 24 hours of LAM pre-incubation in media or serum. Pre-incubation of LAM with the serum lipoproteins prior to exposure to the cells allows for their uptake. **Figure 9.2a** demonstrates differential expression

of cytokines induced by macrophages, measured using qPCR, in the presence of 10 μg/mL of Man LAM in either condition 3a (media) or condition 1 (serum). Table S3 shows the CT values and raw data. Cells growth in the absence of LAM

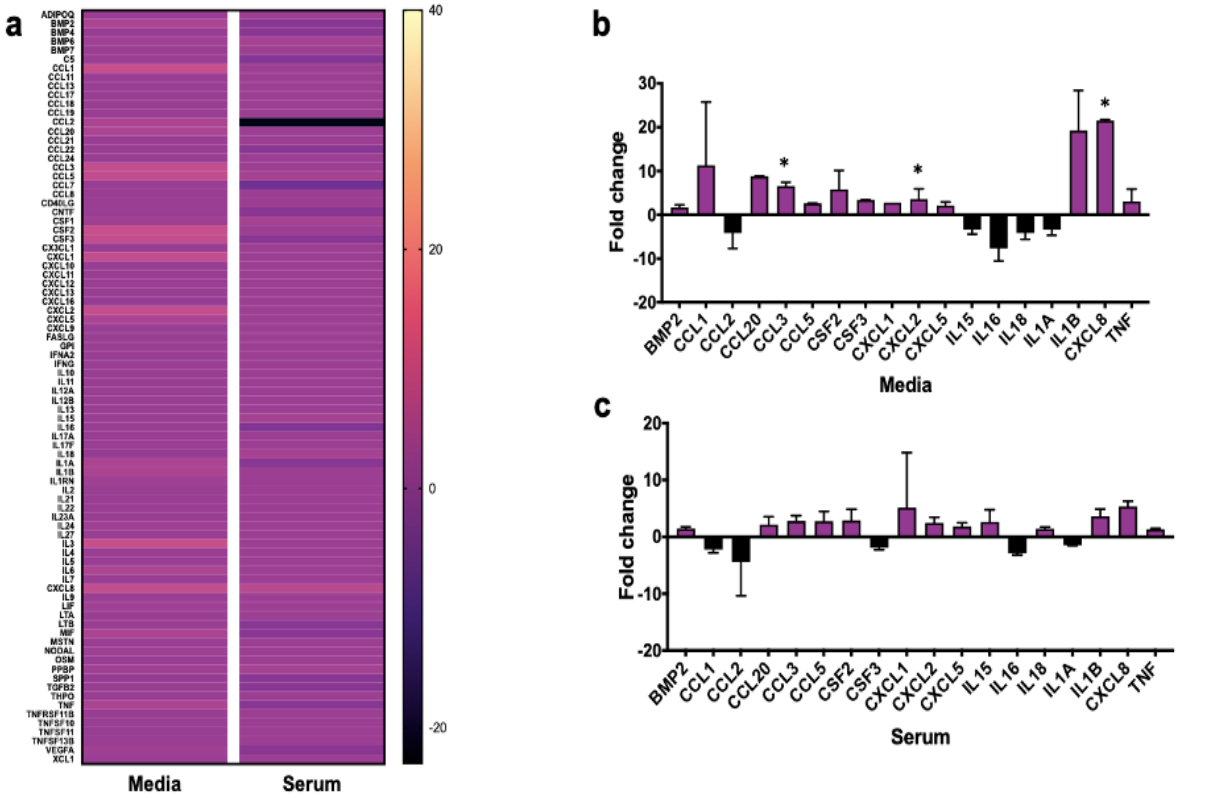

Figure 9.2. Cytokine profile in media and serum. a) Heat map shows fold regulation in gene expression under conditions 3a (just media) and 1 (serum) with 10 μg/ml LAM, incubated overnight. Bar graph represents cytokine response of THP-1 cells with **b)** buffer and **c)** serum. Values are plotted as fold regulation, n=3 with error bars indicating standard deviation of the mean. * indicates significant values with $p < 0.05$.

are used as a baseline for gene expression. Our results demonstrate peak expression of several cytokines in condition 3a (LAM in media). Three cytokines, CCL3, CXCL2 and CXCL8 show significant (p-value < 0.05) up regulation in condition 3a (media) (**Figure 9.2b**). We observed upregulation of CCL1, CCL20, CCL3, CCL5, CSF2, CSF3, IL1B and CXCL8 in condition 3a (LAM in media, Figure 2b) as compared to condition 1 (LAM in serum, **Figure 9.2c**). **Figure 9.2b** shows increased expression of TNF in condition 3a (LAM in media), compared to

condition 1 (LAM in serum). This is in stark contrast to the literature, wherein Man LAM is described as an anti-inflammatory molecule that inhibits TNF and IL-12 while stimulating IL-10 production[39,65,591,592]. We did not observe changes in IL-12 and IL-10 between the different conditions tested either. When comparing the two conditions (3a and 1), it is evident that condition 3a (LAM in media) elicits a much greater cytokine and chemokine response (5-10X increase with select cytokines) compared to condition 1 (LAM in serum, **Figure 9.2b and c**). Yet, LAM is "presented" to TLRs in serum under physiological conditions, rather than blood. **Figure 9.2** shows that the secretion of cytokines is markedly reduced when LAM is presented in association with serum lipoproteins, suggesting a strong protective effect of serum on LAM-mediated cytokine production (n=3). Further analysis of this response was performed using a set of genes selected based on these initial observations. We

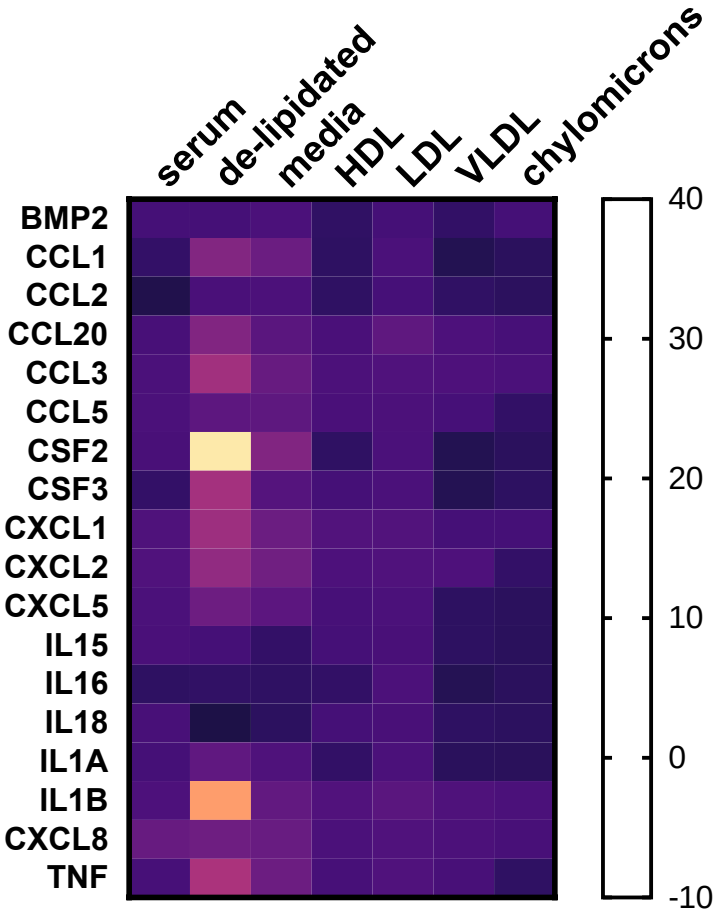

Figure 9.3. Heat map distribution of cytokines in each condition. Display intensity profile of cytokine expression in TLR2 (+) cells in conditions 1, 2, 3 a, b, c, d and e with LAM stimulation against no LAM as control. Scale bar indicates that -10 is the lowest and 40 is the highest intensity. Values are plotted as fold regulation from 3 independent experiments, n=3.

assessed cytokine expression in de-lipidated serum (serum where lipoproteins are inactivated by centrifugation, lipid-free), and media containing purified human lipoproteins (HDL, LDL, VLDL and chylomicrons) in order to further understand the impact of lipoprotein interactions on induction of innate immune cascades by LAM. **Figure 9.3** shows the difference in cytokine/chemokine signaling between conditions 1 (LAM in serum), 2 (LAM in delipidated serum), 3a (LAM in just media), 3b-e (various lipoproteins associated with LAM in media). The heat map indicates an increase in cytokine expression between condition 2 (LAM in delipidated serum) and 3a (LAM in media), compared to condition 1 (LAM in serum) and 3b-e (varied lipoproteins associated with LAM, in media). Interestingly both lipid-free exposure conditions - condition 2 (LAM in delipidated serum) and 3a (LAM in media) - demonstrate a dramatic induction of chemokine/cytokine expression for CCL3, CXCL2 and CXCL8. Condition 2 (LAM in delipidated serum) also shows increase in IL1B and TNF. On the other hand, conditions 3b-e (various lipoproteins associated with LAM in media) show several folds down regulation of most cytokine/chemokines as compared to conditions 2 (LAM in delipidated serum) and 3a (LAM in media). Interestingly, VLDL and chylomicrons show greater suppression of cytokine signaling than HDL and LDL. This could be due to larger particle size of VLDL (30-90 nm) and chylomicrons (200-600 nm) compared to HDL (7-13 nm) and LDL (21-27 nm) which might provide them with greater surface area to associate with LAM[593–596]. Another reason for difference in cytokine expression could be different concentrations of various lipoproteins used based on normal physiological concentration as

described in detail in methods section. Delipidated serum can induce cellular stress, which in itself can contribute to inflammatory signaling. To discriminate between LAM-mediated, TLR2 dependent signaling and other stress induced responses, cytokine expression should be compared between TL2 (+) and TLR2 (-) cell lines.

9.4 Conclusion

The results from this study support the overarching hypothesis that immune responses are affected by the presentation of amphiphilic biomarkers such as LAM, and this physiological context should be considered in the design of *in vitro* experimental systems to study innate immune recognition. Arguably, all bacterial PAMPs are amphiphilic – and this natural biochemistry is critical to their ability to navigate two mutually incompatible regimes – hydrophilic and hydrophobic – in the host. Several chronic inflammatory diseases such as psoriasis, systemic lupus erythematosus, rheumatoid arthritis and infections such as HIV are associated with altered lipoprotein levels[596]. The most common changes are decrease in serum HDL and LDL and increase in serum VLDL. These altered lipoprotein levels and interaction with amphiphilic PAMPs influence the cytokine and chemokine profile. Therefore, it is important to consider this presentation of amphiphiles for accurate understanding of its role in interacting with the host immune system during various inflammatory diseases and infections including TB.

Acknowledgements

We thank Dr. Dominique N. Price and Dr. Zachary R. Stromberg for technical guidance and helpful discussions during the course of this work.

Author contributions

J.Z.K.-S., S.J. and H.M., designed the experiments. S.J., J.Z.K.-S., K.K., LR.S., and K.L. performed experiments. S.J., J.Z.K.-S., K.K., LR.S., and K.L. analyzed the data. S.J., K.L., and J.Z.K.-S. wrote the manuscript. All authors assisted in editing the manuscript.

Competing financial interests

Scientists from the Los Alamos National Laboratories, operated by the Triad LLC, that are authors on this manuscript, do not have competing interests, and are not consultants for any competing interests.

Chapter 10.

Conclusions and Future Directions

This dissertation work has explored the development of novel strategies for the blood-based diagnosis of TB via better understanding of host-pathogen interactions, specifically associated with mycobacterial virulence factor LAM. Previous work from our lab demonstrated that LAM associates with host carriers such as HDL. Based on these findings, we optimized and validated lipoprotein capture assay in adult patients with TB and HIV from Uganda as discussed in chapter 6 of this manuscript. This initial evaluation of serum showed successful detection of LAM in serum but we also saw that a variety of factors can impact host lipoprotein concentrations, including HIV/AIDS which can cause differences in LAM detection by lipoprotein capture assay. Therefore, we developed a membrane insertion assay with sample processing method that is independent of host serum lipoproteins. Compared to lipoprotein capture, the membrane insertion method resulted in higher sensitivity in adult TB patients. Once we established higher sensitivity of membrane insertion in adult cohort, we tested the feasibility of LAM detection and validated the membrane insertion assay in pediatric TB and HIV positive or negative and age matched control serum samples from Kenya as described in chapter 7. We were able to successfully measure LAM in all pediatric samples irrespective of presence or absence of comorbidities. But the sample processing method used to separate lipoproteins from LAM in membrane insertion assay is a crude extraction method which uses chloroform and methanol. To make the method more field and user friendly, our

engineering team has developed a microfluidic chip to be integrated into portable biosensor device. We validated the successful separation of blood from serum and LAM retention using microfluidic device as compared to benchtop method as described in chapter 8. Our results from clinical study in chapter 6 showed dependence of LAM detection on host lipoprotein levels which clearly indicated the need to better understand host- pathogen interaction. Previous work from our lab shows that immune signaling of cells in response to LPS dramatically changes based on its presentation in media versus serum. Therefore, we investigated the impact of LAM- lipoprotein association on immune signaling in a cell-based system as discussed in chapter 9. We successfully demonstrated that the expression profiles of cytokines and chemokines generated in response to LAM induction vary significantly depending on the type of buffer LAM is presented in. This interaction is important to consider while designing studies for LAM in vitro and also during development of LAM detection strategies.

In conclusion, this dissertation work far and wide describes the process and considerations for developing LAM detection strategies to diagnose TB in adult and pediatric populations in presence and absence of comorbidities such as HIV. The assays we have developed here can be transitioned to other amphiphiles which are expressed by pathogens in other infectious diseases and also for non-infectious diseases and used with other detection platforms. Summarized below are some suggested advancements and applications for this technology.

We have shown successful detection of serum LAM using membrane insertion method in both adult and pediatric TB patients. This was first ever serum LAM detection in pediatric patients in presence and absence of co-morbidities.

In future, we would like to evaluate bigger cohort for both adult and pediatric clinical studies. To be able to make more comprehensive comparison, other diagnostics such as culture and GeneXpert and other clinical variables including comorbidities with similarly matched controls would be studied. As the urine LAM assays have already been commercialized and endorsed by WHO, we would like to do a side-by-side assessment of urine and serum detection of LAM on same patient using the waveguide biosensor. To further evaluate the use of LAM in immunocompromised and immunocompetent patients and as a prognostic biomarker, we would perform LAM detection on a longitudinal cohort and correlate the results with CD4 counts and treatment/mortality/morbidity. Since we started these clinical evaluations, FIND has developed much more sensitive antibodies against LAM epitopes. To enhance the sensitivity of LAM detection using membrane insertion, new FIND antibodies would be evaluated

We envisage that in future, we would be able to deploy biosensor device at the point of care in resource limited settings for diagnosis of TB using membrane insertion method. Currently, the separation of amphiphilic biomarkers from blood/lipoproteins is very complicated and almost unattainable in resource limited settings. After successful validation of blood separation from serum and retention of LAM using microfluidic device, the team is working on LAM release from lipoproteins on microfluidic chip. This will automatize the whole process to

be used at the point of care. The engineering and chemistry team is also working on plastic fabrication of multichannel waveguides for multiplexed detection of amphiphiles which will make the chip disposable and usable for several patient samples at one time making the process cheaper and faster.

This whole assay has the advantage of detecting TB by using a prick of blood which will be automatically processed by microfluidic device and detected by using portable biosensor platform attached to a mini computer where the results could be read by a clinician remotely.

Appendix 1

References

1. Sharma, S. K. & Mohan, A. Tuberculosis: From an incurable scourge to a curable disease - journey over a millennium. *Indian J. Med. Res.* **137**, 455–93 (2013).
2. Houben, R. M. G. J. & Dodd, P. J. The Global Burden of Latent Tuberculosis Infection: A Re-estimation Using Mathematical Modelling. *PLOS Med.* **13**, e1002152 (2016).
3. WHO. *Global Tuberculosis Report 2020*. (2020).
4. Hershkovitz, I. *et al.* Tuberculosis origin: The Neolithic scenario. *Tuberculosis* **95**, S122–S126 (2015).
5. WHO Global Tuberculosis Programme. (1994). TB : a global emergency, WHO report on the TB epidemic. World Health Organization. (1994).
6. Paulson, T. Epidemiology: A mortal foe. *Nature* **502**, S2–S3 (2013).
7. Holmes, K. K. *et al.* Major Infectious Diseases: Key Messages from Disease Control Priorities, Third Edition. in *Disease Control Priorities, Third Edition (Volume 6): Major Infectious Diseases* 1–27 (The World Bank, 2017). doi:10.1596/978-1-4648-0524-0_ch1
8. Lienhardt, C. *et al.* Global tuberculosis control: lessons learnt and future prospects. *Nat. Rev. Microbiol.* **10**, 407–416 (2012).
9. Lönnroth, K. *et al.* Tuberculosis control and elimination 2010–50: cure, care, and social development. *Lancet* **375**, 1814–1829 (2010).
10. Lin, H.-H., Ezzati, M. & Murray, M. Tobacco Smoke, Indoor Air Pollution and Tuberculosis: A Systematic Review and Meta-Analysis. *PLoS Med.* **4**, e20 (2007).
11. Bates, M. N. *et al.* Risk of tuberculosis from exposure to tobacco smoke: A systematic review and meta-analysis. *Archives of Internal Medicine* (2007). doi:10.1001/archinte.167.4.335
12. Rehm, J. *et al.* The association between alcohol use, alcohol use disorders and tuberculosis (TB). A systematic review. *BMC Public Health* **9**, 450 (2009).
13. Jeon, C. Y. & Murray, M. B. Diabetes Mellitus Increases the Risk of Active Tuberculosis: A Systematic Review of 13 Observational Studies. *PLoS Med.* **5**, e152 (2008).
14. Havlir, D. V., Getahun, H., Sanne, I. & Nunn, P. Opportunities and Challenges for HIV Care in Overlapping HIV and TB Epidemics. *JAMA* **300**, 423 (2008).
15. Marais, B. J. *et al.* Childhood Pulmonary Tuberculosis. *Am. J. Respir. Crit. Care Med.* **173**, 1078–1090 (2006).
16. van leth, F. Prevalence of tuberculous infection and incidence of tuberculosis; a re-assessment of the Styblo rule. *Bull. World Health Organ.* **86**, 20–26 (2008).
17. Onozaki, I. *et al.* National <scp>tuberculosis</scp> prevalence surveys in Asia, 1990–2012: an overview of results and lessons learned. *Trop. Med.*

Int. Heal. **20**, 1128–1145 (2015).
18. Pai, M. *et al.* Tuberculosis. *Nat. Rev. Dis. Prim.* **2**, 16076 (2016).
19. Roadmap towards ending TB in children and adolescents, second edition. Geneva: World Health Organization; 2018. Licence: CC BY-NC-SA 3.0 IGO. Available at: https://www.who.int/tb/publications/2018/tb-childhoodroadmap/en/. (Accessed: 10th December 2020)
20. Barry, C. E. *et al.* The spectrum of latent tuberculosis: rethinking the biology and intervention strategies. *Nat. Rev. Microbiol.* **7**, 845–855 (2009).
21. Drain, P. K. *et al.* Incipient and Subclinical Tuberculosis: a Clinical Review of Early Stages and Progression of Infection. *Clin. Microbiol. Rev.* **31**, e00021-18 (2018).
22. WHO. *Guidelines on the management of latent tuberculosis infection*. (2015).
23. Nuermberger, E., Bishai, W. R. & Grosset, J. H. Latent Tuberculosis Infection. *Semin. Respir. Crit. Care Med.* **25**, 317–336 (2004).
24. Zhang, M. *et al.* Treatment of Tuberculosis with Rifamycin-containing Regimens in Immune-deficient Mice. *Am. J. Respir. Crit. Care Med.* **183**, 1254–1261 (2011).
25. Chiappini, E. *et al.* Recommendations for the diagnosis of pediatric tuberculosis. *Eur J Clin Microbiol Infect Dis.* **35(1)**, 1–18 (2016).
26. Starke, J. R. Diagnosis of tuberculosis in children. *Pediatric Infectious Disease Journal* (2000). doi:10.1097/00006454-200011000-00015
27. https://www.cdc.gov/tb/topic/populations/tbinchildren/default.htme.
28. Sereti, Irini; Bisson, Gregory P,; Meintjes, G. *HIV and Tuberculosis: A Formidable Alliance*. *Springer International Publishing* (2019). doi:10.1007/978-3-030-29108-2_5
29. Vilchèze, C. Mycobacterial Cell Wall: A Source of Successful Targets for Old and New Drugs. *Appl. Sci.* **10**, 2278 (2020).
30. Brennan, P. J. & Nikaido, H. The Envelope of Mycobacteria. *Annu. Rev. Biochem.* **64**, 29–63 (1995).
31. Brennan, P. . Structure, function, and biogenesis of the cell wall of Mycobacterium tuberculosis. *Tuberculosis* **83(1–3)**, 91–97 (2003).
32. Carranza, C. & Chavez-Galan, L. Several Routes to the Same Destination: Inhibition of Phagosome-Lysosome Fusion by Mycobacterium tuberculosis. *Am. J. Med. Sci.* **357**, 184–194 (2019).
33. Pai, M. *et al.* Tuberculosis. *Nature Reviews Disease Primers* (2016). doi:10.1038/nrdp.2016.76
34. Warner, D. F. & Mizrahi, V. The survival kit of Mycobacterium tuberculosis. *Nature Medicine* (2007). doi:10.1038/nm0307-282
35. Russell, D. G. Mycobacterium tuberculosis: Here today, and here tomorrow. *Nature Reviews Molecular Cell Biology* (2001). doi:10.1038/35085034
36. Chiaradia, L. *et al.* Dissecting the mycobacterial cell envelope and defining the composition of the native mycomembrane. *Sci. Rep.* (2017). doi:10.1038/s41598-017-12718-4
37. Cook, G. M. *et al.* Physiology of Mycobacteria. in *Advances in Microbial*

Physiology 81–319 (2009). doi:10.1016/S0065-2911(09)05502-7
38. Fukuda, T. *et al.* Critical roles for lipomannan and lipoarabinomannan in cell wall integrity of mycobacteria and pathogenesis of tuberculosis. *MBio* (2013). doi:10.1128/mBio.00472-12
39. Nigou, J. *et al.* Mycobacterial lipoarabinomannans: Modulators of dendritic cell function and the apoptotic response. *Microbes and Infection* (2002). doi:10.1016/S1286-4579(02)01621-0
40. Patterson, J. H., Waller, R. F., Jeevarajah, D., Billman-Jacobe, H. & McConville, M. J. Mannose metabolism is required for mycobacterial growth. *Biochem. J.* (2003). doi:10.1042/BJ20021700
41. Stanley, S. A. & Cox, J. S. Host-Pathogen interactions during Mycobacterium tuberculosis infections. *Curr. Top. Microbiol. Immunol.* (2013). doi:10.1007/82-2013-332
42. Watanabe, M. *et al.* Location of functional groups in mycobacterial meromycolate chains; the recognition of new structural principles in mycolic acids. *Microbiology* **148(6)**, 1881–1902 (2002).
43. Qureshi, N., Takayama, K., Jordi, H. C. & Schnoes, H. K. Characterization of the purified components of a new homologous series of α-mycolic acids from Mycobacterium tuberculosis H37Ra. *J Biol Chem.* **253(15)**, 5411–7 (1978).
44. Maitra, A. *et al.* Cell wall peptidoglycan in Mycobacterium tuberculosis: An Achilles' heel for the TB-causing pathogen. *FEMS Microbiol. Rev.* **43**, 548–575 (2019).
45. Lederer, E., Adam, A., Ciorbaru, R., Petit, J.-F. & Wietzerbin, J. Cell walls of mycobacteria and related organisms; Chemistry and immunostimulant properties. *Mol. Cell. Biochem.* **7**, 87–104 (1975).
46. McNeil, M., Daffe, M. & Brennan, P. J. Evidence for the nature of the link between the arabinogalactan and peptidoglycan of mycobacterial cell walls. *J. Biol. Chem.* **265**, 18200–6 (1990).
47. Kleinnijenhuis, J., Oosting, M., Joosten, L. a B., Netea, M. G. & Van Crevel, R. Innate Immune Recognition of Mycobacterium tuberculosis. *Clin. Dev. Immunol.* **2011**, 1–12 (2011).
48. Chatterjee, D. & Khoo, K.-H. Mycobacterial lipoarabinomannan: An extraordinary lipoheteroglycan with profound physiological effects. *Glycobiology* **8**, 113–120 (1998).
49. Lawn, S. D. Point-of-care detection of lipoarabinomannan (LAM) in urine for diagnosis of HIV-associated tuberculosis: a state of the art review. *BMC Infect Dis.* **12(1)**, 103 (2012).
50. Anderson, R. J. *et al.* The Chemistry of the Lipoids of the Tubercle Bacillus and certain other Microorganisms. in *Fortschritte der Chemie Organischer Naturstoffe* (1939). doi:10.1007/978-3-7091-7186-8_4
51. Hunter, S. W. & Brennan, P. J. Evidence for the presence of a phosphatidylinositol anchor on the lipoarabinomannan and lipomannan of Mycobacterium tuberculosis. *J Biol Chem.* **265(16)**, 9272–9 (1990).
52. Chatterjee, D., Lowell, K., Rivoire, B., McNeil, M. R. & Brennan, P. J. Lipoarabinomannan of Mycobacterium tuberculosis. Capping with

mannosyl residues in some strains. *J Biol Chem.* **267(9)**, 6234–9 (1992).
53. Peter, J. G. *et al.* Diagnostic accuracy of induced sputum LAM ELISA for tuberculosis diagnosis in sputum-scarce patients. *InterJ Tuberc Lung Dis.* **16(8)**, 1108–1112 (2012).
54. Guérardel, Y. *et al.* Lipomannan and Lipoarabinomannan from a Clinical Isolate of Mycobacterium kansasii. *J. Biol. Chem.* **278**, 36637–36651 (2003).
55. Nigou, J., Gilleron, M. & Puzo, G. Lipoarabinomannans: From structure to biosynthesis. *Biochimie* (2003). doi:10.1016/S0300-9084(03)00048-8
56. Mukundan, H. *et al.* Understanding the interaction of Lipoarabinomannan with membrane mimetic architectures. *Tuberculosis* **92**, 38–47 (2012).
57. Nigou, J. *et al.* Mannan chain length controls lipoglycans signaling via and binding to TLR2. *J. Immunol.* (2008).
58. Ozinsky, A. *et al.* The repertoire for pattern recognition of pathogens by the innate immune system is defined by cooperation between Toll-like receptors. *Proc. Natl. Acad. Sci. U. S. A.* (2000). doi:10.1073/pnas.250476497
59. Takeuchi, O. *et al.* Discrimination of bacterial lipoproteins by Toll-like recepttor 6. *Int. Immunol.* (2001). doi:10.1093/intimm/13.7.933
60. Takeuchi, O. *et al.* Cutting Edge: Role of Toll-Like Receptor 1 in Mediating Immune Response to Microbial Lipoproteins. *J. Immunol.* (2002). doi:10.4049/jimmunol.169.1.10
61. Rojas, M., Garcia, L. F., Nigou, J., Puzo, G. & Olivier, M. Mannosylated lipoarabinomannan antagonizes Mycobacterium tuberculosis- induced macrophage apoptosis by altering CA+2-dependent cell signaling. *J. Infect. Dis.* (2000). doi:10.1086/315676
62. Szalai, G., Krishnamurthy, R. & Hajnóczky, G. Apoptosis driven by IP3-linked mitochondrial calcium signals. *EMBO J.* (1999). doi:10.1093/emboj/18.22.6349
63. Brazil, D. P., Park, J. & Hemmings, B. A. PKB binding proteins: Getting in on the Akt. *Cell* (2002). doi:10.1016/S0092-8674(02)01083-8
64. Maiti, D., Bhattacharyya, A. & Basu, J. Lipoarabinomannan from Mycobacterium tuberculosis promotes macrophage survival by phosphorylating Bad through a phosphatidylinositol 3-kinase/Akt pathway. *J. Biol. Chem.* (2001). doi:10.1074/jbc.M002650200
65. Geijtenbeek, T. B. H. *et al.* Mycobacteria target DC-SIGN to suppress dendritic cell function. *J. Exp. Med.* (2003). doi:10.1084/jem.20021229
66. Tallieux, L. *et al.* DC-SIGN is the major Mycobacterium tuberculosis receptor on human dendritic cells. *J. Exp. Med.* (2003). doi:10.1084/jem.20021468
67. World Health Organization. *High-priority target product profiles for new tuberculosis diagnostics: report of a consensus meeting. In Proceedings of the WHO/HTM/TB/2014.18* (2014). doi:WHO/HTM/TB/2014.18
68. Chatterjee, D. & Khoo, K. H. The surface glycopeptidolipids of mycobacteria: Structures and biological properties. *Cellular and Molecular Life Sciences* (2001). doi:10.1007/PL00000834

69. Tucci, P., Gonz??lez-Sapienza, G. & Marin, M. Pathogen-derived biomarkers for active tuberculosis diagnosis. *Front. Microbiol.* (2014). doi:10.3389/fmicb.2014.00549
70. Goletti, D., Petruccioli, E., Joosten, S. A. & Ottenhoff, T. H. M. Tuberculosis biomarkers: From diagnosis to protection. *Infect. Dis. Rep.* **8 (2)**, 6568 (2016).
71. Rivière, M., Moisand, A., Lopez, A. & Puzo, G. Highly Ordered Supra-Molecular Organization of the Mycobacterial Lipoarabinomannans in Solution. Evidence of a Relationship Between Supra-Molecular Organization and Biological Activity. *J. Mol. Biol.* **344**, 907–918 (2004).
72. Sakamuri, R. M. *et al.* Association of lipoarabinomannan with high density lipoprotein in blood: Implications for diagnostics. *Tuberculosis* **93**, 301–307 (2013).
73. Kubicek-Sutherland, J. Z., Vu, D. M., Mendez, H. M., Jakhar, S. & Mukundan, H. Detection of lipid and amphiphilic biomarkers for disease diagnostics. *Biosensors* **7**, (2017).
74. Noormohamed, A. *et al.* Detection of lipopolysaccharides in serum using a waveguide-based optical biosensor. in *Optical Diagnostics and Sensing XVII: Toward Point-of-Care Diagnostics* (ed. Coté, G. L.) 100720A (2017). doi:10.1117/12.2253506
75. Nicol, M. P. *et al.* Urine lipoarabinomannan testing for diagnosis of pulmonary tuberculosis in children: A prospective study. *Lancet Glob Heal.* **2(5)**, e278-84 (2014).
76. Kroidl, I. *et al.* Performance of urine lipoarabinomannan assays for paediatric tuberculosis in Tanzania. *Eur Respir J.* **46(3)**, 761–770 (2015).
77. Iskandar, A., Nursiloningrum, E., Arthamin, M. Z., Olivianto, E. & Chandrakusuma, M. S. The diagnostic value of urine lipoarabinomannan (LAM) antigen in childhood tuberculosis. *J Clin Diagn Res.* **11(3)**, EC32–EC35 (2017).
78. Lacourse, S. M. *et al.* Stool Xpert MTB/RIF and urine lipoarabinomannan for the diagnosis of tuberculosis in hospitalized HIV-infected children. *AIDS* **32(1)**, 69–78 (2018).
79. Broger, T. *et al.* Diagnostic accuracy of 3 urine lipoarabinomannan tuberculosis assays in HIV-negative outpatients. *J. Clin. Invest.* (2020). doi:10.1172/JCI140461
80. Magni, R. *et al.* Lipoarabinomannan antigenic epitope differences in tuberculosis disease subtypes. *Sci. Rep.* (2020). doi:10.1038/s41598-020-70669-9
81. Paris, L. *et al.* Urine lipoarabinomannan glycan in HIV-negative patients with pulmonary tuberculosis correlates with disease severity. *Sci. Transl. Med.* (2017). doi:10.1126/scitranslmed.aal2807
82. Peter, J. *et al.* Test characteristics and potential impact of the urine LAM lateral flow assay in HIV-infected outpatients under investigation for TB and able to self-expectorate sputum for diagnostic testing. *BMC Infect. Dis.* (2015). doi:10.1186/s12879-015-0967-z
83. Broger, T. *et al.* Sensitive electrochemiluminescence (ECL) immunoassays

for detecting lipoarabinomannan (LAM) and ESAT-6 in urine and serum from tuberculosis patients. *PLoS One* **14(4)**, e0215443 (2019).
84. Sigal, G. B. *et al.* A Novel Sensitive Immunoassay Targeting the 5-Methylthio-D-Xylofuranose–Lipoarabinomannan Epitope Meets the WHO's Performance Target for Tuberculosis Diagnosis. *J. Clin. Microbiol.* **56**, e01338-18 (2018).
85. Hamasur, B., Bruchfeld, J., VanHelden, P., Källenius, G. & Svenson, S. A sensitive urinary lipoarabinomannan test for tuberculosis. *PLoS One* **10(4)**, e0123457 (2015).
86. Suwanpimolkul, G. *et al.* Utility of urine lipoarabinomannan (LAM) in diagnosing tuberculosis and predicting mortality with and without HIV: prospective TB cohort from the Thailand Big City TB Research Network. *Int. J. Infect. Dis.* (2017). doi:10.1016/j.ijid.2017.04.017
87. Crawford, A. C. *et al.* Detection of the tuberculosis antigenic marker mannose-capped lipoarabinomannan in pretreated serum by surface-enhanced Raman scattering. *Analyst* **142(1)**, 186–196 (2017).
88. Chan, C. E. *et al.* The diagnostic targeting of a carbohydrate virulence factor from M.Tuberculosis. *Sci. Rep.* (2015). doi:10.1038/srep10281
89. Shah, M. *et al.* Diagnostic accuracy of a urine lipoarabinomannan test for tuberculosis in hospitalized patients in a high HIV prevalence setting. *J. Acquir. Immune Defic. Syndr.* (2009). doi:10.1097/QAI.0b013e3181b98430
90. Reither, K. *et al.* Low sensitivity of a urine LAM-ELISA in the diagnosis of pulmonary tuberculosis. *BMC Infect. Dis.* (2009). doi:10.1186/1471-2334-9-141
91. Peter, J. G. *et al.* Diagnostic accuracy of a urine lipoarabinomannan strip-test for TB detection in HIV-infected hospitalised patients. *Eur. Respir. J.* (2012). doi:10.1183/09031936.00201711
92. Dheda, K. *et al.* Clinical utility of a commercial LAM-ELISA assay for TB diagnosis in HIV-infected patients using urine and sputum samples. *PLoS One* (2010). doi:10.1371/journal.pone.0009848
93. Pereira Arias-Bouda, L. M. *et al.* Development of antigen detection assay for diagnosis of tuberculosis using sputum samples. *J. Clin. Microbiol.* (2000). doi:10.1128/jcm.38.6.2278-2283.2000
94. Hamasur, B. *et al.* Rapid diagnosis of tuberculosis by detection of mycobacterial lipoarabinomannan in urine. *J. Microbiol. Methods* **45**, 41–52 (2001).
95. Boehme, C. *et al.* Detection of mycobacterial lipoarabinomannan with an antigen-capture ELISA in unprocessed urine of Tanzanian patients with suspected tuberculosis. *Trans. R. Soc. Trop. Med. Hyg.* (2005). doi:10.1016/j.trstmh.2005.04.014
96. Wood, A. *et al.* Ultrasensitive detection of lipoarabinomannan with plasmonic grating biosensors in clinical samples of HIV negative patients with tuberculosis. *PLoS One* (2019). doi:10.1371/journal.pone.0214161
97. Mutetwa, R. *et al.* Diagnostic accuracy of commercial urinary lipoarabinomannan detection in African tuberculosis suspects and patients. *Int. J. Tuberc. Lung Dis.* (2009).

98. Lawn, S. D. *et al.* Urine lipoarabinomannan assay for tuberculosis screening before antiretroviral therapy diagnostic yield and association with immune reconstitution disease. *AIDS* (2009). doi:10.1097/QAD.0b013e32832e05c8
99. Peter, J. G. *et al.* Effect on mortality of point-of-care, urine-based lipoarabinomannan testing to guide tuberculosis treatment initiation in HIV-positive hospital inpatients: A pragmatic, parallel-group, multicountry, open-label, randomised controlled trial. *Lancet* (2016). doi:10.1016/S0140-6736(15)01092-2
100. Nakiyingi, L. *et al.* Diagnostic Accuracy of a Rapid Urine Lipoarabinomannan Test for Tuberculosis in HIV-Infected Adults. *JAIDS J. Acquir. Immune Defic. Syndr.* **66(3)**, 270–279 (2014).
101. Wood, R. *et al.* Lipoarabinomannan in urine during tuberculosis treatment: Association with host and pathogen factors and mycobacteriuria. *BMC Infect. Dis.* (2012). doi:10.1186/1471-2334-12-47
102. Tessema, T. A., Hamasur, B., Bjune, G., Svenson, S. & Bjorvatn, B. Diagnostic evaluation of urinary lipoarabinomannan at an Ethiopian tuberculosis centre. *Scand. J. Infect. Dis.* (2001). doi:10.1080/003655401300077306
103. Bjerrum, S. *et al.* Diagnostic accuracy of the rapid urine lipoarabinomannan test for pulmonary tuberculosis among HIV-infected adults in Ghana-findings from the DETECT HIV-TB study. *BMC Infect. Dis.* (2015). doi:10.1186/s12879-015-1151-1
104. Huerga, H. *et al.* Diagnostic value of the urine lipoarabinomannan assay in HIV-positive, ambulatory patients with CD4 below 200 cells/μl in 2 low-resource settings: A prospective observational study. *PLoS Medicine* (2019). doi:10.1371/journal.pmed.1002792
105. Daley, P. *et al.* Blinded evaluation of commercial urinary lipoarabinomannan for active tuberculosis: A pilot study. *Int. J. Tuberc. Lung Dis.* (2009).
106. Wang, W. H. *et al.* A novel, rapid (within hours) culture-free diagnostic method for detecting live Mycobacterium tuberculosis with high sensitivity. *EBioMedicine* (2020). doi:10.1016/j.ebiom.2020.103007
107. Ravn, P. *et al.* Prospective evaluation of a whole-blood test using Mycobacterium tuberculosis-specific antigens ESAT-6 and CFP-10 for diagnosis of active tuberculosis. *Clin. Diagn. Lab. Immunol.* (2005). doi:10.1128/CDLI.12.4.491-496.2005
108. Raqib, R. *et al.* Detection of antibodies secreted from circulating mycobacterium tuberculosis-specific plasma cells in the diagnosis of Pediatric tuberculosis. *Clin. Vaccine Immunol.* (2009). doi:10.1128/CVI.00391-08
109. Anderson, S. T. *et al.* Diagnosis of Childhood Tuberculosis and Host RNA Expression in Africa. *N Eng J Med.* **370(18)**, 1712–1723 (2014).
110. Portevin, D. *et al.* Assessment of the novel T-cell activation marker-tuberculosis assay for diagnosis of active tuberculosis in children: A prospective proof-of-concept study. *Lancet Infect. Dis.* (2014).

doi:10.1016/S1473-3099(14)70884-9
111. Tebruegge, M. *et al.* Mycobacteria-specific cytokine responses detect tuberculosis infection and distinguish latent from active tuberculosis. *Am. J. Respir. Crit. Care Med.* (2015). doi:10.1164/rccm.201501-0059OC
112. Tornheim, J. A. *et al.* Transcriptomic Profiles of Confirmed Pediatric Tuberculosis Patients and Household Contacts Identifies Active Tuberculosis, Infection, and Treatment Response Among Indian Children. *J Infect Dis.* **221(10)**, 1647–1658 (2020).
113. Sweeney, T. E., Braviak, L., Tato, C. M. & Khatri, P. Genome-wide expression for diagnosis of pulmonary tuberculosis: a multicohort analysis. *Lancet Respir Med.* **4(3)**, 213–224 (2016).
114. Verhagen, L. M. *et al.* A predictive signature gene set for discriminating active from latent tuberculosis in Warao Amerindian children. *BMC Genomics* **14(1)**, 74 (2013).
115. Iqbal, N. T. *et al.* Antibody-Secreting Cells To Diagnose Mycobacterium tuberculosis Infection in Children in Pakistan . *mSphere* (2020). doi:10.1128/msphere.00632-19
116. Chegou, N. N. *et al.* Utility of Host Markers Detected in Quantiferon Supernatants for the Diagnosis of Tuberculosis in Children in a High-Burden Setting. *PLoS One* (2013). doi:10.1371/journal.pone.0064226
117. Whittaker, E., Gordon, A. & Kampmann, B. Is IP-10 a better biomarker for active and latent tuberculosis in children than IFNγ? *PLoS One* (2008). doi:10.1371/journal.pone.0003901
118. Latorre, I. *et al.* IP-10 is an accurate biomarker for the diagnosis of tuberculosis in children. *J. Infect.* (2014). doi:10.1016/j.jinf.2014.06.013
119. Lighter, J., Rigaud, M., Huie, M., Peng, C. H. & Pollack, H. Chemokine IP-10: An adjunct marker for latent tuberculosis infection in children. *Int. J. Tuberc. Lung Dis.* (2009).
120. Lundtoft, C. *et al.* Alternative Quantiferon cytokines for diagnosis of children with active tuberculosis and HIV co-infection in Ghana. *Med. Microbiol. Immunol.* (2017). doi:10.1007/s00430-017-0501-6
121. Nausch, N. *et al.* Multiple cytokines for the detection of Mycobacterium tuberculosis infection in children with tuberculosis. *Int. J. Tuberc. Lung Dis.* (2017). doi:10.5588/ijtld.16.0351
122. Sudbury, E. L. *et al.* Mycobacterium tuberculosis-specific cytokine biomarkers for the diagnosis of childhood TB in a TB-endemic setting. *J. Clin. Tuberc. Other Mycobact. Dis.* (2019). doi:10.1016/j.jctube.2019.100102
123. Petrone, L. *et al.* Blood or Urine IP-10 cannot discriminate between active tuberculosis and respiratory diseases different from tuberculosis in children. *Biomed Res. Int.* (2015). doi:10.1155/2015/589471
124. Laurenti, P. *et al.* Performance of interferon-γ release assays in the diagnosis of confirmed active tuberculosis in immunocompetent children: A new systematic review and meta-analysis. *BMC Infect. Dis.* (2016). doi:10.1186/s12879-016-1461-y
125. Comella-Del-Barrio, P. *et al.* A model based on the combination of ifn-γ, ip-

10, ferritin and 25-hydroxyvitamin d for discriminating latent from active tuberculosis in children. *Front. Microbiol.* (2019). doi:10.3389/fmicb.2019.01855
126. Gjøen, J. E. *et al.* Novel transcriptional signatures for sputum-independent diagnostics of tuberculosis in children. *Sci Rep.* **7(1)**, 5839 (2017).
127. Albuquerque, V. V. S. *et al.* Plasma levels of C-reactive protein, matrix metalloproteinase-7 and lipopolysaccharide-binding protein distinguish active pulmonary or extrapulmonary tuberculosis from uninfected controls in children. *Cytokine* (2019). doi:10.1016/j.cyto.2019.154773
128. Andreas, N. J. *et al.* Performance of metabonomic serum analysis for diagnostics in paediatric tuberculosis. *Sci Rep.* **10(1)**, 7302 (2020).
129. Nonyane, B. A. S. *et al.* Serologic Responses in Childhood Pulmonary Tuberculosis. *Pediatr. Infect. Dis. J.* (2018). doi:10.1097/INF.0000000000001683
130. Sun, L. *et al.* Utility of Novel Plasma Metabolic Markers in the Diagnosis of Pediatric Tuberculosis: A Classification and Regression Tree Analysis Approach. *J. Proteome Res.* (2016). doi:10.1021/acs.jproteome.6b00228
131. Jenum, S. *et al.* Approaching a diagnostic point-of-care test for pediatric tuberculosis through evaluation of immune biomarkers across the clinical disease spectrum. *Sci Rep.* **6(1)**, 18520 (2016).
132. Dhanasekaran, S. *et al.* Identification of biomarkers for Mycobacterium tuberculosis infection and disease in BCG-vaccinated young children in Southern India. *Genes Immun.* (2013). doi:10.1038/gene.2013.26
133. Zhou, M. *et al.* Circulating microRNAs as biomarkers for the early diagnosis of childhood tuberculosis infection. *Mol Med Rep.* **13(6)**, 4620–4626 (2016).
134. Kumar, N. P. *et al.* Circulating biomarkers of pulmonary and extrapulmonary tuberculosis in children. *Clin. Vaccine Immunol.* (2013). doi:10.1128/CVI.00038-13
135. Perez-Velez, C. M. & Marais, B. J. Tuberculosis in Children. *N. Engl. J. Med.* **367**, 348–361 (2012).
136. Kerkhoff, A. D. *et al.* Disseminated tuberculosis among hospitalised HIV patients in South Africa: A common condition that can be rapidly diagnosed using urine-based assays. *Sci. Rep.* (2017). doi:10.1038/s41598-017-09895-7
137. Jakhar, S., Lenz, K. & Mukundan, H. Current Status of Pediatric Tuberculosis Diagnostics, Needs, and Challenges. in *Diagnosis and management of tuberculosis* 1–13 (2019).
138. Lawn, S. D. & Gupta-Wright, A. Detection of lipoarabinomannan (LAM) in urine is indicative of disseminated TB with renal involvement in patients living with hiv and advanced immunodeficiency: Evidence and implications. *Transactions of the Royal Society of Tropical Medicine and Hygiene* **110**, 180–185 (2015).
139. Broger, T. *et al.* Novel lipoarabinomannan point-of-care tuberculosis test for people with HIV: a diagnostic accuracy study. *Lancet Infect. Dis.* **19**, 852–861 (2019).

140. Kerkhoff, A. D. *et al.* Diagnostic sensitivity of SILVAMP TB-LAM (FujiLAM) point-of-care urine assay for extra-pulmonary tuberculosis in people living with HIV. *Eur. Respir. J.* **55**, 1901259 (2020).
141. Bjerrum, S. *et al.* Diagnostic Accuracy of a Novel and Rapid Lipoarabinomannan Test for Diagnosing Tuberculosis Among People With Human Immunodeficiency Virus. *Open Forum Infect. Dis.* **7**, (2020).
142. Bjerrum, S. *et al.* Lateral flow urine lipoarabinomannan assay for detecting active tuberculosis in people living with HIV. *Cochrane Database Syst Rev.* **10(10)**, CD011420 (2019).
143. Comstock, G. W., Livesay, V. T. & Woolpert, S. F. The prognosis of a positive tuberculin reaction in childhood and adolescence. *Am J Epidemiol* **99(2)**, 131–8 (1974).
144. Mandal, N., Anand, P. K., Gautam, S., Das, S. & Hussain, T. Diagnosis and treatment of paediatric tuberculosis: An insight review. *Crit Rev Microbiol.* **43(4)**, 466–480 (2017).
145. Dodd, P. J., Sismanidis, C. & Seddon, J. A. Global burden of drug-resistant tuberculosis in children: a mathematical modelling study. *Lancet Infect. Dis.* (2016). doi:10.1016/S1473-3099(16)30132-3
146. Marais, B. J. *et al.* A Refined Symptom-Based Approach to Diagnose Pulmonary Tuberculosis in Children. *Pediatrics* **118**, e1350–e1359 (2006).
147. Schumacher, S. G. *et al.* Diagnostic Test Accuracy in Childhood Pulmonary Tuberculosis: A Bayesian Latent Class Analysis. *Am J Epidemiol.* **184(9)**, 690–700 (2016).
148. WHO. *Global tuberculosis report 2018. Geneva: World Health Organization; 2018. WHO Publication* (2018). doi:WHO/HTM/TB/2017.23
149. Esposito, S., Tagliabue, C., & Bosis, S. Tuberculosis in children. *Mediterr. J. Hematol. Infect. Dis.* **5**, (2013).
150. Sakamuri, R. M. *et al.* Current methods for diagnosis of human tuberculosis and considerations for global surveillance. in *Tuberculosis, Leprosy and other Mycobacterial Diseases of Man and Animals* 72–102 (2015). doi:10.1079/9781780643960.0000
151. Bianchi, L. *et al.* Interferon-gamma release assay improves the diagnosis of tuberculosis in children. *Pediatr Infect Dis J.* **28(6)**, 510–514 (2009).
152. Liebeschuetz, S. *et al.* Diagnosis of tuberculosis in South African children with a T-cell-based assay: A prospective cohort study. *Lancet* (2004). doi:10.1016/S0140-6736(04)17592-2
153. Hill, P. C. Comparison of Enzyme-Linked Immunospot Assay and Tuberculin Skin Test in Healthy Children Exposed to Mycobacterium tuberculosis. *Pediatrics* (2006). doi:10.1542/peds.2005-2095
154. Ewer, K. *et al.* Comparison of T-cell-based assay with tuberculin skin test for diagnosis of Mycobacterium tuberculosis infection in a school tuberculosis outbreak. *Lancet* (2003). doi:10.1016/S0140-6736(03)12950-9
155. Nicol, M. P. *et al.* Comparison of T-SPOT.TB Assay and Tuberculin Skin Test for the Evaluation of Young Children at High Risk for Tuberculosis in a Community Setting. *Pediatrics* (2008). doi:10.1542/peds.2008-0611
156. Elliot, C. *et al.* Tuberculin skin test versus interferon-gamma release assay

in refugee children: A retrospective cohort study. *J Paediatr Child Heal.* **54(8)**, 834–839 (2018).
157. Kampmann, B. *et al.* Interferon-γ release assays do not identify more children with active tuberculosis than the tuberculin skin test. *Eur. Respir. J.* (2009). doi:10.1183/09031936.00153408
158. Connell, T. G. *et al.* A Three-Way Comparison of Tuberculin Skin Testing, QuantiFERON-TB Gold and T-SPOT.TB in Children. *PLoS One* **3(7)**, e2624 (2008).
159. MacHingaidze, S. *et al.* The utility of an interferon gamma release assay for diagnosis of latent tuberculosis infection and disease in children: A systematic review and meta-analysis. *Pediatric Infectious Disease Journal* (2011). doi:10.1097/INF.0b013e318214b915
160. Fan, L., Chen, Z., Hao, X. H., Hu, Z. Y. & Xiao, H. P. Interferon-gamma release assays for the diagnosis of extrapulmonary tuberculosis: A systematic review and meta-analysis. *FEMS Immunol. Med. Microbiol.* (2012). doi:10.1111/j.1574-695X.2012.00972.x
161. Detjen, A. K. *et al.* Interferon- Release Assays Improve the Diagnosis of Tuberculosis and Nontuberculous Mycobacterial Disease in Children in a Country with a Low Incidence of Tuberculosis. *Clin Infect Dis.* **45(3)**, 322–8 (2007).
162. Aber, V. R. *et al.* Quality control in tuberculosis bacteriology. I. Laboratory studies on isolated positive cultures and the efficiency of direct smear examination. *Tubercle* **61(3)**, 123–33 (1980).
163. Burdash, N. M., Manos, J. P., Ross, D. & Bannister, E. R. Evaluation of the acid fast smear. *J Clin Microbiol.* **4(2)**, 190–1 (1976).
164. Corper, H. J. & Stoner, R. E. An improved procedure for the diagnostic culture of mammalian tubercle bacilli. *J Lab Clin Med.* **31(12)**, 1364–71 (1946).
165. Dye, C., Watt, C. J., Bleed, D. M. & Williams, B. G. What is the limit to case detection under the DOTS strategy for tuberculosis control? *Tuberculosis* **83(1–3)**, 35–43 (2003).
166. Hopewell, P. C., Pai, M., Maher, D., Uplekar, M. & Raviglione, M. C. International Standards for Tuberculosis Care. *Lancet Infect Dis.* **6(11)**, 710–25 (2006).
167. Perkins, M. D. New diagnostic tools for tuberculosis. in *International Journal of Tuberculosis and Lung Disease* (2000).
168. Desikan, P. Sputum smear microscopy in tuberculosis: Is it still relevant? *Indian Journal of Medical Research* (2013).
169. Frieden, T. *Toman's tuberculosis: case detection, treatment and monitoring. Questions and answers*. *Toman's tuberculosis: case detection, treatment and monitoring. Questions and answers* (2004).
170. Swaminathan, S. & Rekha, B. Pediatric Tuberculosis: Global Overview and Challenges. *Clin. Infect. Dis.* **50**, S184–S194 (2010).
171. Zar, H. J., Hanslo, D., Apolles, P., Swingler, G. & Hussey, G. Induced sputum versus gastric lavage for microbiological confirmation of pulmonary tuberculosis in infants and young children: A prospective study. *Lancet*

(2005). doi:10.1016/S0140-6736(05)17702-2
172. Gomez-Pastrana, D. *et al.* Comparison of Amplicor, In-House Polymerase Chain Reaction, and Conventional Culture for the Diagnosis of Tuberculosis in Children. *Clin. Infect. Dis.* (2002). doi:10.1086/317526
173. Hepple, P., Ford, N. & McNerney, R. Microscopy compared to culture for the diagnosis of tuberculosis in induced sputum samples: A systematic review. *International Journal of Tuberculosis and Lung Disease* **16**, 579–588 (2012).
174. Cuevas, L. E. *et al.* Evaluation of tuberculosis diagnostics in children: 2. Methodological issues for conducting and reporting research evaluations of tuberculosis diagnostics for intrathoracic tuberculosis in children. Consensus from an expert panel. *J. Infect. Dis.* (2012). doi:10.1093/infdis/jir879
175. Marais, B. J. & Pai, M. Recent advances in the diagnosis of childhood tuberculosis. *Archives of Disease in Childhood* (2007). doi:10.1136/adc.2006.104976
176. Ha, D. T. M. *et al.* Microscopic observation drug susceptibility assay (MODS) for early diagnosis of tuberculosis in children. *PLoS One* (2009). doi:10.1371/journal.pone.0008341
177. Connell, T. G., Zar, H. J. & Nicol, M. P. Advances in the diagnosis of pulmonary tuberculosis in HIV-infected and HIV uninfected children. *J. Infect. Dis.* (2011). doi:10.1093/infdis/jir413
178. R, S. K. *et al.* Xpert(R) MTB/RIF assay for pulmonary tuberculosis and rifampicin resistance in adults. *Cochrane Database Syst Rev.* **2014(1)**, CD009593 (2014).
179. Chatterjee, D. & Khoo, K. H. Mycobacterial lipoarabinomannan: An extraordinary lipoheteroglycan with profound physiological effects. *Glycobiology* **8**, 113–120 (1998).
180. Lawn, S. D. Point-of-care detection of lipoarabinomannan (LAM) in urine for diagnosis of HIV-associated tuberculosis: A state of the art review. *BMC Infect. Dis.* **12**, 103 (2012).
181. Tapping, R. I. & Tobias, P. S. Mycobacterial lipoarabinomannan mediates physical interactions between TLR1 and TLR2 to induce signaling. *J. Endotoxin Res.* (2003). doi:10.1179/096805103225001477
182. Sada, E., Aguilar, D., Torres, M. & Herrera, T. Detection of lipoarabinomannan as a diagnostic test for tuberculosis. *J Clin Microbiol.* **30(9)**, 2415–2418 (1992).
183. The use of lateral flow urine lipoarabinomannan assay (LF-LAM) for the diagnosis and screening of active tuberculosis in people living with HIV, policy guidance, WHO 2015. ISBN 978 92 4 150963 3
184. Sakamuri, R. M. *et al.* Detection of stealthy small amphiphilic biomarkers. *J. Microbiol. Methods* **103**, 112–117 (2014).
185. Means, T. K. *et al.* The CD14 ligands lipoarabinomannan and lipopolysaccharide differ in their requirement for Toll-like receptors. *J. Immunol.* (1999).
186. Baumberger, C., Ulevitch, R. J. & Dayer, J. M. Modulation of endotoxic

activity of lipopolysaccharide by high-density lipoprotein. *Pathobiology* **59**, 378–383 (1991).
187. Underhill, D. M., Ozinsky, A., Smith, K. D. & Aderem, A. Toll-like receptor-2 mediates mycobacteria-induced proinflammatory signaling in macrophages. *Proc. Natl. Acad. Sci. U. S. A.* **96**, 14459–63 (1999).
188. Zar, H. J., Connell, T. G. & Nicol, M. Diagnosis of pulmonary tuberculosis in children: New advances. *Expert Rev Anti InfectTher* **8(3)**, 277–88 (2010).
189. Graham, S. M. *et al.* Evaluation of tuberculosis diagnostics in children: 1. Proposed clinical case definitions for classification of intrathoracic tuberculosis disease. Consensus from an expert panel. *J. Infect. Dis.* (2012). doi:10.1093/infdis/jis008
190. Nelson, L. J. & Wells, C. D. Global epidemiology of childhood tuberculosis. *InterJ Tuberc Lung Dis.* **8(5)**, 636–47 (2004).
191. Dodd, P. J., Yuen, C. M., Sismanidis, C., Seddon, J. A. & Jenkins, H. E. The global burden of tuberculosis mortality in children: a mathematical modelling study. *Lancet Glob. Heal.* (2017). doi:10.1016/S2214-109X(17)30289-9
192. Organization, W. H. Global tuberculosis control. *WHO Rep. 2006* (2006).
193. Gordin, F. M. *et al.* The impact of human immunodeficiency virus infection on drug-resistant tuberculosis. *Am. J. Respir. Crit. Care Med.* (1996). doi:10.1164/ajrccm.154.5.8912768
194. Newton, S. M., Brent, A. J., Anderson, S., Whittaker, E. & Kampmann University of Cape Town, Cape Town, South Africa, B. I. of I. D. and M. M. Paediatric tuberculosis TT -. *Lancet Infect. Dis. TA* - **8**, 498–510 (2008).
195. Geneva. *Global Tuberculosis Report 2018*. *Geneva : World Health Organization* (2018). doi:ISBN 978 92 4 156539 4
196. MacLean, E. *et al.* A systematic review of biomarkers to detect active tuberculosis. *Nature Microbiology* (2019). doi:10.1038/s41564-019-0380-2
197. World Health Organization. *Global tuberculosis report*. (2019).
198. Starke, J. R. Transmission of mycobacterium tuberculosis to and from children and adolescents. *Semin. Pediatr. Infect. Dis.* **12**, 115–123 (2001).
199. Flynn, J. L. & Chan, J. Tuberculosis: Latency and reactivation. *Infect Immun.* **69(7)**, 4195–4201 (2001).
200. Kapur, A., Harries, A. D., Lönnroth, K., Wilson, P. & Sulistyowati, L. S. Diabetes and tuberculosis co-epidemic: The Bali Declaration. *Lancet Diabetes Endocrinol* **4(1)**, 8–10 (2016).
201. Sharan, R. *et al.* Chronic Immune Activation in TB/HIV Co-infection. *Trends Microbiol* **28 (8)**, 619–632 (2020).
202. Balasubramanian, V., Wiegeshaus, E. H., Taylor, B. T. & Smith, D. W. Pathogenesis of tuberculosis: pathway to apical localization. *Tuber Lung Dis.* **75(3)**, 68–78 (1994).
203. Riley, R. L. Airborne infection. *Am J Med.* **57(3)**, 466–75 (1974).
204. Whittaker, E., Lopez-Varela, E., Broderick, C. & Seddon, J. A. Examining the complex relationship between tuberculosis and other infectious diseases in children: A review. *Front Pediatr* **7:233**, (2019).

205. Nhu, N. T. Q. *et al.* Evaluation of Xpert MTB/RIF and MODS assay for the diagnosis of pediatric tuberculosis. *BMC Infect Dis.* **13(1): 31**, (2013).
206. Marais, B. J., Graham, S. M., Maeurer, M. & Zumla, A. Progress and challenges in childhood tuberculosis. *Lancet Infect Dis.* **13(4)**, 287–9 (2013).
207. Dunn, J. J., Starke, J. R. & Revell, P. A. Laboratory Diagnosis of Mycobacterium tuberculosis Infection and Disease in Children. *J Clin Microbiol.* **54(6)**, 1434–1441 (2016).
208. Kunkel, A. *et al.* Smear positivity in paediatric and adult tuberculosis: Systematic review and meta-analysis. *BMC Infect Dis.* **16: 282**, (2016).
209. Dorman, S. E. *et al.* Xpert MTB/RIF Ultra for detection of Mycobacterium tuberculosis and rifampicin resistance: a prospective multicentre diagnostic accuracy study. *Lancet Infect Dis.* **18(1)**, 76–84 (2018).
210. Bulterys, M. A. *et al.* Point-Of-Care Urine LAM Tests for Tuberculosis Diagnosis: A Status Update. *J Clin Med.* **9(1):111**, (2019).
211. Mukundan, H. *et al.* Rapid detection of Mycobacterium tuberculosis biomarkers in a sandwich immunoassay format using a waveguide-based optical biosensor. *Tuberculosis* **92(5)**, 407–416 (2012).
212. Amin, A. G. *et al.* Detection of lipoarabinomannan in urine and serum of HIV-positive and HIV-negative TB suspects using an improved capture-enzyme linked immuno absorbent assay and gas chromatography/mass spectrometry. *Tuberculosis* **111:178–18**, (2018).
213. Starke, J. R. Diagnosis of tuberculosis in children. *Pediatr Infect Dis J.* **19(11)**, 1095–1096 (2000).
214. Geyer, P. E., Holdt, L. M., Teupser, D. & Mann, M. Revisiting biomarker discovery by plasma proteomics. *Mol Syst Biol.* **13(9): 942**, (2017).
215. Wetterstrand, K. DNA Sequencing Costs: Data from the NHGRI Genome Sequencing Program (GSP), 2020. (2020). Available at: https://www.genome.gov/about-genomics/fact-sheets/DNA-Sequencing-Costs-Data. (Accessed: 30th August 2020)
216. Colston, S. Field forward sequencing in naval environments. (2019). Available at: https://nanoporetech.com/resource-centre/field-forward-sequencing-naval-environments.
217. Nimmo, C. *et al.* Whole genome sequencing Mycobacterium tuberculosis directly from sputum identifies more genetic diversity than sequencing from culture. *BMC Genomics* **20(389)**, (2019).
218. MD Anderson Center 'Submission, Services and Pricing'. Available at: https://www.mdanderson.org/research/research-resources/core-facilities/functional-proteomics-rppa-core/submission-services-and-pricing.html.
219. Huang, Y. & Zhu, H. Protein Array-based Approaches for Biomarker Discovery in Cancer. *Genom Proteom Bioinf* **15(2)**, 73–81 (2017).
220. Stanislaus, R. *et al.* RPPAML/RIMS: A metadata format and an information management system for reverse phase protein arrays. *BMC Bioinformatics* **9(555)**, (2008).
221. Li, P. E. *et al.* Enabling the democratization of the genomics revolution with

a fully integrated web-based bioinformatics platform. *Nucleic Acids Res.* **45(1)**, 67–80 (2017).
222. Posadas, E. M., Simpkins, F., Liotta, L. A., MacDonald, C. & Kohn, E. C. Proteomic analysis for the early detection and rational treatment of cancer - Realistic hope? *Ann Oncol.* **16(1)**, 16–22 (2005).
223. Gengenbacher, M., Mouritsen, J., Schubert, O. T., Aebersold, R. & Kaufmann, S. H. E. Mycobacterium tuberculosis in the Proteomics Era. *Microbiol Spectr.* **2(2)**, (2014).
224. Köser, C. U. *et al.* Whole-genome sequencing for rapid susceptibility testing of M. tuberculosis. *N Eng J Med.* **369(3)**, 290–2 (2013).
225. Cao, T. *et al.* A Two-Way Proteome Microarray Strategy to Identify Novel Mycobacterium tuberculosis-Human Interactors. *Front. Cell. Infect. Microbiol.* **9**, (2019).
226. Deng, J. *et al.* Mycobacterium Tuberculosis Proteome Microarray for Global Studies of Protein Function and Immunogenicity. *Cell Rep.* **9(6)**, 2317–2329 (2014).
227. Li, J. *et al.* Characterization of plasma proteins in children of different Mycobacterium tuberculosis infection status using label-free quantitative proteomics. *Oncotarget* **8(61)**, 103290–103301 (2017).
228. Layre, E. *et al.* A Comparative Lipidomics Platform for Chemotaxonomic Analysis of Mycobacterium tuberculosis. *Chem Biol.* **18(12)**, 1537–1549 (2011).
229. Shui, G. *et al.* Mycolic acids as diagnostic markers for tuberculosis case detection in humans and drug efficacy in mice. *EMBO Mol Med.* **4(1)**, 27–37 (2012).
230. Zhou, A. *et al.* Application of 1 H NMR Spectroscopy-Based Metabolomics to Sera of Tuberculosis Patients. *J Proteome Res.* **12 (10)**, 4642–4649 (2013).
231. Frediani, J. K. *et al.* Plasma metabolomics in human pulmonary tuberculosis disease: A pilot study. *PLoS One* **9(10)**, e108854 (2014).
232. Lau, S. K. P. *et al.* Metabolomic profiling of plasma from patients with tuberculosis by use of untargeted mass spectrometry reveals novel biomarkers for diagnosis. *J Clin Microbiol.* **53**, 3750–3759 (2015).
233. Haas, C. T., Roe, J. K., Pollara, G., Mehta, M. & Noursadeghi, M. Diagnostic 'omics' for active tuberculosis. *BMC Med.* **14**, 37 (2016).
234. Terwilliger, T. . *et al.* The TB structural genomics consortium: a resource for Mycobacterium tuberculosis biology. *Tuberculosis* **83(4)**, 223–249 (2003).
235. Miotto, P. *et al.* miRNA Signatures in Sera of Patients with Active Pulmonary Tuberculosis. *PLoS One* **8(11)**, e80149 (2013).
236. Yong, Y. K. *et al.* Immune Biomarkers for Diagnosis and Treatment Monitoring of Tuberculosis: Current Developments and Future Prospects. *Front. Microbiol.* **10**, (2019).
237. Schubert, O. T. *et al.* The Mtb Proteome Library: A Resource of Assays to Quantify the Complete Proteome of Mycobacterium tuberculosis. *Cell Host Microbe.* **13(5)**, 602–612 (2013).

238. Cao, S. H. *et al.* Screening of Serum Biomarkers for Distinguishing between Latent and Active Tuberculosis Using Proteome Microarray. *Biomed Env. Sci.* **31(7)**, 515–526 (2018).
239. Kato-Maeda, M. *et al.* Use of Whole Genome Sequencing to Determine the Microevolution of Mycobacterium tuberculosis during an Outbreak. *PLoS One* **8(3)**, e58235 (2013).
240. Guerra-Assunção, J. *et al.* Large-scale whole genome sequencing of M. tuberculosis provides insights into transmission in a high prevalence area. *Elife* **4**, e05166 (2015).
241. Zetola, N. M. *et al.* Mixed Mycobacterium tuberculosis Complex Infections and False-Negative Results for Rifampin Resistance by GeneXpert MTB/RIF Are Associated with Poor Clinical Outcomes. *J Clin Microbiol.* **52(7)**, 2422–2429 (2014).
242. Tang, P. *et al.* Use of DNA microarray chips for the rapid detection of Mycobacterium tuberculosis resistance to rifampicin and isoniazid. *ExpTher Med.* **13(5)**, 2332–2338 (2017).
243. Chen, C. Y. *et al.* A new oligonucleotide array for the detection of multidrug and extensively drug-resistance tuberculosis. *Sci. Rep.* (2019). doi:10.1038/s41598-019-39339-3
244. Iketleng, T. *et al.* Mycobacterium tuberculosis Next-Generation Whole Genome Sequencing: Opportunities and Challenges. *Tuberc ResTreat.* **2018**, 1–8 (2018).
245. Gardy, J. L. *et al.* Whole-Genome Sequencing and Social-Network Analysis of a Tuberculosis Outbreak. *N Eng J Med.* **364(8)**, 730–739 (2011).
246. Ruiz-Tagle, C., Naves, R. & Balcells, M. E. Unraveling the Role of MicroRNAs in Mycobacterium tuberculosis Infection and Disease: Advances and Pitfalls. *Infect Immun.* **88(3)**, (2019).
247. Zhang, H. *et al.* Identification of Serum microRNA Biomarkers for Tuberculosis Using RNA-seq. *PLoS One* **9(2)**, e88909 (2014).
248. de Araujo, L. S. *et al.* Reprogramming of Small Noncoding RNA Populations in Peripheral Blood Reveals Host Biomarkers for Latent and Active Mycobacterium tuberculosis Infection. *MBio* **10(6)**, (2019).
249. Vergne, I., Chua, J., Singh, S. B. & Deretic, V. Cell Biology of Mycobacterium Tuberculosis Phagosome. *Annu. Rev. Cell Dev. Biol.* **20(1)**, 367–394 (2004).
250. Dyer, M. D. *et al.* The Human-Bacterial Pathogen Protein Interaction Networks of Bacillus anthracis, Francisella tularensis, and Yersinia pestis. *PLoS One* **5(8)**, e12089 (2010).
251. König, R. *et al.* Global Analysis of Host-Pathogen Interactions that Regulate Early-Stage HIV-1 Replication. *Cell* **135(1)**, 49–60 (2008).
252. Kunnath-Velayudhan, S. & Porcelli, S. A. Recent Advances in Defining the Immunoproteome of Mycobacterium tuberculosis. *Front Immunol.* **4**, (2013).
253. Kunnath-Velayudhan, S. *et al.* Dynamic antibody responses to the Mycobacterium tuberculosis proteome. *PNAS* **107(33)**, 14703–14708

(2010).
254. Britton, W. J., Hellqvist, L., Ivanyi, J. & Basten, A. Immunopurification of Radiolabelled Antigens of Mycobacterium leprae and Mycobacterium bovis (Bacillus Calmette-Guerin) with Monoclonal Antibodies. *Scand J Immunol.* **26(2)**, 149–159 (1987).
255. Daugelat, S., Guile, H., Schoel, B. & Kaufmann, S. H. E. Secreted Antigens of Mycobacterium tuberculosis: Characterization with T Lymphocytes from Patients and Contacts after Two-Dimensional Separation. *J Infect Dis.* **166(1)**, 186–190 (1992).
256. Wong, D. K., Lee, B.-Y., Horwitz, M. A. & Gibson, B. W. Identification of Fur, Aconitase, and Other Proteins Expressed by Mycobacterium tuberculosis under Conditions of Low and High Concentrations of Iron by Combined Two-Dimensional Gel Electrophoresis and Mass Spectrometry. *Infect Immun.* **67(1)**, 327–336 (1999).
257. Kelkar, D. S. *et al.* Proteogenomic Analysis of Mycobacterium tuberculosis By High Resolution Mass Spectrometry. *Mol Cell Proteomics.* **10(12)**, M111.011627 (2011).
258. Chen, C.-S. *et al.* A proteome chip approach reveals new DNA damage recognition activities in Escherichia coli. *Nat Methods.* **5(1)**, 69–74 (2008).
259. Zhu, H. Global Analysis of Protein Activities Using Proteome Chips. *Science (80-.).* **293(5537)**, 2101–2105 (2001).
260. Li, Y. *et al.* A Proteome-Scale Identification of Novel Antigenic Proteins in Mycobacterium tuberculosis toward Diagnostic and Vaccine Development. *J Proteome Res.* **9(9)**, 4812–4822 (2010).
261. Sette, A. *et al.* Selective CD4+ T Cell Help for Antibody Responses to a Large Viral Pathogen: Deterministic Linkage of Specificities. *Immunity* **28(6)**, 847–858 (2008).
262. Penn-Nicholson, A. *et al.* Discovery and validation of a prognostic proteomic signature for tuberculosis progression: A prospective cohort study. *PLOS Med.* **16**, e1002781 (2019).
263. Perkowski, E. F. *et al.* The EXIT Strategy: an Approach for Identifying Bacterial Proteins Exported during Host Infection. *MBio* **8(2)**, (2017).
264. Yang, Q. *et al.* Identification of eight-protein biosignature for diagnosis of tuberculosis. *Thorax* **75(7)**, 576–583 (2020).
265. Kunnath-Velayudhan, S. & Gennaro, M. L. Immunodiagnosis of Tuberculosis: a Dynamic View of Biomarker Discovery. *Clin Microbiol Rev.* **24(4)**, 792–805 (2011).
266. Pal, R., Hameed, S., Kumar, P., Singh, S. & Fatima, Z. Comparative lipidomics of drug sensitive and resistant Mycobacterium tuberculosis reveals altered lipid imprints. *3 Biotech* **7(5)**, 325 (2017).
267. Raghunandanan, S., Jose, L., Gopinath, V. & Kumar, R. A. Comparative label-free lipidomic analysis of Mycobacterium tuberculosis during dormancy and reactivation. *Sci Rep.* **9(1)**, 3660 (2019).
268. Korf, J., Stoltz, A., Verschoor, J., De Baetselier, P. & Grooten, J. TheMycobacterium tuberculosis cell wall component mycolic acid elicits pathogen-associated host innate immune responses. *Eur J Immunol.*

35(3), 890–900 (2005).
269. Marrakchi, H., Lanéelle, M.-A. & Daffé, M. Mycolic Acids: Structures, Biosynthesis, and Beyond. *Chem Biol.* **21(1)**, 67–85 (2014).
270. Nataraj, V. *et al.* Mycolic acids: deciphering and targeting the Achilles' heel of the tubercle bacillus. *Mol Microbiol.* **98(1)**, 7–16 (2015).
271. Perumal, J. *et al.* Identification of mycolic acid forms using surface-enhanced Raman scattering as a fast detection method for tuberculosis. *Int J Nanomedicine* **13**, 6029–6038 (2018).
272. Ndlandla, F. L. *et al.* Standardization of natural mycolic acid antigen composition and production for use in biomarker antibody detection to diagnose active tuberculosis. *J Immunol Methods.* **435**, 50–59 (2016).
273. Thanyani, S. T., Roberts, V., Siko, D. G. R., Vrey, P. & Verschoor, J. A. A novel application of affinity biosensor technology to detect antibodies to mycolic acid in tuberculosis patients. *J Immunol Methods.* **332(1–2)**, 61–72 (2008).
274. Druszczynska, M., Wawrocki, S., Szewczyk, R. & Rudnicka, W. Mycobacteria-derived biomarkers for tuberculosis diagnosis. *Indian J Med Res.* **146(6)**, 700 (2017).
275. Layre, E., Al-Mubarak, R., Belisle, J. T. & Branch Moody, D. Mycobacterial Lipidomics. *Microbiol Spectr.* **2(3)**, (2014).
276. Astarie-Dequeker, C., Nigou, J., Passemar, C. & Guilhot, C. The role of mycobacterial lipids in host pathogenesis. *Drug DiscovToday.* **7(1)**, e33–e41 (2010).
277. Kurz, S. G. & Rivas-Santiago, B. Time to Expand the Picture of Mycobacterial Lipids: Spotlight on Nontuberculous Mycobacteria. *Am J Respir Cell Mol Biol.* **62(3)**, 275–276 (2020).
278. Correia-Neves, M. *et al.* Biomarkers for tuberculosis: the case for lipoarabinomannan. *ERJ Open Res.* **5(1)**, 00115–02018 (2019).
279. Stromberg, L. R. *et al.* Presentation matters: Impact of association of amphiphilic LPS with serum carrier proteins on innate immune signaling. *PLoS One* **13(6)**, e0198531 (2018).
280. Vu, D. M., Sakamuri, R. M., Waters, W. R., Swanson, B. I. & Mukundan, H. Detection of Lipomannan in Cattle Infected with Bovine Tuberculosis. *Anal. Sci.* **33(4)**, 457–460 (2017).
281. Fukuda, T. *et al.* Critical Roles for Lipomannan and Lipoarabinomannan in Cell Wall Integrity of Mycobacteria and Pathogenesis of Tuberculosis. *MBio* **4(1)**, (2013).
282. Buddle, B., Lisle, G., Waters, W. & Vordermeier, H. Diagnosis of mycobacterium bovis infection in cattle. in *Tuberculosis, Leprosy and Mycobacterial Diseases of Man and Animals: The Many Hosts of Mycobacteria* (eds. Mukundan, H., Chambers, M., Waters, W. & Larsen, M.) 168–184 (CAB International, 2015).
283. Kubicek-Sutherland, J. Z. *et al.* Direct detection of bacteremia by exploiting host-pathogen interactions of lipoteichoic acid and lipopolysaccharide. *Sci. Rep.* (2019). doi:10.1038/s41598-019-42502-5
284. Mukundan, H. *et al.* Immunoassays for the differentiation of bacterial

pathogens in human serum. (2017).
285. Kubicek-Sutherland, J. Z., Vu, D. M., Mendez, H. M., Jakhar, S. & Mukundan, H. Detection of lipid and amphiphilic biomarkers for disease diagnostics. *Biosensors* **7**, 25 (2017).
286. Anes, E. *et al.* Selected lipids activate phagosome actin assembly and maturation resulting in killing of pathogenic mycobacteria. *Nat Cell Biol.* **5**, 793–802 (2003).
287. Ramasamy, R., Gopal, N., Kuzhandaivelu, V. & Murugaiyan, S. Biosensors in clinical chemistry: An overview. *Adv. Biomed. Res.* (2014). doi:10.4103/2277-9175.125848
288. Ridgway, N. D. & McLeod, R. S. *Biochemistry of Lipids, Lipoproteins and Membranes: Sixth Edition*. *Biochemistry of Lipids, Lipoproteins and Membranes: Sixth Edition* (2015).
289. O'Brien, J. S. & Sampson, E. L. Lipid composition of the normal human brain: gray matter, white matter, and myelin. *J. Lipid Res.* (1965). doi:10.1016/S0022-2275(20)39619-X
290. Akira, S. & Hemmi, H. Recognition of pathogen-associated molecular patterns by TLR family. *Immunology Letters* (2003). doi:10.1016/S0165-2478(02)00228-6
291. Kawai, T. & Akira, S. Pathogen recognition with Toll-like receptors. *Current Opinion in Immunology* (2005). doi:10.1016/j.coi.2005.02.007
292. Kumar, H., Kawai, T. & Akira, S. Pathogen recognition in the innate immune response. *Biochemical Journal* (2009). doi:10.1042/BJ20090272
293. Kumar, H., Kawai, T. & Akira, S. Pathogen recognition by the innate immune system. *Int. Rev. Immunol.* (2011). doi:10.3109/08830185.2010.529976
294. Kumagai, Y., Takeuchi, O. & Akira, S. Pathogen recognition by innate receptors. *Journal of Infection and Chemotherapy* (2008). doi:10.1007/s10156-008-0596-1
295. Akira, S. Pathogen recognition by innate immunity and its signaling. *Proceedings of the Japan Academy Series B: Physical and Biological Sciences* (2009). doi:10.2183/pjab.85.143
296. Akira, S., Uematsu, S. & Takeuchi, O. Pathogen recognition and innate immunity. *Cell* (2006). doi:10.1016/j.cell.2006.02.015
297. Sin, M. L., Mach, K. E., Wong, P. K. & Liao, J. C. Advances and challenges in biosensor-based diagnosis of infectious diseases. *Expert Review of Molecular Diagnostics* (2014). doi:10.1586/14737159.2014.888313
298. Zivkovic, A. M. *et al.* Effects of sample handling and storage on quantitative lipid analysis in human serum. *Metabolomics* (2009). doi:10.1007/s11306-009-0174-2
299. Rudy, M. D., Kainz, M. J., Graeve, M., Colombo, S. M. & Arts, M. T. Handling and storage procedures have variable effects on fatty acid content in fishes with different lipid quantities. *PLoS One* (2016). doi:10.1371/journal.pone.0160497
300. Marion, E. *et al.* Photodegradation of the mycobacterium ulcerans toxin, mycolactones: Considerations for handling and storage. *PLoS One* (2012).

doi:10.1371/journal.pone.0033600
301. Harkewicz, R. & Dennis, E. A. Applications of mass spectrometry to lipids and membranes. *Annu. Rev. Biochem.* (2011). doi:10.1146/annurev-biochem-060409-092612
302. Griffiths, W. J. & Wang, Y. Mass spectrometry: From proteomics to metabolomics and lipidomics. *Chem. Soc. Rev.* (2009). doi:10.1039/b618553n
303. Gross, R. W. & Han, X. Lipidomics at the interface of structure and function in systems biology. *Chemistry and Biology* (2011). doi:10.1016/j.chembiol.2011.01.014
304. Brügger, B. Lipidomics: Analysis of the lipid composition of cells and Subcellular organelles by Electrospray ionization mass spectrometry. *Annual Review of Biochemistry* (2014). doi:10.1146/annurev-biochem-060713-035324
305. Hinterwirth, H., Stegemann, C. & Mayr, M. Lipidomics: Quest for molecular lipid biomarkers in cardiovascular disease. *Circ. Cardiovasc. Genet.* (2014). doi:10.1161/CIRCGENETICS.114.000550
306. Li, L. *et al.* Mass spectrometry methodology in lipid analysis. *International Journal of Molecular Sciences* (2014). doi:10.3390/ijms150610492
307. Milne, S., Ivanova, P., Forrester, J. & Alex Brown, H. Lipidomics: An analysis of cellular lipids by ESI-MS. *Methods* (2006). doi:10.1016/j.ymeth.2006.05.014
308. Murphy, R. C. & Gaskell, S. J. New applications of mass spectrometry in lipid analysis. *Journal of Biological Chemistry* (2011). doi:10.1074/jbc.R111.233478
309. FOLCH, J., LEES, M. & SLOANE STANLEY, G. H. A simple method for the isolation and purification of total lipides from animal tissues. *J. Biol. Chem.* (1957). doi:10.1016/s0021-9258(18)64849-5
310. Bligh, E. G. & Dyer, W. J. A rapid method of total lipid extraction and purification. *Can. J. Biochem. Physiol.* **37(8)**, 911–917 (1959).
311. Pati, S., Nie, B., Arnold, R. D. & Cummings, B. S. Extraction, chromatographic and mass spectrometric methods for lipid analysis. *Biomed. Chromatogr.* (2016). doi:10.1002/bmc.3683
312. Cajka, T. & Fiehn, O. Comprehensive analysis of lipids in biological systems by liquid chromatography-mass spectrometry. *TrAC - Trends in Analytical Chemistry* (2014). doi:10.1016/j.trac.2014.04.017
313. Han, X. & Gross, R. W. Shotgun lipidomics: Electrospray ionization mass spectrometric analysis and quantitation of cellular lipidomes directly from crude extracts of biological samples. *Mass Spectrom. Rev.* (2005). doi:10.1002/mas.20023
314. Han, X. & Gross, R. W. Shotgun lipidomics: Multidimensional MS analysis of cellular lipidomes. *Expert Review of Proteomics* (2005). doi:10.1586/14789450.2.2.253
315. Fuchs, B., Süß, R. & Schiller, J. An update of MALDI-TOF mass spectrometry in lipid research. *Progress in Lipid Research* (2010). doi:10.1016/j.plipres.2010.07.001

316. Schiller, J. *et al.* Matrix-assisted laser desorption and ionization time-of-flight (MALDI-TOF) mass spectrometry in lipid and phospholipid research. *Progress in Lipid Research* (2004). doi:10.1016/j.plipres.2004.08.001
317. Bugni, T. S. Review of Mass Spectrometry: Instrumentation, Interpretation, and ApplicationsMass Spectrometry: Instrumentation, Interpretation, and Applications. Edited by Rolf Ekman, Jerzy Silberring, Ann M. Westman-Brinkmalm, and Agnieszka Kraj. Wiley, New York, 2009. *J. Nat. Prod.* (2017). doi:10.1021/acs.jnatprod.7b00030
318. El-Aneed, A., Cohen, A. & Banoub, J. Mass spectrometry, review of the basics: Electrospray, MALDI, and commonly used mass analyzers. *Applied Spectroscopy Reviews* (2009). doi:10.1080/05704920902717872
319. Anand, S. *et al.* Detection and confirmation of serum lipid biomarkers for preeclampsia using direct infusion mass spectrometry. *J. Lipid Res.* (2016). doi:10.1194/jlr.P064451
320. Minkler, P. E. & Hoppel, C. L. Separation and characterization of cardiolipin molecular species by reverse-phase ion pair high-performance liquid chromatography-mass spectrometry. *J. Lipid Res.* (2010). doi:10.1194/jlr.D002857
321. Sparagna, G. C. *et al.* Loss of cardiac tetralinoleoyl cardiolipin in human and experimental heart failure. *J. Lipid Res.* (2007). doi:10.1194/jlr.M600551-JLR200
322. Kiebish, M. A., Han, X., Cheng, H., Chuang, J. H. & Seyfried, T. N. Cardiolipin and electron transport chain abnormalities in mouse brain tumor mitochondria: Lipidomic evidence supporting the Warburg theory of cancer. *J. Lipid Res.* (2008). doi:10.1194/jlr.M800319-JLR200
323. Crutchfield, C. A., Thomas, S. N., Sokoll, L. J. & Chan, D. W. Advances in mass spectrometry-based clinical biomarker discovery. *Clinical Proteomics* (2016). doi:10.1186/s12014-015-9102-9
324. Van, Q. N. *et al.* Comparison of 1D and 2D NMR spectroscopy for metabolic profiling. *J. Proteome Res.* (2008). doi:10.1021/pr700594s
325. Fonville, J. M. *et al.* Evaluation of full-resolution J-resolved1H NMR projections of biofluids for metabonomics information retrieval and biomarker identification. *Anal. Chem.* (2010). doi:10.1021/ac902443k
326. Adosraku, R. K., Choi, G. T. Y., Constantinou-Kokotos, V., Anderson, M. M. & Gibbons, W. A. NMR lipid profiles of cells, tissues, and body fluids: Proton NMR analysis of human erythrocyte lipids. *J. Lipid Res.* (1994). doi:10.1016/S0022-2275(20)39939-9
327. Nicholson, J. K. & Wilson, I. D. High resolution proton magnetic resonance spectroscopy of biological fluids. *Progress in Nuclear Magnetic Resonance Spectroscopy* (1989). doi:10.1016/0079-6565(89)80008-1
328. Beckonert, O. *et al.* High-resolution magic-angle-spinning NMR spectroscopy for metabolic profiling of intact tissues. *Nat. Protoc.* (2010). doi:10.1038/nprot.2010.45
329. Casu, M., Anderson, G. J., Choi, G. & Gibbons, W. A. NMR lipid profiles of cells, tissues and body fluids. I— 1D and 2D Proton NMR of lipids from rat liver. *Magn. Reson. Chem.* (1991). doi:10.1002/mrc.1260290610

330. Kostara, C. E. *et al.* Evaluation of established coronary heart disease on the basis of HDL and non-HDL NMR lipid profiling. *J. Proteome Res.* (2010). doi:10.1021/pr900783x
331. Mahrous, E. A., Lee, R. B. & Lee, R. E. A rapid approach to lipid profiling of mycobacteria using 2D HSQC NMR maps. *J. Lipid Res.* (2008). doi:10.1194/jlr.M700440-JLR200
332. Whitehead, T. L., Monzavi-Karbassi, B. & Kieber-Emmons, T. 1H-NMR metabonomics analysis of sera differentiates between mammary tumor-bearing mice and healthy controls. *Metabolomics* (2005). doi:10.1007/s11306-005-0006-y
333. Beger, R. D., Schnackenberg, L. K., Holland, R. D., Li, D. & Dragan, Y. Metabonomic models of human pancreatic cancer using 1D proton NMR spectra of lipids in plasma. *Metabolomics* (2006). doi:10.1007/s11306-006-0026-2
334. Kostara, C. E. *et al.* NMR-based lipidomic analysis of blood lipoproteins differentiates the progression of coronary heart disease. *J. Proteome Res.* (2014). doi:10.1021/pr500061n
335. Gebregiworgis, T. & Powers, R. Application of NMR Metabolomics to Search for Human Disease Biomarkers. *Comb. Chem. High Throughput Screen.* (2012). doi:10.2174/138620712802650522
336. Giovane, A., Balestrieri, A. & Napoli, C. New insights into cardiovascular and lipid metabolomics. *Journal of Cellular Biochemistry* (2008). doi:10.1002/jcb.21875
337. Zhang, X. *et al.* Metabolic signatures of esophageal cancer: NMR-based metabolomics and UHPLC-based focused metabolomics of blood serum. *Biochim. Biophys. Acta - Mol. Basis Dis.* (2013). doi:10.1016/j.bbadis.2013.03.009
338. Beckonert, O. *et al.* Metabolic profiling, metabolomic and metabonomic procedures for NMR spectroscopy of urine, plasma, serum and tissue extracts. *Nat. Protoc.* (2007). doi:10.1038/nprot.2007.376
339. Monleón, D. *et al.* Metabolite profiling of fecal water extracts from human colorectal cancer. *NMR Biomed.* (2009). doi:10.1002/nbm.1345
340. Yu, Y., Vidalino, L., Anesi, A., Macchi, P. & Guella, G. A lipidomics investigation of the induced hypoxia stress on HeLa cells by using MS and NMR techniques. *Mol. Biosyst.* (2014). doi:10.1039/c3mb70540d
341. Nicholson, J. K. & Lindon, J. C. Systems biology: Metabonomics. *Nature* (2008). doi:10.1038/4551054a
342. Dettmer, K., Aronov, P. A. & Hammock, B. D. Mass spectrometry-based metabolomics. *Mass Spectrometry Reviews* (2007). doi:10.1002/mas.20108
343. Urbina, J. & Waugh, J. S. Proton-enhanced 13C nuclear magnetic resonance of lipids and biomembranes. *Proc. Natl. Acad. Sci. U. S. A.* (1974). doi:10.1073/pnas.71.12.5062
344. Zheng, C., Zhang, S., Ragg, S., Raftery, D. & Vitek, O. Identification and quantification of metabolites in 1H NMR spectra by Bayesian model selection. *Bioinformatics* (2011). doi:10.1093/bioinformatics/btr118

345. Bothwell, J. H. F. & Griffin, J. L. An introduction to biological nuclear magnetic resonance spectroscopy. *Biological Reviews* (2011). doi:10.1111/j.1469-185X.2010.00157.x
346. Bertram, H. C. *et al.* Effect of magnetic field strength on NMR-based metabonomic human urine data. Comparative study of 250, 400, 500, and 800 MHz. *Anal. Chem.* (2007). doi:10.1021/ac070928a
347. Foster, M. P., McElroy, C. A. & Amero, C. D. Solution NMR of large molecules and assemblies. *Biochemistry* (2007). doi:10.1021/bi0621314
348. Lewis, I. A. *et al.* Method for determining molar concentrations of metabolites in complex solutions from two-dimensional 1H-13C NMR spectra. *Anal. Chem.* (2007). doi:10.1021/ac071583z
349. Lindon, J. C., Nicholson, J. K., Holmes, E. & Everett, J. R. Metabonomics: Metabolic processes studied by NMR spectroscopy of biofluids. *Concepts Magn. Reson.* (2000). doi:10.1002/1099-0534(2000)12:5<289::AID-CMR3>3.0.CO;2-W
350. Carrasco-Pancorbo, A., Navas-Iglesias, N. & Cuadros-Rodríguez, L. From lipid analysis towards lipidomics, a new challenge for the analytical chemistry of the 21st century. Part I: Modern lipid analysis. *TrAC - Trends Anal. Chem.* (2009). doi:10.1016/j.trac.2008.12.005
351. Zhang, F., Bruschweiler-Li, L., Robinette, S. L. & Brüschweiler, R. Self-consistent metabolic mixture analysis by heteronuclear NMR. Application to a human cancer cell line. *Anal. Chem.* (2008). doi:10.1021/ac801116u
352. Rai, R. K., Tripathi, P. & Sinha, N. Quantification of metabolites from two-dimensional nuclear magnetic resonance spectroscopy: Application to human urine samples. *Anal. Chem.* (2009). doi:10.1021/ac902405z
353. Smith, I. C. P. & Baert, R. Medical diagnosis by high resolution NMR of human specimens. *IUBMB Life* (2003). doi:10.1080/1521654031000134833
354. Ng, S. M. Portable NMR-Based Sensors in Medical Diagnosis. in *Applications of NMR Spectroscopy* (2015). doi:10.1016/B978-1-60805-999-7.50003-3
355. Maynard, J. A. *et al.* Surface plasmon resonance for high-throughput ligand screening of membrane-bound proteins. *Biotechnology Journal* (2009). doi:10.1002/biot.200900195
356. Hoa, X. D., Kirk, A. G. & Tabrizian, M. Towards integrated and sensitive surface plasmon resonance biosensors: A review of recent progress. *Biosensors and Bioelectronics* (2007). doi:10.1016/j.bios.2007.07.001
357. Kussrow, A., Enders, C. S. & Bornhop, D. J. Interferometric methods for label-free molecular interaction studies. *Analytical Chemistry* (2012). doi:10.1021/ac202812h
358. Baksh, M. M., Kussrow, A. K., Mileni, M., Finn, M. G. & Bornhop, D. J. Label-free quantification of membrane-ligand interactions using backscattering interferometry. *Nat. Biotechnol.* (2011). doi:10.1038/nbt.1790
359. Kussrow, A. *et al.* The potential of backscattering interferometry as an in vitro clinical diagnostic tool for the serological diagnosis of infectious

disease. *Analyst* (2010). doi:10.1039/c0an00098a
360. Anderson, A. S. *et al.* Functional PEG-modified thin films for biological detection. *Langmuir* **24**, 2240–2247 (2008).
361. Liu, L., Viallat, A. & Jin, G. Vesicle adhesion visualized with total internal reflection imaging ellipsometry biosensor. *Sensors Actuators, B Chem.* (2014). doi:10.1016/j.snb.2013.08.044
362. Castellana, E. T., Gamez, R. C. & Russell, D. H. Label-free biosensing with lipid-functionalized gold nanorods. *J. Am. Chem. Soc.* (2011). doi:10.1021/ja109936h
363. Martinez, J. S., Grace, W. K., Grace, K. M., Hartman, N. & Swanson, B. I. Pathogen detection using single mode planar optical waveguides. *J. Mater. Chem.* **15**, 4639 (2005).
364. Mukundan, H. *et al.* Quantitative multiplex detection of pathogen biomarkers on multichannel waveguides. *Anal. Chem.* **82(1)**, 136–44 (2010).
365. Mukundan, H. *et al.* Waveguide-based biosensors for pathogen detection. *Sensors* **9**, 5783–5809 (2009).
366. Stromberg, L. R. *et al.* Membrane insertion for the detection of lipopolysaccharides: Exploring the dynamics of amphiphile-in-lipid assays. *PLoS One* **11**, e0156295 (2016).
367. Kale, R. R. *et al.* Detection of intact influenza viruses using biotinylated biantennary S-sialosides. *J. Am. Chem. Soc.* **130**, 8169–8171 (2008).
368. Mukundan, H. *et al.* Optimizing a waveguide-based sandwich immunoassay for tumor biomarkers: Evaluating fluorescent labels and functional surfaces. *Bioconjug. Chem.* **20**, 222–230 (2009).
369. Mukundan, H. *et al.* Planar optical waveguide-based biosensor for the quantitative detection of tumor markers. *Sensors Actuators, B Chem.* **138**, 453–460 (2009).
370. Sameiro, M. & Gonçalves, T. Fluorescent labeling of biomolecules with organic probes. *Chem. Rev.* (2009). doi:10.1021/cr0783840
371. Grieshaber, D., MacKenzie, R., Vörös, J. & Reimhult, E. Electrochemical biosensors - Sensor principles and architectures. *Sensors* (2008). doi:10.3390/s8031400
372. Ahmed, A., Rushworth, J. V., Hirst, N. A. & Millner, P. A. Biosensors for whole-cell bacterial detection. *Clin. Microbiol. Rev.* (2014). doi:10.1128/CMR.00120-13
373. Peng, T., Cheng, Q. & Stevens, R. C. Amperometric detection of Escherichia coli heat-labile enterotoxin by redox diacetylenic vesicles on a sol-gel thin-film electrode. *Anal. Chem.* (2000). doi:10.1021/ac990406y
374. Cheng, Q., Zhu, S., Song, J. & Zhang, N. Functional lipid microstructures immobilized on a gold electrode for voltammetric biosensing of cholera toxin. *Analyst* (2004). doi:10.1039/b315656g
375. Shiba, K., Umezawa, Y., Watanabe, T., Ogawa, S. & Fujiwara, S. Thin-Layer Potentiometric Analysis of Lipid Antigen-Antibody Reaction by Tetrapentylammonium (TPA+) Ion Loaded Liposomes and TPA+ Ion Selective Electrode. *Anal. Chem.* (1980). doi:10.1021/ac50061a018

376. Psychoyios, V. N. *et al.* Potentiometric Cholesterol Biosensor Based on ZnO Nanowalls and Stabilized Polymerized Lipid Film. *Electroanalysis* (2013). doi:10.1002/elan.201200591
377. Nikoleli, G. P. *et al.* Potentiometric cholesterol biosensing application of graphene electrode with stabilized polymeric lipid membrane. *Cent. Eur. J. Chem.* (2013). doi:10.2478/s11532-013-0285-5
378. Ali, M. A. *et al.* Protein-conjugated quantum dots interface: Binding kinetics and label-free lipid detection. *Anal. Chem.* (2014). doi:10.1021/ac403543g
379. Ali, M. A. *et al.* Protein Functionalized Carbon Nanotubes-based Smart Lab-on-a-Chip. *ACS Appl. Mater. Interfaces* (2015). doi:10.1021/am509002h
380. Cho, N. J., Frank, C. W., Kasemo, B. & Höök, F. Quartz crystal microbalance with dissipation monitoring of supported lipid bilayers on various substrates. *Nat. Protoc.* (2010). doi:10.1038/nprot.2010.65
381. Edvardsson, M. *et al.* QCM-D and reflectometry instrument: Applications to supported lipid structures and their biomolecular interactions. *Anal. Chem.* (2009). doi:10.1021/ac801523w
382. Nieradka, K. *et al.* Microcantilever array biosensors for detection and recognition of Gram-negative bacterial endotoxins. *Sensors Actuators, B Chem.* (2014). doi:10.1016/j.snb.2014.03.023
383. Zhang, Z. *et al.* A Cantilever-based Biosensor for Real-time Monitoring of Interactions between Amyloid-β(1–40) and Membranes Comprised of Phosphatidylcholine Lipids with Different Hydrophobic Acyl Chains. *Electroanalysis* (2017). doi:10.1002/elan.201600416
384. O'Neill, J. *Tackling drug-resistant infections globally: final report and recommendations: the review on antimicrobial resistance; 2016 [Available from: https://amr-review. org*. *Publications. html* (2019).
385. Washington, J. A. Chapter 10 Principles of Diagnosis. in *Medical Microbiology* (1996).
386. Levin, J., Poore, T. E., Zauber, N. P. & Oser, R. S. Detection of Endotoxin in the Blood of Patients with Sepsis Due to Gram-Negative Bacteria. *N. Engl. J. Med.* (1970). doi:10.1056/nejm197012102832404
387. Feingold, K. R. & Grunfeld, C. The role of HDL in innate immunity. *Journal of Lipid Research* (2011). doi:10.1194/jlr.E012138
388. Triantafilou, M. *et al.* Serum proteins modulate lipopolysaccharide and lipoteichoic acid-induced activation and contribute to the clinical outcome of sepsis. *Virulence* (2012). doi:10.4161/viru.19077
389. Matsumoto, T. *et al.* Significance of urinary endotoxin concentration in patients with urinary tract infection. *Urol. Res.* (1991). doi:10.1007/BF00299061
390. Hrabák, J., Chudáčková, E. & Walková, R. Matrix-assisted laser desorption ionization-time of flight (MALDITOF) mass spectrometry for detection of antibiotic resistance mechanisms: From research to routine diagnosis. *Clin. Microbiol. Rev.* (2013). doi:10.1128/CMR.00058-12
391. Levels, J. H. M., Abraham, P. R., Van Barreveld, E. P., Meijers, J. C. M. & Van Deventer, S. J. H. Distribution and kinetics of lipoprotein-bound

lipoteichoic acid. *Infect. Immun.* (2003). doi:10.1128/IAI.71.6.3280-3284.2003
392. Kassa, F. A. *et al.* New inflammation-related biomarkers during malaria infection. *PLoS One* (2011). doi:10.1371/journal.pone.0026495
393. Biron, B. M., Ayala, A. & Lomas-Neira, J. L. Biomarkers for sepsis: What is and what might be? *Biomarker Insights* (2015). doi:10.4137/BMI.S29519
394. Faix, J. D. Biomarkers of sepsis. *Critical Reviews in Clinical Laboratory Sciences* (2013). doi:10.3109/10408363.2013.764490
395. Aderem, A. & Ulevitch, R. J. Toll-like receptors in the induction of the innate immune response. *Nature* (2000). doi:10.1038/35021228
396. Chaby, R. Lipopolysaccharide-binding molecules: Transporters, blockers and sensors. *Cellular and Molecular Life Sciences* (2004). doi:10.1007/s00018-004-4020-4
397. Pathak, S. K. *et al.* Mycobacterium tuberculosis lipoarabinomannan-mediated IRAK-M induction negatively regulates toll-like receptor-dependent interleukin-12 p40 production in macrophages. *J. Biol. Chem.* (2005). doi:10.1074/jbc.M506471200
398. Kohanski, M. A., Dwyer, D. J. & Collins, J. J. How antibiotics kill bacteria: From targets to networks. *Nature Reviews Microbiology* (2010). doi:10.1038/nrmicro2333
399. Kubicek-Sutherland, J. Z. *et al.* Antimicrobial peptide exposure selects for Staphylococcus aureus resistance to human defence peptides. *J. Antimicrob. Chemother.* (2017). doi:10.1093/jac/dkw381
400. Kubicek-Sutherland, J. Z. *et al.* Host-dependent Induction of Transient Antibiotic Resistance: A Prelude to Treatment Failure. *EBioMedicine* (2015). doi:10.1016/j.ebiom.2015.08.012
401. Olivier, M., Van Den Ham, K., Shio, M. T., Kassa, F. A. & Fougeray, S. Malarial pigment hemozoin and the innate inflammatory response. *Frontiers in Immunology* (2014). doi:10.3389/fimmu.2014.00025
402. Frita, R. *et al.* Simple flow cytometric detection of haemozoin containing leukocytes and erythrocytes for research on diagnosis, immunology and drug sensitivity testing. *Malar. J.* (2011). doi:10.1186/1475-2875-10-74
403. Tabas, I. Cholesterol in health and disease. *Journal of Clinical Investigation* (2002). doi:10.1172/JCI0216381
404. Miller, M. *et al.* Triglycerides and cardiovascular disease: A scientific statement from the American Heart Association. *Circulation* (2011). doi:10.1161/CIR.0b013e3182160726
405. Henry, N. L. & Hayes, D. F. Cancer biomarkers. *Molecular Oncology* (2012). doi:10.1016/j.molonc.2012.01.010
406. Rader, D. J. & Hovingh, G. K. HDL and cardiovascular disease. *The Lancet* (2014). doi:10.1016/S0140-6736(14)61217-4
407. Wadhera, R. K., Steen, D. L., Khan, I., Giugliano, R. P. & Foody, J. M. A review of low-density lipoprotein cholesterol, treatment strategies, and its impact on cardiovascular disease morbidity and mortality. *Journal of Clinical Lipidology* (2016). doi:10.1016/j.jacl.2015.11.010
408. Bielecka-Dąbrowa, A. Malignancy-Associated Dyslipidemia. *Open*

Cardiovasc. Med. J. (2011). doi:10.2174/1874192401105010035
409. Solomon, K. R. & Freeman, M. R. The complex interplay between cholesterol and prostate malignancy. *Urologic Clinics of North America* (2011). doi:10.1016/j.ucl.2011.04.001
410. Bartsch, E. *et al.* Clinical risk factors for pre-eclampsia determined in early pregnancy: Systematic review and meta-analysis of large cohort studies. *BMJ* (2016). doi:10.1136/bmj.i1753
411. Spracklen, C. N., Smith, C. J., Saftlas, A. F., Robinson, J. G. & Ryckman, K. K. Maternal hyperlipidemia and the risk of preeclampsia: A meta-analysis. *American Journal of Epidemiology* (2014). doi:10.1093/aje/kwu145
412. Bedogni, G. *et al.* The fatty liver index: A simple and accurate predictor of hepatic steatosis in the general population. *BMC Gastroenterol.* (2006). doi:10.1186/1471-230X-6-33
413. Nordestgaard, B. G. & Varbo, A. Triglycerides and cardiovascular disease. *The Lancet* (2014). doi:10.1016/S0140-6736(14)61177-6
414. Singh, A. & Singh, R. Triglyceride and cardiovascular risk: A critical appraisal. *Indian Journal of Endocrinology and Metabolism* (2016). doi:10.4103/2230-8210.183460
415. Rodrigues Dos Santos, C. *et al.* LDL-cholesterol signaling induces breast cancer proliferation and invasion. *Lipids Health Dis.* (2014). doi:10.1186/1476-511X-13-16
416. Esposito, K. *et al.* Effect ofmetabolic syndrome and its components on prostate cancer risk:Meta-analysis. *Journal of Endocrinological Investigation* (2013). doi:10.1007/BF03346748
417. Kitahara, C. M. *et al.* Total cholesterol and cancer risk in a large prospective study in Korea. *J. Clin. Oncol.* (2011). doi:10.1200/JCO.2010.31.5200
418. Magura, L. *et al.* Hypercholesterolemia and prostate cancer: A hospital-based case-control study. *Cancer Causes Control* (2008). doi:10.1007/s10552-008-9197-7
419. Pelton, K., Freeman, M. R. & Solomon, K. R. Cholesterol and prostate cancer. *Current Opinion in Pharmacology* (2012). doi:10.1016/j.coph.2012.07.006
420. Ray, G. & Husain, S. A. Role of lipids, lipoproteins and vitamins in women with breast cancer. *Clin. Biochem.* (2001). doi:10.1016/S0009-9120(00)00200-9
421. Gallos, I. D. *et al.* Pre-eclampsia is associated with, and preceded by, hypertriglyceridaemia: A meta-analysis. *BJOG: An International Journal of Obstetrics and Gynaecology* (2013). doi:10.1111/1471-0528.12375
422. Ray, J. G., Diamond, P., Singh, G. & Bell, C. M. Brief overview of maternal triglycerides as a risk factor for pre-eclampsia. *BJOG: An International Journal of Obstetrics and Gynaecology* (2006). doi:10.1111/j.1471-0528.2006.00889.x
423. Ibrahim, S. H., Kohli, R. & Gores, G. J. Mechanisms of lipotoxicity in NAFLD and clinical implications. *Journal of Pediatric Gastroenterology and*

Nutrition (2011). doi:10.1097/MPG.0b013e31822578db
424. Wende, A. R. & Abel, E. D. Lipotoxicity in the heart. *Biochimica et Biophysica Acta - Molecular and Cell Biology of Lipids* (2010). doi:10.1016/j.bbalip.2009.09.023
425. Deguchi, H., Fernández, J. A., Hackeng, T. M., Banka, C. L. & Griffin, J. H. Cardiolipin is a normal component of human plasma lipoproteins. *Proc. Natl. Acad. Sci. U. S. A.* (2000). doi:10.1073/pnas.97.4.1743
426. Sapandowski, A. *et al.* Cardiolipin composition correlates with prostate cancer cell proliferation. *Mol. Cell. Biochem.* (2015). doi:10.1007/s11010-015-2549-1
427. World Health Organization. WHO | Cardiovascular diseases (CVDs) factsheet. *http://www.who.int/mediacentre/factsheets/fs317/en/index.html* (2013).
428. Mearns, B. M. Editorial: Targeting levels and functions of blood lipids in the prevention of CVD. *Nature Reviews Cardiology* (2011). doi:10.1038/nrcardio.2011.42
429. Tabatabaei-Malazy, O. *et al.* Prevalence of dyslipidemia in Iran: A systematic review and meta-analysis study. *International Journal of Preventive Medicine* (2014).
430. Arsenault, B. J., Boekholdt, S. M. & Kastelein, J. J. P. Lipid parameters for measuring risk of cardiovascular disease. *Nat. Rev. Cardiol.* (2011). doi:10.1038/nrcardio.2010.223
431. Hu, J., Zhang, Z., Shen, W. J. & Azhar, S. Cellular cholesterol delivery, intracellular processing and utilization for biosynthesis of steroid hormones. *Nutrition and Metabolism* (2010). doi:10.1186/1743-7075-7-47
432. Bhatnagar, D., Soran, H. & Durrington, P. N. Hypercholesterolaemia and its management. *BMJ* (2008). doi:10.1136/bmj.a993
433. Ridker, P. M. LDL cholesterol: Controversies and future therapeutic directions. *The Lancet* (2014). doi:10.1016/S0140-6736(14)61009-6
434. National Cholesterol Education Program. *Third report of the expert panel on detection, evaluation and treatment of high blood cholesterol in adults - Adult Treatment Panel III*. *National Institutes of Health* (2002).
435. Kwiterovich, P. Total cholesterol, HDL-cholesterol, triglycerides, and LDL-cholesterol. *Lab. Proced. Man. Anal.* (2004).
436. Schaefer, E. J. *et al. The Measurement of Lipids, Lipoproteins, Apolipoproteins, Fatty Acids, and Sterols, and Next Generation Sequencing for the Diagnosis and Treatment of Lipid Disorders*. *Endotext* (2000).
437. Evans, K. & Laker, M. F. Intra-individual factors affecting lipid, lipoprotein and apolipoprotein measurement: A review. *Annals of Clinical Biochemistry* (1995). doi:10.1177/000456329503200303
438. Hafiane, A. & Genest, J. High density lipoproteins: Measurement techniques and potential biomarkers of cardiovascular risk. *BBA Clinical* (2015). doi:10.1016/j.bbacli.2015.01.005
439. Friedewald, W. T., Levy, R. I. & Fredrickson, D. S. Estimation of the concentration of low-density lipoprotein cholesterol in plasma, without use

of the preparative ultracentrifuge. *Clin. Chem.* (1972). doi:10.1093/clinchem/18.6.499
440. Nauck, M., Warnick, G. R. & Rifai, N. Methods for measurement of LDL-cholesterol: A critical assessment of direct measurement by homogeneous assays versus calculation. *Clinical Chemistry* (2002). doi:10.1093/clinchem/48.2.236
441. Ekroos, K., Jänis, M., Tarasov, K., Hurme, R. & Laaksonen, R. Lipidomics: A tool for studies of atherosclerosis. *Current Atherosclerosis Reports* (2010). doi:10.1007/s11883-010-0110-y
442. Schlame, M. & Ren, M. Barth syndrome, a human disorder of cardiolipin metabolism. *FEBS Letters* (2006). doi:10.1016/j.febslet.2006.07.022
443. Shen, Z., Ye, C., McCain, K. & Greenberg, M. L. The Role of Cardiolipin in Cardiovascular Health. *BioMed Research International* (2015). doi:10.1155/2015/891707
444. Han, X. *et al.* Alterations in myocardial cardiolipin content and composition occur at the very earliest stages of diabetes: A shotgun lipidomics study. *Biochemistry* (2007). doi:10.1021/bi7004015
445. Petrosillo, G. *et al.* Mitochondrial dysfunction associated with cardiac ischemia/reperfusion can be attenuated by oxygen tension control. Role of oxygen-free radicals and cardiolipin. *Biochim. Biophys. Acta - Bioenerg.* (2005). doi:10.1016/j.bbabio.2005.10.003
446. Frostegård, A. G. *et al.* Antibodies against native and oxidized Cardiolipin and Phosphatidylserine and phosphorylcholine in atherosclerosis development. *PLoS One* (2014). doi:10.1371/journal.pone.0111764
447. Stewart, B. & Wild, C. World Cancer Report 2014. *Int. Agency Res. Cancer* (2014).
448. Laisupasin, P., Thompat, W., Sukarayodhin, S., Sornprom, A. & Sudjaroen, Y. Comparison of Serum Lipid Profiles between Normal Controls and Breast Cancer Patients. *J. Lab. Physicians* (2013). doi:10.4103/0974-2727.115934
449. Ni, H., Liu, H. & Gao, R. Serum lipids and breast cancer risk: A meta-Analysis of prospective cohort studies. *PLoS One* (2015). doi:10.1371/journal.pone.0142669
450. Gacci, M. *et al.* Meta-Analysis of metabolic syndrome and prostate cancer. *Prostate Cancer and Prostatic Diseases* (2017). doi:10.1038/pcan.2017.1
451. Heir, T. *et al.* Cholesterol and prostate cancer risk: A long-term prospective cohort study. *BMC Cancer* (2016). doi:10.1186/s12885-016-2691-5
452. Yu Peng, L. *et al.* Cholesterol levels in blood and the risk of prostate cancer: A meta-analysis of 14 prospective studies. *Cancer Epidemiol. Biomarkers Prev.* (2015). doi:10.1158/1055-9965.EPI-14-1329
453. Boland, M. L., Chourasia, A. H. & Macleod, K. F. Mitochondrial dysfunction in cancer. *Frontiers in Oncology* (2013). doi:10.3389/fonc.2013.00292
454. Warburg, O. On the origin of cancer cells. *Science (80-.).* (1956). doi:10.1126/science.123.3191.309
455. Chen, X. *et al.* Plasma lipidomics profiling identified lipid biomarkers in distinguishing early-stage breast cancer from benign lesions. *Oncotarget*

(2016). doi:10.18632/oncotarget.9124
456. Li, J. *et al.* Integration of lipidomics and transcriptomics unravels aberrant lipid metabolism and defines cholesteryl oleate as potential biomarker of prostate cancer. *Sci. Rep.* (2016). doi:10.1038/srep20984
457. Mistry, D. A. H. & French, P. W. Circulating phospholipids as biomarkers of breast cancer: A review. *Breast Cancer: Basic and Clinical Research* (2016). doi:10.4137/BCBCR.S40693
458. Perrotti, F. *et al.* Advances in lipidomics for cancer biomarkers discovery. *International Journal of Molecular Sciences* (2016). doi:10.3390/ijms17121992
459. Berinstein, N. L. Carcinoembryonic antigen as a target for therapeutic anticancer vaccines: A review. *Journal of Clinical Oncology* (2002). doi:10.1200/JCO.2002.08.017
460. Duffy, M. J. Carcinoembryonic antigen as a marker for colorectal cancer: Is it clinically useful? *Clinical Chemistry* (2001). doi:10.1093/clinchem/47.4.624
461. Hammarström, S. The carcinoembryonic antigen (CEA) family: Structures, suggested functions and expression in normal and malignant tissues. *Semin. Cancer Biol.* (1999). doi:10.1006/scbi.1998.0119
462. Beard, D. B. & Haskell, C. M. Carcinoembryonic antigen in breast cancer. Clinical review. *The American Journal of Medicine* (1986). doi:10.1016/0002-9343(86)90015-X
463. Huyghe, J. CEA radioimmunoassay. Clinical applications in colorectal cancer. *Acta Chir. Belg.* (1983).
464. Chester, S. J. *et al.* A new radioimmunoassay detecting early stages of colon cancer: A comparison with CEA, AFP, and Ca 19-9. *Dis. Markers* (1991).
465. Staab, H. J., Ahlemann, L. M., Koch, H. L. & Anderer, F. A. Serial carcinoembryonic antigen (CEA) determinations in the management of patients with breast cancer. *Oncodevelopmental Biol. Med.* (1980).
466. Chan, D. W. *et al.* Use of truquant BR radioimmunoassay for early detection of breast cancer recurrence in patients with stage II and stage III disease. *J. Clin. Oncol.* (1997). doi:10.1200/JCO.1997.15.6.2322
467. Borthwick, N. M., Wilson, D. W. & Bell, P. A. Carcinoembryonic antigen (CEA) in patients with breast cancer. *Eur. J. Cancer* (1977). doi:10.1016/0014-2964(77)90196-7
468. Kufe, D. W. Mucins in cancer: Function, prognosis and therapy. *Nature Reviews Cancer* (2009). doi:10.1038/nrc2761
469. Duffy, M. J. *et al.* CA125 in ovarian cancer: European Group on Tumor Markers guidelines for clinical use. *International Journal of Gynecological Cancer* (2005). doi:10.1111/j.1525-1438.2005.00130.x
470. Sturgeon, C. M. *et al.* National Academy of Clinical Biochemistry Laboratory Medicine Practice Guidelines for use of tumor markers in testicular, prostate, colorectal, breast, and ovarian cancers. *Clinical Chemistry* (2008). doi:10.1373/clinchem.2008.105601
471. Kallioniemi, O. P. *et al.* Serum ca 15-3 assay in the diagnosis and follow-up

of breast cancer. *Br. J. Cancer* (1988). doi:10.1038/bjc.1988.196
472. Kalluri, R. The biology and function of exosomes in cancer. *Journal of Clinical Investigation* (2016). doi:10.1172/JCI81135
473. Mollaei, H., Safaralizadeh, R. & Pouladi, N. A brief review of exosomes and their roles in cancer. *Meta Gene* (2017). doi:10.1016/j.mgene.2016.11.010
474. Soung, Y. H., Ford, S., Zhang, V. & Chung, J. Exosomes in cancer diagnostics. *Cancers* (2017). doi:10.3390/cancers9010008
475. Zhang, X. *et al.* Exosomes in cancer: Small particle, big player. *Journal of Hematology and Oncology* (2015). doi:10.1186/s13045-015-0181-x
476. Ko, J., Carpenter, E. & Issadore, D. Detection and isolation of circulating exosomes and microvesicles for cancer monitoring and diagnostics using micro-/nano-based devices. *Analyst* (2016). doi:10.1039/c5an01610j
477. Uzan, J., Carbonnel, M., Piconne, O., Asmar, R. & Ayoubi, J. M. Pre-eclampsia: Pathophysiology, diagnosis, and management. *Vascular Health and Risk Management* (2011). doi:10.2147/VHRM.S2018
478. Backes, C. H. *et al.* Maternal preeclampsia and neonatal outcomes. *Journal of pregnancy* (2011). doi:10.1155/2011/214365
479. Meads, C. A. *et al.* Methods of prediction and prevention of pre-eclampsia: Systematic reviews of accuracy and effectiveness literature with economic modelling. *Health Technology Assessment* (2008). doi:10.3310/hta12060
480. Siddiqui, I. Maternal serum lipids in women with pre-eclampsia. *Ann. Med. Health Sci. Res.* (2014). doi:10.4103/2141-9248.139358
481. Brown, S. H. J., Eather, S. R., Freeman, D. J., Meyer, B. J. & Mitchell, T. W. A lipidomic analysis of placenta in preeclampsia: Evidence for lipid storage. *PLoS One* (2016). doi:10.1371/journal.pone.0163972
482. Schweiger, M. *et al.* Measurement of lipolysis. in *Methods in Enzymology* (2014). doi:10.1016/B978-0-12-800280-3.00010-4
483. Scha. Lipotoxicity: when tissues overeat. *Curr. Opin. Lipidol.* (2003). doi:10.1097/01.mol.0000073508.41685.7f
484. Konige, M., Wang, H. & Sztalryd, C. Role of adipose specific lipid droplet proteins in maintaining whole body energy homeostasis. *Biochimica et Biophysica Acta - Molecular Basis of Disease* (2014). doi:10.1016/j.bbadis.2013.05.007
485. Schaffer, J. E. Fatty acid transport: The roads taken. *American Journal of Physiology - Endocrinology and Metabolism* (2002). doi:10.1152/ajpendo.00462.2001
486. Brasaemle, D. L. The perilipin family of structural lipid droplet proteins: Stabilization of lipid droplets and control of lipolysis. *Journal of Lipid Research* (2007). doi:10.1194/jlr.R700014-JLR200
487. Zechner, R. *et al.* FAT SIGNALS - Lipases and lipolysis in lipid metabolism and signaling. *Cell Metabolism* (2012). doi:10.1016/j.cmet.2011.12.018
488. Farese, R. V. & Walther, T. C. Lipid Droplets Finally Get a Little R-E-S-P-E-C-T. *Cell* (2009). doi:10.1016/j.cell.2009.11.005
489. Murphy, D. J. The biogenesis and functions of lipid bodies in animals, plants and microorganisms. *Progress in Lipid Research* (2001). doi:10.1016/S0163-7827(01)00013-3

490. Walther, T. C. & Farese, R. V. Lipid droplets and cellular lipid metabolism. *Annu. Rev. Biochem.* (2012). doi:10.1146/annurev-biochem-061009-102430
491. Malhi, H. & Gores, G. J. Molecular mechanisms of lipotoxicity in nonalcoholic fatty liver disease. *Seminars in Liver Disease* (2008). doi:10.1055/s-0028-1091980
492. Maaetoft-Udsen, K. *et al.* Comparative analysis of lipotoxicity induced by endocrine, pharmacological, and innate immune stimuli in rat basophilic leukemia cells. *J. Immunotoxicol.* (2015). doi:10.3109/1547691X.2014.990655
493. Ahmed, M. H. & Byrne, C. D. Modulation of sterol regulatory element binding proteins (SREBPs) as potential treatments for non-alcoholic fatty liver disease (NAFLD). *Drug Discovery Today* (2007). doi:10.1016/j.drudis.2007.07.009
494. Angulo, P. & Lindor, K. D. Non-alcoholic fatty liver disease. in *Journal of Gastroenterology and Hepatology (Australia)* (2002). doi:10.1046/j.1440-1746.17.s1.10.x
495. Kawano, Y. & Cohen, D. E. Mechanisms of hepatic triglyceride accumulation in non-alcoholic fatty liver disease. *Journal of Gastroenterology* (2013). doi:10.1007/s00535-013-0758-5
496. Postic, C. & Girard, J. Contribution of de novo fatty acid synthesis to hepatic steatosis and insulin resistance: Lessons from genetically engineered mice. *Journal of Clinical Investigation* (2008). doi:10.1172/JCI34275
497. Tucci, P., GonzÃ¡lez-Sapienza, G. & Marin, M. Pathogen-derived biomarkers for active tuberculosis diagnosis. *Front. Microbiol.* **5**, 549 (2014).
498. Walzl, G., Ronacher, K., Hanekom, W., Scriba, T. J. & Zumla, A. Immunological biomarkers of tuberculosis. *Nat. Rev. Immunol.* **11**, 343–345 (2011).
499. Gupta-Wright, A., Peters, J. A., Flach, C. & Lawn, S. D. Detection of lipoarabinomannan (LAM) in urine is an independent predictor of mortality risk in patients receiving treatment for HIV-associated tuberculosis in sub-Saharan Africa: A systematic review and meta-analysis. *BMC Med.* **14**, 53 (2016).
500. Dudchenko, A., Averbakh, M., Karpina, N. & Ergeshov, A. Capacities of blood serum lipoarabinomannan in the diagnosis of tuberculosis at a late stage of HIV infection. in (2018). doi:10.1183/13993003.congress-2018.pa4738
501. Sigal, G. B. *et al.* A novel sensitive immunoassay targeting the 5-methylthio-ᴅ-xylofuranose–lipoarabinomannan epitope meets the WHO's performance target for tuberculosis diagnosis. *J. Clin. Microbiol.* (2018). doi:10.1128/JCM.01338-18
502. Broger, T. *et al.* Novel lipoarabinomannan point-of-care tuberculosis test for people with HIV: a diagnostic accuracy study. *Lancet Infect. Dis.* **19**, 852–861 (2019).

503. Reid, M. J. & Shah, N. S. Approaches to tuberculosis screening and diagnosis in people with HIV in resource-limited settings. *Lancet Infect. Dis.* **9(3)**, 173–84 (2009).
504. Dudchenko, A., Averbakh, M., Karpina, N. & Ergeshov, A. Capacities of blood serum lipoarabinomannan in the diagnosis of tuberculosis at a late stage of HIV infection. *Eur. Respir. J.* **52**, PA4738 (2018).
505. Owens, N. A. *et al.* Detection of the tuberculosis biomarker mannose-capped lipoarabinomannan in human serum: Impact of sample pretreatment with perchloric acid. *Anal. Chim. Acta* **1046**, 140–147 (2019).
506. Kubicek-Sutherland, J. Z. *et al.* Direct detection of bacteremia by exploiting host-pathogen interactions of lipoteichoic acid and lipopolysaccharide. *Sci. Rep.* **9**, 6203 (2019).
507. Rose, H. *et al.* HIV infection and high density lipoprotein metabolism. *Atherosclerosis* **199**, 79–86 (2008).
508. Njoroge, A. *et al.* Low HDL-cholesterol among HIV-1 infected and HIV-1 uninfected individuals in Nairobi, Kenya. *Lipids Health Dis.* (2017). doi:10.1186/s12944-017-0503-9
509. Duprez, D. A. *et al.* Lipoprotein particle subclasses, cardiovascular disease and HIV infection. *Atherosclerosis* (2009). doi:10.1016/j.atherosclerosis.2009.05.001
510. Enkhmaa, B. *et al.* HIV disease activity as a modulator of lipoprotein(a) and allele-specific apolipoprotein(a) levels. *Arterioscler. Thromb. Vasc. Biol.* (2013). doi:10.1161/ATVBAHA.112.300125
511. Riddler, S. A. *et al.* Impact of HIV Infection and HAART on Serum Lipids in Men. *J. Am. Med. Assoc.* (2003). doi:10.1001/jama.289.22.2978
512. Esmail, H., Barry, C. E., Young, D. B. & Wilkinson, R. J. The ongoing challenge of latent tuberculosis. *Philosophical Transactions of the Royal Society B: Biological Sciences* (2014). doi:10.1098/rstb.2013.0437
513. Chintu, C. *et al.* Lung diseases at necropsy in African children dying from respiratory illnesses: A descriptive necropsy study. *Lancet* (2002). doi:10.1016/S0140-6736(02)11082-8
514. Oliwa, J. N., Karumbi, J. M., Marais, B. J., Madhi, S. A. & Graham, S. M. Tuberculosis as a cause or comorbidity of childhood pneumonia in tuberculosis-endemic areas: A systematic review. *The Lancet Respiratory Medicine* (2015). doi:10.1016/S2213-2600(15)00028-4
515. Jenkins, H. E. *et al.* Mortality in children diagnosed with tuberculosis: a systematic review and meta-analysis. *Lancet Infect. Dis.* (2017). doi:10.1016/S1473-3099(16)30474-1
516. Shata, A. M. A. *et al.* Sputum induction for the diagnosis of tuberculosis. *Arch. Dis. Child.* (1996). doi:10.1136/adc.74.6.535
517. Osório, D.-V. *et al.* Lipoarabinomannan Antigen Assay (TB-LAM) for Diagnosing Pulmonary Tuberculosis in Children with Severe Acute Malnutrition in Mozambique. *J. Trop. Pediatr.* (2020). doi:10.1093/tropej/fmaa072
518. Nicol, M. P. & Zar, H. J. New specimens and laboratory diagnostics for childhood pulmonary TB: Progress and prospects. *Paediatric Respiratory*

Reviews (2011). doi:10.1016/j.prrv.2010.09.008
519. Zar, H. J., Tannenbaum, E., Hanslo, D. & Hussey, G. Sputum induction as a diagnostic tool for community-acquired pneumonia in infants and young children from a high HIV prevalence area. *Pediatr. Pulmonol.* (2003). doi:10.1002/ppul.10302
520. Iriso, R., Mudido, P. M., Karamagi, C. & Whalen, C. The diagnosis of childhood tuberculosis in an HIV-endemic setting and the use of induced sputum. *International Journal of Tuberculosis and Lung Disease* (2005).
521. Qureshi, U. A. *et al.* Microbiological diagnosis of pulmonary tuberculosis in children: Comparative study of induced sputum and gastric lavage. *Indian Journal of Pediatrics* (2011). doi:10.1007/s12098-011-0452-7
522. Joel, D. R. *et al.* Diagnosis of paediatric tuberculosis using sputum induction in Botswana: Programme description and findings. *Int. J. Tuberc. Lung Dis.* (2014). doi:10.5588/ijtld.13.0243
523. World Health Organization. *Automated real-time nucleic acid amplification technology for rapid and simultaneous detection of tuberculosis and rifampicin resistance: Xpert MTB/RIF assay for the diagnosis of pulmonary and extrapulmonary TB in adults and children: policy update*. (2013).
524. Marais, B. J. Urine lipoarabinomannan testing in children with tuberculosis. *Lancet Glob. Heal.* **2**, e245–e246 (2018).
525. *Lateral flow urine lipoarabinomannan assay (LF-LAM) for the diagnosis of active tuberculosis in people living with HIV*.
526. Nicol, M. P. *et al.* Accuracy of a Novel Urine Test, Fujifilm SILVAMP Tuberculosis Lipoarabinomannan, for the Diagnosis of Pulmonary Tuberculosis in Children. *Clin. Infect. Dis.* (2020). doi:10.1093/cid/ciaa1052
527. Mukundan, H. *et al.* Planar optical waveguide-based biosensor for the quantitative detection of tumor markers. *Sensors Actuators, B Chem.* (2009). doi:10.1016/j.snb.2009.01.073
528. Stromberg, L. R., Mendez, H. M. & Mukundan, H. *Escherichia coli - Recent Advances on Physiology, Pathogenesis and Biotechnological Applications*. *Escherichia coli-Recent Advances on Physiology, Pathogenesis and Biotechnological Applications* (InTech, 2017). doi:10.5772/63146
529. Kubicek-Sutherland, J. Z., Hengartner, A. C. & Mukundan, H. Membrane Insertion for Direct Detection of Lipoteichoic Acid. *Trans. Mater. Res. Soc. Japan* (2017). doi:10.14723/tmrsj.42.101
530. Kale, R. R. *et al.* Detection of intact influenza viruses using biotinylated biantennary S-sialosides. *J. Am. Chem. Soc.* (2008). doi:10.1021/ja800842v
531. Jakhar, S. *et al.* Interaction of amphiphilic lipoarabinomannan with host carrier lipoproteins in tuberculosis patients: Implications for blood-based diagnostics. *bioRxiv* (2020). doi:10.1101/2020.11.20.391037
532. Guwatudde, D. *et al.* Tuberculosis in Household Contacts of Infectious Cases in Kampala, Uganda. *Am. J. Epidemiol.* (2003). doi:10.1093/aje/kwg227
533. Lemos, A. C., Matos, E. D., Pedral-Sampaio, D. B. & Netto, E. M. Risk of tuberculosis among household contacts in Salvador, Bahia. *Braz. J. Infect.*

Dis. (2004). doi:10.1590/S1413-86702004000600006
534. Batra, S. *et al.* Childhood tuberculosis in household contacts of newly diagnosed TB patients. *PLoS ONE* (2012). doi:10.1371/journal.pone.0040880
535. Song, Y. *et al.* Point-of-care technologies for molecular diagnostics using a drop of blood. *Trends in Biotechnology* (2014). doi:10.1016/j.tibtech.2014.01.003
536. Mielczarek, W. S., Obaje, E. A., Bachmann, T. T. & Kersaudy-Kerhoas, M. Microfluidic blood plasma separation for medical diagnostics: Is it worth it? *Lab Chip* (2016). doi:10.1039/c6lc00833j
537. Sun, K., Oh, H., Emerson, J. F. & Raghavan, S. R. A new method for centrifugal separation of blood components: Creating a rigid barrier between density-stratified layers using a UV-curable thixotropic gel. *J. Mater. Chem.* (2012). doi:10.1039/c2jm14818h
538. Stromberg, L. R., Mendez, H. M. & Mukundan, H. *Escherichia coli - Recent Advances on Physiology, Pathogenesis and Biotechnological Applications*. *Escherichia coli-Recent Advances on Physiology, Pathogenesis and Biotechnological Applications* (InTech, 2017). doi:10.5772/63146
539. Hin, S. *et al.* Membrane-based sample inlet for centrifugal microfluidic cartridges. *Microelectron. Eng.* (2018). doi:10.1016/j.mee.2017.12.006
540. Phurimsak, C., Tarn, M. D. & Pamme, N. Magnetic particle plug-based assays for biomarker analysis. *Micromachines* (2016). doi:10.3390/mi7050077
541. Liu, W. *et al.* A fully-integrated and automated testing device for PCR-free viral nucleic acid detection in whole blood. *Lab Chip* (2018). doi:10.1039/c8lc00371h
542. Tripathi, S., Kumar, Y. V. B., Agrawal, A., Prabhakar, A. & Joshi, S. S. Microdevice for plasma separation from whole human blood using bio-physical and geometrical effects. *Sci. Rep.* (2016). doi:10.1038/srep26749
543. Kuo, J. N. & Chen, X. F. Plasma separation and preparation on centrifugal microfluidic disk for blood assays. *Microsyst. Technol.* (2015). doi:10.1007/s00542-015-2408-8
544. Dimov, I. K. *et al.* Stand-alone self-powered integrated microfluidic blood analysis system (SIMBAS). *Lab Chip* (2011). doi:10.1039/c0lc00403k
545. Lee, B. S. *et al.* A fully automated immunoassay from whole blood on a disc. *Lab Chip* (2009). doi:10.1039/b820321k
546. Browne, A. W., Ramasamy, L., Cripe, T. P. & Ahn, C. H. A lab-on-a-chip for rapid blood separation and quantification of hematocrit and serum analytes. *Lab Chip* (2011). doi:10.1039/c1lc20144a
547. Valera, E. *et al.* A microfluidic biochip platform for electrical quantification of proteins. *Lab Chip* (2018). doi:10.1039/c8lc00033f
548. Wang, J. *et al.* A self-powered, one-step chip for rapid, quantitative and multiplexed detection of proteins from pinpricks of whole blood. *Lab Chip* (2010). doi:10.1039/c0lc00132e
549. Homsy, A. *et al.* Development and validation of a low cost blood filtration element separating plasma from undiluted whole blood. *Biomicrofluidics*

(2012). doi:10.1063/1.3672188
550. Kim, C. J. *et al.* Fully automated, on-site isolation of cfDNA from whole blood for cancer therapy monitoring. *Lab Chip* (2018). doi:10.1039/c8lc00165k
551. Cho, Y. K. Centrifugal microfluidics. in *15th International Conference on Miniaturized Systems for Chemistry and Life Sciences 2011, MicroTAS 2011* (2011). doi:10.1007/978-3-642-27758-0_203-2
552. Gorkin, R. *et al.* Centrifugal microfluidics for biomedical applications. *Lab on a Chip* (2010). doi:10.1039/b924109d
553. Tang, M., Wang, G., Kong, S. K. & Ho, H. P. A review of biomedical centrifugal microfluidic platforms. *Micromachines* (2016). doi:10.3390/mi7020026
554. Sano, M. B. & Davalos, R. V. Microfluidic techniques for the detection, manipulation and isolation of rare cells. in *MEMS for Biomedical Applications* (2012). doi:10.1533/9780857096272.3.337
555. Bowen, W. R. & Jenner, F. Theoretical descriptions of membrane filtration of colloids and fine particles: An assessment and review. *Advances in Colloid and Interface Science* (1995). doi:10.1016/0001-8686(94)00232-2
556. Anand, B. S. S. & Sujatha, N. Fluorescence quenching effects of hemoglobin on simulated tissue phantoms in the UVVis range. *Meas. Sci. Technol.* (2012). doi:10.1088/0957-0233/23/2/025502
557. Moneriz, C., Marín-García, P., Bautista, J. M., Diez, A. & Puyet, A. Haemoglobin interference and increased sensitivity of fluorimetric assays for quantification of low-parasitaemia Plasmodium infected erythrocytes. *Malar. J.* (2009). doi:10.1186/1475-2875-8-279
558. Simoni, J., Simoni, G., Lox, C. D., Prien, S. D. & Shires, G. T. Hemoglobin interference with an enzyme-linked immunosorbent assay for the detection of tumor necrosis factor-alpha. *Anal. Chim. Acta* (1995). doi:10.1016/0003-2670(95)00169-Z
559. Kim, T. H. *et al.* FAST: Size-Selective, clog-free isolation of rare cancer cells from whole blood at a liquid-liquid interface. *Anal. Chem.* (2017). doi:10.1021/acs.analchem.6b03534
560. Lee, A. *et al.* All-in-one centrifugal microfluidic device for size-selective circulating tumor cell isolation with high purity. *Anal. Chem.* (2014). doi:10.1021/ac5035049
561. Wang, Y., Keller, K. & Cheng, X. Tangential flow microfiltration for viral separation and concentration. *Micromachines* (2019). doi:10.3390/mi10050320
562. Sterlitech, C. Polyester membrane filter data sheet. Available at: https://www.sterlitech.com/polyester-membrane-filter-pet2020030.html. (Accessed: 13th January 2021)
563. Li, T., Zhang, L., Leung, K. M. & Yang, J. Out-of-plane microvalves for whole blood separation on lab-on-a-CD. *J. Micromechanics Microengineering* (2010). doi:10.1088/0960-1317/20/10/105024
564. Zhou, K. L., Li, X., Zhang, X. L. & Pan, Q. Mycobacterial mannose-capped lipoarabinomannan: a modulator bridging innate and adaptive immunity.

Emerging Microbes and Infections (2019). doi:10.1080/22221751.2019.1649097
565. Turner, J. & Torrelles, J. B. Mannose-capped lipoarabinomannan in Mycobacterium tuberculosis pathogenesis. *Pathogens and Disease* (2018). doi:10.1093/femspd/fty026
566. Brightbill, H. D. *et al.* Host defense mechanisms triggered by microbial lipoproteins through toll-like receptors. *Science (80-.).* **285**, 732–736 (1999).
567. Hunter, S. W., Gaylor, H. & Brennan, P. J. Structure and antigenicity of the phosphorylated lipopolysaccharide antigens from the leprosy and tubercle bacilli. *J. Biol. Chem.* (1986). doi:10.1016/s0021-9258(18)67246-1
568. Gilleron, M., Nigou, J., Nicolle, D., Quesniaux, V. & Puzo, G. The acylation state of mycobacterial lipomannans modulates innate immunity response through toll-like receptor 2. *Chem. Biol.* (2006). doi:10.1016/j.chembiol.2005.10.013
569. Yuan, C. *et al.* Mycobacterium tuberculosis Mannose-Capped Lipoarabinomannan Induces IL-10-Producing B Cells and Hinders CD4+Th1 Immunity. *iScience* (2019). doi:10.1016/j.isci.2018.11.039
570. Huang, Z. *et al.* Mannose-capped lipoarabinomannan from mycobacterium tuberculosis induces IL-37 production via upregulating ERK1/2 and p38 in human type ii alveolar epithelial cells. *Int. J. Clin. Exp. Med.* (2015).
571. Piermattei, A. *et al.* Toll-like receptor 2 mediates in vivo pro- and anti-inflammatory effects of Mycobacterium Tuberculosis and modulates autoimmune encephalomyelitis. *Front. Immunol.* (2016). doi:10.3389/fimmu.2016.00191
572. Shukla, S., Richardson, E. T., Drage, M. G., Boom, W. H. & Harding, C. V. Mycobacterium tuberculosis lipoprotein and lipoglycan binding to toll-like receptor 2 correlates with agonist activity and functional outcomes. *Infect. Immun.* (2018). doi:10.1128/IAI.00450-18
573. Means, T. K. *et al.* Human toll-like receptors mediate cellular activation by Mycobacterium tuberculosis. *J. Immunol.* (1999).
574. Vreugdenhil, A. C. E., Snoek, A. M. P., Van 'T Veer, C., Greve, J. W. M. & Buurman, W. A. LPS-binding protein circulates in association with apoB-containing lipoproteins and enhances endotoxin-LDL/VLDL interaction. *J. Clin. Invest.* (2001). doi:10.1172/JCI10832
575. Viles-Gonzalez, J. F., Fuster, V., Corti, R. & Badimon, J. J. Emerging importance of HDL cholesterol in developing high-risk coronary plaques in acute coronary syndromes. *Curr. Opin. Cardiol.* (2003). doi:10.1097/00001573-200307000-00008
576. Sathiyakumar, V. *et al.* Fasting versus nonfasting and low- density lipoprotein cholesterol accuracy. *Circulation* (2018). doi:10.1161/CIRCULATIONAHA.117.030677
577. Desmarchelier, C., Borel, P., Lairon, D., Maraninchi, M. & Valéro, R. Effect of nutrient and micronutrient intake on chylomicron production and postprandial lipemia. *Nutrients* (2019). doi:10.3390/nu11061299
578. Riendeau, C. J. & Kornfeld, H. THP-1 cell apoptosis in response to

Mycobacterial infection. *Infect. Immun.* (2003). doi:10.1128/IAI.71.1.254-259.2003
579. Aldo, P. B., Craveiro, V., Guller, S. & Mor, G. Effect of culture conditions on the phenotype of THP-1 monocyte cell line. *Am. J. Reprod. Immunol.* (2013). doi:10.1111/aji.12129
580. Lund, M. E., To, J., O'Brien, B. A. & Donnelly, S. The choice of phorbol 12-myristate 13-acetate differentiation protocol influences the response of THP-1 macrophages to a pro-inflammatory stimulus. *J. Immunol. Methods* (2016). doi:10.1016/j.jim.2016.01.012
581. Park, E. K. *et al.* Optimized THP-1 differentiation is required for the detection of responses to weak stimuli. *Inflamm. Res.* (2007). doi:10.1007/s00011-007-6115-5
582. Tsuchiya, S. *et al.* Establishment and characterization of a human acute monocytic leukemia cell line (THP-1). *Int. J. Cancer* (1980). doi:10.1002/ijc.2910260208
583. Tsuchiya, S. *et al.* Induction of Maturation in Cultured Human Monocytic Leukemia Cells by a Phorbol Diester. *Cancer Res.* (1982).
584. Alonso, H. *et al.* Protein O-mannosylation deficiency increases LprG-associated lipoarabinomannan release by Mycobacterium tuberculosis and enhances the TLR2-associated inflammatory response. *Sci. Rep.* (2017). doi:10.1038/s41598-017-08489-7
585. Baxter, E. W. *et al.* Standardized protocols for differentiation of THP-1 cells to macrophages with distinct M(IFNγ+LPS), M(IL-4) and M(IL-10) phenotypes. *J. Immunol. Methods* (2020). doi:10.1016/j.jim.2019.112721
586. Elass, E. *et al.* Mycobacterial lipomannan induces matrix metalloproteinase-9 expression in human macrophagic cells through a toll-like receptor 1 (TLR1)/TLR2- and CD14-dependent mechanism. *Infect. Immun.* (2005). doi:10.1128/IAI.73.10.7064-7068.2005
587. Huang, H., Fletcher, A., Niu, Y., Wang, T. T. Y. & Yu, L. Characterization of lipopolysaccharide-stimulated cytokine expression in macrophages and monocytes. *Inflamm. Res.* (2012). doi:10.1007/s00011-012-0533-8
588. Hook, J. S., Cao, M., Weng, K., Kinnare, N. & Moreland, J. G. Mycobacterium tuberculosis Lipoarabinomannan Activates Human Neutrophils via a TLR2/1 Mechanism Distinct from Pam 3 CSK 4 . *J. Immunol.* (2020). doi:10.4049/jimmunol.1900919
589. Sibley, L. D., Hunter, S. W., Brennan, P. J. & Krahenbuhl, J. L. Mycobacterial lipoarabinomannan inhibits gamma interferon-mediated activation of macrophages. *Infect. Immun.* (1988). doi:10.1128/iai.56.5.1232-1236.1988
590. Daigneault, M., Preston, J. A., Marriott, H. M., Whyte, M. K. B. & Dockrell, D. H. The identification of markers of macrophage differentiation in PMA-stimulated THP-1 cells and monocyte-derived macrophages. *PLoS One* (2010). doi:10.1371/journal.pone.0008668
591. Kang, P. B. *et al.* The human macrophage mannose receptor directs Mycobacterium tuberculosis lipoarabinomannan-mediated phagosome biogenesis. *J. Exp. Med.* (2005). doi:10.1084/jem.20051239

592. Knutson, K. L., Hmama, Z., Herrera-Velit, P., Rochford, R. & Reiner, N. E. Lipoarabinomannan of Mycobacterium tuberculosis promotes protein tyrosine dephosphorylation and inhibition of mitogen-activated protein kinase in human mononuclear phagocytes: Role of the Src homology 2 containing tyrosine phosphatase 1. *J. Biol. Chem.* (1998). doi:10.1074/jbc.273.1.645
593. Martins, I. J., Mortimer, B. C., Miller, J. & Redgrave, T. G. Effects of particle size and number on the plasma clearance of chylomicrons and remnants. *J. Lipid Res.* (1996). doi:10.1016/s0022-2275(20)37472-1
594. Krauss, R. M. Lipids and lipoproteins in patients with type 2 diabetes. *Diabetes Care* (2004). doi:10.2337/diacare.27.6.1496
595. Vance, J. E. & Vance, D. E. *Biochemistry Of Lipids, Lipoproteins And Membranes*. *Biochemistry of Lipids, Lipoproteins and Membranes* (2008). doi:10.1016/B978-0-444-53219-0.X5001-6
596. Rensen, P. C. N. *et al.* Recombinant lipoproteins: Lipoprotein-like lipid particles for drug targeting. *Adv. Drug Deliv. Rev.* (2001). doi:10.1016/S0169-409X(01)00109-0

Appendix 2

Additional information for Chapter 6

Supplemental Information

Section S1

Selection of antibodies for assay development

In order to determine the optimal antibodies for use in the lipoprotein capture assay, we systematically assessed the performance of several antibodies that were available to us, including two from BEI Resources (monoclonal antibody CS40, anti-LAM polyclonal antibody (LAM-pab), and five different monoclonal antibody clones (24, 27, 29, 31 and 171) that were generously provided by the Foundation for Innovative New Diagnostics (FIND) (Figure S1) using a conventional sandwich ELISA. Although reagent intensive and associated with lower sensitivity for detection of LAM (LoD 300-500 nM)[72,211] compared to the waveguide platform[364], ELISA is a useful tool for the high-throughput screening of antibodies.

A typical ELISA experiment for the detection of LAM at various concentrations using FIND clones 24, 29 and 31 as the capture, and clone 171 as the reporter is shown in Fig S1. The limit of detection (LoD) for LAM using this assay was found to be 62.5 nM (assuming a molecular weight of 19 KDa for LAM) (n=3, per experimental condition) using clone 31 as the capture and clone 171 as the reporter. LoD was defined as 3 (s/n) where s/n is the standard deviation in observed measurements, and summary of s/n for the measurements is shown in Fig S1. Statistical significance was determined using one-way ANOVA with Fisher's least significant different test used for *post-hoc* analysis (**P<0.05).

Antibodies were assessed for suitability for use in the lipoprotein capture assay based on three parameters (Table S1): a) stability (>6 weeks after labeling with either horse radish peroxidase (HRP) or Alexa fluor 647, under refrigeration), b) specificity (no cross reactivity with *M. smegmatis* LAM), and c) sensitivity (use of <30 nM of antibody to obtain a limit of detection of ≤ 62.5 nM of LAM, which is the maximal sensitivity obtainable for this antigen by ELISA in our hands). Antibodies that did not satisfy all three criteria were not used in the waveguide-assays. For instance, the best sensitivity for detection of LAM using this method incorporated clone 31 as capture, and clone 171 as the reporter (Fig S1). However, clone 31 was unstable upon HRP labeling, and demonstrated cross reactivity with *M. smegmatis* LAM, and therefore, was not selected for further development. Using a similar assessment metric (Fig S1), FIND clones 171 and 24 were chosen for use in the lipoprotein capture assay.

Table S1. Selection of monoclonal antibodies

Antibody	**Source**	**Properties**	**Parameter**		
			Stability	Specificity	Sensitivity
CS40	BEI	Monoclonal	***	***	**
Pab	BEI	Polyclonal	*	*	**
24	FIND	Monoclonal	***	***	***
27	FIND	Monoclonal	***	**	***
29	FIND	Monoclonal	***	*	**
31	FIND	Monoclonal	*	**	***
171	FIND	Monoclonal	***	***	***

Characterization, selection, labeling and preparation of antibodies

Five different FIND monoclonal antibodies (clones 24, 27, 29, 31 and 171) were evaluated for sensitivity and specificity of detection of LAM by Enzyme Linked Immunosorbent Assays (ELISA), and optimal antibodies were selected for further use. For ELISA screening, a sandwich assay protocol was used. The conditions described for this screening assay were shown to provide good sensitivity for detection from early screening measurements at various antibody concentrations using the BEI antibodies, and H37RV LAM. All the FIND antibodies evaluated in the screening ELISA were first labelled with Horse Radish Peroxidase (HRP) using the EZ-Link Plus Activated Peroxidase Kit from ThermoFisher.

Rabbit polyclonal anti-LAM antibody from BEI Resources was diluted 100-fold in carbonate buffer, and 100μl of this dilution was added to each well of a 96 well polystyrene ELISA plate, sealed, and incubated overnight at 4°C. Then, plates were washed thrice with PBS-0.5% Tween 20 (PBST, room temperature (RT), 2 min each), and PBS containing 2% BSA was added to each well as a blocking agent 2 hr, RT). After washing (2X, PBST and 2X, PBS), LAM (500nM), diluted fresh in PBS in silanized plastic tubes was added and incubated for 2 hrs at 37°C. Following wash, varying concentrations (20-150 nM each, based on the manufacturer's recommendation) of each of the reporter antibodies being evaluated were added and incubated for 2 hours at 37°C. It was determined that 100 nM of the reporter antibody offers maximal sensitivity of detection. Following the quantification of binding affinity and signal resolution with individual

antibodies, combinations of antibodies were evaluated (all five, sets of 2, 3 and 4). From this antibody characterization, performance sensitivities were found to be even better using a cocktail of two antibodies, FIND clones 24 and 171. With this choice of antibodies, cross-reactivity studies were performed to determine binding of these antibodies with H37RV LAM, ara-LAM from *M. smegmatis* and Lipomannan from *M. bovis*.

For use in the waveguide assay, the chosen reporter antibodies, FIND clones 24 and 171, were labeled using Alexa Fluor 647 fluorescent labeling kit from Life Technologies Inc, as per manufacturer's instructions. Each antibody was purified by gel filtration, and tested for binding activity (immunoblot). The concentration of the labeled antibody, and the degree of labeling were measured by ultra-violet visible (UV-Vis) spectroscopy. Three different batch aliquots were prepared and characterized. The degree of labeling for FIND 171 was 6, 7.6, 5.2 for each of these batches, and for FIND 24 was 7.5, 9.1 and 5.03. Aliquots of each antibody were prepared and stored at 4 °C. They were combined to make a cocktail of 15nM total antibody concentration before each experiment. Lipoprotein capture assay is a sandwich immunoassay, where the capture antibody targets the coat-protein of HDL nanodiscs, namely Apolipoprotein A1. This capture antibody, goat polyclonal anti-ApoA1 (1mg/ml), was purchased in biotinylated form and activity was measured by ELISA, and subsequently evaluated by immunoblot at periodic intervals (once every month). Aliquots of the capture antibody were stored at -20 °C, 100nM of the antibody being used as effective concentration in each experiment.

Table S2: Patient demographics

Patient ID	Sex	Age (years)	CD4 cells/mm3	Infiltrates	Miliary infiltrates	Cavity	Urine LAM result
1	FEMALE	28	32				1
2	FEMALE	58	57	YES	NO	NO	1
3	FEMALE	39	1				1
4	MALE	31	5	YES	NO	NO	1
5	FEMALE	38	202				1
6	MALE	35	125	YES	NO	NO	1
7	MALE	35	32				1
8	FEMALE	25	25	YES	YES	NO	1
9	MALE	30	18	YES	NO	NO	1
10	MALE	45	230	YES	NO	NO	1
11	MALE	37	2				1
12	FEMALE	35	313	YES	NO	NO	0
13	FEMALE	27	59	YES	NO	NO	1
14	FEMALE	29	10	YES	YES	NO	1
15	MALE	43	10	YES	NO	NO	1
16	FEMALE	21	138	YES	NO	NO	1
17	FEMALE	38	27				1
18	MALE	25	14	YES	NO	NO	1
19	FEMALE	38	28	YES	YES	NO	1
20	MALE	30	61	YES	YES	NO	1
21	FEMALE	30	31	YES	YES	NO	0
22	FEMALE	.	305	YES	NO	YES	0
23	MALE	28	109	YES	NO	NO	0
24	FEMALE	21	199	YES	NO	NO	0
25	MALE	50	2	YES	NO	NO	0
26	FEMALE	32	348	YES	NO	NO	0

27	FEMALE	28	117	YES	NO	NO	0
28	FEMALE	34	7				0
29	FEMALE	29	616	YES	NO	YES	0
30	FEMALE	18	13	YES	NO	NO	0
31	FEMALE	48	56	YES	YES	NO	0
32	FEMALE	24	81	YES	NO	NO	0
33	MALE	33	14	YES	NO	NO	0
34	FEMALE	24	354				0
35	MALE	50	54	YES	NO	NO	0
36	FEMALE	37	67	YES	NO	NO	1
37	FEMALE	40	25				1
38	MALE	44	36	YES	YES	NO	0
39	FEMALE	29	.				
40	MALE	.	626	YES	NO	NO	1
41	FEMALE	19	19				0
42	FEMALE	29	635	YES	NO	NO	0
43	FEMALE	20	73				0
44	MALE	.	28	YES	NO	NO	0
45	MALE	.	206	NO	NO	NO	0
46	FEMALE	30	138	YES	NO	NO	0
47	FEMALE	28	36	YES	NO	NO	0
48	FEMALE	33	140	YES	NO	NO	0

. represents missing data, Urine LAM result- positive=1, negative=0

Appendix 3

Additional information for Chapter 9
Supplemental Information

Table S3- CT values for gene expression analysis in THP-1 cells under different physiological conditions

Sample	HDL	HDL	HDL	HDL + LAM	HDL + LAM	HDL + LAM
Round	1	2	3	1	2	3
BMP2	32.01	35.38	31.96	32.14	35.35	32.66
CCL1	33.71	36.28	30.68	31.57	34.22	37.11
CCL2	30.23	35.83	35.45	31.31	37.01	35.93
CCL20	31.38	31.92	31.17	30.31	31.67	30.00
CCL3	30.80	32.91	30.92	29.70	32.32	29.47
CCL5	29.43	31.47	28.60	28.90	31.86	25.97
CSF2	33.76	UD	36.47	37.14	37.12	35.31
CSF3	35.58	36.31	36.71	34.02	35.97	35.57
CXCL1	31.96	35.39	33.96	31.01	33.72	31.73
CXCL2	28.91	31.79	28.18	28.23	30.91	26.38
CXCL5	29.58	37.04	36.51	28.69	35.90	34.35
IL15	34.97	34.12	33.47	34.52	37.06	32.48
IL16	37.09	36.93	35.36	35.62	UD	35.24
IL18	32.97	35.47	33.49	33.60	35.40	32.50
IL1A	35.88	36.97	35.88	35.89	36.92	35.63
IL1B	33.04	33.77	34.59	31.93	32.93	32.23
CXCL8	22.90	24.68	22.49	22.23	24.27	20.66
TNF	32.96	36.42	31.92	32.94	33.97	31.49
ACTB	21.91	25.40	21.59	22.51	24.69	20.92
HPRT1	30.19	33.38	30.91	30.62	33.47	29.92
RPLP0	23.36	25.90	22.87	23.84	26.67	21.88
GDC	31.83	UD	UD	33.75	36.99	UD
RTC	24.71	24.11	23.90	24.96	23.91	23.43

Sample	LDL	LD	LD	LDL + LAM	LDL + LAM	LDL + LAM
Round	1	2	3	1	2	3
BMP2	33.45	29.59	29.90	37.05	29.92	30.34
CCL1	34.00	37.93	34.20	37.13	37.15	33.25
CCL2	33.19	36.63	36.66	37.11	36.90	35.74
CCL20	33.91	31.62	31.01	34.15	30.90	27.91
CCL3	33.88	30.29	31.17	34.92	30.40	28.91
CCL5	30.74	29.95	28.72	31.94	29.69	27.55
CSF2	39.30	36.63	UD	UD	36.37	37.12
CSF3	36.98	36.87	36.92	36.29	36.53	35.86
CXCL1	36.45	35.94	33.91	36.95	35.24	32.48
CXCL2	33.48	32.30	29.84	34.93	31.57	27.91
CXCL5	34.91	33.61	37.07	37.24	34.01	34.65
IL15	35.42	34.09	33.90	36.90	34.93	33.88
IL16	UD	UD	33.16	UD	36.99	32.91
IL18	34.19	32.92	31.92	36.91	33.34	31.50
IL1A	35.83	34.14	35.87	UD	34.77	34.47
IL1B	36.33	32.57	32.14	36.93	31.87	29.93
CXCL8	25.45	23.26	23.90	26.79	22.91	21.81
TNF	36.90	34.91	32.49	UD	34.92	31.34
ACTB	25.18	22.85	20.84	28.70	22.91	20.68
HPRT1	32.36	30.61	30.33	34.92	30.91	29.87
RPLP0	24.79	24.45	22.19	26.90	24.80	21.91
GDC	37.14	UD	UD	UD	UD	UD
RTC	24.89	23.48	23.84	26.75	23.41	23.77

Sample	media + LAM	media + LAM	media + LAM	media	media	media
Round	1	2	3	1	2	3
BMP2	29.90	29.91	28.91	31.90	31.90	28.97
CCL1	31.91	33.91	21.94	35.92	37.13	30.24
CCL2	30.92	33.92	32.93	32.91	34.92	34.74
CCL20	22.91	23.91	23.92	24.91	25.90	26.71
CCL3	23.90	24.90	24.92	26.91	26.90	28.61
CCL5	23.93	26.96	24.97	26.91	28.93	27.36
CSF2	31.90	32.90	29.60	35.91	35.90	37.11
CSF3	30.91	31.91	32.68	33.91	33.90	35.76
CXCL1	25.90	26.91	28.92	28.90	28.90	33.05
CXCL2	25.90	25.92	25.91	28.90	28.90	29.83
CXCL5	31.90	31.90	30.54	33.90	34.90	33.14
IL15	34.89	36.89	33.93	36.89	37.01	34.82
IL16	33.92	34.91	31.91	33.91	36.91	31.00
IL18	33.91	34.92	31.98	32.91	34.91	30.64
IL1A	31.89	32.89	31.90	33.88	34.90	33.43
IL1B	20.91	20.92	23.93	22.92	23.91	26.88
CXCL8	19.91	20.90	19.92	22.90	22.89	23.63
TNF	27.93	26.91	27.22	29.91	30.93	30.60
ACTB	21.91	22.94	20.92	21.90	22.91	19.95
HPRT1	29.91	30.92	29.18	30.91	31.91	28.91
RPLP0	22.91	23.91	21.89	23.91	24.91	21.60
GDC	UD	36.97	UD	UD	UD	UD
RTC	23.89	21.91	23.90	23.89	22.89	23.64

Sample	VLDL	VLDL	VLDL	VLDL + LAM	VLDL + LAM	VLDL + LAM
Round	1	2	3	1	2	3
BMP2	33.89	35.94	30.44	31.36	33.39	30.46
CCL1	37.11	37.16	UD	UD	35.61	37.14
CCL2	37.09	35.28	35.21	33.11	34.25	34.24
CCL20	32.81	30.91	29.52	29.91	28.98	26.85
CCL3	32.71	33.88	31.27	29.64	31.80	28.58
CCL5	30.55	33.86	29.13	27.95	31.81	28.28
CSF2	UD	UD	UD	37.11	36.67	35.82
CSF3	36.73	35.95	34.92	34.83	36.84	35.33
CXCL1	34.92	36.87	35.90	33.46	33.92	32.82
CXCL2	30.91	33.73	31.43	28.74	30.92	28.62
CXCL5	37.06	37.05	37.09	33.47	34.84	34.32
IL15	35.06	36.99	33.91	32.63	35.40	33.74
IL16	37.00	37.00	34.13	37.00	34.86	33.97
IL18	33.53	36.91	32.05	31.45	34.46	31.92
IL1A	35.17	UD	35.41	33.99	34.46	36.37
IL1B	35.59	32.25	32.82	32.93	28.92	30.23
CXCL8	22.76	27.57	24.63	20.29	25.15	22.25
TNF	35.02	35.95	33.91	32.91	33.52	31.30
ACTB	23.37	26.36	21.91	21.52	23.91	21.88
HPRT1	31.89	34.18	30.77	29.38	31.91	30.56
RPLP0	24.26	27.44	22.91	21.92	25.62	22.82
GDC	UD	UD	UD	UD	UD	UD
RTC	24.62	23.92	23.86	22.91	23.91	23.94

Sample	serum	serum	serum	serum + LAM	serum + LAM	serum + LAM
Round	1	2	3	1	2	3
BMP2	30.90	33.44	34.94	31.92	34.45	32.64
CCL1	36.92	UD	UD	37.06	37.80	UD
CCL2	28.92	37.08	36.94	33.91	35.64	35.24
CCL20	25.90	27.30	27.76	25.90	27.45	25.87
CCL3	27.90	32.77	30.92	27.90	32.92	28.06
CCL5	27.96	31.51	29.76	26.91	31.95	27.74
CSF2	37.03	UD	37.12	36.89	37.11	32.98
CSF3	33.90	35.74	35.61	34.92	35.92	33.97
CXCL1	26.91	36.86	33.33	26.90	34.95	29.70
CXCL2	26.91	31.82	29.98	26.91	30.97	26.96
CXCL5	32.90	34.89	35.92	32.89	35.74	32.25
IL15	34.89	36.28	34.94	33.89	36.62	33.86
IL16	32.91	34.71	36.97	35.91	UD	34.19
IL18	31.92	33.29	32.17	30.90	33.91	30.92
IL1A	32.88	34.57	36.37	33.88	37.05	33.33
IL1B	25.91	29.95	30.93	25.91	29.58	28.18
CXCL8	26.90	24.91	24.15	21.90	24.90	21.83
TNF	30.91	34.96	33.41	31.91	34.90	31.10
ACTB	20.91	24.53	23.84	21.92	24.93	21.66
HPRT1	28.90	32.89	31.55	29.90	33.32	29.91
RPLP0	22.91	25.91	23.33	23.92	26.34	22.47
GDC	UD	UD	UD	UD	UD	UD
RTC	24.90	23.60	23.78	24.89	23.66	23.58

Sample	de-lip	de-lip	de-lip	de-lip + LAM	de-lip + LAM	de-lip + LAM
Round	1	2	3	1	2	3
BMP2	33.20	35.90	29.45	31.27	32.62	31.91
CCL1	UD	UD	37.04	29.00	33.20	31.62
CCL2	33.34	32.72	32.05	29.12	32.49	32.40
CCL20	27.13	28.45	26.95	23.65	23.91	23.91
CCL3	30.73	31.41	27.92	25.91	26.39	25.01
CCL5	29.40	31.98	27.74	26.52	28.78	25.95
CSF2	35.97	UD	35.40	29.37	28.74	29.33
CSF3	36.93	32.92	34.78	30.41	29.91	29.53
CXCL1	31.93	35.92	33.06	29.75	29.72	27.93
CXCL2	28.75	31.36	28.91	25.12	26.62	25.31
CXCL5	32.74	36.92	36.27	29.39	32.16	31.56
IL15	35.91	36.99	33.91	33.76	34.07	34.11
IL16	34.28	36.94	32.60	32.17	36.39	33.91
IL18	31.15	35.73	31.05	32.93	34.92	33.23
IL1A	35.93	37.00	33.86	31.78	31.88	31.90
IL1B	30.61	30.96	29.53	24.93	25.35	24.31
CXCL8	23.06	25.91	23.90	20.91	21.46	20.83
TNF	33.04	33.56	30.51	27.59	28.46	27.91
ACTB	22.80	25.71	20.92	21.91	23.88	22.48
HPRT1	30.45	33.25	28.95	28.92	30.76	29.65
RPLP0	23.71	26.24	21.79	23.29	24.55	22.91
GDC	UD	UD	37.08	35.92	29.94	UD
RTC	25.82	23.65	23.76	24.66	23.44	23.89

Sample	chyl	chyl	chyl	chyl + LAM	chyl + LAM	chyl + LAM
Round	1	2	3	1	2	3
BMP2	29.92	35.94	30.91	30.89	30.94	30.55
CCL1	37.08	UD	33.38	35.83	37.14	31.15
CCL2	36.70	37.11	21.32	37.05	34.84	19.91
CCL20	32.26	34.92	37.14	32.27	32.50	UD
CCL3	28.91	33.62	28.78	29.08	29.91	26.90
CCL5	29.95	33.34	31.92	30.20	31.48	30.68
CSF2	37.13	UD	30.27	35.70	37.00	30.18
CSF3	34.39	35.92	35.80	33.55	35.01	35.75
CXCL1	35.42	37.04	21.18	35.30	34.09	20.76
CXCL2	32.17	35.96	29.65	32.90	33.27	27.97
CXCL5	35.88	UD	32.91	34.96	36.96	32.75
IL15	34.27	36.96	29.91	34.54	35.92	29.57
IL16	35.42	UD	29.80	35.92	37.07	27.92
IL18	33.91	36.94	34.92	34.78	34.14	34.89
IL1A	32.76	36.41	21.91	34.53	34.92	21.55
IL1B	30.92	35.69	27.97	30.84	31.60	27.25
CXCL8	23.27	27.75	30.26	23.54	24.61	29.88
TNF	35.12	UD	37.20	35.90	36.90	31.23
ACTB	22.61	27.63	37.10	22.89	23.90	35.48
HPRT1	30.90	35.30	34.94	31.26	31.92	33.66
RPLP0	23.91	27.19	23.12	24.32	25.42	22.91
GDC	38.18	UD	36.92	37.16	UD	36.96
RTC	24.89	23.99	31.93	25.39	23.68	30.04

UD- Undetermined, Chyl- Chylomicrons, De-lip- Delipidataed serum

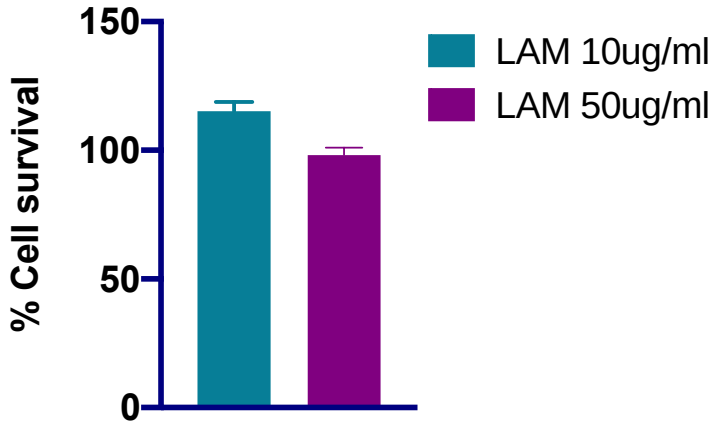

Figure S2: Cell viability assay for THP-1 cells exposed to LAM